frontiers | Research Topics

Case reports in cardiac rhythmology 2022

Edited by
Matteo Anselmino, Masateru Takigawa, Giovanni Peretto,
Elsayed Z. Soliman and Alexander H. Maass

Published in
Frontiers in Cardiovascular Medicine

ISSN 1664-8714
ISBN 978-2-8325-3462-5
DOI 10.3389/978-2-8325-3462-5

About Frontiers

Frontiers is more than just an open access publisher of scholarly articles: it is a pioneering approach to the world of academia, radically improving the way scholarly research is managed. The grand vision of Frontiers is a world where all people have an equal opportunity to seek, share and generate knowledge. Frontiers provides immediate and permanent online open access to all its publications, but this alone is not enough to realize our grand goals.

Frontiers journal series

The Frontiers journal series is a multi-tier and interdisciplinary set of open-access, online journals, promising a paradigm shift from the current review, selection and dissemination processes in academic publishing. All Frontiers journals are driven by researchers for researchers; therefore, they constitute a service to the scholarly community. At the same time, the *Frontiers journal series* operates on a revolutionary invention, the tiered publishing system, initially addressing specific communities of scholars, and gradually climbing up to broader public understanding, thus serving the interests of the lay society, too.

Dedication to quality

Each Frontiers article is a landmark of the highest quality, thanks to genuinely collaborative interactions between authors and review editors, who include some of the world's best academicians. Research must be certified by peers before entering a stream of knowledge that may eventually reach the public - and shape society; therefore, Frontiers only applies the most rigorous and unbiased reviews. Frontiers revolutionizes research publishing by freely delivering the most outstanding research, evaluated with no bias from both the academic and social point of view. By applying the most advanced information technologies, Frontiers is catapulting scholarly publishing into a new generation.

What are Frontiers Research Topics?

Frontiers Research Topics are very popular trademarks of the *Frontiers journals series*: they are collections of at least ten articles, all centered on a particular subject. With their unique mix of varied contributions from Original Research to Review Articles, Frontiers Research Topics unify the most influential researchers, the latest key findings and historical advances in a hot research area.

Find out more on how to host your own Frontiers Research Topic or contribute to one as an author by contacting the Frontiers editorial office: frontiersin.org/about/contact

Case reports in cardiac rhythmology: 2022

Topic editors

Matteo Anselmino — University of Turin, Italy
Masateru Takigawa — Tokyo Medical and Dental University, Japan
Giovanni Peretto — San Raffaele Hospital (IRCCS), Italy
Elsayed Z. Soliman — Wake Forest University, United States
Alexander H. Maass — University Medical Center Groningen, Netherlands

Citation

Anselmino, M., Takigawa, M., Peretto, G., Soliman, E. Z., Maass, A. H., eds. (2023). *Case reports in cardiac rhythmology: 2022*. Lausanne: Frontiers Media SA.
doi: 10.3389/978-2-8325-3462-5

Table of contents

frontiers | Frontiers in Cardiovascular Medicine

TYPE Editorial
PUBLISHED 29 August 2023
DOI 10.3389/fcvm.2023.1276721

OPEN ACCESS

EDITED AND REVIEWED BY
Sing-Chien Yap,
Erasmus Medical Center, Netherlands

*CORRESPONDENCE
Matteo Anselmino
matteo.anselmino@unito.it

RECEIVED 12 August 2023
ACCEPTED 18 August 2023
PUBLISHED 29 August 2023

CITATION
Ballatore A, Maass AH, Peretto G, Soliman EZ, Takigawa M and Anselmino M (2023) Editorial: Case reports in cardiac rhythmology: 2022. Front. Cardiovasc. Med. 10:1276721. doi: 10.3389/fcvm.2023.1276721

Editorial: Case reports in cardiac rhythmology: 2022

Andrea Ballatore[1,2], Alexander H. Maass[3], Giovanni Peretto[4], Elsayed Z. Soliman[5], Masateru Takigawa[6] and Matteo Anselmino[1,2]*

[1]Division of Cardiology, Cardiovascular and Thoracic Department, "Citta della Salute e della Scienza" Hospital, Turin, Italy, [2]Department of Medical Sciences, University of Turin, Turin, Italy, [3]Department of Cardiology, University Medical Center Groningen, University of Groningen, Groningen, Netherlands, [4]Department of Cardiac Electrophysiology and Arrhythmology, IRCCS San Raffaele Scientific Institute, Milan, Italy, [5]Section on Cardiovascular Medicine, Epidemiological Cardiology Research Center, Wake Forest School of Medicine, Winston Salem, NC, United States, [6]Division of Advanced Arrhythmia Research, Department of Cardiovascular Medicine, Tokyo Medical and Dental University, Tokyo, Japan

KEYWORDS

electrophysiology, case reports, cardiac arrhythmias, cardiac pacing, catheter ablation

Editorial on the Research Topic
Case reports in cardiac rhythmology: 2022

Medical science is characterized by profound interactions among different disciplines, with each discipline impacting the other in different ways. Cardiac electrophysiology is no exception, as several alterations in the cardiac rhythm can be secondary to medical disorders otherwise unrelated to the development of arrhythmias. In the present volume of the *Journal*, three great examples of these interactions are reported: Omer et al. described a case in which initiation of lamotrigine in a patient with history of epilepsy lead to the unmasking of a type 1 Brugada pattern, the development of arrhythmic syncopal events, and the induction of ventricular fibrillation during ventricular programmed electrical stimulation. Duon-Quy et al. reported the use of plasmapheresis for the treatment of heart block secondary to Guillain-Barré syndrome elicited by COVID-19 infection. Finally, Duan et al. showed a case in which a carotid body tumor resection was complicated by 40 s of asystole and cardiac arrest due to carotid sinus hypersensitivity highlighting the interplay between the heart and the autonomic nervous system. In addition to the connection between systemic disease and the heart, specific cardiac pathologies can also impact electrophysiological properties. For example, coronary artery disease is frequently associated with both brady- and tachy-arrhythmias. Development of heart block in the acute phases of myocardial infarction is a common complication; however, Zhang et al. and Wu et al. described two peculiar cases in which myocardial infarction was associated with pacemaker loss of capture, pointing out a new possible mechanism of pacemaker dysfunction.

In recent years, cardiac electrophysiology has undergone significant transformation and witnessed remarkable advancements in technologies and instruments, proving to be highly efficient and helpful in several occasions as described by Li et al. Nevertheless, critical reasoning and maintaining a logical approach to electrical signals continue to play a fundamental role, and despite the advancements, the "traditional" 12-lead electrocardiography has stood the test of time, persisting as the initial and often adequate step in diagnosing cardiac arrhythmias. Ren et al. described a case of dual atrioventricular nodal non-reentrant tachycardia, an easily missed arrhythmia with potential deleterious effects, that, however, can be "simply" diagnosed on surface ECG. On the other hand, an

"old" technique can benefit from renowned instruments, as demonstrated by the report of Hawryszko et al. in which a common smartwatch with the possibility to record a single lead ECG helped in the diagnosis of atrioventricular nodal reentrant tachycardia in a pregnant woman. In this delicate scenario, the use of a non-invasive technique helped in ruling out more severe cardiac arrhythmias leading to the correct management of the case. Use of wearable devices has grown exponentially in recent years and physicians will have to face increasing demand for the interpretation of a significant amount of data (1, 2). The clinical implications, as suggested the results of the LOOP study for the screening of atrial fibrillation (3), still need to be clarified. These reports, moreover, highlight recent and renewed attention to the AV node physiology and anatomy (4), an extremely complex structure, as originally claimed by the seminal work of Tawara. Similarly, in WPW cases, precise knowledge of the ECG and the correlation between ECG waveforms and cardiac anatomy are necessary to appropriately plan the ablation procedure. Yang et al. described a brilliant example in which correct ECG interpretation, at baseline and during programmed stimulation, led to the prompt identification of an atypical bypass tract. Similarly, Zhao et al. reported a case in which surface ECG helped in raising the suspicion of dextrocardia and finally guided the identification and ablation of an atrioventricular accessory pathway in this peculiar scenario.

Evidence-based approach in Medicine is founded on the results of properly conducted randomized controlled trials, with a large number of patients to guarantee the necessary statistical power to confirm, or reject, a thorough scientific hypothesis. However, cardiac electrophysiology has traditionally grown on the observation of an event in a small number of cases, providing insights into the mechanism underlying a specific phenomenon. The cornerstone of atrial fibrillation ablation is currently obtaining pulmonary vein isolation by means of different sources of energy, on the basis of the landmark study by Haissaguerre et al. (5); nevertheless, atrial fibrillation is a complex arrhythmia and further lesion sets may be warranted both to modify the substrate that sustains the arrhythmia (6) than to eliminate extra pulmonary vein triggers, as shown by Tao et al.

The anatomical substrate is the determinant of the development of arrhythmias and of their characteristics, therefore, precise knowledge of the anatomy is crucial for understanding and correctly treating arrhythmias, as in the case reported by Raina et al. Moreover, correct knowledge of cardiac anatomy is fundamental in preventing the occurrence of complications. New tools such as 3D printing and creation of accurate anatomical models can help with training, learning new techniques, and planning for a complex procedure (Wei et al.). Complications are intrinsically related to invasive procedures and, at times, are unpredictable and almost inevitable (De Innocentiis et al., Huang et al., Kim et al., Lo and Chen, Sha et al.); however, accurate knowledge of the anatomical relationship and caution during the planning of the procedure may surely help to reduce the possibility of severe complications.

> "*Doctors without [knowledge of] anatomy are like moles. They work in the dark and the work of their hands are mounds.*" Tiedemann, Heidelberg, 1781–1861.

Author contributions

AB: Writing – original draft. AM: Writing – review and editing. GP: Writing – review and editing. ES: Writing – review and editing. MT: Writing – review and editing. MA: Writing – original draft.

Funding

The author(s) declare that no financial support was received for the research, authorship, and/or publication of this article.

Conflict of interest

The authors declare that the research was conducted in the absence of any commercial or financial relationships that could be construed as a potential conflict of interest.

The author(s) declared that they were an editorial board member of Frontiers, at the time of submission. This had no impact on the peer review process and the final decision.

The handling editor S-CY declared a past co-authorship with the author AM.

Publisher's note

References

1. Leclercq C, Witt H, Hindricks G, Katra RP, Albert D, Belliger A, et al. Wearables, telemedicine, and artificial intelligence in arrhythmias and heart failure: proceedings of the European society of cardiology cardiovascular round table. *Europace*. (2022) 24:1372–83. doi: 10.1093/EUROPACE/EUAC052

2. Svennberg E, Tjong F, Goette A, Akoum N, Di Biase L, Bordachar P, et al. How to use digital devices to detect and manage arrhythmias: an EHRA practical guide. *Europace*. (2022) 24:979–1005. doi: 10.1093/EUROPACE/EUAC038

3. Svendsen JH, Diederichsen SZ, Højberg S, Krieger DW, Graff C, Kronborg C, et al. Implantable loop recorder detection of atrial fibrillation to prevent stroke (the LOOP study): a randomised controlled trial. *Lancet*. (2021) 398:1507–16. doi: 10.1016/S0140-6736(21)01698-6

4. Pandozi C, Matteucci A, Galeazzi M, Russo M, Lavalle C, Ficili S, et al. New insights into atrioventricular nodal anatomy, physiology, and immunochemistry: a comprehensive review and a proposed model of the slow-fast atrioventricular nodal reentrant tachycardia circuit in agreement with direct potential recordings in the Koch's triangle area. *Heart Rhythm*. (2023) 20:614–26. doi: 10.1016/J.HRTHM.2023.01.004

5. Haïssaguerre M, Jaïs P, Shah DC, Takahashi A, Hocini M, Quiniou G, et al. Spontaneous initiation of atrial fibrillation by ectopic beats originating in the pulmonary veins. *N Engl J Med*. (1998) 339:659–66. doi: 10.1056/NEJM199809033391003

6. Saglietto A, Ballatore A, Gaita F, Scaglione M, De Ponti R, De Ferrari GM, et al. Comparative efficacy and safety of different catheter ablation strategies for persistent atrial fibrillation: a network meta-analysis of randomized clinical trials. *Eur Heart J Qual Care Clin Outcomes* (2022) 8(6):619–29. doi: 10.1093/EHJQCCO/QCAB066

frontiers in Cardiovascular Medicine

CASE REPORT
published: 18 February 2022
doi: 10.3389/fcvm.2022.818275

Case Report: An Unusual Case of Fasciculoventricular Pathway

*Liu Yang, Zhijian Chen and Min Zhang**

Department of Cardiology, Union Hospital, Tongji Medical College, Huazhong University of Science and Technology, Wuhan, China

A 30-year-old man with an ECG demonstrating ventricular preexcitation with a normal PR interval and a QR pattern in lead V1 was evaluated. Electrophysiology studies showed a normal AH interval and a shortened HV interval at sinus rhythm; while the degree of preexcitation (QRS waveform) and HV interval were not affected by multisite or incremental atrial pacing. These findings implied ventricular preexcitation due to a fasciculoventricular pathway (FVP). Moreover, temporarily blocking FVP conduction mechanically resulted in normal HV interval, absence of delta wave, and an rSR pattern in V1, which indicated incomplete right bundle branch block (IRBBB). These findings suggested the coexistence of FVP and IRBBB, which is very rare.

Keywords: electrophysiology, arrhythmia, ventricular preexcitation, fasciculoventricular pathway, ablation

OPEN ACCESS

Edited by:
Richard Hauer, University Medical Center Utrecht, Netherlands

Reviewed by:
Hussam Ali, MultiMedica Holding SpA (IRCCS), Italy
Naotaka Hashiguchi, Japanese Red Cross Narita Hospital, Japan

***Correspondence:**
Min Zhang
zm429800@qq.com

Specialty section:
This article was submitted to Cardiac Rhythmology, a section of the journal Frontiers in Cardiovascular Medicine

Received: *19 November 2021*
Accepted: *17 January 2022*
Published: *18 February 2022*

Citation:
Yang L, Chen Z and Zhang M (2022) Case Report: An Unusual Case of Fasciculoventricular Pathway. Front. Cardiovasc. Med. 9:818275. doi: 10.3389/fcvm.2022.818275

INTRODUCTION

Fasciculoventricular pathways (FVPs) are uncommon preexcitation variants. Of note, a combination of FVPs with bundle branch blocks is barely observed. In this report, we describe a rare case of FVP with the presence of an incomplete right bundle branch block (IRBBB).

CASE REPORT

A 30-year-old man presented with an aberrant ECG performed 2 years ago. He was asymptomatic with unremarkable medical history. Physical examination findings, laboratory test results, and echocardiographic measurements were within normal range. A 12-lead ECG demonstrated ventricular preexcitation (**Figure 1**). The patient was admitted to the cardiology unit for consideration of an electrophysiology study (EPS).

The ECG demonstrated the presence of delta waves during sinus rhythm (**Figure 1**), suggesting a manifest accessory pathway (AP) with antegrade conduction property. Based on the deflection of the delta wave (negative in V1 and positive in lead I and aVL) and very early R-wave progression in the precordial leads (by V2), the ventricular preexcitation is likely mediated by a right septal AP. However, unlike a typical Wolff-Parkinson-White (WPW) pattern, the PR interval of this patient is within normal range with an obvious PR segment (**Figure 1**). In addition, the QR pattern in V1 is different from what we usually see (a QS or rS pattern) in a patient with ventricular preexcitation conducted over a right septal AP. This necessitates an EPS for accurate diagnosis.

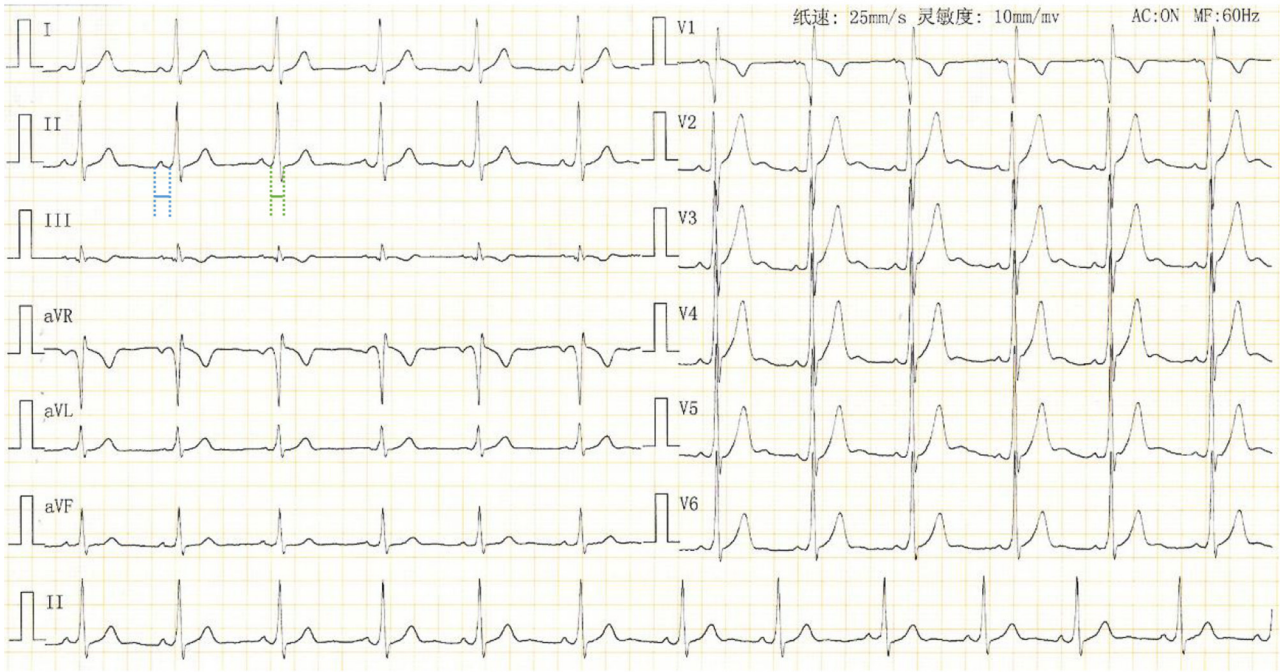

FIGURE 1 | Standard 12-lead surface ECG of the patient upon admission. QRS duration: 102 ms (in green); PR interval: 124 ms (in blue).

The patient had an EPS performed 3 days later. The baseline intracardiac recording demonstrated normal PR and atrial-His (AH) intervals (130 and 77 ms, respectively) but a shortened His-ventricular (HV) interval (24 ms) (**Figure 2A**). Right ventricular pacing showed a decremental and concentric ventriculoatrial conduction (**Figure 2B**). Programed incremental atrial pacing demonstrated a prolonged AV interval (**Figure 2C**). From sinus rhythm to atrial S1S1 pacing at 180 and 200 bpm, gradually prolonged AH intervals and short but fixed HV intervals at 24 ms were observed (**Figure 2D**). Notably, the QRS waveform remained unchanged during atrial pacing (**Figures 2C,D**), or in spontaneous paroxysmal atrial flutter or junctional beats (data not shown). These suggested that the degree of ventricular preexcitation was not affected by the frequency or location of supraventricular stimulation. All these findings favored the diagnosis of fasciculoventricular pathway (FVP) with an anterograde conduction capacity. In addition, three-dimensional (3D) mapping suggested that the earliest ventricular preexcitation occurred in the para-Hisian area (**Figure 3**). Temporarily blocking FVP conduction mechanically resulted in normal HV interval (**Figure 3**), absence of delta wave, and an rSR' pattern in V1, which indicated incomplete right bundle branch block (IRBBB) (**Figure 4**). This explained the QR pattern in V1 in the ECG upon admission. Thus, the final diagnosis of this patient was FVP with IRBBB. No ablation was performed due to the innocent nature of this AP and the non-inducibility of any tachycardia.

DISCUSSION

The presence of a delta wave with normal PR interval can be seen in the following situations: (1) An AP with a slow antegrade conduction property, such as the Mahaim fiber. The Mahaim fiber is initially identified as a conducting tissue extending from the AV node or His bundle to the ventricular myocardium to form nodoventricular fibers or fasciculoventricular fibers (as it is in this case) (1). Later studies show that Mahaim conduction appears more frequently in atriofascicular pathways, connecting usually the lateral right atrium with the right bundle fascicle (2). It is usually capable of antegrade but not retrograde conduction with a long and decremental conduction property. Preexcitation through the Mahaim fiber displays a small or no delta wave and a normal PR interval, suggesting subtle or non-recognizable ventricular preexcitation. (2) Some left-sided atrioventricular AP. Due to the long distance from the sinus node, conduction to this pathway may be delayed and ventricular preexcitation is not as obvious as APs on the right side. Thus, the PR interval can be within the normal range. (3) AP with delayed intra-atrial conduction. In such a case, the impulse that reaches the AP is delayed and a normal PR interval is displayed.

Fasciculoventricular pathways (FVPs) are the rarest variant of preexcitation (1.2–5.1% in all preexcitation cases) (3, 4), connecting His bundle or bundle branches to the ventricular septum. They are characterized by the presence of a small

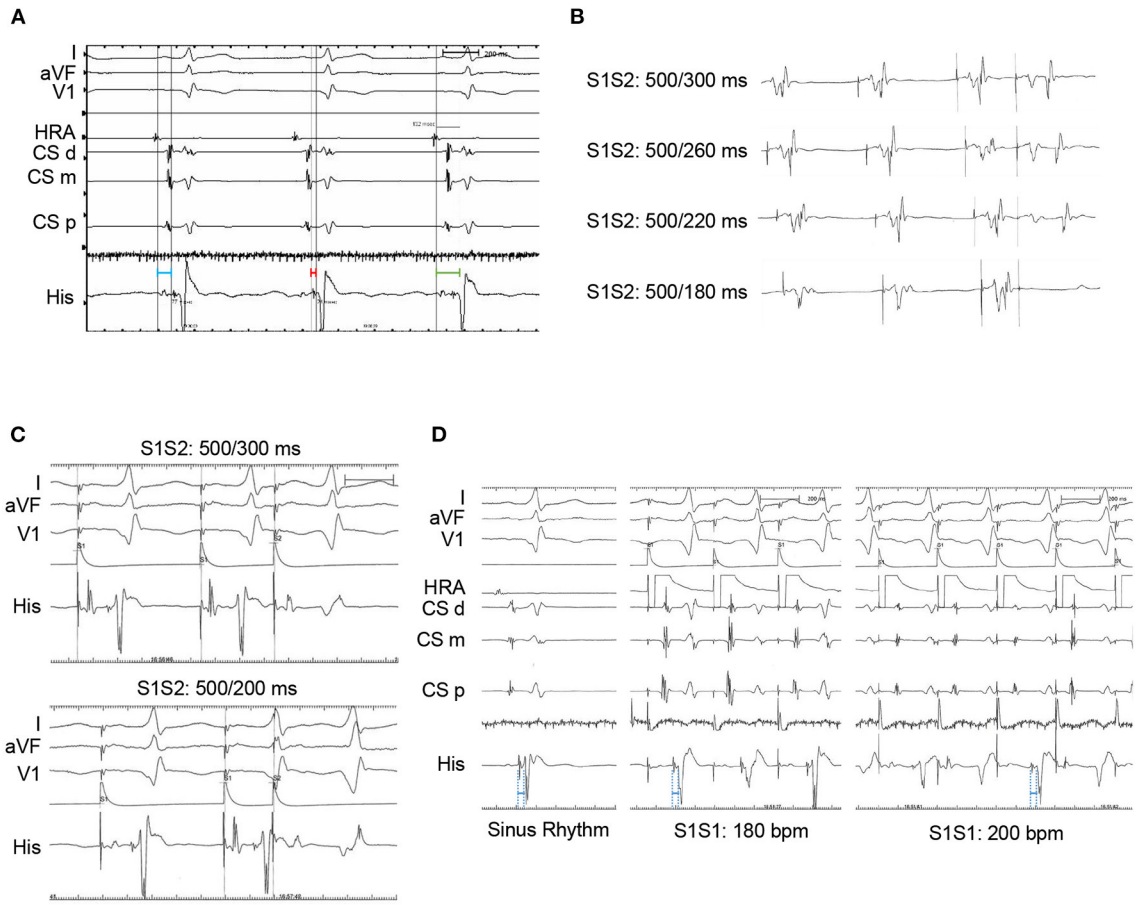

FIGURE 2 | Electrophysiological study. **(A)** Intracardiac electrograms at baseline. PR interval: 130 ms (in green); atrial-His interval: 77 ms (in blue); His-ventricular interval: 24 ms (in red). **(B)** Intracardiac electrograms in His bundle after programed incremental pacing at the right ventricular apex. **(C)** Intracardiac electrograms after programed pacing at right atrium. **(D)** Intracardiac electrograms during sinus rhythm (left panel) or atrial S1S1 stimulation at 180 bpm (middle panel) or 200 bpm (right panel). HV intervals: 24 ms (in blue). HRA, high right atrium; CS, coronary sinus; His, His bundle; d, distal; m, middle; p, proximal; bpm, beats per minute.

delta wave, with a normal AH interval and a shortened HV interval at sinus rhythm; while the degree of preexcitation is not affected by multisite or incremental atrial pacing. The main differential diagnosis is anteroseptal AP with rapid conduction property. The criteria that favor an FVP over an anteroseptal AP are: (1) a shorter QRS duration (120 vs. 140 ms); (2) a not-so-short PR interval; (3) a flat or negative delta wave in V1; (4) a narrow delta/R wave in V2; (5) S wave amplitude <20 mm in V1; (6) notching in the descending limb of the S wave in V1; and (7) prolongation of PR interval without changes in the delta wave during intravenous adenosine infusion testing (5). Another differential diagnosis is FVPs that are directly connected from the proximal RBB to the septal ventricle. Mechanically induced proximal RBBB can "correct" aberrant electrical activities (presence of delta wave and shortened HV interval) caused by FVP. However, proximal RBBB is usually more complete (duration of QRS wave > 120 ms) and the basal QR pattern in V1 as well as S waves at the end of QRS complexes in leads I, aVL, V5, and V6 should not be observed prior to EPS. Thus, the concomitant presence of FVPs and IRBBB is more reasonable. FVPs are frequently accompanied by other tachycardia, but they play no active role in producing re-entrant circuits (6, 7). Thus, ablation for FVP is usually not necessary.

To the best of our knowledge, this is the first report demonstrating the coexistence of FVP with IRBBB. In surface ECG, the QR pattern in V1 serves as a hint for the existence of IRBBB. The electrophysiological study is the golden standard for diagnosis. Although the IRBBB, in this case, does not affect the therapeutic strategy for this patient, it broadens our understanding of the co-existence of FVPs with other aberrant electrical activities in the heart.

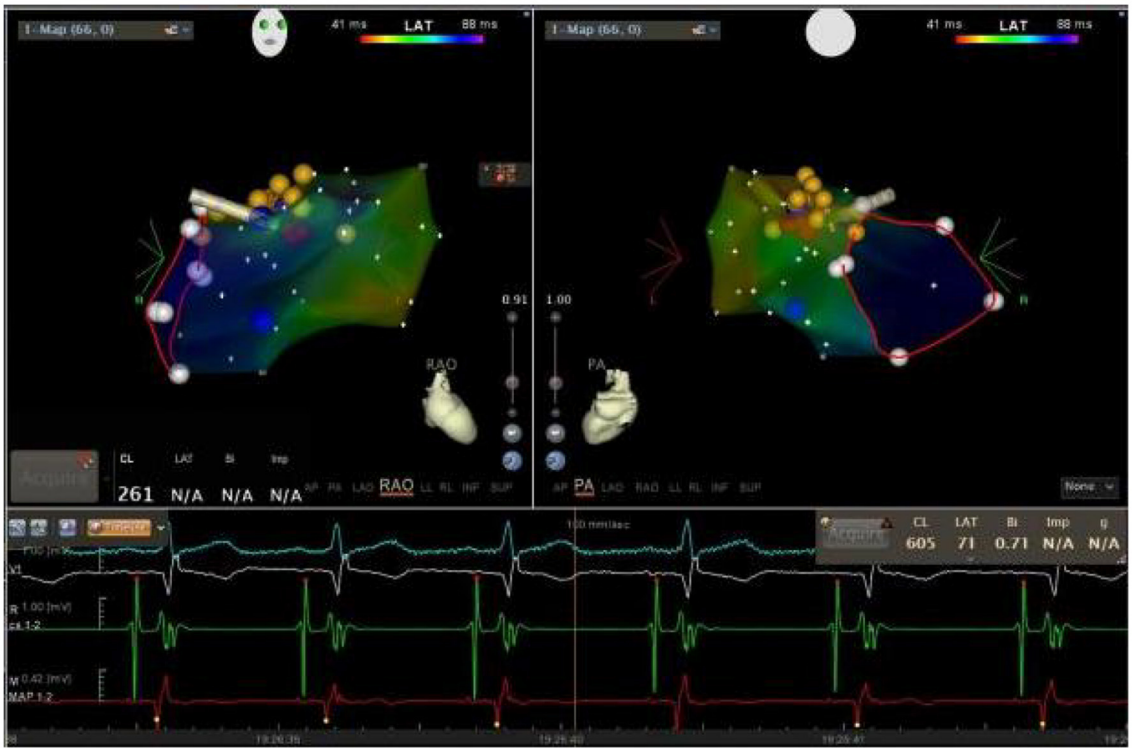

FIGURE 3 | Three-dimensional (3D) mapping of the fasciculoventricular pathway (FVP) using a Carto3 mapping system. The bipolar electrogram of the ablation catheter is shown in red (MAP 1–2). Yellow dots indicate the location where the electrical activity of His bundle was recorded, while the red dots indicate the position where the FVP was mechanically blocked.

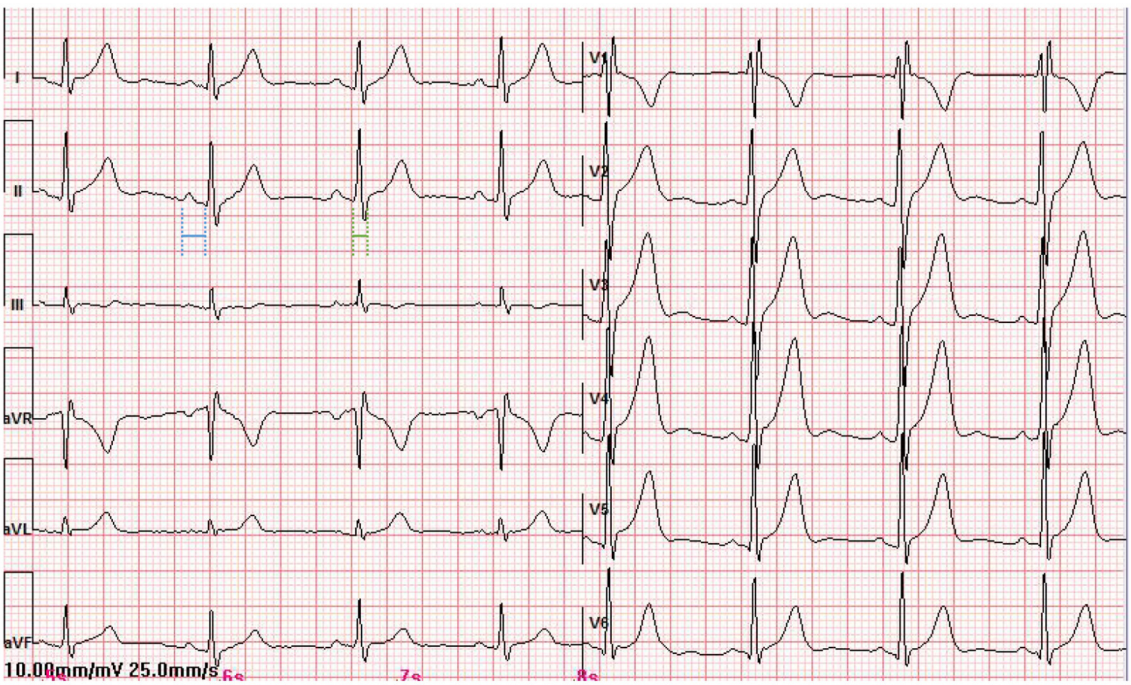

FIGURE 4 | The standard 12-lead surface ECG of the patient when the conductivity of the FVP was temporarily disturbed. QRS duration: 90 ms (in green); PR interval: 135 ms (in blue).

CONCLUSION

Fasciculoventricular pathways (FVPs) are the rarest variant of preexcitation, connecting His bundle or bundle branches to the ventricular septum. A careful evaluation of surface ECGs and EPS findings will help to recognize these pathways. Although radiofrequency ablation is usually not needed for FVPs, a combination of FVPs with other aberrant electrical activities should be noted before a clinical decision is made.

DATA AVAILABILITY STATEMENT

The original contributions presented in the study are included in the article/supplementary material, further inquiries can be directed to the corresponding author.

ETHICS STATEMENT

Written informed consent was obtained from the individual(s) for the publication of any potentially identifiable images or data included in this article.

AUTHOR CONTRIBUTIONS

MZ conceptualized the study. LY, ZC, and MZ collected all the clinical data. LY and MZ wrote the manuscript. All authors contributed to the article and approved the submitted version.

REFERENCES

1. Gallagher JJ, Smith WM, Kasell JH, Benson Jr. DW, Sterba R, Grant AO. Role of Mahaim fibers in cardiac arrhythmias in man. *Circulation.* (1981) 64:176–89. doi: 10.1161/01.CIR.64.1.176
2. Balaji S, Tchou P, Kanter R. Mahaim fibers: should they be renamed? *Heart Rhythm.* (2020) 17:161–2. doi: 10.1016/j.hrthm.2019.07.025
3. Sternick EB, Rodriguez LM, Gerken LM, Wellens HJ. Electrocardiogram in patients with fasciculoventricular pathways: a comparative study with anteroseptal and midseptal accessory pathways. *Heart Rhythm.* (2005) 2:1–6. doi: 10.1016/j.hrthm.2004.10.009
4. Suzuki T, Nakamura Y, Yoshida S, Yoshida Y, Shintaku H. Differentiating fasciculoventricular pathway from Wolff-Parkinson-White syndrome by electrocardiography. *Heart Rhythm.* (2014) 11:686–90. doi: 10.1016/j.hrthm.2013.11.018
5. de Alencar Neto JN, Ramalho de. Moraes SR, Back Sternick E, Wellens HJJ. Atypical bypass tracts: can they be recognized during sinus rhythm? *Europace.* (2019) 21:208–18. doi: 10.1093/europace/euy079
6. O'Leary ET, Dewitt ES, Mah DY, Gauvreau K, Walsh EP, Bezzerides VJ. Differentiation of fasciculoventricular fibers from anteroseptal accessory pathways using the surface electrocardiogram. *Heart Rhythm.* (2019) 16:1072–9. doi: 10.1016/j.hrthm.2019.02.011
7. Kim YG, Nam GB, Cho MS, et al. Impact of fasciculoventricular bypass tracts on the diagnosis and treatment of concomitant arrhythmias and cardiac diseases. *J Electrocardiol.* (2019) 55:34–40. doi: 10.1016/j.jelectrocard.2019.04.002

Conflict of Interest: The authors declare that the research was conducted in the absence of any commercial or financial relationships that could be construed as a potential conflict of interest.

frontiers | Frontiers in Cardiovascular Medicine

CASE REPORT
published: 02 May 2022
doi: 10.3389/fcvm.2022.889761

Case Report: A Rare Case of Severe Coronary Venous Spasm During Radiofrequency Ablation of Premature Ventricular Contraction

Rina Sha[1†], *Bing Rong*[1†], *Kellina Maduray*[1] *and Jingquan Zhong*[1,2*]

[1] *The Key Laboratory of Cardiovascular Remodeling and Function Research, Chinese Ministry of Education, Chinese National Health Commission and Chinese Academy of Medical Sciences, The State and Shandong Province Joint Key Laboratory of Translational Cardiovascular Medicine, Department of Cardiology, Qilu Hospital, Cheeloo College of Medicine, Shandong University, Jinan, China,* [2] *Department of Cardiology, Qilu Hospital (Qingdao), Cheeloo College of Medicine, Shandong University, Qingdao, China*

OPEN ACCESS

Edited by:
Matteo Anselmino, University of Turin, Italy

Reviewed by:
Hiroki Teragawa, JR Hiroshima Hospital, Japan
Kensuke Nishimiya, Tohoku University, Japan

***Correspondence:**
Jingquan Zhong
18560086597@163.com

[†]*These authors have contributed equally to this work and share first authorship*

Specialty section:
This article was submitted to Cardiac Rhythmology, a section of the journal Frontiers in Cardiovascular Medicine

Received: *04 March 2022*
Accepted: *30 March 2022*
Published: *02 May 2022*

Citation:
Sha R, Rong B, Maduray K and Zhong J (2022) Case Report: A Rare Case of Severe Coronary Venous Spasm During Radiofrequency Ablation of Premature Ventricular Contraction. Front. Cardiovasc. Med. 9:889761. doi: 10.3389/fcvm.2022.889761

Coronary venous spasm has never been reported during premature ventricular extrasystole ablation. We report a 20-year-old female patient who experienced a severe spasm of the great cardiac vein during radiofrequency ablation for premature ventricular contractions, which were relieved eventually by the administration of intracoronary nitroglycerine. The operation was successfully completed, leading to a long-term resolution of her palpitation symptoms.

Keywords: coronary venous spasm, premature ventricular contraction, radiofrequency ablation, mechanism, coronary artery spasm

INTRODUCTION

The great cardiac vein is often used as a target site for radiofrequency ablation (RFA) when treating premature ventricular contraction (PVC) in an atypical site (1). In previous reports, RFA was associated with a rare but serious side effect, coronary artery spasm, whose major possible mechanism may be catheter ablation energy inflicting direct thermal trauma near the coronary artery or impairment of the autonomic nervous system (2–4). However, coronary venous spasm (CVS) is an under-recognized phenomenon. In this report, we describe a case of CVS during the RFA of PVC.

CASE DESCRIPTION

The patient was a 20-year-old female with a history of PVCs. Her medical history stated she had no known allergies, history of tobacco or alcohol usage, family history of sudden death or cardiac disease, or history of surgery. With the aim of treating her palpitations, she was admitted to Ningjin County PPL's Hospital in Shandong province for RFA. Before the ablation, a 12-lead electrocardiogram showed frequent PVCs (**Figure 1**). There was no significant abnormity in her transthoracic echocardiogram or biochemical indexes.

After discontinuation of all anti-arrhythmic medications for at least five half-lives, the patient underwent an electrophysiologic study under local anesthesia, and then mapping and ablation were performed with an 8-Fr decapolar catheter (SmartTouch, Biosense Webster, United States). PVCs were demonstrated in the great cardiac vein, and then the catheter was positioned (**Figure 2** and **Supplementary Video 1**). The impedance at the ideal mapping position immediately increased to about 300 Ω, and radiofrequency energy was delivered at a power of 25 W with a saline irrigation flow velocity of 17 ml/min. After 20 s, an X-ray revealed that the catheter was impacted at this position (**Supplementary Video 1**). After several failed attempts to extract the catheter, the abnormality was considered to be vasospasm. A venogram was immediately manipulated to confirm great cardiac vein flow and rule out cardiac tamponade (**Figure 2**). Saline was simultaneously injected at a rate of 1 ml/min *via* the intracoronary vein. The angiography showed pericardial effusion. Pericardiocentesis was performed by extracting a 40 ml colorless transparent liquid, which appeared to be saline that was effused from the catheter. Approximately, 4 min after intracoronary injection of nitroglycerin (200 ug), the vasoconstriction was rapidly relieved (**Supplementary Video 2**). An angiogram *via* the coronary sinus was performed, which showed no signs of exudation, suggesting effusion of pericardial fluid from the catheter but not perforation. Mapping and ablation were continued, with vasoconstriction ceased to persist, and the patient ultimately converted to sinus rhythm twice, each time with 60 s. The procedure was finalized uneventfully.

DISCUSSION

The differential diagnosis includes (1) venous thrombosis, which is not consistent with the X-ray results, (2) local hematoma resulting in an impacted catheter, which was excluded considering that the venogram showed blood flow in the great cardiac vein, (3) angioedema caused by ablation energy, which was unlikely, since there were no associated signs on X-ray, and (4) severe venous spasm was the maximum possibility since it can be alleviated by vasodilation, in this case, with nitroglycerin.

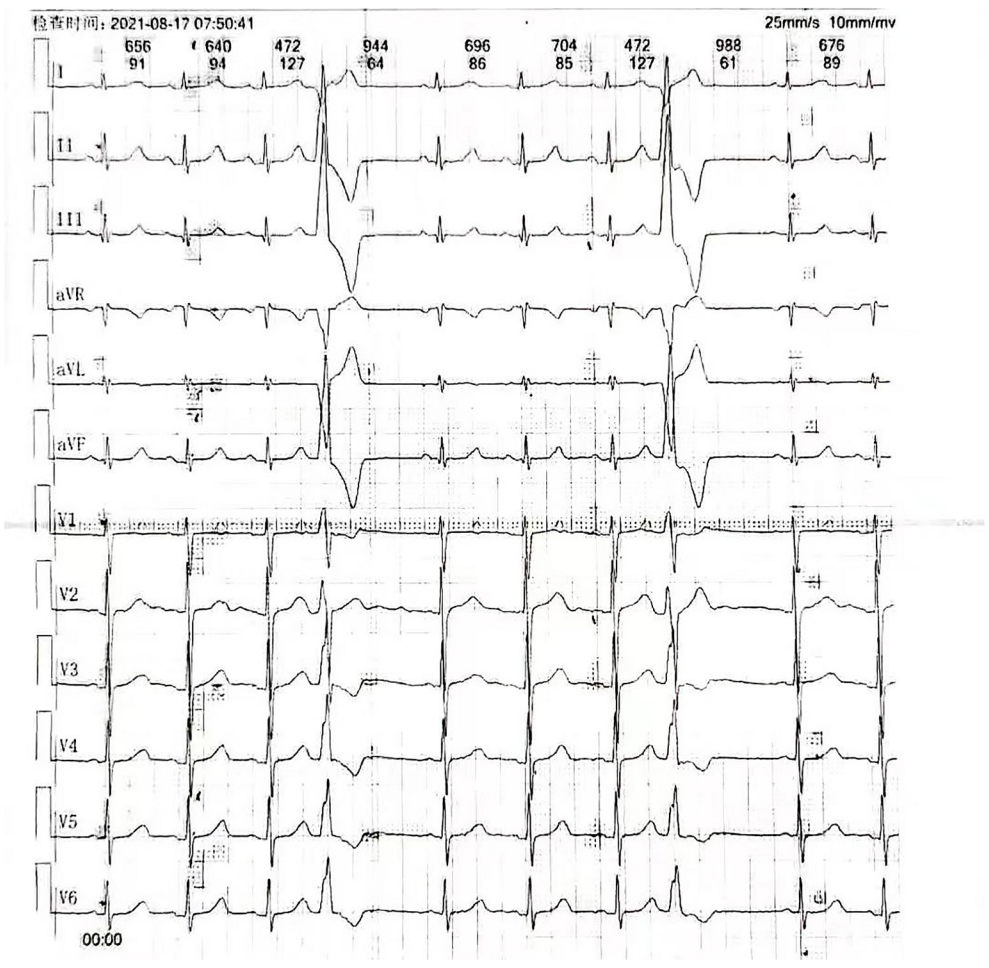

FIGURE 1 | Twelve-lead electrocardiogram displaying premature ventricular contractions.

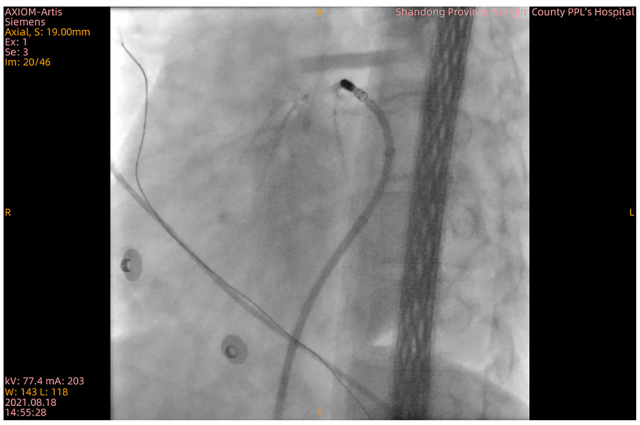

FIGURE 2 | X-ray confirming blood circulation in the great cardiac vein.

As mentioned above, coronary artery spasm has been well-documented. Peripheral venous spasm (5), central venous spasm during pacemaker implantation (6–8), and saphenous venous graft spasm causing recurrent angina (9) have been previously reported. CVS has never been reported in the literature. The pathophysiological explanation may be the same as arterial spasm.

Vasospasm could be induced by certain stimulants, such as mechanical stimulation, nerve stimulation, platelet dysfunction, and vasoconstrictor substances (9, 10). During ablation, simple mechanical stimulation to the venous vascular smooth muscle layer with a large ablation catheter could cause an imbalance between vasoconstrictors and vasodilators, resulting in vasospasm. It could also be associated with endothelial dysfunction as a consequence of direct thermal damage, since a healthy intact endothelium may prevent vasoconstriction by releasing endothelium-derived relaxing factors. Moreover, considering the great cardiac vein is surrounded by epicardial adipose tissue, which produces a large amount of metabolically active substances with both endocrine and paracrine actions, the vasospasm may have been the result of an injured adipocyte tissue (11). However, we are uncertain whether the great cardiac vein or the epicardial adipose tissue was injured through direct thermal trauma. We suggest that the most likely cause of the CVS was chemical autoregulatory imbalance. However, the definitive mechanism remains undetermined and requires further studies. Regarding precautionary measures, the operator should focus on impedance. If it reaches 300 Ω, radiofrequency ablation should be stopped. After impedance is reduced to a normal range with saline irrigation, the operator may proceed.

LIMITATIONS

The activity of the vasoconstrictors and vasodilators in the great cardiac vein during an ablation procedure could not be directly confirmed. Therefore, we were unable to ensure a cause-and-effect relationship in this case.

CONCLUSION

We reported a rare clinical case of CVS during PVC ablation, which was alleviated by intracoronary infusion of nitroglycerin. We suspect that the vasospasm was induced by the application of catheter ablation energy and catheterization in the great cardiac vein, which may result in an imbalance between vasoconstrictors and vasodilators.

DATA AVAILABILITY STATEMENT

The raw data supporting the conclusions of this article will be made available by the authors, without undue reservation.

ETHICS STATEMENT

The studies involving human participants were reviewed and approved by Ethics Committee of Shandong University Qilu Hospital. The patients/participants provided their written informed consent to participate in this study. Written informed consent was obtained from the individual(s) for the publication of any potentially identifiable images or data included in this article.

AUTHOR CONTRIBUTIONS

RS and BR contributed to the clinical treatment of this case. RS and KM contributed to the writing of the manuscript. JZ contributed to the review of the manuscript. All the authors listed have contributed sufficiently to the project in order to be included as authors and approved the final version of the manuscript for publication.

ACKNOWLEDGMENTS

This study was supported by the Natural Science Foundation of China (81970282), Qingdao Key Health Discipline Development Fund, and Shandong Provincial Natural Science Foundation, China, (ZR2018MH002).

SUPPLEMENTARY MATERIAL

The Supplementary Material for this article can be found online at: https://www.frontiersin.org/articles/10.3389/fcvm.2022.889761/full#supplementary-material

Supplementary Video 1 | X-ray showing the vasospasm and an impacted catheter at the site of the great cardiac vein.

Supplementary Video 2 | X-ray showing that the vasospasm was rapidly relieved.

REFERENCES

1. Li T, Xu Q, Zhan XZ, Xue YM, Liao HT Li YF, Letsas KP, et al. Unique electrocardiographic pattern "w" wave in lead I of idiopathic ventricular arrhythmias arising from the distal great cardiac vein. *BMC Cardiovasc Disord.* (2019) 19:90. doi: 10.1186/s12872-019-1064-9
2. Yamashita E, Tada H, Tadokoro K, Hashimoto T, Kaseno K, Miyaji K, et al. Left atrial catheter ablation promotes vasoconstriction of the right coronary artery. *Pacing Clin Electrophysiol.* (2007) 30:S98–102. doi: 10.1111/j.1540-8159.2007.00615.x
3. Tada H, Naito S, Oshima S, Taniguchi K. Vasospastic angina shortly after left atrial catheter ablation for atrial fibrillation. *Heart Rhythm.* (2005) 2:867–70. doi: 10.1016/j.hrthm.2005.05.009
4. Honda N, Takase S, Tashiro H. Severe coronary artery spasm repeatedly induced after left pulmonary vein isolation in patient with atrial fibrillation. *HeartRhythm Case Rep.* (2018) 4:501–5. doi: 10.1016/j.hrcr.2018.07.010
5. Wennevold A, Christiansen I, Lindeneg O. Complications in 4,413 catheterizations of the right side of the heart. *Am Heart J.* (1965) 69:173–80. doi: 10.1016/0002-8703(65)90034-7
6. Cooper RM, Krishnan U, Pyatt JR. Central venous spasm during pacemaker insertion. *Heart.* (2010) 96:1484. doi: 10.1136/hrt.2010.203919
7. Clemens RK, Lillis AP, Alomari AI. Catheter-induced venous spasm. *Circulation.* (2012) 126:2363–5. doi: 10.1161/CIRCULATIONAHA.112.112946
8. Vemuri KS, Parashar N, Bootla D, Revaiah PC, Kanabar K, Nevali KP, et al. Refractory axillary venous spasm during permanent pacemaker implantation. *Egypt Heart J.* (2020) 72:71. doi: 10.1186/s43044-020-00102-z
9. Victor MF, Kimbiris D, Iskandrian AS, Mintz GS, Bemis CE, Procacci PM, et al. Spasm of a saphenous vein bypass graft. A possible mechanism for occlusion of the venous graft. *Chest.* (1981) 80:413–5. doi: 10.1378/chest.80.4.413
10. He GW, Rosenfeldt FL, Buxton BF, Angus JA. Reactivity of human isolated internal mammary artery to constrictor and dilator agents. Implications for treatment of internal mammary artery spasm. *Circulation.* (1989) 80:I141–150.
11. Villasante Fricke AC, Iacobellis G. Epicardial adipose tissue: clinical biomarker of cardio-metabolic risk. *Int J Mol Sci.* (2019) 20. doi: 10.3390/ijms20235989

Conflict of Interest: The authors declare that the research was conducted in the absence of any commercial or financial relationships that could be construed as a potential conflict of interest.

frontiers | Frontiers in Cardiovascular Medicine

CASE REPORT
published: 15 June 2022
doi: 10.3389/fcvm.2022.887190

Case Report: Delayed Ventricular Pseudoaneurysm After Radiofrequency Ablation of Left Posteromedial Papillary Muscle Ventricular Tachycardia

*Min Kim[1], Yoon Jung Park[2], Hee Tae Yu[2], Tae-Hoon Kim[2], Jae-Sun Uhm[2], Boyoung Joung[2], Hui-Nam Pak[2] and Moon-Hyoung Lee[2]**

[1] Division of Cardiology, Chungbuk National University Hospital, Cheongju, South Korea, [2] Division of Cardiology, Yonsei University Health System, Seoul, South Korea

OPEN ACCESS

Edited by:
Claudio Tondo,
Monzino Cardiology Center (IRCCS), Italy

Reviewed by:
Roberto Spina,
Gosford Hospital, Australia
Saima Karim,
Case Western Reserve University, United States

***Correspondence:**
Moon-Hyoung Lee
mhlee@yuhs.ac

Specialty section:
This article was submitted to Cardiac Rhythmology, a section of the journal Frontiers in Cardiovascular Medicine

Received: 01 March 2022
Accepted: 30 May 2022
Published: 15 June 2022

Citation:
Kim M, Park YJ, Yu HT, Kim T-H, Uhm J-S, Joung B, Pak H-N and Lee M-H (2022) Case Report: Delayed Ventricular Pseudoaneurysm After Radiofrequency Ablation of Left Posteromedial Papillary Muscle Ventricular Tachycardia. Front. Cardiovasc. Med. 9:887190. doi: 10.3389/fcvm.2022.887190

A 74-year-old woman presented with incessant wide complex tachycardia that was refractory to cardioversions. Successful radiofrequency catheter ablation was performed on the left ventricular posteromedial papillary muscle. An inaudible steam pop has occurred during the procedure, but we confirmed that there were no complications during the procedure and short-term follow-up of echocardiography. Two months after the procedure, an asymptomatic pseudoaneurysm was identified at the ablation site that had not been observed in the short-term follow-up.

Keywords: ventricular tachycardia, catheter ablation, pseudoaneurysm, complication, intracardiac echocardiography

INTRODUCTION

Radiofrequency ablation is a surgical procedure used to resolve ventricular arrhythmias originating from the papillary muscle of the left ventricle (LV). Although usually challenging due to anatomical constraints and catheter instability, intracardiac echocardiography assists in achieving a high procedural success rate and immediate identification of procedural complications. The risk of cardiac perforation in catheter ablation of ventricular arrhythmia is less than 1%, which is relatively small compared to the risk of atrial catheter ablation and inaudible steam pop during catheter ablation is the most plausible mechanism for this complication (1–3). Delayed pseudoaneurysm in the LV is a very rare manifestation of catheter ablation (4), and information about its prognosis and management is limited, especially when surgical treatment is not necessary. Here we report a case of ventricular tachycardia (VT) inducing a delayed LV pseudoaneurysm on the radiofrequency catheter ablation site of the left posteromedial papillary muscle, which was absent during the short-term echocardiographic follow-up.

Abbreviations: CT, computed tomography; ICE, intracardiac echocardiography; LV, left ventricle; VT, ventricular tachycardia.

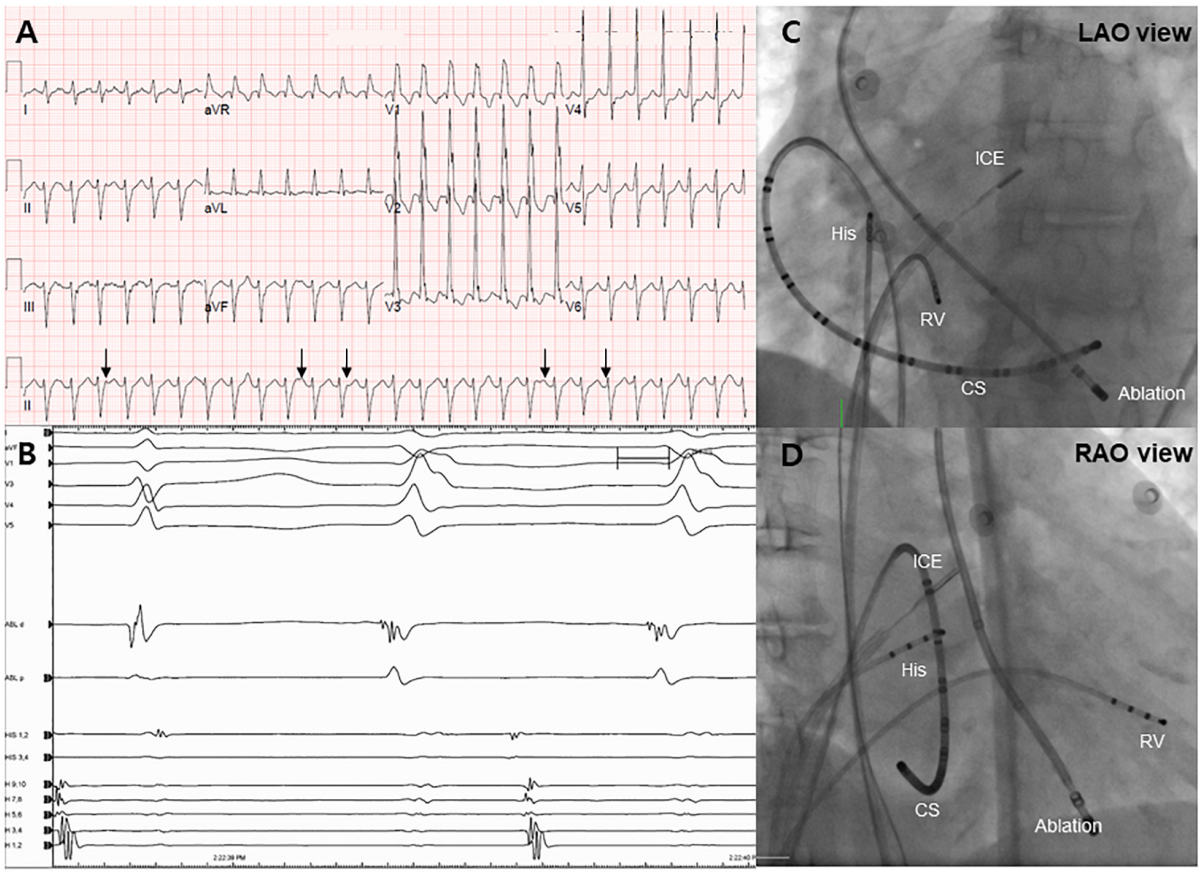

FIGURE 1 | Electrocardiogram and endocardial mapping. **(A)** Electrocardiogram of monomorphic ventricular tachycardia showing ventriculoatrial dissociation (black arrows). **(B)** Intracardiac electrogram revealing an early signal (−40 ms) before the QRS complex during the ventricular tachycardia rhythm. **(C,D)** Right and left anterior oblique projections of endocardial mapping using intracardiac echocardiography. CS, coronary sinus; RV, right ventricle.

CASE PRESENTATION

A 74-year-old woman presented to the emergency department with symptomatic wide complex tachycardia in the absence of hemodynamic deterioration. On admission, electrocardiography demonstrated monomorphic VT with a right bundle branch block pattern, a Q wave in lead V_1, left superior axis deviation, and ventriculoatrial dissociation, suggesting an exit site in the posteromedial papillary muscle region of the left ventricle (**Figure 1A**). Despite the patient undergoing electrical and pharmacological cardioversions, the VT remained unresponsive. The patient had a history of hypertension with antihypertensive drug use but no history of structural heart disease or tobacco or alcohol use. On the baseline examination, transthoracic echocardiography estimated LV end-diastolic dimension and LV ejection fraction to be 62 mm and 26%, respectively. Cardiac computed tomography (CT) revealed no significant stenotic lesions in the coronary arteries and no structural heart disease (**Supplementary Figures 1A,B**), indicating tachycardia-induced cardiomyopathy.

Following admission to the cardiac intensive care unit, the patient underwent a percutaneous left-sided stellate ganglion block with bupivacaine, a cardiac sympathetic intervention suppressing sympathetic activity for controlling VT. However, the cardiac sympathetic intervention was unsuccessful. Given that the VT remained unresolved and the driving cause of electrical instability was unclear, radiofrequency catheter ablation was decided as the most appropriate treatment strategy. Endocardial electroanatomical mapping of the LV using a CARTO-3 system (Biosense Webster) was performed through both transseptal and retroaortic approaches using a multi-electrode catheter. The procedure was performed using intracardiac echocardiography (ICE) through a transseptal approach and viewing the LV structure in real-time. The ablation catheter was positioned through the retroaortic approach. During endocardial mapping, intracardiac electrograms showed fractionated potentials around the posteromedial papillary muscle with the earliest activation (−40 ms) (**Figures 1B–D**). Endocardial bipolar voltage mapping revealed no scarring (0.5–1.5 mV), and the activation map was consistent with an exit site in the posteromedial papillary muscle region. Under direct ICE visualization (**Figure 2A**), endocardial ablation using an irrigated-tip catheter (SmartTouch, Biosense Webster) and 40 W was applied to target the earliest site that showed the

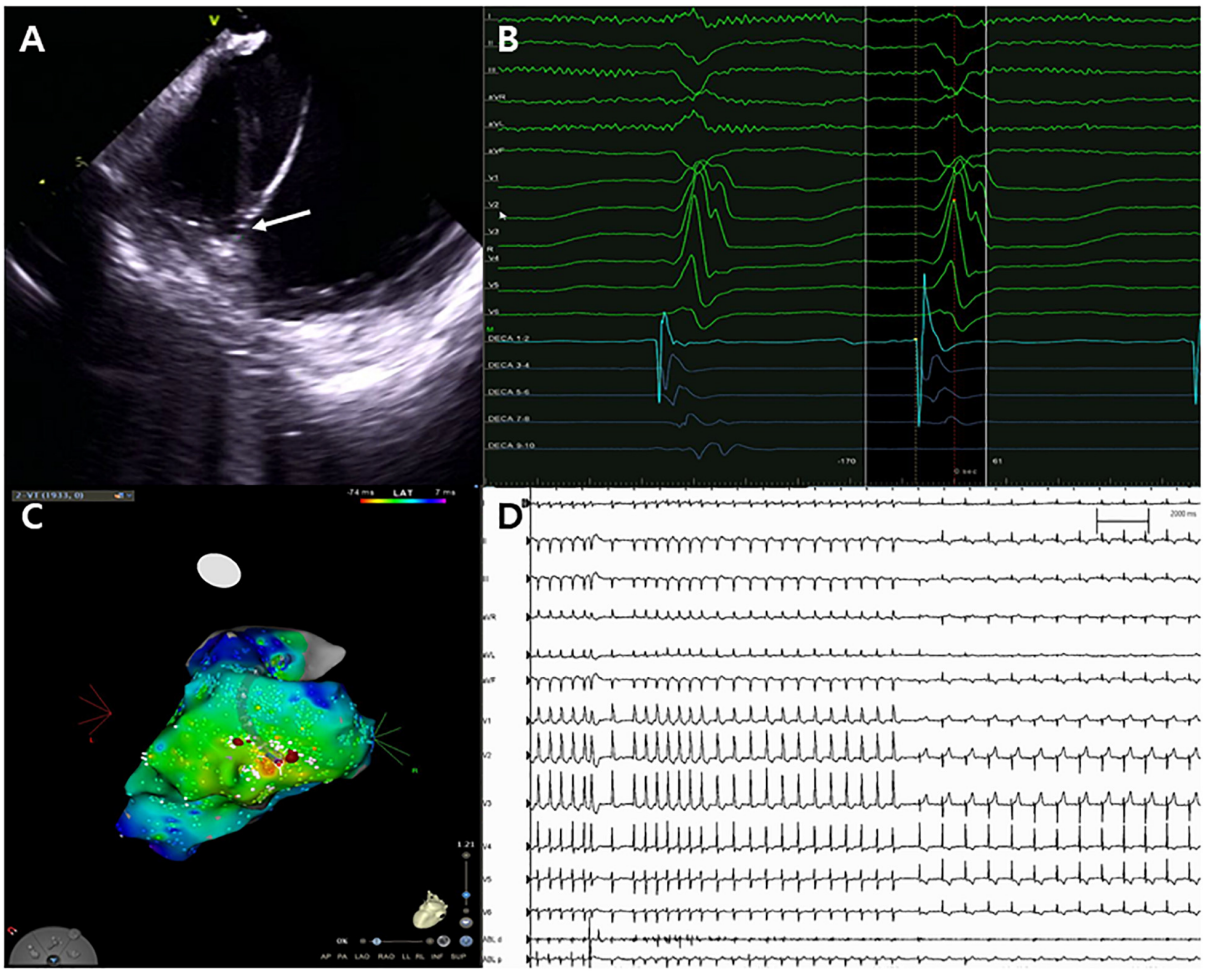

FIGURE 2 | Catheter ablation for ventricular tachycardia. **(A)** Successful ablation site on the left posteromedial papillary muscle (white arrow). **(B,C)** Unipolar Q signal on successful ablation site and three-dimensional activation map. **(D)** Termination of ventricular tachycardia with steam pops.

initial Q wave in the unipolar signal with 10–15 g of contact force (**Figures 2B,C**). During the first ablation, the VT was terminated for 30 s with an inaudible steam pop recorded by ICE (**Figure 2D** and **Supplementary Video 1**), and a sudden rise in electrical impedance was not noted. After confirming that no evidence of perforation or tissue defects were present in the first ablation site, multiple circumferential ablations were performed in the area surrounding the posteromedial papillary muscle without further steam pops. Repeated programmed electrical stimulation failed to induce VT following the ablation. Before the end of the procedure, the ICE operator confirmed that there was no evidence of procedure-related complications. The transthoracic echocardiography performed the next day showed no evidence of mitral regurgitation or tissue defects in the ablation sites (**Figure 3A**).

After 2 months of follow-up, the patient remained free of VT. Echocardiography showed improved LV systolic function with LV ejection fraction of 50% and a decreased LV size with LV end-diastolic dimension of 52 mm, but a pseudoaneurysm (26 × 9 mm) that has the ratio of the maximum diameter of the orifice to the maximum internal diameter of the cavity was lesser than 0.50 was identified at the base of the LV posteromedial papillary muscle where a steam pop had occurred without pericardial effusion (**Figure 3B** and **Supplementary Video 2**). The patient was asymptomatic; therefore, she was referred to the outpatient clinic for observational follow-up during the following year without anticoagulation or antiplatelet agents; the patient underwent no further interventions. One year later, cardiac CT revealed that the pseudoaneurysm that typically has a neck narrower than the diameter of the aneurysm remained present but showed no signs of a size change or other complications such as thrombus formation (**Figure 3C**).

DISCUSSION

Left ventricle pseudoaneurysm is a very rare complication of catheter ablation for ventricular arrhythmias that occurs regardless of the presence or absence of structural heart disease (4, 5). It is a form of cardiac rupture concealed by the adherent

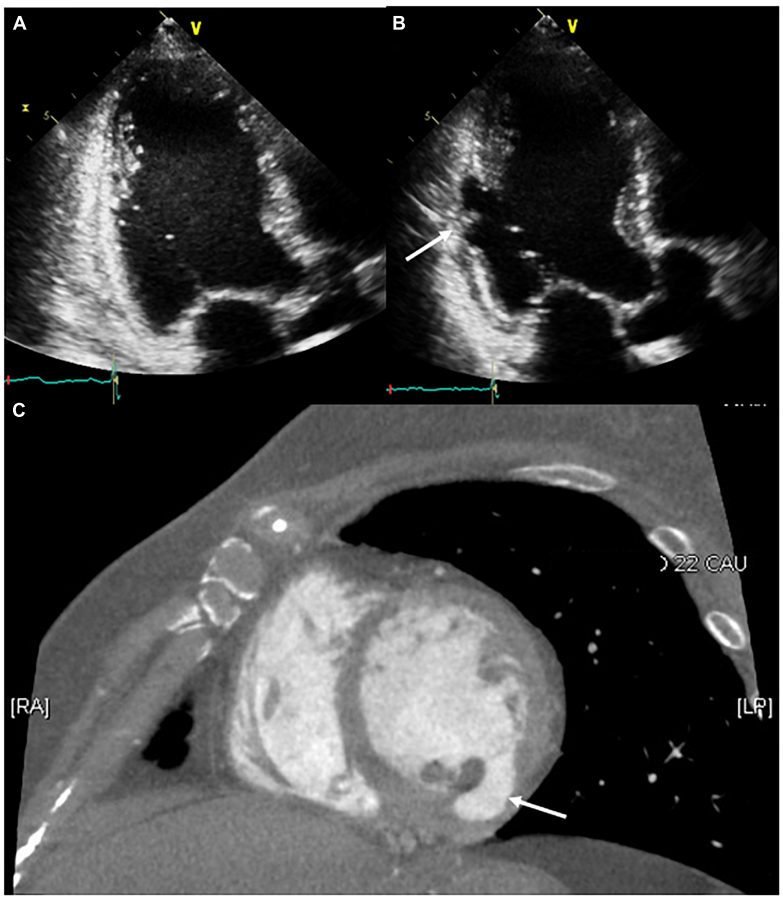

FIGURE 3 | Serial follow-up of the ablation site using transthoracic echocardiography. **(A)** The day after the procedure, no structural changes around the ablation site were observed. **(B,C)** After 2 months of follow-up, the development of a pseudoaneurysm on the ablation site (white arrow) was confirmed through transthoracic echocardiography and contrast-enhanced computed tomography.

pericardium or scar tissue and has a wide range of clinical manifestations (6). Identifying LV pseudoaneurysm is often difficult, but very important because it may cause significant complications including cardiac perforation (2), hemodynamic deterioration by compressing adjacent coronary arteries (7), and thromboembolism (8). To reduce structural defects during catheter ablation, careful monitoring of the ablation parameters, including tissue temperature changes, impedance changes, electrical potentials, and catheter position, is essential for all team members and the primary operator.

It is often challenging to differentiate between LV pseudo aneurysms and true aneurysms. Although magnetic resonance imaging is the most useful for differentiation, it is still helpful for differentiation by comparing the ratio of end-systolic orifice diameter to maximal aneurysmal diameter through echocardiography or CT. The presence of turbulent flow by pulsed Doppler at the neck of a cavity or within the cavity by echocardiography can help differentiation (9).

In the case reported here, although the presence of turbulent flow by pulsed Doppler was unclear, other echocardiography and CT findings suggested a pseudoaneurysm. Most plausible cause of the pseudoaneurysm was an inaudible steam pop that occurred during the ablation. A steam pop occurs by the myocardial explosion when the tissue temperature reaches 100°C high enough to cause tissue vaporization and gas production; by ICE visualization, it appears as a sudden hyperechogenic intramyocardial microbubble formation around the catheter. It is a potentially life-threatening complication of radiofrequency ablation because it can cause structural defects (10). Intraprocedural ICE and transthoracic echocardiogram 1 day after the procedure revealed no tissue defects around the ablation site and no pericardial effusion. However, echocardiography performed at 2 months of follow-up confirmed the delayed development of a pseudoaneurysm at the first ablation site. We speculated that an inaudible steam pop cause both acute denuding and delayed endocardial necrosis. Here we reported a rare case of delayed LV pseudoaneurysm confirmed by echocardiography and cardiac CT that developed on an inaudible steam pop site occurring during ablation for the treatment of VT originating from the papillary muscle of the LV. However, magnetic resonance imaging is thought to be more useful when considering the diagnosis and follow-up of

structural defects such as pseudoaneurysm. Serial imaging-based follow-up can facilitate the identification of pseudoaneurysms with delayed development, even when intraprocedural and short-term imaging-based follow-up confirms no procedure-related complications.

DATA AVAILABILITY STATEMENT

The original contributions presented in this study are included in the article/**Supplementary Material**, further inquiries can be directed to the corresponding author.

ETHICS STATEMENT

Written informed consent was obtained from the participant for the publication of this case report. Written informed consent was obtained from the participant for the publication of any potentially identifiable images or data included in this article.

AUTHOR CONTRIBUTIONS

MK and M-HL drafted the manuscript and were involved directly in treating the patient. YP provided figures and formalized the manuscript. HY, T-HK, J-SU, BJ, and H-NP reviewed the drafts and made contributions to proofreading. All authors approved the submitted version.

SUPPLEMENTARY MATERIAL

The Supplementary Material for this article can be found online at: https://www.frontiersin.org/articles/10.3389/fcvm.2022.887190/full#supplementary-material

Supplementary Figure 1 | Pre-procedural cardiac computed tomography short-axis **(A)** and 2-chamber **(B)** cines reveal no evidence of aneurysm or structural defect at baseline.

Supplementary Video 1 | Intracardiac echocardiography showing steam pops and termination of the ventricular tachycardia.

Supplementary Video 2 | A 2-month follow-up transthoracic echocardiographic view of the delayed left ventricular pseudoaneurysm.

REFERENCES

1. Stevenson WG, Wilber DJ, Natale A, Jackman WM, Marchlinski FE, Talbert T, et al. Irrigated radiofrequency catheter ablation guided by electroanatomic mapping for recurrent ventricular tachycardia after myocardial infarction: the multicenter thermocool ventricular tachycardia ablation trial. *Circulation.* (2008) 118:2773–82. doi: 10.1161/CIRCULATIONAHA.108.788604
2. Tokuda M, Kojodjojo P, Epstein M, Koplan BA, Michaud GF, Tedrow UB, et al. Outcomes of cardiac perforation complicating catheter ablation of ventricular arrhythmias. *Circ Arrhythm Electrophysiol.* (2011) 4:660–6. doi: 10.1161/CIRCEP.111.963413
3. Seiler J, Roberts-Thomson KC, Raymond JM, Vest J, Delacretaz E, Stevenson WG. Steam pops during irrigated radiofrequency ablation: feasibility of impedance monitoring for prevention. *Heart Rhythm.* (2008) 5:1411–6. doi: 10.1016/j.hrthm.2008.07.011
4. Koch KE, Raiszadeh F, Godelman A, Palma E, Forman R. Giant left ventricular pseudoaneurysm and myocardial dissection as a complication of multiple ventricular tachycardia ablations in a patient with cardiac sarcoidosis. *Clin Med Insights Cardiol.* (2015) 9:105–7. doi: 10.4137/CMC.S23863
5. Gill KS, Bansal RC, Pai S, Timothy P. Left ventricular pseudoaneurysm as a complication of electrophysiologic study. *J Am Soc Echocardiogr.* (2001) 14:228–30. doi: 10.1067/mje.2001.108540
6. Frances C, Romero A, Grady D. Left ventricular pseudoaneurysm. *J Am Coll Cardiol.* (1998) 32:557–61.
7. Mansour F, Basmadjian AJ, Bouchard D, Ibrahim R, Guerra PG, Khairy P. Images in cardiovascular medicine. Left ventricular pseudoaneurysm: a late complication of low-energy DC ablation. *Circulation.* (2006) 113:e780–1.
8. Hulten EA, Blankstein R. Pseudoaneurysms of the heart. *Circulation.* (2012) 125:1920–5.
9. Tuan J, Kaivani F, Fewins H. Left ventricular pseudoaneurysm. *Eur J Echocardiogr.* (2008) 9:107–9.
10. Nakagawa H, Yamanashi WS, Pitha JV, Arruda M, Wang X, Ohtomo K, et al. Comparison of in vivo tissue temperature profile and lesion geometry for radiofrequency ablation with a saline-irrigated electrode versus temperature control in a canine thigh muscle preparation. *Circulation.* (1995) 91:2264–73. doi: 10.1161/01.cir.91.8.2264

Conflict of Interest: The authors declare that the research was conducted in the absence of any commercial or financial relationships that could be construed as a potential conflict of interest.

frontiers | Frontiers in Cardiovascular Medicine

CASE REPORT
published: 04 July 2022
doi: 10.3389/fcvm.2022.935524

Paroxysmal Atrial Fibrillation Originating From the Inferior Vena Cava: A Case Report and Literature Review

*Yirao Tao, Donghui Yang and Liang Chen**

Department of Cardiology, The Second Affiliated Hospital of Dalian Medical University, Dalian, China

Atrial fibrillation is a common arrhythmia, but atrial fibrillation originating in the inferior vena cava is extremely rare. Here, we present a case of a 51-year-old woman with symptomatic paroxysmal atrial fibrillation, who was admitted to the Second Affiliated Hospital of Dalian Medical University and underwent radiofrequency ablation. The atrial fibrillation persisted despite pulmonary vein isolation. The inferior vena cava was then identified not only as a trigger but also as the driver to maintain atrial fibrillation, and tachycardia terminated successfully by discharging at the inferior vena cava. Furthermore, we performed a literature review of five previous case reports on this subject.

Keywords: atrial fibrillation, inferior vena cava, trigger, driver, catheter ablation

OPEN ACCESS

Edited by:
Rajeev Gupta,
Medicilinic, United Arab Emirates

Reviewed by:
Jaganmohan Tharakan,
Cardiologist Researcher India, India
Roddy Hiram,
Université de Montréal, Canada

***Correspondence:**
Liang Chen
panlongqi@163.com

Specialty section:
This article was submitted to Cardiac Rhythmology, a section of the journal Frontiers in Cardiovascular Medicine

Received: *04 May 2022*
Accepted: *15 June 2022*
Published: *04 July 2022*

Citation:
Tao Y, Yang D and Chen L (2022) Paroxysmal Atrial Fibrillation Originating From the Inferior Vena Cava: A Case Report and Literature Review. Front. Cardiovasc. Med. 9:935524. doi: 10.3389/fcvm.2022.935524

HIGHLIGHTS

- It is extremely rare for atrial fibrillation to originate from inferior vena cava. We present the first report to show inferior vena cava acts as both the trigger and the driver of atrial fibrillation using a three-dimensional imaging system.
- The electrocardiogram pattern of atrial tachycardia or premature atrial complex in individuals with paroxysmal atrial fibrillation originating from the inferior vena cava shows a narrow positive ectopic P wave in lead V1 and a negative ectopic P wave in inferior leads.
- Tachycardia terminates successfully by discharging at the inferior vena cava.

INTRODUCTION

Paroxysmal atrial fibrillation (AF) is mostly initiated by triggers (1), usually from pulmonary veins. Therefore, pulmonary veins disconnection is the cornerstone for paroxysmal AF ablation. Nevertheless, about 11% of cases of AF are elicited by other triggers (2). These triggers include the crista terminalis, the superior vena cava, the posterior wall of the left atrium, and the coronary sinus (CS) (2). Moreover, the Marshall buddle (3) and left atrial appendage (4) have also been implicated in AF initiation. The reports about AF raising from the inferior vena cava (IVC) are extremely rare.

We presented a case of paroxysmal AF originating in the IVC, in whom the tachycardia was successfully eliminated by discharging at IVC.

TABLE 1 | Baseline characteristics.

Baseline characteristics	
Sex	Female
Age, years	51
Weight, Kg	45
Height, cm	150
BMI, kg/m^2	20
Ethnicity	Asian
Hypertension	No
Diabetes	No
Coronary artery disease	No
Heart failure	No
Family history	No
Smoking	No
Alcohol	No
Atrial fibrillation duration, month	4
CHA_2DS_2-VASc score	1
HAS-BLED score	0
Antiarrhythmic drug	Propafenone
BNP, pg/mL	34.7
eGFR, mL/min. 1.73 m^2	>90

BMI, body mass index; BNP, B-type natriuretic peptide; eGFR, estimate glomerular filtration rate.

CASE PRESENTATION

A 51-year-old woman suffered from symptomatic paroxysmal AF with a 4-month history. Her AF episodes did not respond to treatment with propafenone, and then she was admitted to the Second Affiliated Hospital of Dalian Medical University. The baseline characteristics of this patient were presented in **Table 1**. Her admission electrocardiogram (ECG), echocardiography, physical examination, and blood test results were unremarkable. The surface ECG recorded when the patient experienced palpitations during hospitalization presented episodes of atrial tachycardia/atrial flutter with a negative atrial wave morphology in inferior leads (II, III, and avF), and narrow positive atrial wave morphology in lead V1 (**Figure 1**). The patient was diagnosed with paroxysmal AF, atrial flutter, and atrial tachycardia. The diagnostic assessment is shown in **Supplementary Table 1**. The patient participated in a discussion and was fully informed of the state of the illness and the possible benefits and risks of various treatments and then chose radiofrequency ablation.

The patient presented the sinus rhythm at the beginning of the radiofrequency ablation procedure. However, an AF episode started during the procedure of circumferential pulmonary veins isolation, and AF persisted after all four pulmonary veins were isolated. Tachycardia was able to terminate spontaneously, followed by several sinus beats; then, AF was triggered again by a premature atrial complex, which displayed a similar ECG appearance to atrial arrhythmia during palpitations recorded before the procedure—negative P wave in inferior leads and positive narrow P wave in lead V1 (**Figure 2**). Meanwhile, the CS catheter displayed a proximal-to-distal activation pattern, and the activation of the premature atrial complex on the CS catheter was not earlier than the P wave on surface ECG. Subsequently, the activation mapping procedure of the premature atrial complex in the right atrium was performed using a circular diagnostic catheter guided by the EnSite NavX system (St. Jude Medical, St. Paul, MN, United States). The superior vena cava showed passive conduction. The activation at the posteromedial wall of IVC was identified as the earliest activation, where rapid and disorganized electrical activities were recorded. Some of the electrical activities were conducted to the right atrium (IVC 9–10) and left atrium (CS) and drove tachyarrhythmia (**Figure 3A**). AF terminated immediately after radiofrequency ablation was performed at the earliest activation site, with a target temperature of 43°C, a maximal power of 40 W, and a flow rate of 20 mL/min (**Figure 3B**). Adenosine triphosphate infusion did not induce any atrial arrhythmia.

The patient has remained asymptomatic following the session without any need for antiarrhythmic drugs and no ECG evidence of tachycardia during the 2-month follow-up.

DISCUSSION

It has been established that pulmonary veins are the most common site for initiation of AF. Herein, we presented a case of paroxysmal AF originating from a very unusual location, such as the posteromedial wall of IVC. The earliest activation of the premature atrial complex which induced AF was located at the posteromedial wall of IVC by three-dimensional mapping systems, suggesting that the IVC triggered of AF. The electrical activity recorded in IVC during AF was significantly faster than in the atrium, and focal ablation of earliest atrial activation in IVC immediately terminated AF, suggesting that the IVC was also responsible for the maintenance of AF.

To the best of our knowledge, five previous reports have described AF originating from the IVC, and their baseline characteristics are summarized in **Table 2** (5–9). These five case reports included six patients, aged from 22 to 83 years, and the follow-up time was from 2 to 14 months. All of the patients were free of AF during the follow-up. The majority of the cases underwent first-time AF ablation, except for a recent report (9) of a recurrent AF despite two previous AF ablations. The role of the IVC differed among these reports: it acted as the trigger in three reports and both as the trigger and the driver in two reports. Four of the five reports were published before 2010, and manipulation was mainly performed under fluoroscopy guidance. Because of the limited accuracy of fluoroscopy guidance, it is challenging to distinguish the IVC from adjacent origin locations, such as the CS ostium. Until 2021, Alonso-Martín et al. reported a case of AF originating from the IVC under three-dimensional electroanatomic mapping systems navigation (9).

In a histological study from two cadavers in 1995, Hashizume et al. (10) reported that the IVC included both smooth and cardiac muscle fibers covering a length of 18 mm from the right atrium. They demonstrated that the cardiac muscle fibers in the IVC were more plentiful in the anterior aspect than in the posterior aspect. Interestingly, in our case and most of the previous cases (5, 6, 8, 9) in which AF originated in the IVC,

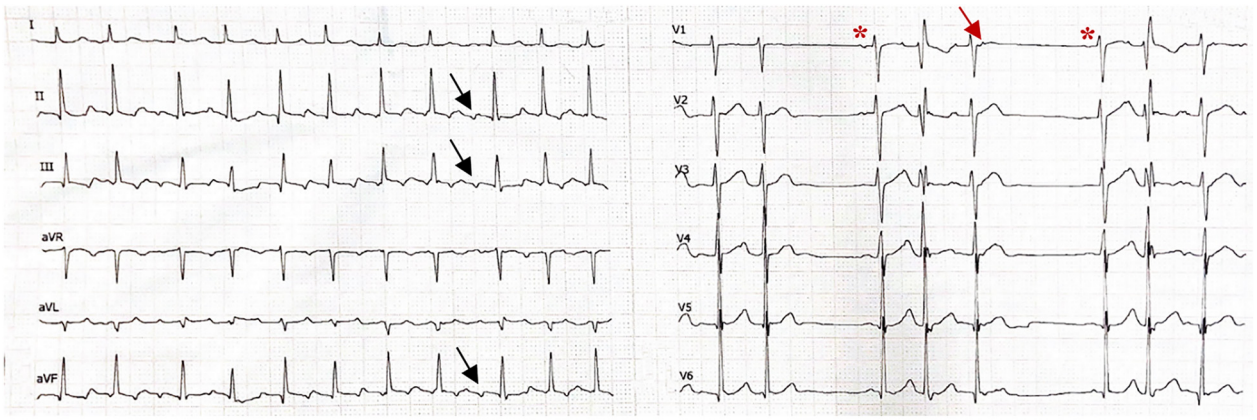

FIGURE 1 | Electrocardiogram showing atrial flutter with atrial rate 280–290/min with variable atrioventricular conduction in the limb leads, the atrial wave displayed negative wave in inferior leads (II, III, and avF, black arrow). The precordial 6 lead rhythm strip shows termination of atrial flutter with a sinus beat (red asterisk), followed by four consecutive ectopic atrial beats at rate 250/min, which showed a narrow positive wave in lead V1 (red arrow). The first conducted beat occurred with the right brunch block, the second was blocked, the third conducted a with a narrow QRS, and the fourth was blocked. This followed by another sinus beat followed by the same atrial tachycardia/atrial flutter at a rate of 260/min. The ECG was recorded at a speed of 25 mm/s (x axis) and an amplitude of 10 mm/mV (y axis).

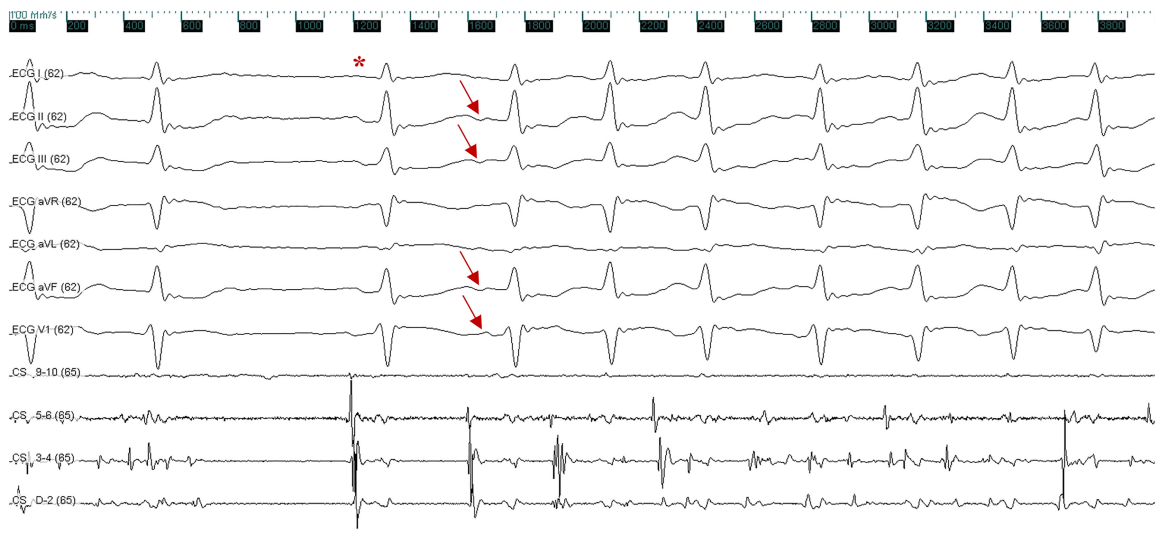

FIGURE 2 | Surface and intracardiac electrocardiogram indicate the termination of atrial fibrillation, followed by a sinus beat (red asterisk); atrial fibrillation was triggered again by a premature atrial complex, which exhibited a negative P wave in inferior leads (II, III, and aVF) and a positive P wave in lead V1 (red arrow). The ECG was recorded at a speed of 100 mm/s. X axis, time line; y axis: gain. CS, coronary sinus; ECG, electrocardiogram.

the posterior wall was identified as the trigger. It is unknown whether this is just an accidental phenomenon or there are differences in electrical activity properties between the anterior and posterior IVC sleeves. Further investigations are required to clarify this issue.

The ECG features of ectopic P wave from the IVC were clearly visible in three of the above five reports. The ECG from our case presented a negative ectopic P wave in inferior leads, which is in line with these three cases (6, 7, 9), and the complete or dominant positive ectopic P wave in lead V1 was consistent with two of the cases (6, 9). Furthermore, all available ECG recordings displayed a narrow ectopic P wave. Several studies have demonstrated a narrow positive P wave in lead V1, suggesting that the trigger originates from the right pulmonary vein (11, 12). However, deeper inversion of P wave in inferior leads was rare even the trigger originates from the right inferior pulmonary vein. Considering that the anatomical location of the IVC is nearby the right inferior pulmonary vein but lower, we suggest that the ECG features described above may indicate the ectopic P wave originating from the IVC.

The IVC ablation schemes were not consistent among the past five case reports. In two cases (5, 8), focal ablation (like in our case) was chosen; in one case (6), IVC isolation was selected; and in two cases (7, 9), radiofrequency was applied in addition to target ablation, consequently achieving IVC isolation. All of the above patients were free of AF during the

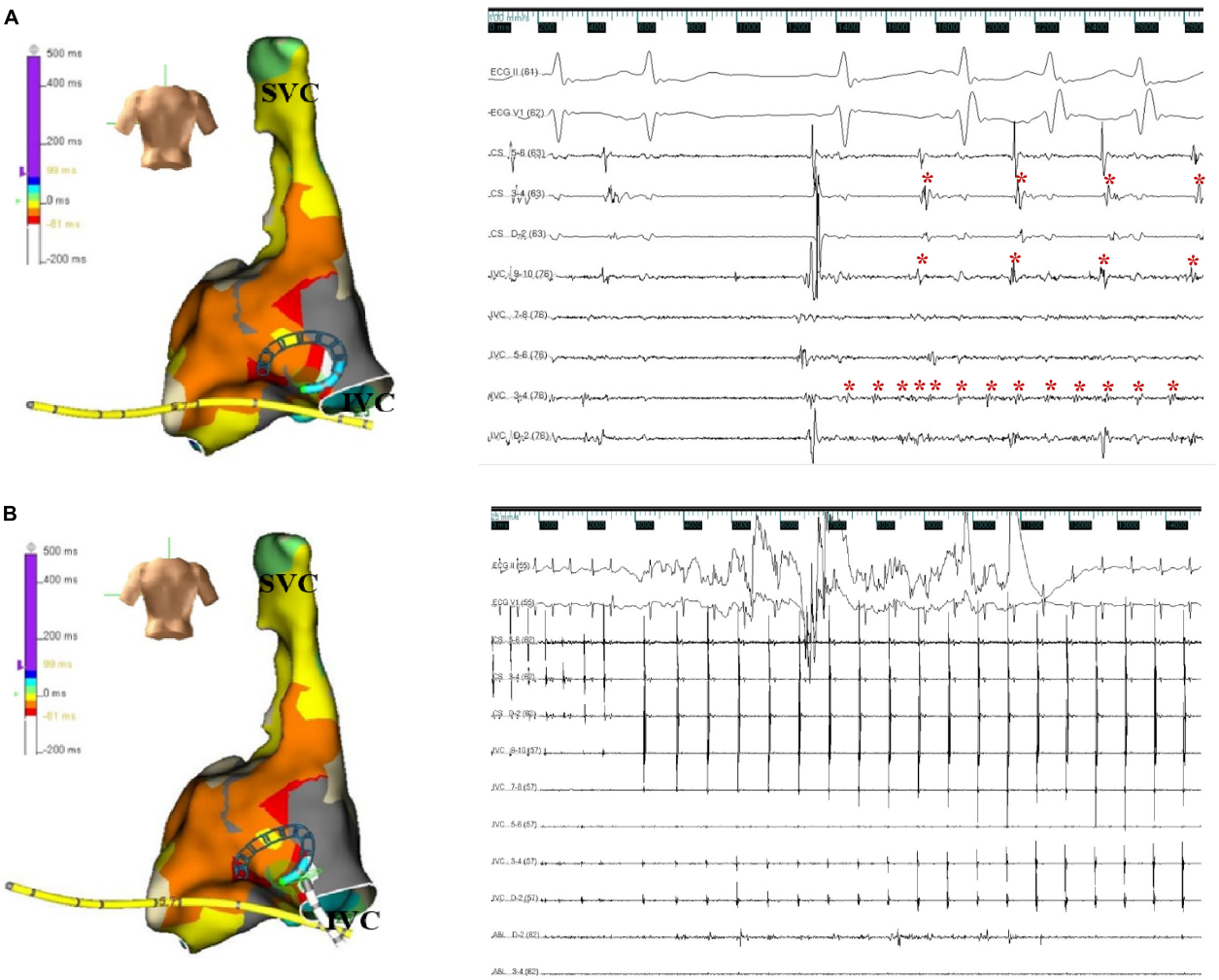

FIGURE 3 | (A) Activation map and electrograms. Activation mapping shows that the earliest activity was at the posteromedial wall of the inferior vena cava. The intracardiac electrocardiogram indicates rapid discharges from the inferior vena cava; some of them were conducted to the right atrium (IVC 9-10) and left atrium (CS). The red asterisk represents the electrical activation recorded by the electrode. The ECG was recorded at a speed of 100 mm/s. **(B)** Successful ablation site. Atrial fibrillation terminated immediately after radiofrequency ablation at the earliest activation site in the posteromedial inferior vena cava. The ECG was recorded at a speed of 25 mm/s. X axis, time line; y axis, gain. CS, coronary sinus; ECG, electrocardiogram; IVC, inferior vena cava; SVC, superior vena cava.

TABLE 2 | Baseline characteristics of previous case reports.

References	Year	Age	Sex	Target location of IVC	Surface ECG feature of ectopic P wave	PVI	Imaging	IVC role	IVC ablation schemes	Follow-up
Mansour et al. (5)	2002	22/60	Male/ female	Posterolateral ostium	NA	No	3-D	Trigger	Foci ablation	2 months/ 9 months
Scavée et al. (6)	2003	44	NA	Posteromedial wall	Negative P wave in leads II, III, avF, and V1	Yes	Fluoroscopy	Trigger	IVC disconnection	14 months
Yamane et al. (7)	2005	57	Male	Anteromedial ostium	Negative P wave in leads II and III, and positive P wave in lead V1	No	Fluoroscopy	Trigger and driver	Foci ablation and IVC disconnection	12 months
Mizobuchi et al. (8)	2006	83	Female	Posterior wall	NA	No	Fluoroscopy	Trigger and driver	Foci ablation	12 months
Alonso-Martín et al. (9)	2021	47	Male	Posteromedial aspect	Negative P wave in inferior leads and positive P wave in lead V1	Yes	3-D	Trigger	Foci ablation and IVC disconnection	6 months

3-D, 3-dimensional; ECG, electrocardiogram; IVC, inferior vena cava; NA, not available; PVI, pulmonary vein isolation.

follow-up without complications. Because of the difference in anatomy and adjacent structures, the ablation strategies between non-pulmonary vein and pulmonary vein foci are different (13). The optimum ablation scheme of AF originating from the IVC remains unknown because of the limited experience, and it requires further studies.

To the best of our knowledge, this is the first report to show that IVC acts as both the trigger and the driver of AF using a three-dimensional imaging system. One limitation in the present study was that no intracardiac echocardiography or high-density mapping catheters were used. These tools may provide a more accurate assessment of the anatomical structure and more precise activation conduction mapping.

CONCLUSION

We presented an extremely rare case of paroxysmal AF originating in the IVC. Moreover, we performed a literature review of five previous case reports on this subject. AF originating in the IVC is mostly initiated at the posterior wall of the IVC, and the role of the IVC is not only that of the trigger but also of the driver. The ECG pattern of AT or premature atrial complex in individuals with paroxysmal AF originating from the IVC shows a narrow positive ectopic P wave in lead V1 and a negative ectopic P wave in inferior leads. Tachycardia terminates successfully by discharging at the IVC.

DATA AVAILABILITY STATEMENT

The original contributions presented in this study are included in the article/**Supplementary Material**, further inquiries can be directed to the corresponding author/s.

ETHICS STATEMENT

Written informed consent was obtained from the participant for the publication of this case report. Written informed consent was obtained from the individual(s) for the publication of any potentially identifiable images or data included in this article.

AUTHOR CONTRIBUTIONS

YT, LC, and DY conceived the study. YT drafted the manuscript. LC and DY checked it and performed critical revision. All authors contributed to the article and approved the submitted version.

SUPPLEMENTARY MATERIAL

The Supplementary Material for this article can be found online at: https://www.frontiersin.org/articles/10.3389/fcvm.2022.935524/full#supplementary-material

REFERENCES

1. Margulescu AD, Mont L. Persistent atrial fibrillation vs paroxysmal atrial fibrillation: differences in management. *Expert Rev Cardiovasc Ther.* (2017) 15:601–18. doi: 10.1080/14779072.2017.1355237
2. Santangeli P, Zado ES, Hutchinson MD, Riley MP, Lin D, Frankel DS, et al. Prevalence and distribution of focal triggers in persistent and long-standing persistent atrial fibrillation. *Heart Rhythm.* (2016) 13:374–82. doi: 10.1016/j.hrthm.2015.10.023
3. Lador A, Valderrábano M. Atrial fibrillation ablation using vein of marshall ethanol infusion. *Methodist Debakey Cardiovasc J.* (2021) 17:52–5. doi: 10.14797/zqme8581
4. Di Biase L, Burkhardt JD, Mohanty P, Sanchez J, Mohanty S, Horton R, et al. Left atrial appendage: an underrecognized trigger site of atrial fibrillation. *Circulation.* (2010) 122:109–18. doi: 10.1161/circulationaha.109.928903
5. Mansour M, Ruskin J, Keane D. Initiation of atrial fibrillation by ectopic beats originating from the ostium of the inferior vena cava. *J Cardiovasc Electrophysiol.* (2002) 13:1292–5. doi: 10.1046/j.1540-8167.2002.01292.x
6. Scavée C, Jaïs P, Weerasooriya R, Haïssaguerre M. The inferior vena cava: an exceptional source of atrial fibrillation. *J Cardiovasc Electrophysiol.* (2003) 14:659–62. doi: 10.1046/j.1540-8167.2003.03027.x
7. Yamane T, Miyazaki H, Inada K, Matsuo S, Miyanaga S, Date T, et al. Focal source of atrial fibrillation arising from the ostium of the inferior vena cava. *Circ J.* (2005) 69:756–9. doi: 10.1253/circj.69.756
8. Mizobuchi M, Enjoji Y, Shibata K, Funatsu A, Yokouchi I, Kambayashi D, et al. Case report: focal ablation for atrial fibrillation originating from the inferior vena cava and the posterior left atrium. *J Interv Card Electrophysiol.* (2006) 16:131–4. doi: 10.1007/s10840-006-9037-1
9. Alonso-Martín C, García Mancebo S, Campos García B, Guerra Ramos J, Moreno Weidman Z, Méndez Zurita F, et al. Atrial fibrillation originating in the inferior vena cava: a typical presentation of an atypical location. *JACC Case Rep.* (2021) 3:1918–23. doi: 10.1016/j.jaccas.2021.11.001
10. Hashizume H, Ushiki T, Abe K. A histological study of the cardiac muscle of the human superior and inferior venae cavae. *Arch Histol Cytol.* (1995) 58:457–64. doi: 10.1679/aohc.58.457
11. Kistler PM, Roberts-Thomson KC, Haqqani HM, Fynn SP, Singarayar S, Vohra JK, et al. P-wave morphology in focal atrial tachycardia: development of an algorithm to predict the anatomic site of origin. *J Am Coll Cardiol.* (2006) 48:1010–7. doi: 10.1016/j.jacc.2006.03.058
12. Yamada T, Murakami Y, Muto M, Okada T, Okamoto M, Toyama J, et al. Electrophysiologic characteristics of atrial tachycardia originating from the right pulmonary veins or posterior right atrium: double potentials obtained from the posterior wall of the right atrium can be useful to predict foci of atrial tachycardia in right pulmonary veins or posterior right atrium. *J Cardiovasc Electrophysiol.* (2004) 15:745–51. doi: 10.1046/j.1540-8167.2004.03513.x
13. Higa S, Lo LW, Chen SA. Catheter ablation of paroxysmal atrial fibrillation originating from non-pulmonary vein areas. *Arrhythm Electrophysiol Rev.* (2018) 7:273–81. doi: 10.15420/aer.2018.50.3

Conflict of Interest: The authors declare that the research was conducted in the absence of any commercial or financial relationships that could be construed as a potential conflict of interest.

frontiers | Frontiers in Cardiovascular Medicine

TYPE Case Report
PUBLISHED 18 August 2022
DOI 10.3389/fcvm.2022.938735

OPEN ACCESS

EDITED BY
Matteo Anselmino,
University of Turin, Italy

REVIEWED BY
Federico Migliore,
University of Padua, Italy
Ewa Jędrzejczyk-Patej,
Silesian Center for Heart Disease, Poland
Mohamed Yassin,
University of Pittsburgh, United States
Richard Gary Trohman,
Rush University, United States

*CORRESPONDENCE
Ju-Yi Chen
juyi@mail.ncku.edu.tw

SPECIALTY SECTION
This article was submitted to Cardiac Rhythmology, a section of the journal Frontiers in Cardiovascular Medicine

RECEIVED 08 May 2022
ACCEPTED 25 July 2022
PUBLISHED 18 August 2022

CITATION
Lo S-W and Chen J-Y (2022) Case report: A rare complication after the implantation of a cardiac implantable electronic device: Contralateral pneumothorax with pneumopericardium and pneumomediastinum. *Front. Cardiovasc. Med.* 9:938735. doi: 10.3389/fcvm.2022.938735

Case report: A rare complication after the implantation of a cardiac implantable electronic device: Contralateral pneumothorax with pneumopericardium and pneumomediastinum

Shao-Wei Lo and Ju-Yi Chen*

Department of Internal Medicine, College of Medicine, National Cheng Kung University Hospital, National Cheng Kung University, Tainan, Taiwan

Cardiac implantable electronic devices (CIED) including pacemakers (PM), implantable cardioverter defibrillators (ICD), and cardiac resynchronized therapy (CRT) have become the mainstay of therapy for many cardiac conditions, consequently drawing attention to the risks and benefits of these procedures. Although CIED implantation is usually a safe procedure, pneumothorax remains an important complication and may contribute to increased morbidity, mortality, length of stay, and hospital costs. On the other hand, pneumopericardium and pneumomediastinum are rare but potentially fatal complications. Accordingly, a high degree of awareness about these complications is important. Pneumothorax almost always occurs on the ipsilateral side of implantation. The development of contralateral pneumothorax is uncommon and may be undetected on an initial chest radiograph. Contralateral pneumothorax with concurrent pneumopericardium and pneumomediastinum is much rarer. We describe a rare case of concurrent right-sided pneumothorax with pneumopericardium and pneumomediastinum after left-sided pacemaker implantation and highlight the risk factors, management, and possible ways to prevent the complications.

KEYWORDS

contralateral pneumothorax, pneumopericardium, pneumomediastinum, cardiac implantable electronic device, pacemaker

Introduction

Cardiac implantable electronic devices (CIED) including pacemakers (PM), implantable cardioverter defibrillators (ICD), and cardiac resynchronized therapy (CRT) have become the mainstay of therapy for many cardiac conditions, consequently drawing attention to the risks and benefits of these procedures (1, 2). Although CIED

implantation is usually safe, pneumothorax has been reported to occur in 0.51–2.24%, however this reported incidence may have been overestimated (3). In recent years, many CIED implantations have moved to outpatient settings. Outpatient CIED implantations are not included in the National Inpatient Sample (NIS) database, which is the largest publicly available all-payer inpatient care database in the United States. Since the subgroup of outpatients who developed CIED-associated pneumothorax and were later hospitalized (included in the NIS, while outpatients without pneumothorax were not), the NIS database incidence of pneumothorax may have been artificially elevated (an accurate numerator with a falsely low denominator) (3). Furthermore, it seems likely that improved medical knowledge and the development of safer procedures, would have reduced the incidence of pneumothorax over time (3). Nevertheless, pneumothorax remains an important complication of CIED implants and may contribute to increased morbidity, mortality, length of stay, and hospital costs, especially when a chest tube is required (4–7). On the other hand, pneumopericardium and pneumomediastinum are rare but potentially fatal complications (8). Accordingly, a high degree of awareness about these complications is important.

Pneumothorax almost always occurs on the ipsilateral side of implantation. The development of contralateral pneumothorax is uncommon and may be undetected on an initial chest radiograph (9, 10). Contralateral pneumothorax with concurrent pneumopericardium and pneumomediastinum is much rarer (11). We describe a rare case of concurrent right-sided pneumothorax with pneumopericardium and pneumomediastinum after left-sided pacemaker implantation and highlight the risk factors, management, and possible ways to prevent these complications.

Case presentation

A 76-year-old man underwent dual-chamber permanent pacemaker (PPM) implantation due to sick sinus syndrome. He was 173 cm in height, 59 kg in weight, and had a body mass index (BMI) of 20 kg/m^2. He had a past medical history of heavy smoking, paroxysmal atrial fibrillation, coronary atherosclerosis, and bilateral pulmonary emphysema.

A dual-chamber pacemaker (BIOTRONIK EVIA DR) was inserted using active fixation leads (Biotronik Solia S60, Biotronik Solia S53) through the left subclavian vein into the right ventricular outflow tract (RVOT) and the right atrial appendage respectively. At implantation, the parameters of the pacemaker were satisfactory. The atrial lead pacing threshold was 0.6 V at 0.4 ms and the impedance was 532 Ω. The sensed P wave was 2.3 mV. The pacing threshold of the ventricular lead was also appropriate measuring 0.4 V at 0.4 ms and the impedance 661 Ω. The sensed R wave was 11.2 mV.

The implantation procedure was completed uneventfully. Two h after the implantation, the chest radiographs revealed acceptable lead positions and no evidence of pneumothorax. There was no pericardial effusion on echocardiography. About 5 h after the procedure, the patient suddenly reported dyspnea, severe headache, neck stiffness, and shoulder pain. A chest X-ray (CXR) revealed a 3.5 cm right-sided apical pneumothorax as well as small amounts of gas as linear or curvilinear lucencies in the mediastinum, indicating pneumomediastinum. Non-contrast computed tomography (CT) of the chest showed bilateral emphysema, right-sided pneumothorax with pneumopericardium and pneumomediastinum, a small right-sided pleural effusion, and the atrial lead crossing the cardiac contour, suggesting lead perforation through the pericardium and directly into the pleural cavity (Figure 1).

The patient's symptoms improved significantly after receiving high-flow oxygen through a nasal cannula. Nevertheless, the follow-up CXR showed no improvement. The patient, therefore, underwent insertion of a small-bore pigtail chest drain on the 3rd day, evacuating more than 80 ml of air. Serial CXRs showed significant improvement in the pneumopericardium and gradual resolution of the pneumothorax over the next few days. The electrocardiogram (ECG) showed no abnormal changes suggesting lead displacement, and interrogation of the pacemaker parameters remained fine with no significant alterations in the pacing thresholds, sensing or impedance. It was decided to leave the atrial lead in place.

During several days of in-hospital observation, the patient remained stable with no breathing difficulties, pleuritic chest discomfort, or pericardial signs and symptoms. The pigtail was then removed on day 6. The CXR verified the complete resolution of the pneumothorax and pneumopericardium before the patient was discharged on day 8. Since discharge, we have followed up on his signs and symptoms, pacemaker parameters, and ECG. The patient has remained stable for 15 months, and the pacemaker parameters and ECG have demonstrated no abnormalities.

Discussion

Mechanisms of ipsilateral/contralateral pneumothorax with concurrent pneumopericardium/pneumomediastinum

Ipsilateral pneumothorax is commonly caused by needle penetration of the pleura during venous access (Figure 2) (5, 10, 12–14). Concurrent pneumopericardium and pneumomediastinum can occur when the leaking air

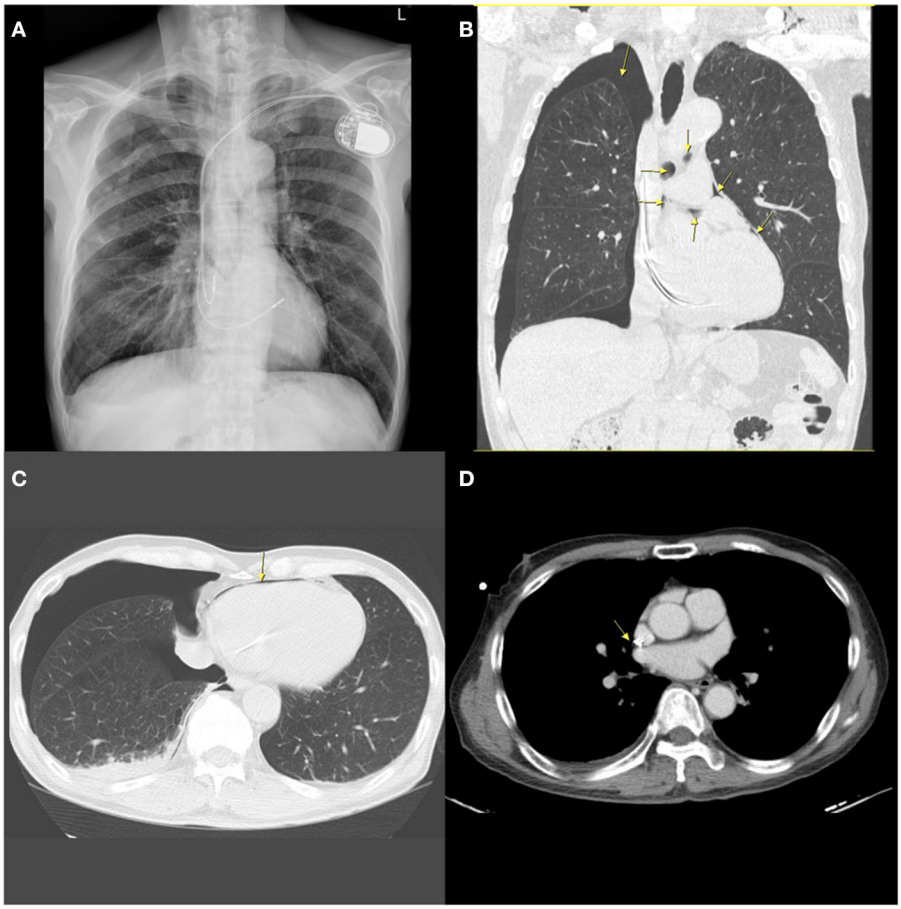

FIGURE 1
A chest radiograph performed 5 h after implantation showing contralateral pneumothorax, pneumopericardium, and pneumomediastinum. **(A)** Posterior-anterior (PA) chest X-ray demonstrating contralateral pneumothorax and mild pneumomediastinum. **(B)** Coronal chest non-contrast computed tomography (CT) scan image showing right-sided pneumothorax, pneumomediastinum, and pneumopericardium (arrows). **(C)** Horizontal CT image showing pneumopericardium (arrow) and pneumothorax. **(D)** Horizontal slices of CT scan suggesting possible extrusion of the atrial lead through the right atrium (arrow).

passes through the lung parenchyma along the perivascular sheaths to the hilum and the mediastinum (15, 16). At its reflection enclosing the ostia of the pulmonary veins, the pericardium is most fragile, and air can thus pour into the pericardial cavity.

There are two potential causes of contralateral pneumothorax and pneumopericardium. One is that the active fixation lead protrudes through the right atrium injuring the pericardium and right pleura (16). Another one could be incidental venous puncture of the right pleura while using the Seldinger technique to insert a dilator and sheath (17). An injury to the superior vena cava (SVC) near the pericardium could allow air (blood and/or intravenous fluid) to leak into the pericardial space through a congenital pericardial defect or tiny pleuro-pericardial fistulas (11).

Risk factors for atrial lead protrusion and venous perforation

Complications from pacemaker implantation are 30% more likely in females than in males (3). The incidence of both venipuncture related injury and cardiac perforation is higher in patients with bullous emphysema, chronic obstructive pulmonary disease (COPD), congenital defects such as persistent left superior vena cava, age >80 years, Caucasian ethnicity, steroid treatment within 7 days, anticoagulant and antiplatelet therapy, urgent surgery, low BMI (<18.5), or agitation (1, 8, 15, 18–20). Prior procedures, operation (such as sternotomies), trauma, or irradiation therapy in the affected area, clavicle/chest deformity, and previous fractures, are all significant risk factors. Difficult or lengthy procedures, large

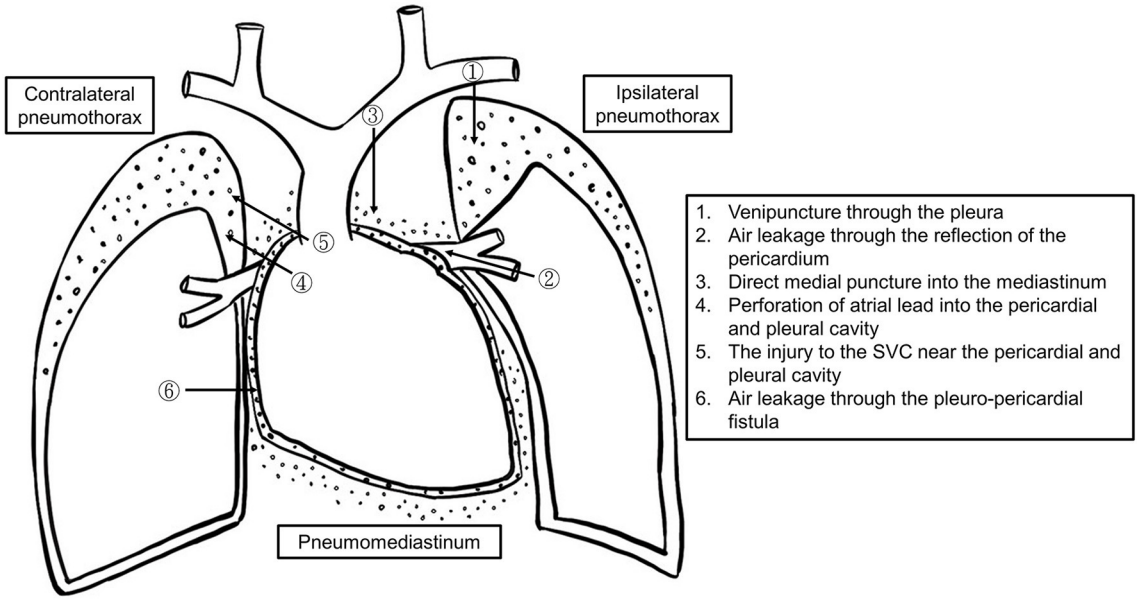

FIGURE 2
The schematic diagram of the mechanisms of pneumothorax, pneumopericardium, and pneumomediastinum formation.

diameter (≥12 French) sheaths, more than one attempt at venipuncture, implantation of multiple electrodes, and a dual-chamber device (versus a single chamber device), are all linked to a higher risk for complications (1, 12, 14, 18, 21).

In comparison to passive fixation leads, active fixation leads provide several benefits, such as simple fixation, the capacity to be deployed at alternate pacing sites with ideal pacing and sensing parameters, decreased rates of dislodgement, and they are easier to extract (22). Because of these advantages, they are more frequently employed. Nevertheless, active fixation and over-screwing increase the risk of perforation (8, 16, 17, 20). Lead and helix design also play a role, particularly in the case of magnetic resonance imaging (MRI) compatible leads due to their greater diameter and stiffness (20). As a result, these active fixation leads should be implanted cautiously. Anatomic variations, such as multilobed or a thin-walled atrial appendage, fatty infiltration of the myocardium due to myotonic dystrophy, ischemic and dilated cardiomyopathy, are variables that increase the likelihood of atrial perforation (10, 11, 13, 15, 20, 23–29).

The mechanism and risk factors in our case

In our case, there were no apparent problems throughout the procedure. Over-screwing of the atrial lead seems unlikely because the requisite number of clockwise turns were performed under fluoroscopic guidance. Importantly, our patient had several risk factors including a history of longstanding smoking with bilateral emphysema. These risk factors increased the risk of pneumothorax. However, non-contrast chest CT raised suspicion of atrial lead perforation. Thus, we hypothesized that the atrial lead protruded through the pericardium directly into the pleural cavity, causing contralateral pneumothorax with concurrent pneumomediastinum and pneumopericardium.

Diagnosis of lead perforation and CIED-associated pneumothorax

A patient can manifest signs and symptoms during the procedure or up to 72 hours after implantation (20). Every patient should receive a chest x-ray within 4 h post-procedure (30). Patients discharged from the hospital shortly after outpatient procedures should remain in contact with the CIED center (17).

In concerning cases, fluoroscopy, chest CT with three-dimensional reconstruction, and echocardiography assist in diagnosing lead perforation (13, 31); however, they are not as sensitive for tiny perforation (15, 19, 23, 32). ECG-gated high-resolution CT (HRCT) remains the diagnostic gold standard although the perforation may be over-diagnosed (19, 25, 27). To

reduce imaging distortions caused by heart motion, prospective ECG triggering and retrospective ECG gating methods are introduced (33). Prospective ECG triggering, for instance, allows the ECG signal to regulate scanning such that projection data is only collected during diastole, which is the period of the least amount of cardiac movement. Thus, HRCT maximizes spatial resolution and results in optimal delineation of the myocardium, blood, and fat interfaces (19). HRCT also aids in lead retrieval planning because it provides a reliable estimation of the orientation of important structures around the misplaced lead (23, 32).

The management of CIED-associated pneumothorax

The management depends on the presence or absence of symptoms, the hemodynamic condition, and the extent of the lesions. Although the American College of Chest Physicians (ACCP) proposed guidelines for the management of spontaneous pneumothorax (34), which were updated by the British Thoracic Society (BTS) (35), there is no consensus on the management of iatrogenic pneumothorax, let alone CIED-induced pneumothorax. We propose a flow chart for the management of CIED-associated pneumothorax (Figure 3), which was adapted from the recommended treatment for iatrogenic pneumothorax (36).

High flow (10 L) 100% nasal oxygen, which theoretically accelerates air absorption, is generally recommended as the first step despite conflicting evidence suggesting that it has probably no effect on large pneumothoraces (13, 37, 38). A clinically stable patient with a small pneumothorax (<20%) can be observed since it may resolve on its own (12, 36). After 12–24 h, further imaging should be acquired (36). If the pneumothorax is enlarging or once symptoms worsen, drainage should be considered (36).

Needle or cannula aspiration is advocated for patients with a small (<20%) pneumothorax, minimal symptoms, and no previous parenchymal disease (36). If the patients are asymptomatic after aspiration, and repeat imaging shows resolution of the pneumothorax or no progression, they can be discharged with a 48-h follow-up (36). However, observation alone may sufficient for small iatrogenic pneumothoraces. Of note, evacuated volumes >543 mL indicate the need for further intervention with a chest tube (39).

Patients with a large (>20%) pneumothorax or those presenting moderate-to-severe symptoms should be treated with a chest tube (12–16 French) for at least 24 h (11–13, 36). If the pneumothorax improves, the absence of an air leak should be confirmed before the chest tube is removed (36). Even though a pneumothorax appears to be resolved on imaging, there may still be an air leak, which is masked by an equilibrium between the air evacuation and the air flowing into the lung through the site of puncture (36). The removal of the chest tube under this condition may lead to the reoccurrence of the pneumothorax (36).

In the majority of pneumothoraces, air leakage will stop <48 h after the placement of a chest tube (40, 41). For patients with a persistent gas leak for more than 48 h, consulting a cardiothoracic surgeon or an interventional pulmonologist is recommended (42).

Consideration of lead extraction and repositioning

The symptoms, imaging findings, and lead parameters are used to determine if lead extraction or repositioning is necessary (Figure 4). The lead parameters usually alter following a lead perforation (43); however, they may remain unchanged, and the patient may be asymptomatic in certain circumstances (8, 11, 13, 20, 31). The proper management of asymptomatic lead perforation is still up for debate. Despite the uncertainty, it is generally suggested the lead be extracted or repositioned because there is a chance that it will perforate the surrounding structures over time, causing catastrophic harm (27, 28, 31, 44).

Transvenous lead extraction is effective and safe management in the majority of cases. It is conducted under fluoroscopic guidance with echocardiographic and hemodynamic monitoring. Additional precautions such as placement of a pericardial drain for emergent pericardiocentesis and having cardiac surgeons on standby help assure procedural safety (15, 23, 25, 27, 28, 31, 45). Postprocedural follow-up is recommended due to the risks of constrictive pericarditis and infections (31).

Atrial lead extraction is not always required. When there is an improvement in the pneumothorax, no pericardial effusion, minimal symptoms, and satisfactory lead parameters, it is preferable to keep the electrode in place until the fibrous tissue thickens and/or wraps around the helix, especially in the elderly and weak patients who are at higher risk for complications associated with lead extraction or repositioning. It should be noted that this strategy's long-term effectiveness is unverified (11, 46).

Prevention during venipuncture

Figure 5 provides a clinical algorithm for early identification of individuals at high risk and appropriate preventative measures.

The subclavian vein has served as the most widely used venous access for CIEDs (47). In a patient with risk factors venography is recommended prior to subclavian vein puncture.

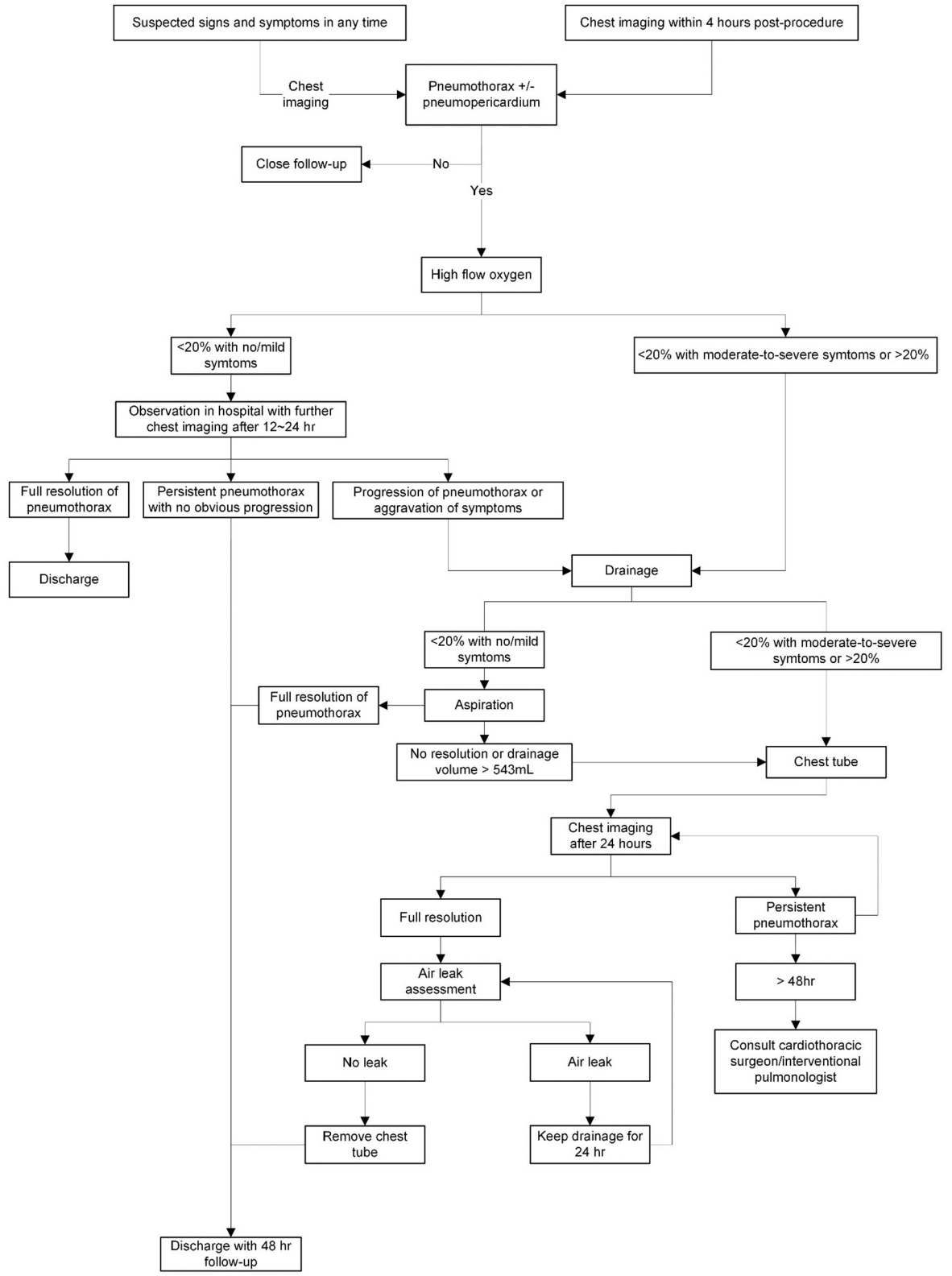

FIGURE 3
The management of cardiac implantable electronic device (CIED)-induced pneumothorax and concurrent pneumopericardium.

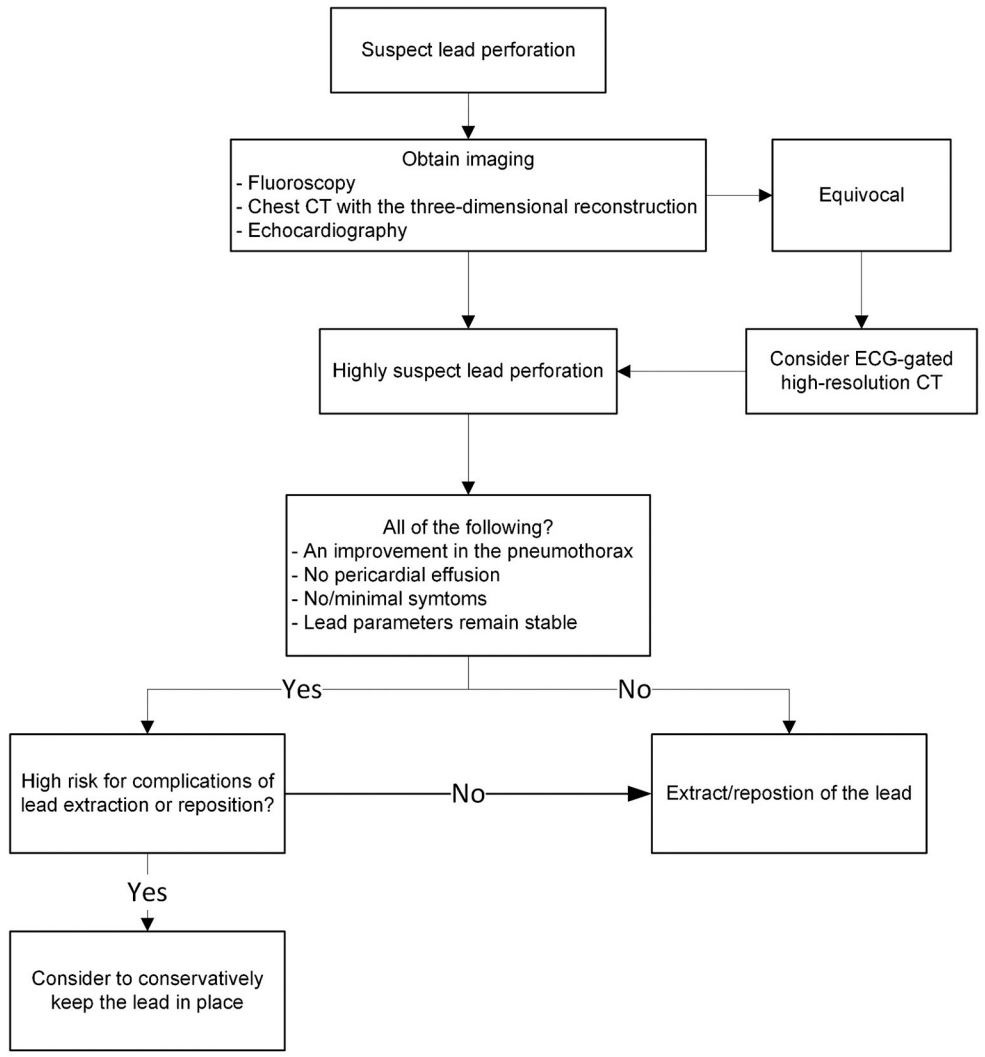

FIGURE 4
The evaluation of the need for lead extraction or repositioning.

Ultrasound guidance and/or fluoroscopic guidance may also be useful (48, 49). In a patient with unilateral pulmonary lesions, it's preferred to use the subclavian approach on the ipsilateral side of the diseased lung since there may be less severe complications (13). When venous access is not possible to establish, particularly after exhaustively looking for the subclavian vein on a specific side, the pacemaker-implanting physicians should rule out pneumothorax before shifting to the opposite side (13).

In terms of preventing pneumothorax, axillary venous access or cephalic vein cut-down is better than the subclavian vein approach (18, 47). The cephalic vein cut-down technique has been well-recognized for fewer occurrences of pneumothorax (50); however, the axillary approach is still not widely used due to inadequate training and a lack of familiarity (51).

Axillary vein access decreases the risk of complications due to its extra-thoracic anatomic location (52). Although "blind" puncture using anatomical landmarks is common, it is constrained by the variable relationship between the first rib and the axillary vein. About 5% of patients need a contrast-guided technique due to anatomical variations (52–54). As a result of inexperience, failed attempts, probable complications, and radiation exposure for both patients and physicians unavoidably increase (55).

Ultrasound guidance provides a direct view of the vessel, allowing the operator to monitor the needle's passage onto the subcutaneous tissue, assessing the depth of the vein, and preventing accidental arterial puncture, thus minimizing the probability of complications (52). A

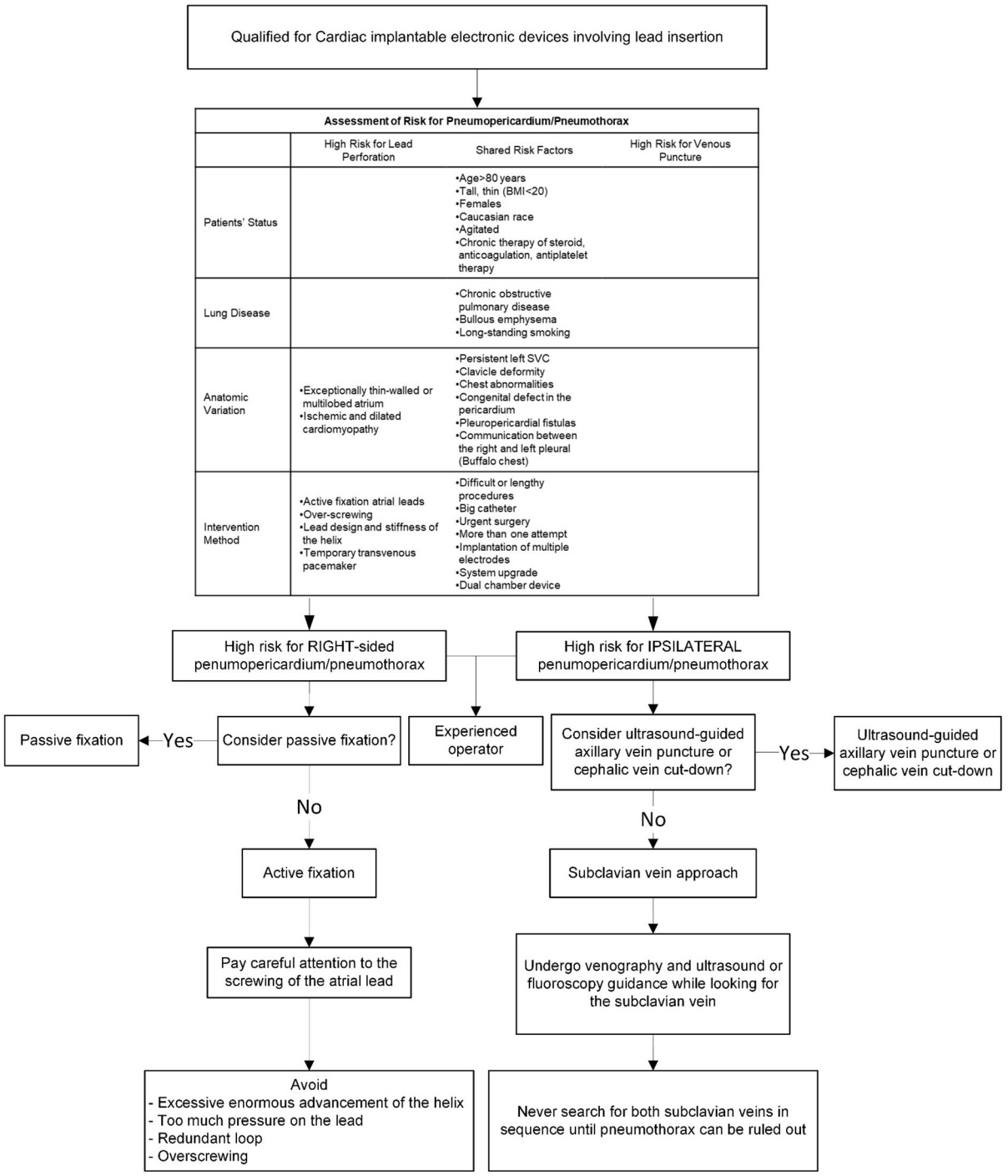

FIGURE 5
A clinical algorithm for early identification of patients at high risk of developing pneumothorax or pneumopericardium and corresponding preventive measures.

randomized clinical trial demonstrated that even when carried out by inexperienced operators, the ultrasound-guided axillary vein technique was much superior to cephalic vein cut-down (47). Therefore, we suggest ultrasound-guided axillary venous access as the preferred choice for CIED implantation.

Conclusion

This case highlights the risks of pneumothorax and pneumopericardium associated with CIEDs, as well as the recommended treatment. Operators should be aware of these potential, unusual complications and precautions that can be taken to avoid them. However, there is currently no definitive guidance on the management of CIED-associated pneumothorax or pneumopericardium. We recommend more multicenter randomized, trials to compare conservative vs. invasive therapy for CIED-associated pneumothorax of varying severity and to compare the long-term outcome between conservative management and lead extraction in patients with asymptomatic lead perforation.

Data availability statement

The raw data supporting the conclusions of this article will be made available by the authors, without undue reservation.

Ethics statement

The study involving human participants has been reviewed and approved by National Cheng Kung University Hospital Institutional Review Board (NCKUH IRB) on Jun 28th, 2022. IRB No: A-EC-111-023. Written informed consent for participation was not required for this study in accordance with the national legislation and the institutional requirements.

Author contributions

Conception and design, data acquisition, and critical revision of the article for important intellectual content: S-WL and J-YC. Literature review and drafting and finalizing the article: S-WL. Supervised the literature search and revision and approved the final version: J-YC. All authors contributed to the article and approved the submitted version.

Funding

This study was supported by the Ministry of Science and Technology of Taiwan, China (MOST 110-2218-E-006-017 and MOST 110-2218-E-006-015) and Higher Education Sprout Project, Ministry of Education to the Headquarters of University Advancement at National Cheng Kung University (NCKU).

Acknowledgments

The authors would like to thank the Ministry of Science and Technology of the Republic of China, Taiwan, for financially supporting this research under contract MOST 110-2218-E-006-017 and MOST 110-2218-E-006-015.

Conflict of interest

The authors declare that the research was conducted in the absence of any commercial or financial relationships that could be construed as a potential conflict of interest.

Publisher's note

References

1. Kirkfeldt RE, Johansen JB, Nohr EA, Jorgensen OD, Nielsen JC. Complications after cardiac implantable electronic device implantations: an analysis of a complete, nationwide cohort in Denmark. *Eur Heart J.* (2014) 35:1186–94. doi: 10.1093/eurheartj/eht511

2. Merenkov VV, Monahov YE, Kovalev AN, Ustinov AA. Pneumothorax after pacemaker implantation: a diagnostic value of sonography. *J Cardiothorac Vasc Anesth.* (2013) 27:e73–5. doi: 10.1053/j.jvca.2013.07.003

3. Ogunbayo GO, Charnigo R, Darrat Y, Morales G, Kotter J, Olorunfemi O, et al. Incidence, predictors, and outcomes associated with pneumothorax during cardiac electronic device implantation: a 16-year review in over 3. 7 million patients. *Heart Rhythm.* (2017) 14:1764–70. doi: 10.1016/j.hrthm.2017.07.024

4. Kirkfeldt RE, Johansen JB, Nohr EA, Moller M, Arnsbo P, Nielsen JC. Risk factors for lead complications in cardiac pacing: a population-based cohort study of 28,860 Danish patients. *Heart Rhythm.* (2011) 8:1622–8. doi: 10.1016/j.hrthm.2011.04.014

5. Kirkfeldt RE, Johansen JB, Nohr EA, Moller M, Arnsbo P, Nielsen JC. Pneumothorax in cardiac pacing: a population-based cohort study of 28,860 Danish patients. *Europace.* (2012) 14:1132–8. doi: 10.1093/europace/eus054

6. Udo EO, Zuithoff NP, van Hemel NM, de Cock CC, Hendriks T, Doevendans PA, et al. Incidence and predictors of short- and long-term complications in pacemaker therapy: the FOLLOWPACE study. *Heart Rhythm.* (2012) 9:728–35. doi: 10.1016/j.hrthm.2011.12.014

7. van Rees JB, de Bie MK, Thijssen J, Borleffs CJ, Schalij MJ, van Erven L. Implantation-related complications of implantable cardioverter-defibrillators and cardiac resynchronization therapy devices: a systematic review of randomized clinical trials. *J Am Coll Cardiol.* (2011) 58:995–1000. doi: 10.1016/j.jacc.2011.06.007

8. Sebastian CC, Wu WC, Shafer M, Choudhary G, Patel PM. Pneumopericardium and pneumothorax after permanent

pacemaker implantation. *Pacing Clin Electrophysiol.* (2005) 28:466–8. doi: 10.1111/j.1540-8159.2005.40063.x

9. Schorlemmer GR, Khouri RK, Murray GF, Johnson G Jr. Bilateral pneumothoraces secondary to latrogenic buffalo chest an unusual complication of median sternotomy and subclavian vein catheterization. *Ann Surg.* (1984) 199:372–4. doi: 10.1097/00000658-198403000-00021

10. Ayati M, Menon SD, Morillo CA, Healey J, Connolly SJ. Bilateral pneumothorax post insertion of intracardiac defibrillator, a rare condition, risk factors and prevention. *Eu J Arrhyth Electrophysiol.* (2016) 2:40. doi: 10.17925/EJAE.2016.02.01.40

11. Parashar NK, Deepti S, Yadav R, Sinha M, Ramakumar V. An unexpected complication of intracardiac device implantation: contralateral pneumothorax and pneumopericardium. *Indian Pacing Electrophysiol J.* (2019) 19:167–70. doi: 10.1016/j.ipej.2019.04.001

12. Rodriguez JAO, Hipskind JE. *Iatrogenic Pneumothorax*. StatPearls Publishing (2021).

13. Olesen LL. Bilateral pneumothorax complicating pacemaker implantation, due to puncture of the left subclavian vein and electrode perforation of the right atrium. *Cureus.* (2020) 12:11302. doi: 10.7759/cureus.11302

14. Res JC, de Priester JA, van Lier AA, van Engelen CL, Bronzwaer PN, Tan PH, et al. Pneumothorax resulting from subclavian puncture: a complication of permanent pacemaker lead implantation. *Neth Heart J.* (2004) 12:101–5.

15. Dilling-Boer D, Ector H, Willems R, Heidbüchel H. Pericardial effusion and right-sided pneumothorax resulting from an atrial active-fixation lead. *EP Europace.* (2003) 5:419–23. doi: 10.1016/S1099-5129(03)00079-5

16. Oginosawa Y, Abe H, Nakashima Y. Right pneumothorax resulting from an endocardial screw-in atrial lead in an implantable cardioverter defibrillator system. *Pac Clin Electrophysiol.* (2002) 25:1278–9. doi: 10.1046/j.1460-9592.2002.01278.x

17. Grabowski M. Pneumothorax after pacemaker implantation localized contralaterally to the side of implantation–a rare but possible complication. *Heart Beat J.* (2017) 2:1611. doi: 10.24255/hbj/81611

18. Kotsakou M, Kioumis I, Lazaridis G, Pitsiou G, Lampaki S, Papaiwannou A, et al. Pacemaker insertion. *Ann Trans Med.* (2015) 3:42. doi: 10.3978/j.issn.2305-5839.2015.02.06

19. Saradna A, Sinha A, Abduraimova M, Rodriguez D, Yang F. Tale of a wandering lead: late atrial lead perforation into right lung following pacemaker implantation. *Cureus.* (2017) 9:1865. doi: 10.7759/cureus.1865

20. Srivathsan K, Byrne R, Appleton C, Scott LR. Pneumopericardium and pneumothorax contralateral to venous access site after permanent pacemaker implantation. *EP Europace.* (2003) 5:361–3. doi: 10.1016/S1099-5129(03)00093-X

21. Tsotsolis N, Tsirgogianni K, Kioumis I, Pitsiou G, Baka S, Papaiwannou A, et al. Pneumothorax as a complication of central venous catheter insertion. *Ann Trans Med.* (2015) 3:40. doi: 10.3978/j.issn.2305-5839.2015.02.11

22. Hao Y, Li Y, Liao D, Yang L, Liu F, A. comparative analysis of the effectiveness of active versus passive atrial lead fixation in Chinese patients with cardiac implantable electrical devices: a long term, retrospective, observational, single-center study. *Curr Med Res Opin.* (2017) 33:573–8. doi: 10.1080/03007995.2016.1275938

23. Banaszewski M, Stepińska J. Right heart perforation by pacemaker leads. *Archives of medical science: AMS.* (2012) 8:11. doi: 10.5114/aoms.2012.27273

24. Glikson M, VON FELDT LK, Suman VJ, Hayes DL. Clinical surveillance of an active fixation, bipolar, polyurethane insulated pacing lead, part I: the atrial lead. *Pacing Clin Electrophysiol.* (1994) 17:1399–404. doi: 10.1111/j.1540-8159.1994.tb02459.x

25. Kumar S, Yassin H, Esan O, Budzikowski AS, Kassotis JT. Mechanism and management of pacing lead related cardiac perforation. *Curr Iss Rec Adv Pacemaker Therapy: IntechOpen.* (2012). doi: 10.5772/48630

26. Martos R, Khadadah S, Alsaleh H, Foley B, Dodd J. Pneumopericardium and contralateral pneumothorax to venous access site after a biventricular permanent pacemaker implantation. *J Clinic Experiment Cardiol.* (2011) 2:2. doi: 10.4172/2155-9880.1000150

27. Sadamatsu K. Complication of pacemaker implantation: an atrial lead perforation. *Mod Pacemakers-Pre Fut: IntechOpen.* (2011). doi: 10.5772/13854

28. Van Gelder BM, Verberkmoes N, Nathoe R, Bracke FA. Late asymptomatic atrial lead perforation, a fortuitous finding during lead extraction using thoracoscopic surveillance: a case report and review of the literature. *EP Europace.* (2016) 18:1773–8. doi: 10.1093/europace/euw054

29. Mahadevan MS, Yadava RS, Mandal M. Cardiac pathology in myotonic dystrophy type 1. *Int J Mol Sci.* (2021) 22:11874. doi: 10.3390/ijms222111874

30. Thomas GR, Kumar SK, Turner S, Moussa F, Singh SM. The natural history and treatment of cardiac implantable electronic device associated pneumothorax—A 10-year single-centre experience. *CJC open.* (2021) 3:176–81. doi: 10.1016/j.cjco.2020.10.011

31. HUANG XM FU HX, Zhong L, Osborn MJ, Asirvatham SJ, Sinak LJ, et al. Outcomes of lead revision for myocardial perforation after cardiac implantable electronic device placement. *J Cardiovasc Electrophysiol.* (2014) 25:1119–24. doi: 10.1111/jce.12457

32. Balabanoff C, Gaffney CE, Ghersin E, Okamoto Y, Carrillo R, Fishman JE. Radiographic and electrocardiography-gated noncontrast cardiac CT assessment of lead perforation: modality comparison and interobserver agreement. *J Cardiovasc Comput Tomogr.* (2014) 8:384–90. doi: 10.1016/j.jcct.2014.08.004

33. Feng Q, Yin Y, Hua X, Zhu R, Hua J, Xu J. Prospective ECG triggering versus low-dose retrospective ECG-gated 128-channel CT coronary angiography: comparison of image quality and radiation dose. *Clin Radiol.* (2010) 65:809–14. doi: 10.1016/j.crad.2010.05.005

34. Baumann MH, Strange C, Heffner JE, Light R, Kirby TJ, Klein J, et al. Management of spontaneous pneumothorax: an American college of chest physicians Delphi consensus statement. *Chest.* (2001) 119:590–602. doi: 10.1378/chest.119.2.590

35. MacDuff A, Arnold A, Harvey J. Management of spontaneous pneumothorax: British thoracic society pleural disease guideline 2010. *Thorax.* (2010) 65:ii18–31. doi: 10.1136/thx.2010.136986

36. Loiselle A, Parish JM, Wilkens JA, Jaroszewski DE. Managing iatrogenic pneumothorax and chest tubes. *J Hosp Med.* (2013) 8:402–8. doi: 10.1002/jhm.2053

37. Chadha TS, Cohn MA. Noninvasive treatment of pneumothorax with oxygen inhalation. *Respiration.* (1983) 44:147–52. doi: 10.1159/000194541

38. Clark S, Saker F, Schneeberger M, Park E, Sutton D, Littner Y. Administration of 100% oxygen does not hasten resolution of symptomatic spontaneous pneumothorax in neonates. *J Perinatol.* (2014) 34:528–31. doi: 10.1038/jp.2014.55

39. Yamagami T, Kato T, Iida S, Hirota T, Yoshimatsu R, Nishimura T. Efficacy of manual aspiration immediately after complicated pneumothorax in CT-guided lung biopsy. *J Vasc Intervent Radiol.* (2005) 16:477–83. doi: 10.1097/01.RVI.0000150032.12842.9E

40. Baumann MH, Strange C. The clinician's perspective on pneumothorax management. *Chest.* (1997) 112:822–8. doi: 10.1378/chest.112.3.822

41. Schoenenberger RA, Haefeli WE, Weiss P, Ritz RF. Timing of invasive procedures in therapy for primary and secondary spontaneous pneumothorax. *Arch Surg.* (1991) 126:764–6. doi: 10.1001/archsurg.1991.01410300110017

42. Schoenenberger RA, Haefeli WE, Weiss P, Ritz R. Evaluation of conventional chest tube therapy for iatrogenic pneumothorax. *Chest.* (1993) 104:1770–2. doi: 10.1378/chest.104.6.1770

43. Ellenbogen KA, Wood MA, Shepard RK. Delayed complications following pacemaker implantation. *Pacing Clin Electrophysiol.* (2002) 25:1155–8. doi: 10.1046/j.1460-9592.2002.01155.x

44. Sadamatsu K, Enomoto N, Tsuji M, Tashiro H. Progressive atrial lead perforation developed 5 years after pacemaker replacement. *J Cardiol.* (2009) 53:150–3. doi: 10.1016/j.jjcc.2008.07.006

45. Migliore F, Zorzi A, Bertaglia E, Leoni L, Siciliano M, De Lazzari M, et al. Incidence, management, and prevention of right ventricular perforation by pacemaker and implantable cardioverter defibrillator leads. *Pacing Clin Electrophysiol.* (2014) 37:1602–9. doi: 10.1111/pace.12472

46. Nantsupawat T, Li J-M, Benditt DG, Adabag S. Contralateral pneumothorax and pneumopericardium after dual-chamber pacemaker implantation: Mechanism, diagnosis, and treatment. *HeartRhythm Case Reports.* (2018) 4:256–9. doi: 10.1016/j.hrcr.2018.03.001

47. Tagliari AP, Kochi AN, Mastella B, Saadi RP, di Leoni Ferrari A, Saadi EK, et al. Axillary vein puncture guided by ultrasound vs cephalic vein dissection in pacemaker and defibrillator implant: a multicenter randomized clinical trial. *Heart Rhythm.* (2020) 17:1554–60. doi: 10.1016/j.hrthm.2020.04.030

48. Ahmed AS, Gilge JL, Clark BA, Shah A, Bagga S, Padanilam MS, et al. Predictors of successful ultrasound-guided lead implantation. *Pacing Clin Electrophysiol.* (2020) 43:217–22. doi: 10.1111/pace.13855

49. Harada Y, Katsume A, Kimata M, Hikosaka T, Yamanaka S, Akashi K, et al. Placement of pacemaker leads via the extrathoracic subclavian vein guided by fluoroscopy and venography in the oblique projection. *Heart Vessels.* (2005) 20:19–22. doi: 10.1007/s00380-004-0797-1

50. Chauhan A, Grace A, Newell S, Stone D, Shapiro L, Schofield P, et al. Early complications after dual chamber versus single chamber pacemaker implantation. *Pacing Clin Electrophysiol.* (1994) 17:2012–5. doi: 10.1111/j.1540-8159.1994.tb03791.x

51. Migliore F, Fais L, Vio R, De Lazzari M, Zorzi A, Bertaglia E, et al. Axillary vein access for permanent pacemaker and implantable cardioverter defibrillator implantation: fluoroscopy compared to ultrasound. *Pacing Clin Electrophysiol.* (2020) 43:566–72. doi: 10.1111/pace.13940

52. Migliore F, Siciliano M, De Lazzari M, Ferretto S, Valle CD, Zorzi A, et al. Axillary vein puncture using fluoroscopic landmarks: a safe and effective approach for implantable cardioverter defibrillator leads. *J Intervent Card Electrophysiol.* (2015) 43:263–7. doi: 10.1007/s10840-015-0011-7

53. De Sensi F, Miracapillo G, Addonisio L, Breschi M, Paneni F, Cresti A, et al. Axillary vein access with or without venography: is this the dilemma in the ultrasounds era? *EP Euro.* (2018) 20:1389–90. doi: 10.1093/europace/euy048

54. Antonelli D, Feldman A, Freedberg NA, Turgeman Y. Axillary vein puncture without contrast venography for pacemaker and defibrillator leads implantation. *Pacing Clin Electrophysiol.* (2013) 36:1107–10. doi: 10.1111/pace.12181

55. Squara F, Tomi J, Scarlatti D, Theodore G, Moceri P, Ferrari E. Self-taught axillary vein access without venography for pacemaker implantation: prospective randomized comparison with the cephalic vein access. *EP Europace.* (2017) 19:2001–6. doi: 10.1093/europace/euw363

frontiers | Frontiers in Cardiovascular Medicine

TYPE Case Report
PUBLISHED 15 September 2022
DOI 10.3389/fcvm.2022.973480

OPEN ACCESS

EDITED BY
Young Keun On,
Sungkyunkwan University, South Korea

REVIEWED BY
Jiangang Zou,
Nanjing Medical University, China
Jean-benoît Le Polain de Waroux,
AZ Sint-Jan Brugge-Oostende
AV, Belgium

*CORRESPONDENCE
Xianhong Fang
drfangxh@163.com

SPECIALTY SECTION
This article was submitted to
Cardiac Rhythmology,
a section of the journal
Frontiers in Cardiovascular Medicine

RECEIVED 20 June 2022
ACCEPTED 22 August 2022
PUBLISHED 15 September 2022

CITATION
Wei H-Q, Xue Y, Wu S and Fang X
(2022) Case report: Three-dimensional
printing as an educational tool for
optimal lead positioning to left bundle
branch pacing.
Front. Cardiovasc. Med. 9:973480.
doi: 10.3389/fcvm.2022.973480

Case report: Three-dimensional printing as an educational tool for optimal lead positioning to left bundle branch pacing

Hui-Qiang Wei, Yumei Xue, Shulin Wu and Xianhong Fang*

Department of Cardiology, Guangdong Cardiovascular Institute, Guangdong Provincial People's Hospital, Guangdong Academy of Medical Sciences, Guangzhou, China

Left bundle branch pacing (LBBP) has been widely adopted as a physiological pacing approach. However, LBBP fails to achieve in some cases because it is difficult to maintain the orientation of the lead tip perpendicular to the interventricular septum (IVS). Three-dimensional (3D) printing technology has emerged as a promising tool for modeling and teaching cardiovascular interventions. Seeking confirmation of optimal lead placement relative to the IVS, we used 3D printing technology to generate a 3D printed heart from a selected patient with successful and proven LBBP. Our model successfully illustrated that the lead tip was perpendicular to the IVS. Application of the 3D technology has potential to help the early-operator understand the optimal lead placement relative to IVS and diminish the learning-curve.

KEYWORDS

left bundle branch area, physiological pacing, 3-dimensional printing, interventricular septum, pacing lead

Introduction

Medical 3-dimensional (3D) printing has been applied to cardiovascular diseases in recent years (1). 3D printing has become a promising tool for modeling and teaching cardiovascular interventions. Left bundle branch pacing (LBBP), a new physiological pacing strategy, is considered as a feasible and safe approach characterized by a narrow QRS duration and low and stable capture threshold (2). Ideally, the pacing lead is screwed-in perpendicular to the interventricular septum (IVS) during the implantation procedure (3). However, LBBP cannot be achieved in some cases because it is difficult to maintain the orientation of the lead tip perpendicular to the IVS. To better examine the position of the lead relative to the IVS, we reviewed clinically indicated cardiac computed tomography (CT) scan of a patient with LBBP lead and generated 3D-printed model.

Case report

A 61-year-old male presented with recurrent syncope and was found to have high-degree atrioventricular block. He was admitted to our institution for pacemaker implantation. We intended to place the ventricular lead in the left bundle branch (LBB) area to deliver physiological pacing. The 3830 pacing lead (SelectSecure, Medtronic, Minneapolis, MN, USA) was delivered through a fixed-curve sheath (C315 His, Medtronic, Minneapolis, MN, USA) inserted *via* the left axillary vein. Then the sheath and the lead were advanced to the ventricular side inferior to the septal leaflet of tricuspid valves and rotated in a counterclockwise fashion to place the lead tip in a perpendicular orientation toward the IVS. The pacing lead was successfully placed in the LBB area and LBB potential was recorded with a low capture threshold of 0.75V/0.5ms (Figure 1A). The transition from non-selective LBBP to selective LBBP was recorded with the same peak LV activation time of 75 ms (Figure 1B). No complications occurred during the procedure.

Cardiac CT was performed in this patient due to the chest pain evaluation. CT scans were obtained with a 64-slice spiral CT system (GE Healthcare, Milwaukee, WI, USA), with retrospective gating and a slice thickness of 0.75 mm. Then 3D reconstruction of the heart was performed using the Mimics software (Materialize NV, Leuven, Belgium). Model was printed using the J501Pro printer (Zhuhai Seine Technology Co., Ltd., Zhuhai, China) with photosensitive resin. The printing procedure took ∼5 h to complete. The result of the model is shown in Figure 1C.

Discussion

LBBP has been widely used in clinical practice since it was initially described by Huang in 2017 (4). Several methods for guiding LBBP lead implantation have been reported (5, 6). However, the failure rate of LBBP was 10–20% (7). One of possible explanations may be related to the oblique lead fixation. 3D printing technology is a promising tool for modeling and teaching cardiovascular interventions. Patient-specific 3D models may offer useful anatomic information and guide the operators how to rotate the sheath. The example of our 3D printing model as an educational tool for optimal lead positioning to LBBP showed that the lead tip was perpendicular to the IVS. The LBB potential was recorded during the procedure and selective LBBP was successfully achieved in this patient.

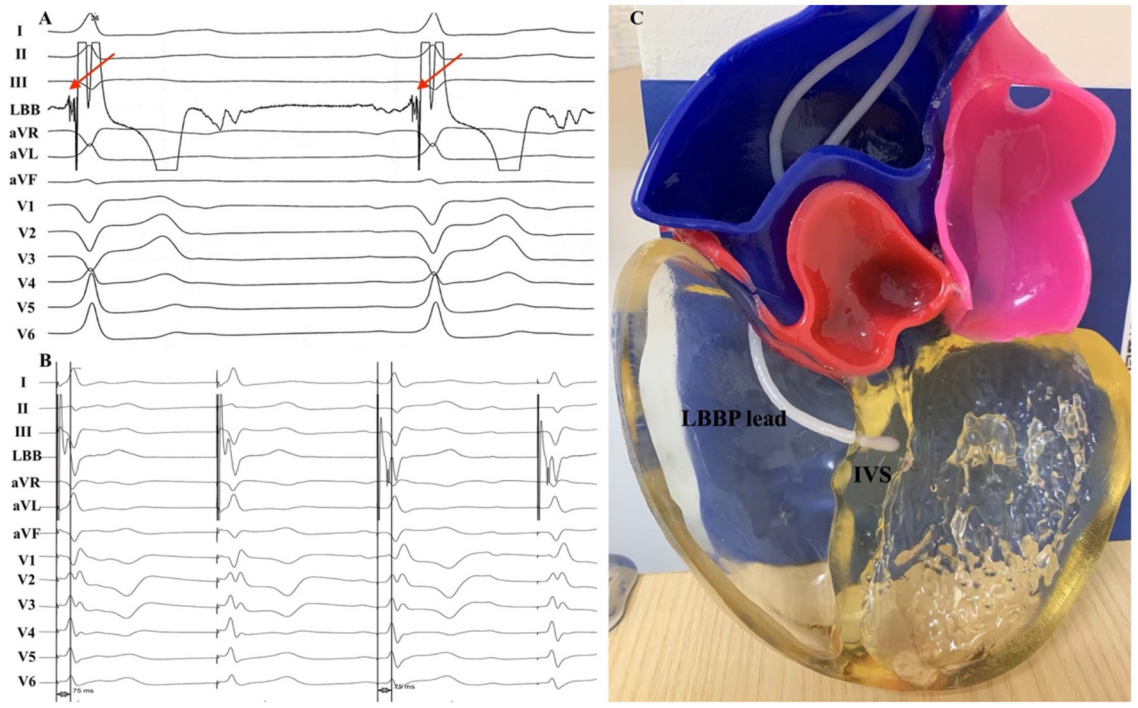

FIGURE 1
(A) 12-lead ECG and unipolar tip electrode electrogram obtained during sinus rhythm and **(B)** LBBP. **(C)** Three-dimensional printed model. **(A)** A LBB potential (red arrow) was recorded during the implant procedure. **(B)** During the threshold test, a transition from non-selective to selective LBBP was observed with a stable peak LV activation time of 75 ms. LBB, left bundle branch; LBBP, left bundle branch pacing; LV, left ventricular; IVS, interventricular septum.

Application of the 3D technology has potential to help the early-operator understand the optimal lead placement relative to IVS and diminish the learning-curve.

Conclusion

The 3D printed model may help to better understand the relationship between the lead and IVS. Future applications of 3D printing might include facilitating research focusing on optimal lead positioning, understand complex anatomy and plan complex implantation procedure.

Data availability statement

The raw data supporting the conclusions of this article will be made available by the authors, without undue reservation.

Ethics statement

The studies involving human participants were reviewed and approved by Guangdong Provincial People's Hospital. The patients/participants provided their written informed consent to participate in this case study. Written informed consent was obtained from the individual(s) for the publication of any potentially identifiable images or data included in this article.

Author contributions

All authors listed have made a substantial, direct, and intellectual contribution to the work and approved it for publication.

Funding

This work was supported by the Science and Technology Planning Program of Guangdong Province (grant number 2019B020230004).

Conflict of interest

The authors declare that the research was conducted in the absence of any commercial or financial relationships that could be construed as a potential conflict of interest.

Publisher's note

All claims expressed in this article are solely those of the authors and do not necessarily represent those of their affiliated organizations, or those of the publisher, the editors and the reviewers. Any product that may be evaluated in this article, or claim that may be made by its manufacturer, is not guaranteed or endorsed by the publisher.

References

1. Wang DD, Qian Z, Vukicevic M, Engelhardt S, Kheradvar A, Zhang C, et al. 3d printing, computational modeling, and artificial intelligence for structural heart disease. *JACC Cardiovasc Imaging.* (2021) 14:41–60. doi: 10.1016/j.jcmg.2019.12.022

2. Vijayaraman P, Subzposh FA, Naperkowski A, Panikkath R, John K, Mascarenhas V, et al. Prospective evaluation of feasibility and electrophysiologic and echocardiographic characteristics of left bundle branch area pacing. *Heart Rhythm.* (2019) 16:1774–82. doi: 10.1016/j.hrthm.2019.05.011

3. Huang W, Chen X, Su L, Wu S, Xia X, Vijayaraman P. A beginner's guide to permanent left bundle branch pacing. *Heart Rhythm.* (2019) 16:1791–6. doi: 10.1016/j.hrthm.2019.06.016

4. Huang W, Su L, Wu S, Xu L, Xiao F, Zhou X, et al. A novel pacing strategy with low and stable output: pacing the left bundle branch immediately beyond the conduction block. *Can J Cardiol.* (2017) 33:1736 e1–3. doi: 10.1016/j.cjca.2017.09.013

5. Jiang H, Hou X, Qian Z, Wang Y, Tang L, Qiu Y, et al. A novel 9-partition method using fluoroscopic images for guiding left bundle branch pacing. *Heart Rhythm.* (2020) 17:1759–67. doi: 10.1016/j.hrthm.2020.05.018

6. Liu X, Niu HX, Gu M, Chen X, Hu Y, Cai M, et al. Contrast-enhanced image-guided lead deployment for left bundle branch pacing. *Heart Rhythm.* (2021) 18:1318–25. doi: 10.1016/j.hrthm.2021.04.015

7. Li Y, Chen K, Dai Y, Li C, Sun Q, Chen R, et al. Left bundle branch pacing for symptomatic bradycardia: implant success rate, safety, and pacing characteristics. *Heart Rhythm.* (2019) 16:1758–65. doi: 10.1016/j.hrthm.2019.05.014

frontiers | Frontiers in Cardiovascular Medicine

TYPE Case Report
PUBLISHED 03 October 2022
DOI 10.3389/fcvm.2022.969192

OPEN ACCESS

EDITED BY
Matteo Anselmino,
University of Turin, Italy

REVIEWED BY
Richard Gary Trohman,
Rush University, United States
Maciej M. Sterlinski,
National Institute of
Cardiology, Poland

*CORRESPONDENCE
Shuying Qi
qsy304@126.com

SPECIALTY SECTION
This article was submitted to
Cardiac Rhythmology,
a section of the journal
Frontiers in Cardiovascular Medicine

RECEIVED 14 June 2022
ACCEPTED 06 September 2022
PUBLISHED 03 October 2022

CITATION
Zhang X, Ma Y, Ru L, Wang D, Li J and Qi S (2022) Case report: What course to follow when left bundle branch pacing encounters acute myocardial infarction?.
Front. Cardiovasc. Med. 9:969192.
doi: 10.3389/fcvm.2022.969192

Case report: What course to follow when left bundle branch pacing encounters acute myocardial infarction?

Xiaojiang Zhang, Yanzhuo Ma, Leisheng Ru, Dongmei Wang, Jie Li and Shuying Qi*

980th Hospital of the Joint Logistic Support Force of PLA, Shijiazhuang, China

Compared with traditional right ventricular apical pacing, His-bundle pacing (HBP) provides more physiologic pacing by activating the normal conduction system. However, HBP has some limitations including higher pacing thresholds. In addition, disease in the distal His-Purkinje system may prevent the correction of abnormal conduction. Left bundle branch pacing (LBBP) may overcome these disadvantages by providing lower pacing thresholds and relatively narrow QRS duration that improve cardiac function. Here, we describe a rare case of a transient loss of ventricular capture due to acute anterior wall myocardial infarction in an LBB-paced patient. With the improvement of the ischemia, the function of the pacemaker partly recovered. We review the adaptations, advantages, and limitations, and long-term safety of LBBP.

KEYWORDS

left bundle branch pacing (LBBP), acute myocardial infarction (AMI), AV block, pacemaker dysfunction, the pacing threshold

Case presentation

Treatment of AMI

An 82-year-old man who was treated with LBBP in 2018 for atrioventricular (AV) conduction disorder was admitted to the Chest Pain Center of the 980th Hospital of the Joint Logistic Support Force of the People's Liberation Army (PLA) in 2021. Based on typical acute chest pain, the elevation of the ST segment in leads V1–V4 of the electrocardiogram (ECG) (Figure 1B), and positive cardiac troponin I (12.34 ng/ml), the patient was diagnosed with an acute anterior wall myocardial infarction (AMI). According to the AMI treatment guidelines, the patient underwent emergency coronary angiography. In his left anterior descending (LAD) artery, there was thrombosis with fixed stenosis in the proximal segment, whereas no significant stenosis was observed in the left circumflex artery and the right coronary artery (Figures 2A,B). Because thrombolysis resulted in grade 3 flow in the distal part of the LAD, we prepared

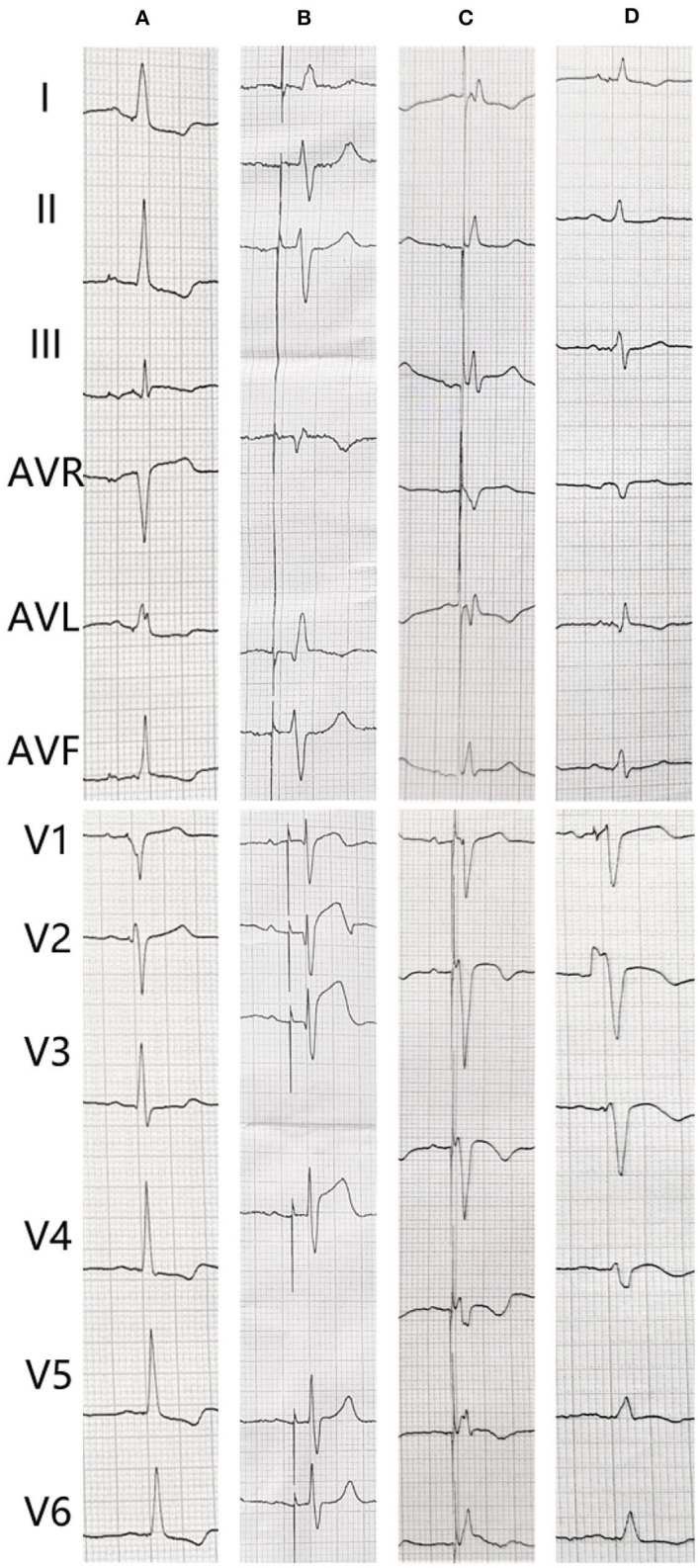

FIGURE 1
The electrocardiogram (ECG) changes of the patient. **(A)** After pacemaker implantation. **(B)** The transient loss of capture when acute myocardial infarction. **(C)** Second day after coronary angiography. **(D)** After percutaneous coronary intervention.

to perform percutaneous coronary intervention (PCI) after initiating standard drug therapy that included dual antiplatelets, statin, metoprolol, and diuretics. A subsequent laboratory test revealed no pathologic features except for 88.3% of white blood cells being neutrophils (40–75%), creatine kinase (CK) of 2,179 U/l (50–301 U/l), CK isoenzyme of 140 U/l (0–24 U/l), creatinine of 117 μmol/l (57–111 μmol/l), and D-dimer of 1.227 mg/l (0–0.243 mg/l), which led to a diagnosis of AMI. A computed tomography (CT) scan of the lung revealed bilateral pneumonia and hydrothorax that was related to the heart failure. Echocardiography revealed a left ventricular end-diastolic diameter of 56 mm, ejection fraction of 42%, interventricular septal thickness of 11.8 mm, and decreased diastolic function. The second day after AMI, the ST segments on his ECG declined toward the baseline value with inverted T waves in the anterior leads (Figure 1C).

Adjustment of LBBP parameters

The patient underwent LBB pacemaker implantation for second-degree type II AV block according to the treatment guidelines. A 3,830 lead (Medtronic, Inc. Minneapolis, MN, US) was advanced and positioned *via* a transventricular septal approach (Figures 3A,B). The procedure was performed successfully, with a pacing threshold of 0.5 V/0.4 ms and a QRS duration of 110 ms on the ECG (Figures 1A,C, 3C). The pacemaker had a normal function in subsequent examinations until the occurrence of AMI (Table 1). Compared with the previous ECG, there was a transient loss of capture and an increase in the LBBP threshold at the time of AMI (Figure 1B; Table 1). Pectoral muscle twitching was noted which indicated some changes in the electrical performance of the pacing system. The pacemaker and electrode were immediately tested; the ventricular pacing threshold had increased to 5 V/0.4 ms (Table 1) whereas that of the right atrium remained stable compared with the value recorded at implantation. After parameters adjustment, the symptoms disappeared and the threshold decreased to 3.5 V/0.4 ms. Three days after AMI, in the absence of additional acute ischemia, the pacing threshold had decreased to 2.5 V/0.4 ms and was stable. The LAD PCI was performed after 2 weeks (Table 1). A 3.5 × 28 mm drug-coated stent (Boston Scientific, Marlborough, Massachusetts, US) was placed in the proximal segment of the LAD (Figures 2D–F). A routine test showed that the pacing threshold had decreased to 2 V/0.4 ms (Figure 1D, Table 1).

Outcome and follow-up

The patient recovered well and was discharged. After more than 1.4 years of follow-up, the patient showed good recovery with no complications and a septal thickness of 9 mm. The ventricular pacing threshold remained relatively steady with a slight decrease to 1.75 V/0.4 ms (Table 1).

Discussion

To overcome the limitations of right ventricular apical pacing (RVAP) such as electrical and mechanical dysynchrony and a high risk of heart failure (1), two physiologic stimulation techniques have been employed—namely, HBP and LBBP (2). Although HBP has some demonstrated benefits (3) such as specific activation of the conduction system and has been broadly adopted, it has certain drawbacks including the difficulty of identifying the precise location of the His bundle, unstable pacing threshold, or lead dislodgement rate of 5–10%, large atrial signals, or low R-wave amplitude that complicate pacing management, and heart block distal to the pacing cite (4). The LBBP is a novel technique for stimulating the cardiac conduction system. Direct LBBP, another physiologic pacing method, was first used during pacemaker implantation to restore the impaired His-Purkinje conduction system in a patient with heart failure and LBB block (5). From 2018 to the present, our center has performed more than 100 LBBP procedures and has described the advantages of LBBP such as a lower and more stable pacing threshold, reduced heart failure rate, narrow QRS duration, high success rate, and few complications. The LBBP is gaining rapid acceptance among clinicians (6).

In this report, we described a patient with AV block and a high percentage of right ventricular pacing rate that was successfully treated with LBBP. After the implantation in 2018, the threshold of the pacemaker remained stable and was similar to that observed at the time of implantation, and the patient was asymptomatic without heart failure for more than 2 years till the year 2021.

Many articles and systematic reviews have demonstrated the effectiveness of LBBP (3), which was confirmed in our patient. However, some researchers have cautioned that additional studies are needed to validate the safety of LBBP (6) as some complications have been reported including septal perforation and thromboembolism (7), septal arterial injury (8), and lead dislodgement (9). Our patient was diagnosed with an acute anterior wall myocardial infarction 2 years after LBBP, and emergency coronary angiography revealed LAD stenosis in the proximal segment with transient loss of LBBP capture in the ECG. During testing the LBB pacing threshold of had increased to 5 V/0.4 ms, which was related to the myocardial ischemia in the septum. To investigate whether the infarction scar also contributed to this increase, we further tested the pacemaker 3 days after the AMI and found that the threshold had decreased to

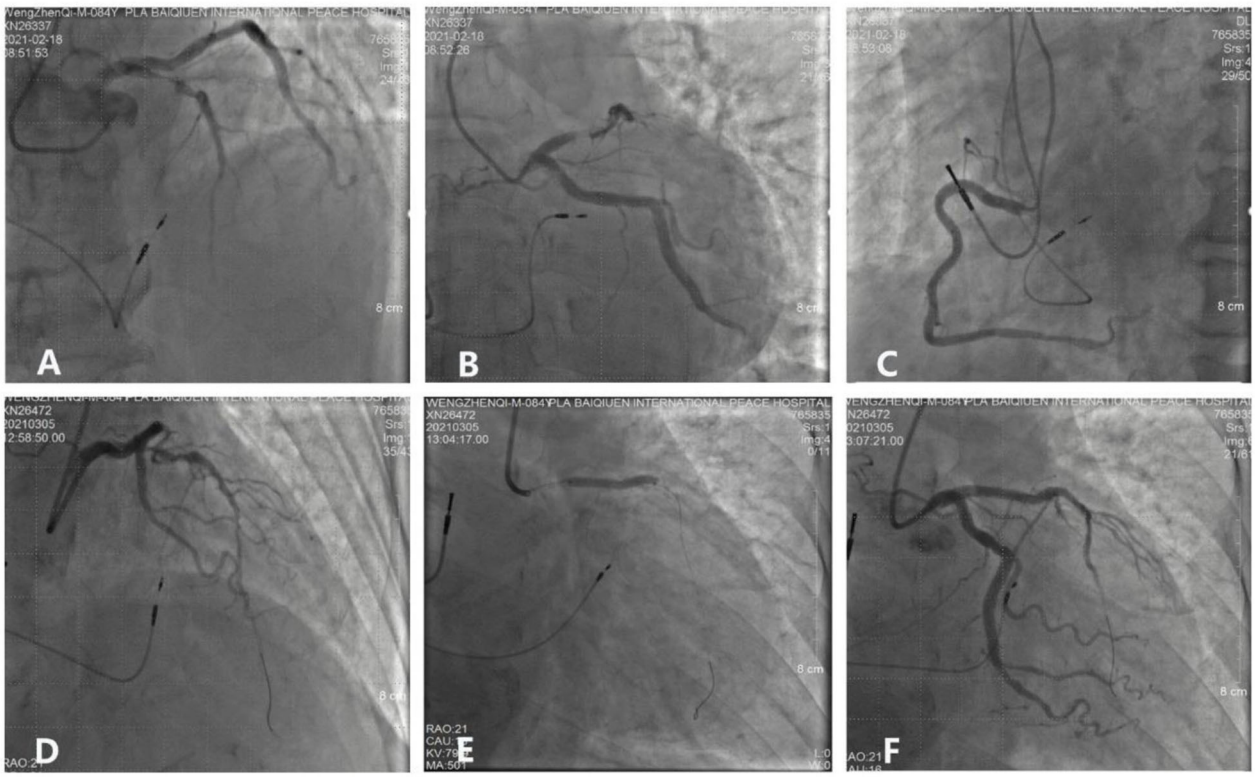

FIGURE 2
Process and visualization of percutaneous coronary intervention (PCI). **(A,B)** A fixed stenosis in the left anterior descending artery. **(C)** No severe stenosis in the right coronary. **(D)** NS guidewire was placed in the targeted artery. **(E)** A stent was placed in the proximal segment of the left anterior descending artery. **(F)** No residual stenosis after stent implantation.

2.5 V/0.4 ms. After standard drug therapy for 2 weeks and selective PCI for the LAD stenosis, the pacing threshold further declined to 2 V/0.4 ms, likely due to the additional improvement of the myocardial blood supply. This suggests that ischemia played a pivotal role in the threshold change. As for the cardiac scar, there was no evidence that it was a contributing factor. After discharge, the patient was followed up for more than 1.4 years, during which time the pacing threshold remained almost the same as that recorded at the time of PCI, with only a minor decline after 1.4 years.

Compared with RVAP and HBP, LBBP has technical advantages, especially in terms of physiologic pacing, but there are still some aspects that warrant consideration (10). First, it is essential to strictly comply with the LBBP operation procedure, which is summarized as follows: (1) determine the initial LBBP site; (2) introduce a pacing lead into the interventricular septum (IVS) and reach the LBB area; (3) assess the lead depth and confirm LBB capture; (4) remove the sheath and provide slack; and (5) program the pulse generator (10). Second, after assessing cardiac ischemia and scarring of the myocardium (especially the septum), it is important to avoid pacing dysfunctions such as a high threshold or unstable electrode. Coronary computed tomography angiography and magnetic resonance imaging of the heart can provide valuable information. Third, the patient should be closely followed up to monitor pacemaker function so that pacing problems can be detected and corrected in a timely manner.

Short-term clinical outcomes of physiologic pacing, especially LBBP, have been promising (11, 12). Nonetheless, prospective clinical trials and mechanistic studies are needed to better understand this technique and improve its safety and reliability.

Conclusion

The IVS ischemia may occur more frequently than with RVAP in patients with LBBP, making them more prone to loss of capture, which should be taken into account when selecting the mode of pacing.

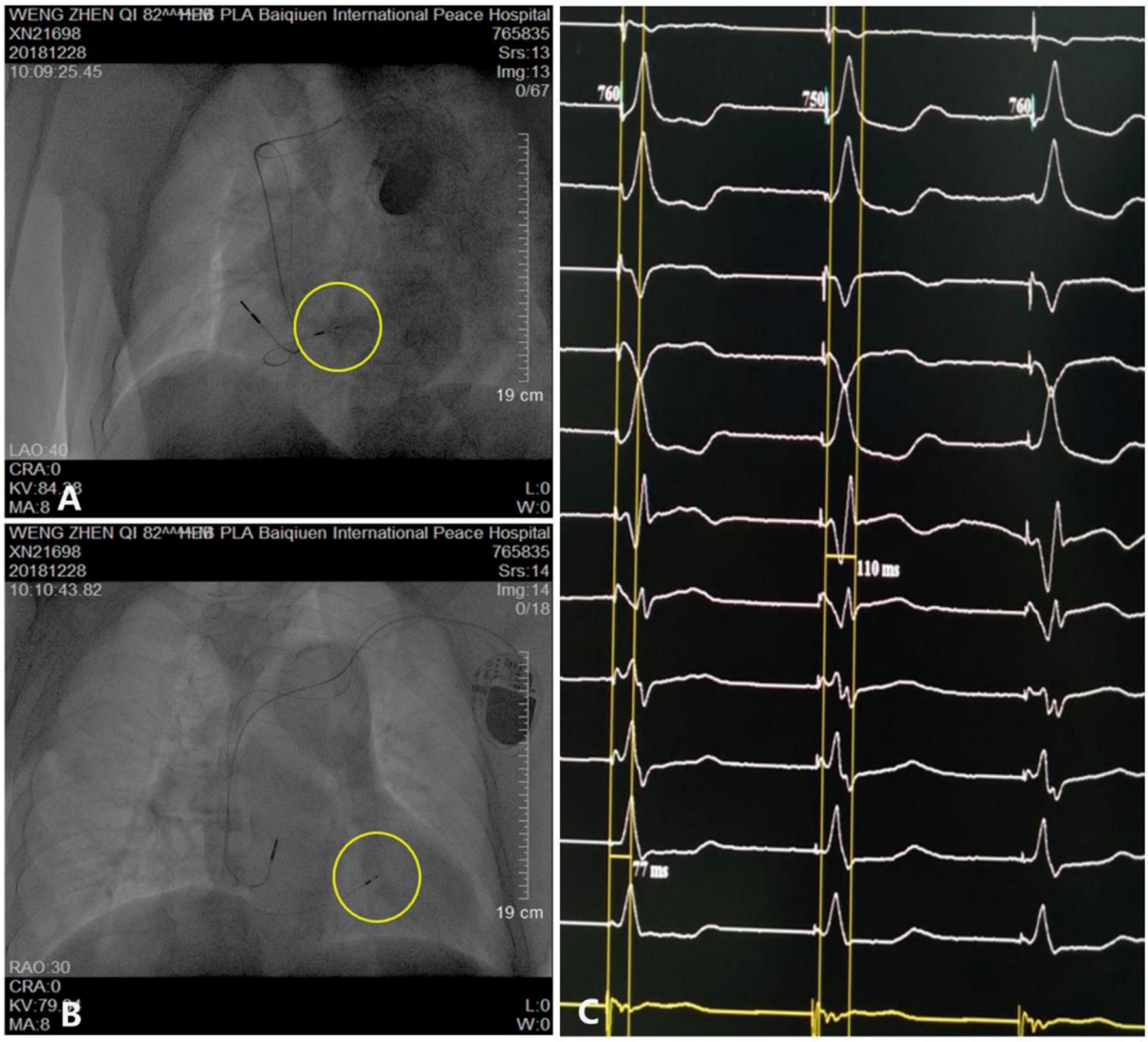

FIGURE 3
Parameters and visualization of pacemaker implantation. **(A,B)** Pacing electrode of the left bundle branch (yellow circle). **(C)** Electrocardiogram showing a QRS duration of 110 ms.

TABLE 1 Pacemaker pacing and sensing thresholds of the right atrium and left bundle branch at the time of implantation and acute myocardial infarction and during follow-up.

	2018.12.18 Pacemaker implantation	2021.02.19 AMI	2021.02.21 3 days after AMI	2021.03.05 2 weeks after AMI	2021.03.12 3 weeks after AMI	2021.04.27 2 months after AMI	2022.05.11 1.4 years after AMI
LBB pacing threshold	0.5 V/0.4 ms	5.0 V/0.4 ms	2.5 V/0.4 ms	2.0 V/0.4 ms	2.0 V/0.4 ms	2.0 V/0.4 ms	1.75 V/0.4 ms
LBB sensing threshold	10 mV	11–15.6 mV	15.6 mV	Dependence	Dependence	Dependence	Dependence
RA pacing threshold	0.5 V/0.4 ms	0.25 V/0.4 ms	0.25 V/0.4 ms	0.25 V/0.4 ms	0.25 V/0.4 ms	0.25 V/0.4 ms	0.25 V/0.4 ms
RA sensing threshold	5.0 mV	2.8 mV	2.8 mV	4.0 mV	4.0–5.6 mV	2.8 mV	4.0–5.6 mV

AMI, acute myocardial infarction; LBB, left bundle branch; RA, right atrium.

Data availability statement

The original contributions presented in the study are included in the article/supplementary material, further inquiries can be directed to the corresponding author/s.

Ethics statement

The studies involving human participants were reviewed and approved by the Ethics Committee of 980th Hospital of the Joint Logistic Support Force of PLA, Hebei Medical University. Written informed consent to participate in this study was provided by the In review participants' legal guardian/next of kin. Written informed consent was obtained from the minor(s)' legal guardian/next of kin for the publication of any potentially identifiable images or data included in this article.

Author contributions

XZ, SQ, and DW were responsible for study design and manuscript preparation. XZ, YM, and JL performed clinical data acquisition. LR contributed to the operation of PCI. XZ wrote the manuscript. All the authors contributed to the article and approved the submitted version.

Funding

This work was supported by the Key Project of Medical Science Research in the Hebei Province (grant no. 20200232).

Conflict of interest

The authors declare that the research was conducted in the absence of any commercial or financial relationships that could be construed as a potential conflict of interest.

Publisher's note

All claims expressed in this article are solely those of the authors and do not necessarily represent those of their affiliated organizations, or those of the publisher, the editors and the reviewers. Any product that may be evaluated in this article, or claim that may be made by its manufacturer, is not guaranteed or endorsed by the publisher.

References

1. Slotwiner DJ, Raitt MH, Del-Carpio Munoz F, Mulpuru SK, Nasser N, Peterson PN. Impact of physiologic pacing versus right ventricular pacing among patients with left ventricular ejection fraction greater than 35%: a systematic review for the 2018 ACC/AHA/HRS Guideline on the Evaluation and Management of Patients with Bradycardia and Cardiac Conduction Delay: A Report of the American College of Cardiology/American Heart Association Task Force on Clinical Practice Guidelines and the Heart Rhythm Society. *Circulation.* (2019) 140:e483–503. doi: 10.1161/CIR.0000000000000629

2. Upadhyay GA, Cherian T, Shatz DY, Beaser AD, Aziz Z, Ozcan C, et al. Intracardiac delineation of septal conduction in left bundle-branch block patterns. *Circulation.* (2019) 139:1876–88. doi: 10.1161/CIRCULATIONAHA.118.038648

3. Pestrea C, Gherghina A, Ortan F, Cismaru G, Radu R. Left bundle branch area pacing – restoring the natural order: a case report. *Medicine (Baltimore).* (2020) 99:e21602. doi: 10.1097/MD.0000000000021602

4. Sharma PS, Ellenbogen KA, Trohman RG. Permanent His bundle pacing: the past, present, and future. *J Cardiovasc Electrophysiol.* (2017) 28:458–65. doi: 10.1111/jce.13154

5. Huang W, Su L, Wu S, Xu L, Xiao F, Zhou X, et al. A novel pacing strategy with low and stable output: Pacing the left bundle branch immediately beyond the conduction block. *Can J Cardiol.* (2017) 33:1736.e1–e3. doi: 10.1016/j.cjca.2017.09.013

6. Liu P, Wang Q, Sun H, Qin X, Zheng Q. Left bundle branch pacing: Current knowledge and future prospects. *Front Cardiovasc Med.* (2021) 8:630399. doi: 10.3389/fcvm.2021.630399

7. Ravi V, Larsen T, Ooms S, Trohman R, Sharma PS. Late-onset interventricular septal perforation from left bundle branch pacing. *Heart Rhythm Case Rep.* (2020) 6:627–31. doi: 10.1016/j.hrcr.2020.06.008

8. Ponnusamy SS, Vijayaraman P. Aborted ST-elevation myocardial infarction – An unusual complication of left bundle branch pacing. *Heart Rhythm Case Rep.* (2020) 6:520–2. doi: 10.1016/j.hrcr.2020.05.010

9. Vijayaraman P, Subzposh FA, Naperkowski A, Panikkath R, John K, Mascarenhas V, et al. Prospective evaluation of feasibility and electrophysiologic and echocardiographic characteristics of left bundle branch area pacing. *Heart Rhythm.* (2019) 16:1774–82. doi: 10.1016/j.hrthm.2019.05.011

10. Zhang S, Zhou X, Gold MR. Left bundle branch pacing: JACC review topic of the week. *J Am Coll Cardiol.* (2019) 74:3039–49. doi: 10.1016/j.jacc.2019.10.039

11. Hou X, Qian Z, Wang Y, Qiu Y, Chen X, Jiang H, et al. Feasibility and cardiac synchrony of permanent left bundle branch pacing through the interventricular septum. *Europace.* (2019) 21:1694–702. doi: 10.1093/europace/euz188

12. Jastrzebski M, Moskal P, Bednarek A, Kielbasa G, Kusiak A, Sondej T, et al. Programmed deep septal stimulation: a novel maneuver for the diagnosis of left bundle branch capture during permanent pacing. *J Cardiovasc Electrophysiol.* (2020) 31:485–93. doi: 10.1111/jce.14352

frontiers | Frontiers in Cardiovascular Medicine

TYPE Case Report
PUBLISHED 12 October 2022
DOI 10.3389/fcvm.2022.998453

OPEN ACCESS

EDITED BY
Matteo Anselmino,
University of Turin, Italy

REVIEWED BY
Pedro Brugada,
UZ Brussel - VUB, Belgium
Hussam Ali,
Center for Clinical Arrhythmology and Electrophysiology, MultiMedica Holding SpA (IRCCS), Italy

*CORRESPONDENCE
Ying-Long Hou
houyinglong@sina.com

SPECIALTY SECTION
This article was submitted to Cardiac Rhythmology, a section of the journal Frontiers in Cardiovascular Medicine

RECEIVED 20 July 2022
ACCEPTED 26 September 2022
PUBLISHED 12 October 2022

CITATION
Ren M-Y, Zhang Y, Zhang Y-J, Gao M, Sang C-H, Cha Y-M and Hou Y-L (2022) Case report: Dual atrioventricular nodal non-reentrant tachycardia with six types of ECG patterns leading to tachycardia-induced cardiomyopathy in a 51-year-old man. *Front. Cardiovasc. Med.* 9:998453. doi: 10.3389/fcvm.2022.998453

Case report: Dual atrioventricular nodal non-reentrant tachycardia with six types of ECG patterns leading to tachycardia-induced cardiomyopathy in a 51-year-old man

Man-Yi Ren[1], Yong Zhang[1], Yu-Jiao Zhang[1], Mei Gao[1], Cai-Hua Sang[2], Yong-Mei Cha[3] and Ying-Long Hou[1]*

[1]Shandong Medicine and Health Key Laboratory of Cardiac Electrophysiology and Arrhythmia, Department of Cardiology, The First Affiliated Hospital of Shandong First Medical University & Shandong Provincial Qianfoshan Hospital, Jinan, China, [2]Department of Cardiology, Beijing Anzhen Hospital, National Clinical Research Centre for Cardiovascular Diseases, Capital Medical University, Beijing, China, [3]Division of Electrophysiology, Department of Cardiovascular Diseases, Mayo Clinic, Rochester, MN, United States

More than three types of ECG manifestations in one patient with dual atrioventricular nodal non-reentrant tachycardia (DAVNNT) are rare. We report a 51-year-old male patient with DAVNNT consisting of six types of ECG patterns leading to tachycardia-induced cardiomyopathy. After radiofrequency ablation of the slow pathway, DAVNNT was eliminated and cardiac function was restored.

KEYWORDS

dual atrioventricular nodal non-reentrant tachycardia, electrocardiogram, cardiomyopathy, slow pathway, catheter ablation

Introduction

Dual atrioventricular (AV) nodal non-reentrant tachycardia (DAVNNT) is characterized by a sinus beat resulting in consecutive double antegrade conduction via the fast and slow pathways, which produces two ventricular depolarizations (1). The 12-lead surface ECG has been regarded as the gold standard for the diagnosis of DAVNNT with "2 QRS for 1 P" manifestation (2). However, apart from the typical ECG pattern with 1:2 AV conduction over the fast and slow pathways (3–12), there are six atypical types of ECG patterns including either slow or fast pathway antegrade block

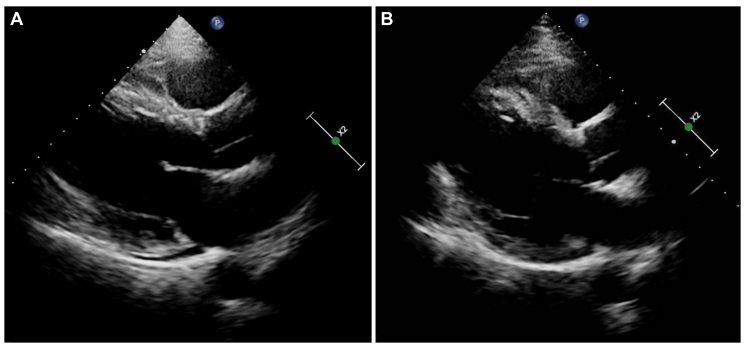

FIGURE 1
Results of transthoracic echocardiography. **(A)** On admission. **(B)** At the 3-month follow-up.

(3, 4, 6, 7), both fast and slow pathway block (4, 5), alternating pathway block (3, 4), functional bundle branch block (4, 10), and atrioventricular nodal reentry tachycardia (AVNRT) (3, 10) during 1:2 AV conduction. Additionally, DAVNNT could result in tachycardia-induced cardiomyopathy (TIC) (2, 6, 10). Nevertheless, more than three types of ECG manifestations in one patient are rare. Herein, we report a case with DAVNNT consisting of six types of ECG patterns leading to TIC.

Case description

A 51-year-old man was presented with palpitations for 9 years and had a documented history of premature atrial and ventricular contractions and paroxysmal atrial fibrillation. He was admitted for incessant narrow complex tachycardia and New York Heart Association class III heart failure. He took perindopril 4 mg twice daily, metoprolol succinate 23.75 mg once daily, furosemide 20 mg every other day, and aldosterone 20 mg every other day for half a month, which failed to alleviate his symptoms. His physical examination and laboratory tests were unremarkable. Computed tomography angiography excluded coronary artery disease. Transthoracic echocardiography (TTE) revealed a dilated cardiomyopathy with global hypokinesis, left ventricular end-diastolic diameter (LVEDD) 68 mm, and left ventricular ejection fraction (LVEF) 39% (**Figure 1A**). A 12-lead ECG showed a narrow complex tachycardia with 510 and 400 msec alternating R-R intervals. Each P wave was followed by 2 QRS, suggesting 1:2 AV conduction through the fast and slow AV nodal pathways and possible DAVNNT (**Figure 2A**).

Different patterns of AV conduction recorded from Holter monitoring were displayed in **Figure 3**. Pattern 1 showed a continuous manifest 1:2 AV conduction over the fast and slow pathways (**Figure 3A**). Pattern 2 was defined as the slow pathway with a 2:1 conduction block (**Figure 3B**). Pattern 3 occurred when the conduction of the fast pathway was intermittently blocked (2:1) (**Figure 3C**). Pattern 4 was classified as the alternating conduction block of the fast and slow pathways (**Figure 3D**). Pattern 5 was typified by the simultaneous antegrade 2:1 conduction block with the dual AV pathways (**Figure 3E**). In pattern 6, there was 1:2 conduction with persistent or intermittent left or right bundle branch block (**Figures 3F,G**).

The electrophysiological study (EPS) revealed that each sinus beat was conducted down both the fast and slow pathways, resulting in 2 QRS, which could be reproduced by atrial extra stimulus (**Figure 4**). Atrial programmed extra stimulation at $CS_{7,8}$ was performed using a driving cycle length (S_1) of 600 msec. When the S_1S_2 interval was reduced to 350 msec, a marked AH jump from 172 to 328 msec was observed, which did not trigger an atrial echo and AVNRT even with intravenous isoprenaline. There was no retrograde ventriculoatrial (VA) conduction. Radiofrequency ablation of the slow pathway subsequently eliminated the tachycardia and restored 1:1 AV conduction (**Figure 2B**). Oral medications except metoprolol succinate 11.875 mg once daily after discharge was the same as at admission. At the 3-month follow-up, the patient was free of symptoms. Holter recordings showed no recurrent 1:2 AV conduction. LVEF improved to 67% and the LVEDD decreased to 56 mm (**Figure 1B**).

Discussion

In 1975, the dual ventricular response was first described as a manifestation of dual AV nodal physiology in which a premature atrial depolarization was conducted down both the fast and slow pathways, called "double fire" (9) and subsequently named DAVNNT (12). The surface ECG characterizes a sinus P wave followed by two narrow QRS complexes (2). However, when the frequency of the sinus P wave is over 100 bpm, the ventricular rate will amount to 200 bpm or more. Meanwhile, the sinus P waves could be superimposed on the preceding QRS complexes, T waves, and ST segments, making DAVNNT diagnosis difficult

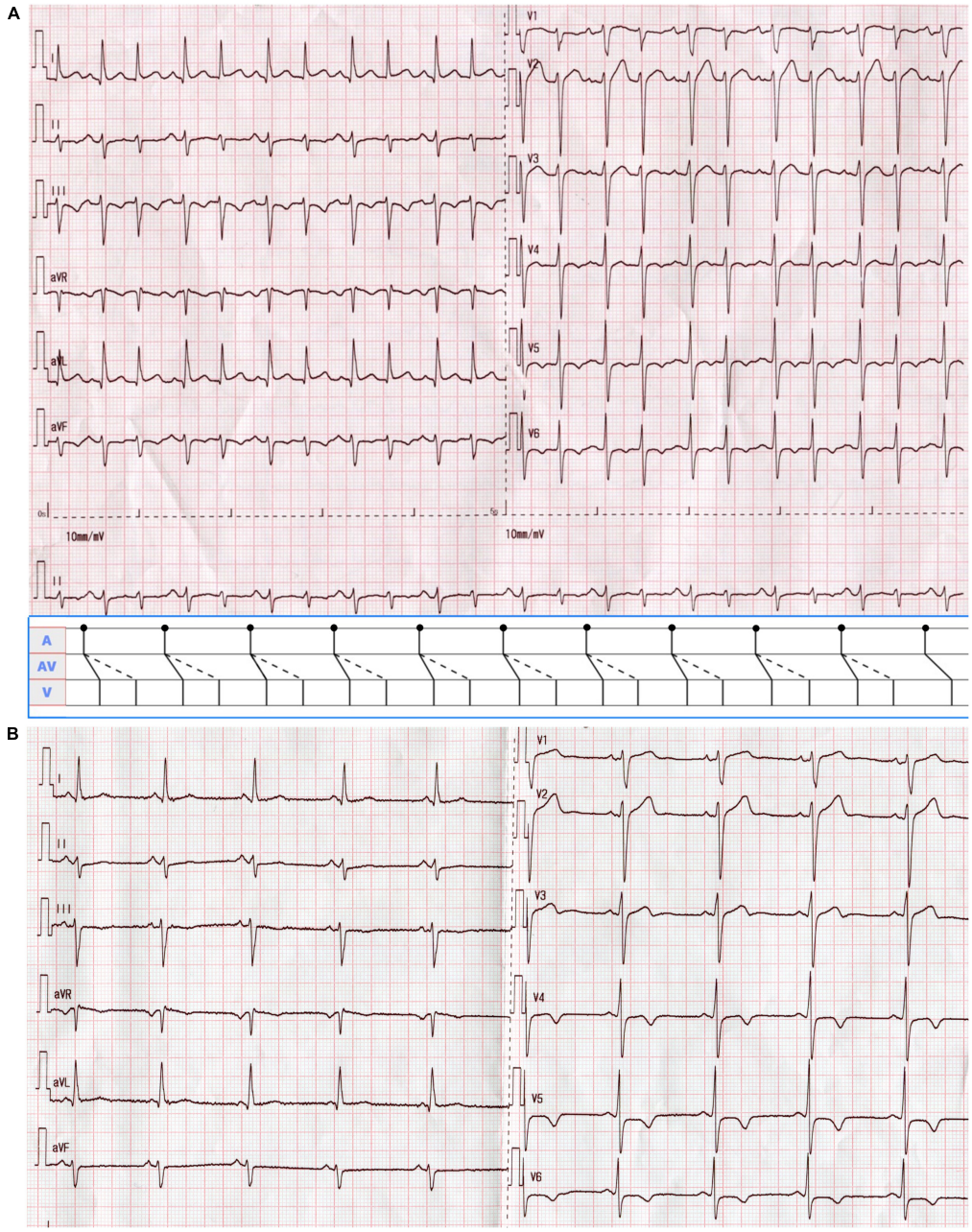

FIGURE 2
(A) A 12-lead ECG on admission showed supraventricular tachycardia with alternating RR intervals at a rate of 133 beats/min. The P wave was positive in lead II, negative in aVR, and biphasic in V_1, suggesting a sinus rhythm of 66 beats/min. Each sinus beat was simultaneously conducted through the anterograde fast and slow AV nodal pathways, giving rise to a double ventricular response. QRS alternans were present as the first and second QRS complexes during 1:2 AV conduction were of different amplitudes. As shown in the ladder diagram, dots indicate the beginnings of the P waves. Solid oblique and dashed lines in the AV portion of the diagram denote conduction over the fast and slow pathways, respectively. **(B)** The surface ECG returned to normal after radiofrequency ablation.

(**Figures 3E–G**). Hence, DAVNNT is often misdiagnosed as premature atrial or ventricular complexes, supraventricular tachycardia, atrial fibrillation, and ventricular tachycardia, leading to inappropriate referral for pulmonary vein isolation (11) and improper implantation of a pacemaker (7). A misdiagnosis (1) may result in TIC, as in our case, for 9 years.

Seven ECG patterns of DAVNNT from different patients have been reported. More than three ECG manifestations in one patient are rare (3, 4). Our case showed six different

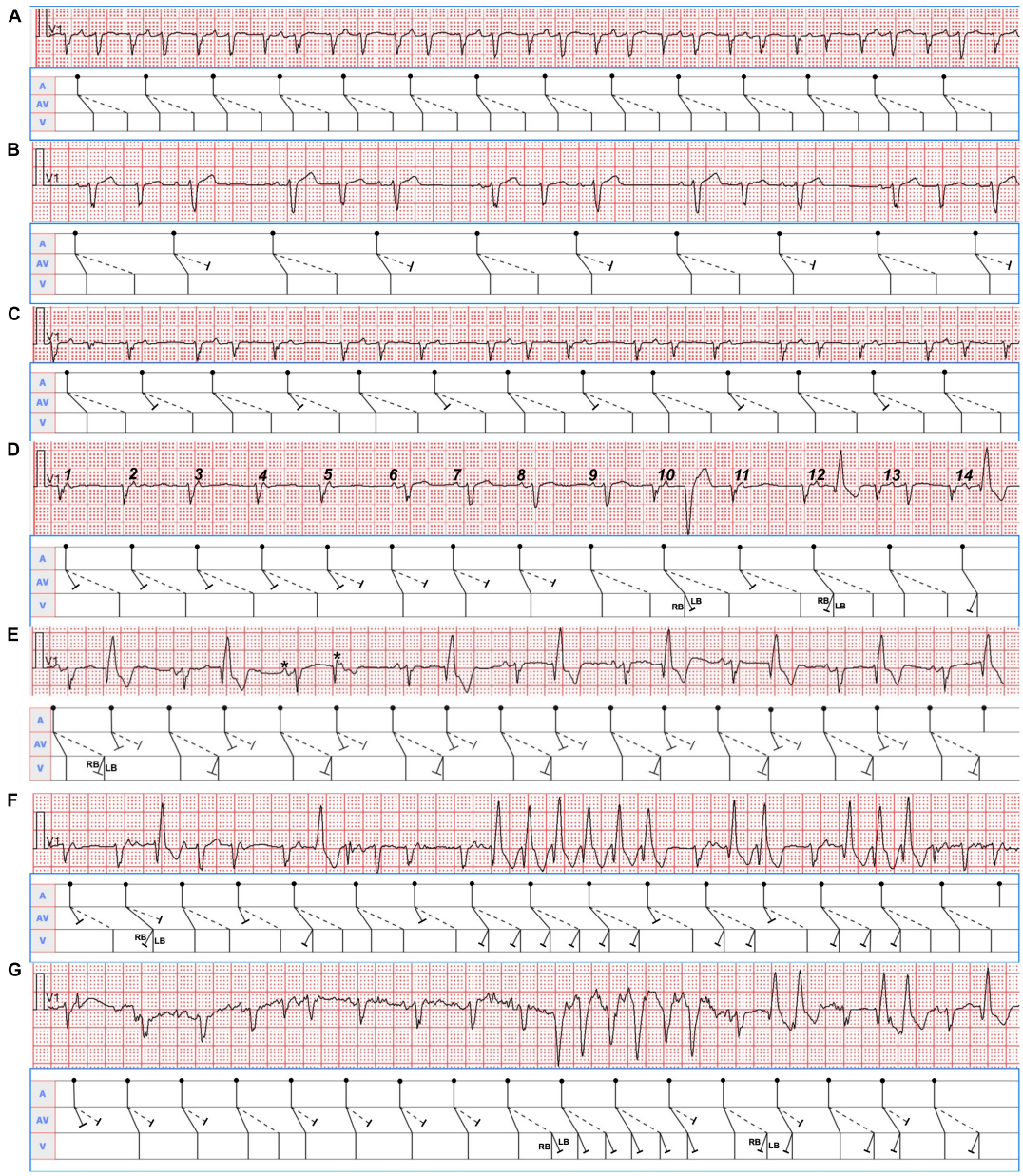

FIGURE 3
Seven typical Holter recording strips in lead V_1 were shown. The corresponding mechanism was explained in the ladder diagram below each of them. RB, right bundle; LB, left bundle. **(A)** The sinus P waves (PP intervals 740 msec) were conducted simultaneously over the dual AV nodal pathways, producing a double ventricular response. **(B)** Group beatings with PP intervals of 1,120 msec were presented. A group of three was seen throughout the tracing follow by a pause, suggesting sinus beats conducted with alternating 1:2 and 1:1 AV ratios with longer PR intervals (160 msec) during 1:1 conduction over the fast pathways. **(C)** The sinus beats (PP intervals 820 msec) in the group beatings conducted with alternating 1:1 and 1:2 AV ratios with shorter PR intervals (580 msec) during 1:1 conduction over the slow pathways. **(D)** The front 5 and eleventh P waves were conducted only through the slow pathways, then the sixth to eighth P waves only *via* the fast pathways, and the ninth, tenth, twelfth, and thirteenth P waves simultaneously over the dual AV pathways. The tenth P wave with a PR interval of 240 msec gave rise to a QRS complex with left bundle branch block (LBBB) morphology, whereas the twelfth and fourteenth P waves with a PR interval of 220 msec produced a QRS wave with right bundle block (RBBB) pattern. The front 7 PP intervals were 720 msec, whereas the remaining PP intervals were approximately 840 msec. **(E)** The remaining adjacent PP intervals will be determined according to the PP interval of 600 msec consisting of two P waves marked with asterisks. The 2:1 conduction block occurred when the sinus beats were conducted simultaneously *via* the fast and slow pathways. Additionally, RBBB aberrancy except the sixth QRS complex were presented with conduction through the slow pathways. **(F)** Single, double, triple, and especially six consecutive QRS complexes with RBBB configuration from the conduction *via* the fast and slow pathways were shown in the lead V_1 rhythm strip. It was the most difficult to identify them due to the superimposition of the P waves (PP intervals 640 msec) on the QRS complexes. **(G)** As a result of the conduction *via* the fast and (or) slow pathways, single and double QRS complexes with RBBB pattern as well as six consecutive QRS complexes with LBBB morphology coexisted in the lead V_1 rhythm strip. Likewise, the P waves with PP intervals of 620 msec were superimposed on the QRS complexes when LBBB or RBBB occurred, which made them unrecognizable.

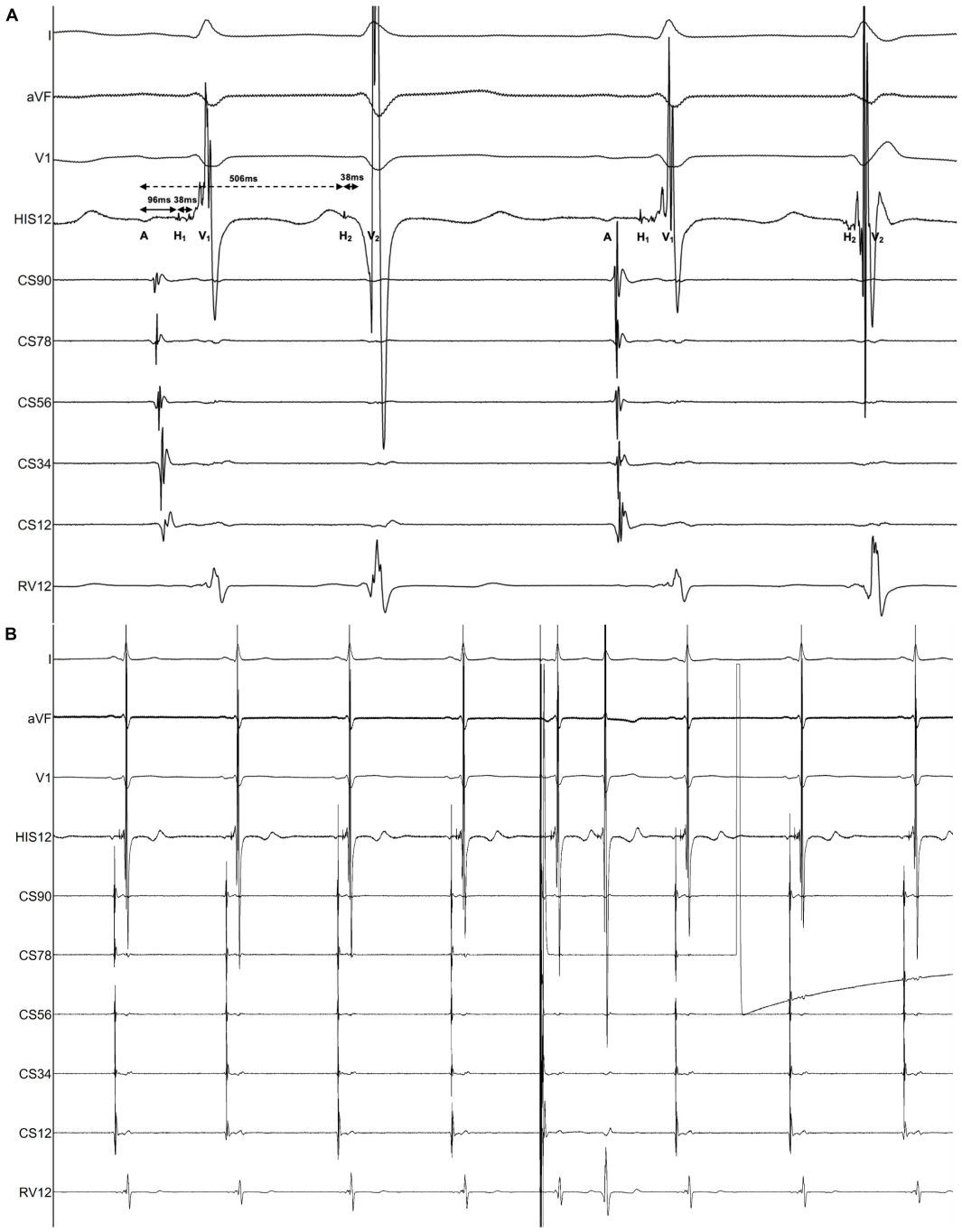

FIGURE 4
Findings of the electrophysiological study. The intracardiac recording confirmed the diagnosis of dual AV nodal non-reentrant tachycardia (DAVNNT). **(A)** One atrial impulse (A) triggered one hissian potential (H_1) and one ventricular potential (V_1) through the fast pathway, and then one H_2 and one V_2 through the slow pathway. The time difference between the fast pathway with an AH interval of 96 msec and the slow pathway with an AH interval of 506 msec was long enough to result in a double ventricular response. The HV interval of both fast and slow pathways was 38 msec. This recording was taken at a sweep speed of 100 mm/s. **(B)** Atrial extra systolic stimulation can reproducibly induce a 1:2 conduction over the fast and slow pathways, corroborating the diagnosis of DAVNNT. A paper speed was 25 mm/s.

ECG presentations. The variable ECG manifestations are attributable to the fact that dual AV nodal pathways have distinct refractory periods, different conduction velocities, Wenckebach-type block, and unidirectional block (3), and various degrees of concealed retrograde conduction under different physiologic states (7). Specifically, in **Figure 3B**, slow

pathway conduction prolonged the following fast pathway conduction by retrograde concealed penetration of the fast pathway, which made the ensuing slow pathway conduction blocked due to concealed conduction. As the second P wave did not conduct down the slow pathway, there was no retrograde concealed conduction to the fast pathway, elucidating the short fast pathway conduction following the third P wave. Similarly, in **Figure 3C**, slow pathway conduction blocked the following fast pathway conduction by retrograde concealed penetration of the fast pathway, making the second PR interval of slow pathway conduction 80 msec shorter compared with the first PR interval. In **Figure 3D**, after Mobitz type I AV block (Wenckebach) conduction in the front 5 P waves occurred only along with slow pathway, the fast pathway exhibited Wenckebach conduction in the sixth to eleventh P waves. In **Figure 3E**, the third PR interval down the slow pathway was 20 msec longer than the remaining PR intervals, so the fifth P wave can conduct through the slow pathway and produce a normal QRS complex. In **Figures 3F,G**, the QRS complexes displayed functional RBBB and LBBB morphologies because of different PP intervals (rate-dependent aberrancy), retrograde concealed conductions, and changes in autonomic nervous tension. Taken together, different sinus rates led to different manifestations of DAVNNT. Therefore, knowing all of the six ECG presentations of DAVNNT will help early diagnosis and management.

The differential diagnosis of 12-lead ECG presentation, in this case, included (1) orthodromic atrioventricular reentry tachycardia (AVRT) with alternating AV conduction over a slow and a fast AV nodal pathway as well as VA conduction over an accessory pathway, (2) AVNRT with reentrant circuit using two distinct, beat-to-beat alternating slow AV nodal pathways anterogradely and a single fast pathway retrogradely, (3) atrial bigeminy, and (4) junctional bigeminy with a retrograde conduction block. However, the regular presence of sinus P waves excluded both AVRT and AVNRT. Additionally, atrial bigeminy can be ruled out due to the absence of atrial P waves preceding the QRS complexes with a short cycle length. In addition, some typical rhythm strips in lead V_1 from Holter ECG tracings (**Figure 3**) demonstrated that each sinus P wave was conducted simultaneously over the fast and slow pathways, and produced two QRS complexes, which were further corroborated by EPS. Remarkably, the antegrade fast pathway is more sensitive to the effects of adenosine than the slow pathway. A positive adenosine test verified by a PR jump can identify dual AV node physiology on surface ECG recording (13).

No medications appear highly successful in suppressing DAVNNT. Radiofrequency ablation or cryoablation of the slow pathway can eliminate DAVNNT and restore left ventricular function (1).

Limitations

The Holter tracings in **Figures 3B–G** were not verified by EPS, which did not influence the correct explanations in the ladder diagrams.

Conclusion

This is the first case that reveals six ECG patterns of DAVNNT leading to TIC. Radiofrequency ablation of the slow pathway eliminated DAVNNT and restored cardiac function.

Data availability statement

The raw data supporting the conclusions of this article will be made available by the authors, without undue reservation.

Ethics statement

The studies involving human participants were reviewed and approved by the Ethics Committee of the First Affiliated Hospital of Shandong First Medical University. The patients/participants provided their written informed consent to participate in this study and for the publication of this case report.

Author contributions

M-YR, YZ, Y-JZ, and C-HS contributed to the clinical treatment of this case. M-YR wrote the manuscript. Y-MC, Y-LH, and MG revised the manuscript. All authors contributed to the article and approved the submitted version.

Funding

This work was supported by the Shandong Medical and Health Science and Technology Development Plan Project (Grant No. 202003010975).

Conflict of interest

The authors declare that the research was conducted in the absence of any commercial or financial relationships that could be construed as a potential conflict of interest.

Publisher's note

References

1. Wang NC. Dual atrioventricular nodal nonreentrant tachycardia: a systematic review. *Pacing Clin Electrophysiol.* (2011) 34:1671–81. doi: 10.1111/j.1540-8159.2011.03218.x

2. Peiker C, Pott C, Eckardt L, Kelm M, Shin DI, Willems S, et al. Dual atrioventricular nodal non-re-entrant tachycardia. *Europace.* (2016) 18:332–9. doi: 10.1093/Europace/euv056

3. Elizari MV, Sanchez RA, Chiale PA. Manifest fast and slow pathway conduction patterns and reentry in a patient with dual av nodal physiology. *J Cardiovasc Electrophysiol.* (1991) 2:98–102. doi: 10.1111/j.1540-8167.1991.tb01308.x

4. Ajiki K, Murakawa Y, Yamashita T, Oikawa N, Sezaki K, Otsuka Y, et al. Nonreentrant supraventricular tachycardia due to double ventricular response via dual atrioventricular nodal pathways. *J Electrocardiol.* (1996) 2:155–60. doi: 10.1016/s0022-0736(96)80126-9

5. Germano JJ, Essebag V, Papageorgiou P, Josephson ME. Concealed and manifest 1:2 tachycardia and atrioventricular nodal reentrant tachycardia: manifestations of dual atrioventricular nodal physiology. *Heart Rhythm.* (2005) 2:536–9. doi: 10.1016/j.hrthm.2005.01.025

6. Clementy N, Casset-Senon D, Giraudeau C, Rosnay P. Tachycardiomyopathy secondary to nonreentrant atrioventricular nodal tachycardia: recovery after slow pathway ablation. *Pacing Clin Electrophysiol.* (2007) 30:925–8. doi: 10.1111/j.1540-8159.2007.00784.x

7. Wang NC, Shah H, Jain SK, Saba S. Dual atrioventricular nodal nonreentrant tachycardia with alternating 1:1 and 1:2 AV conduction: mechanistic hypotheses and total suppression using right atrial pacing. *Ann Noninvasive Electrocardiol.* (2013) 18:199–203. doi: 10.1111/j.1542-474X.2012.00539.x

8. Zhao YT, Wang L, Yi Z. Tachycardia-induced cardiomyopathy in a 43-year-old man. *Circulation.* (2016) 134:1198–201. doi: 10.1161/CIRCULATIONAHA.116.024208

9. Wu D, Denes P, Dhingra R, Pietras RJ, Rosen KM. New manifestations of Dual A-V nodal pathways. *Eur J Cardiol.* (1975) 2:459–66.

10. Anselme F, Frederiks J, Boyle NG, Papageorgiou P, Josephson ME. An unusual cause of tachycardia-induced myopathy. *Pacing Clin Electrophysiol.* (1996) 19:115–9. doi: 10.1111/j.1540-8159.1996.tb04800.x

11. Mansour M, Marrouche N, Ruskin J, Natale A, Keane D. Incessant nonreentrant tachycardia due to simultaneous conduction over dual atrioventricular nodal pathways mimicking atrial fibrillation in patients referred for pulmonary vein isolation. *J Cardiovasc Electrophysiol.* (2003) 14:752–5. doi: 10.1046/j.1540-8167.2003.02527.x

12. Wang NC, Razak EA, Jain SK, Saba S. Isoproterenol facilitation of slow pathway ablation in incessant dual atrioventricular nodal nonreentrant tachycardia. *Pacing Clin Electrophysiol.* (2012) 35:e31–4. doi: 10.1111/j.1540-8159.2010.02875.x

13. Toal SC, Vajifdar BU, Gupta AK, Vora AM, Lokhandwala YY. Adenosine induced PR jump on surface ECG to differentiate atrioventricular nodal re-entrant tachycardia from concealed accessory pathway mediated tachycardia: a bedside test. *Heart.* (2002) 87:37–40. doi: 10.1136/heart.87.1.37

frontiers | Frontiers in Cardiovascular Medicine

TYPE Case Report
PUBLISHED 24 October 2022
DOI 10.3389/fcvm.2022.1005596

OPEN ACCESS

EDITED BY
Matteo Anselmino,
University of Turin, Italy

REVIEWED BY
Jean-Benoît Le Polain de Waroux,
AZ Sint-Jan Brugge-Oostende AV, Belgium
Nikolaos Fragakis,
Aristotle University Medical School, Greece

*CORRESPONDENCE
Cheng-Han Lee
appollolee@yahoo.com.tw
Ju-Yi Chen
juyi@mail.ncku.edu.tw

SPECIALTY SECTION
This article was submitted to Cardiac Rhythmology, a section of the journal Frontiers in Cardiovascular Medicine

RECEIVED 28 July 2022
ACCEPTED 10 October 2022
PUBLISHED 24 October 2022

CITATION
Li Y-P, Lee C-H and Chen J-Y (2022) Proposed strategies to overcome venous occlusion in the implantation of a cardiac implantable electronic device: A case report and literature review.
Front. Cardiovasc. Med. 9:1005596.
doi: 10.3389/fcvm.2022.1005596

Proposed strategies to overcome venous occlusion in the implantation of a cardiac implantable electronic device: A case report and literature review

Yi-Pan Li, Cheng-Han Lee* and Ju-Yi Chen*

Division of Cardiology, Department of Internal Medicine, National Cheng Kung University Hospital, College of Medicine, National Cheng Kung University, Tainan, Taiwan

This case report describes a successful balloon venoplasty to overcome a total occlusion from the brachiocephalic vein to the superior vena cava in a patient undergoing cardiac resynchronization therapy. It is crucial for implanting physicians to be familiar with strategies to overcome venous occlusion in lead implantation, especially balloon venoplasty, which is an effective and safe approach.

KEYWORDS

venous occlusion, balloon venoplasty, cardiac implantable electronic device, cardiac synchronization therapy, pacemaker

Introduction

Cardiac synchronization therapy (CRT) has been shown to reduce morbidity and mortality in patients with symptomatic heart failure with left ventricular (LV) systolic dysfunction with broad QRS duration and is strongly recommended in the clinical guidelines (1). Venous occlusion is not an uncommon condition, with an incidence rate of 13.7% in patients without a previous transvenous implanted device. Approximately 31–67% of patients with previous transvenous cardiac implantable electronic devices (CIED) experience some degree of venous occlusion (2, 3), which causes difficulty in lead implantation. We report a successful implantation of three leads after balloon venoplasty to recanalize the total occlusion of the brachiocephalic vein and superior vena cava (SVC) for CRT.

Case presentation

A 78-year-old woman was admitted to our department with the diagnosis of New York Heart Association class III heart failure with a reduced ejection fraction (HFrEF) (LV ejection fraction: 19%) and one prior drug-eluting stent for the left anterior descending artery. The 12-lead electrocardiography (ECG) showed complete left bundle branch block (LBBB) with QRS duration of 174 msec. In the past 2 years, her LV systolic function didn't improve despite optimal guideline-directed medical therapy with

sacubitril/valsartan, spironolactone, and furosemide. We didn't prescribe beta-blockers due to intolerance. CRT was indicated according to the 2021 ESC guideline (1).

She was diagnosed with right breast cancer 14 years ago in 2008 and underwent neoadjuvant chemotherapy and modified radical mastectomy, followed by adjuvant radiotherapy with 5,000 cGY and hormone therapy with letrozole for 2 years. A Port-a-Cath was implanted *via* her left subclavian vein (SCV) in 2008 and was removed in 2014. The preprocedural venogram showed partial stenosis in the proximal left SCV, severe stenosis in brachiocephalic vein and Standford type III SVC occlusion (4) (Figure 1A). The SVC chronic complete occlusion was compensated by collateral flow and thus prevented this patient from clinical symptoms.

We performed a balloon venoplasty and biventricular pacing CRT(BiV-CRT) implantation with the assistance of a vascular interventionist. We inserted a 6-French (Fr) Merit sheath *via* the left SCV. With the support of a Mustang balloon (3.0 × 40 mm), we passed a 0.035-inch TERUMO GLIDEWIRE® through the stenotic lesion of the left SCV and the brachiocephalic vein but could not cross the SVC total occlusion (Figure 1B). We escalated the wire to a 0.018-inch Hi-Torque Connect™ wire (Figure 1C) but we still failed to pass it through the lesion. Thus, we used right femoral venous access with an 8-Fr Cordis sheath.

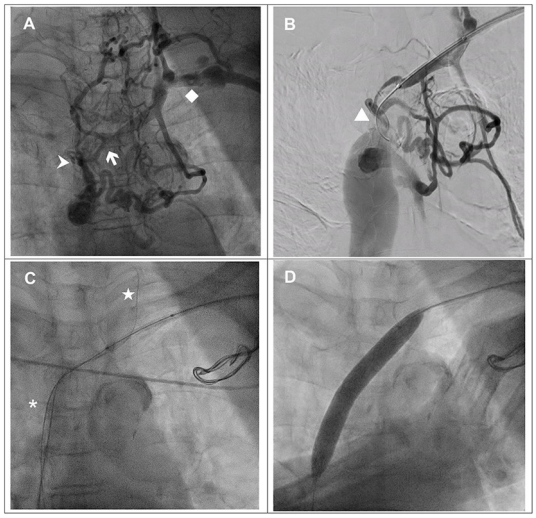

FIGURE 1
(A) Venography *via* the left upper arm demonstrated total occlusion from the brachiocephalic vein (white arrow) to the superior vena cava (SVC) (arrowhead) with abundant collaterals. Left subclavian vein (♦). **(B)** TERUMO GLIDEWIRE® (▲) with support of a Mustang balloon (3.0 × 40 mm) failed to cross the junction of the brachiocephalic vein and SVC. **(C)** TERUMO GLIDEWIRE® (★) with the support of a multipurpose catheter was advanced to the left internal jugular vein. The antegrade Hi-Torque Connect™ guidewire was successfully advanced to the inferior vena cava. **(D)** A Mustang balloon (12.0 × 80 mm) was used to dilate the SVC and brachiocephalic vein with 6 atm.

With the support of a 6-Fr Multipurpose (MP-1) catheter, the TERUMO GLIDEWIRE® was advanced to left IJV. Under the guidance of the retrograde guidewire, the antegrade Hi-Torque Connect™ wire crossed the SVC total occlusion and was advanced to the inferior vena cava (Figure 1C). A Mustang balloon (3.0 × 40 mm) and a Mustang balloon (12.0 × 80 mm) were used to dilate the brachiocephalic vein and the SVC sequentially (Figure 1D). The post-dilation angiogram revealed patent flow (Figure 2A).

Subsequently, the coronary sinus was cannulated, and a passive fixation LV lead (Medtronic 4598–88 cm) was implanted in the lateral vein with the parameters of *R* wave 0.6 mV, impedance 652 ohm, threshold 0.8 V @ 0.5 ms and 93.3% biventricular pacing. An active fixation lead in the right ventricle (Medtronic 5076–58 cm), an active fixation lead in the right atrium (Medtronic 5076–52 cm) and a generator (Medtronic Percepta™) with DDDR mode were implanted smoothly (Figure 2B). The total procedural time was 152 min, and the fluoroscopy time was 16 min. Postprocedural chest X-ray revealed no pneumothorax. The 12-lead ECG after CRT implantation showed a narrower QRS of 150 ms with biventricular paced rhythm.

Discussion

Consideration of BiV CRT and conduction system pacing for CRT

The conduction system pacing with His-bundle pacing (HBP) or left bundle branch area pacing (LBBAP) for cardiac resynchronization has become promising as an alternative for BiV-CRT, especially in patients with unsuitable coronary sinus anatomy. Currently, the majority of the studies are observational and nonrandomized (5). A recent small, randomized study including 40 patients demonstrated that LBBAP for CRT had greater LVEF improvement than BiV-CRT in heart failure with non-ischemic cardiomyopathy and LBBB (6). Large randomized

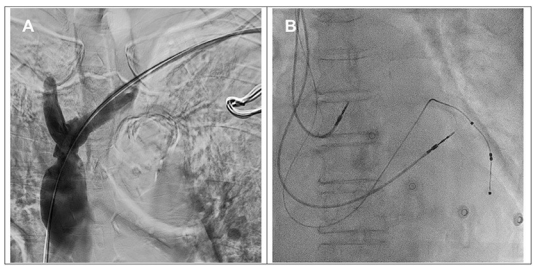

FIGURE 2
(A) The angiogram showed a patent brachiocephalic vein and superior vena cava after balloon venoplasty. **(B)** Implantation of right atrial, right ventricular and left ventricular leads.

controlled studies are required to verify the possible morbidity and mortality benefit of conduction system pacing for CRT. According to the current guideline, BiV-CRT has more solid evidence of efficacy and safety and is the first-line therapy. In CRT candidates with unsuccessful coronary sinus lead implantation, HBP should be considered as an option along with other techniques such as surgical epicardial lead (Class IIa recommendation in ESC 2021 guideline). LBBAP has not yet been recommended as an alternative option for BiV-CRT in current guideline (1).

Risk factors for venous occlusion and re-occlusion after lead implantation in our case

Venous occlusion due to fibrosis or thrombosis is not uncommon. The incidence of venous occlusion of various degrees was reported to be 13.7–25% with a total occlusion rate of 6.8–26% in patients without preexisting CIED. After prior lead implantation, the incidence raised to 31–67% (2, 3, 7). Due to the development of adequate venous collateral circulation, patients seldom present with clinical symptoms (2). Other etiologies of venous occlusion include a history of venous thrombosis, hypercoagulable state, use of temporary pacing lead, hormone therapy, temporary or implanted venous access for hemodialysis, chemotherapy and parenteral nutrition (8). Therefore, venography prior to CIED implantation should be considered for planning venous access and identifying venous occlusion (1, 9).

Our patient had Port-A-Cath implantation *via* the left SVC and the catheter remained for 6 years. She underwent radiotherapy and hormone therapy for right breast cancer, which could contribute to venous occlusion. Venous access *via* the right side was abandoned due to the history of right breast cancer and radiotherapy.

For patients with an implanted transvenous device, the rate of occlusion increases over time. The incidence of occlusion was 23% between 1 and 6 months and increased to 35% between 6 and 12 months after transvenous device implantation (10). The bending point of the vessel with persistent contact to the endothelium irritates the vessel wall and leads to fibrosis and occlusion (10). Radiation would injure the microvasculature of the vessel walls, lead to hypoxia, stimulate proliferation in the intima and then cause thickening or focal plaque. The neurotransmitters are also released in damaged vessels and cause vascular spasm or occlusion (11).

Our purpose of venoplasty was to create the route for lead implantation in an asymptomatic patient. According to the current guideline (9), it is considered reasonable that up to 5 leads are implanted in the SVC of older patients, and 3 to 4 leads are implanted in the SCV. The number of leads and sum of the lead diameters have been reported to be independent predictors of risk for venous stenosis and occlusion after CIED implantation (3, 9). The re-occlusion risk is high after lead implantation, but venous occlusion is generally asymptomatic due to gradual development of collaterals. The pacemaker-induced SVC syndrome has been reported to be 0.1% (9). Lead removal, venoplasty and subsequent stent placement in SVC are recommended in patients with SVC syndrome (9).

Strategies to overcome a difficult venous access

Strategies to overcome venous occlusion in lead implantation have been reviewed (12). In patients with previously implanted pacemaker leads requiring upgrading or revision, there were several approaches for venous occlusion, including contralateral implantation of a new system, new lead with subcutaneous tunneling to the old pocket, recanalization by lead extraction (*via* extraction sheaths, creating access for new leads) and recanalization without lead extraction requiring special equipment, such as a laser tool (12). Other vascular access options include gaining access medially to the occlusive site *via* internal jugular vein, external jugular vein or supraclavicular approach for subclavian vein, and femoral/iliac vein access with abdominal/femoral pockets (13). Alternatively, Elayi et al. (14) detailed inside-out central venous access (IOCVA) retrogradely from the right femoral vein to facilitate lead placement in patients with central venous occlusion.

Implantable leadless pacemakers have become a reality since 2012. Leadless pacemaker systems, including FDA-approved Nanostim™ and Micra™, are suitable for patients with indications for VVI pacing, such as fixed atrial arrhythmia with symptomatic bradycardia. The VVI pacing mode cannot maintain AV synchrony and sometimes causes pacemaker syndrome. It was also shown that leadless pacemaker therapy resulted in worsening biventricular function and mitral regurgitation and had an equivalent rate of deterioration in tricuspid regurgitation compared to a transvenous pacemaker (15). Although one study including 198 patients with 100% right ventricular pacing reported a 3 vs. 14% incidence of pacing-induced cardiomyopathy (PICM) in leadless and transvenous pacemaker groups, larger studies are required to confirm the stated lower incidence of PICM in patients with leadless pacemakers (16). Surgical epicardial lead implantation or endocardial lead placement *via* trans-atrial access should be the last resort due to invasiveness. Our patient needed CRT to restore LV systolic function; therefore, a current FDA-approved leadless pacemaker was not indicated. It has been reported in the WiSE-CRT study that the WiCS®-LV system for leadless CRT was successfully implanted in 13 patients (76%). Although the study showed short-term effectiveness of QRS duration shortening and LVEF improvement, the long-term effectiveness and safety were unclear. In addition, three patients developed

TABLE 1 Characteristics and disadvantages of strategies to overcome venous occlusion in lead implantation (7, 9, 13).

	Characteristics	Disadvantages
Contralateral implantation		
A. Create a new system or	✓ Straightforward option at the time of upgrade or revision	× Adding leads without extraction, causing the future lead revision more challenging
B. Tunneling to the old pocket	✓ Fast and effective	× Increased rate of SVC occlusion due to greater sum of the lead diameters
	✓ Lower risk of vascular injury	× New pocket or tunneling requiring second incision, associated with risk of infection
		× Tunneled leads fracture and erosion
Restore venous patency		
Recanalization with lead extraction	✓ Preserves the contralateral side for potential future use	× Risk of major complications including cardiac avulsion, vascular laceration, pericardial effusion and death, etc.
	✓ Reduced overall lead burden	× Loss of functional lead
Recanalization without lead extraction		
Antegrade and retrograde wiring with balloon venoplasty	✓ Fast and effective	× Risk of vascular perforation during inflation or advancement of lead after venoplasty
	✓ Preserve contralateral venous access	× Increased overall lead burden by leaving redundant lead(s) behind
Excimer laser	✓ Can be used to cross wire-refractory chronic total occlusion	× Risk of vascular perforation or arteriovenous fistula
		× Thermal damage to surrounding tissue
		× Require special skill and equipment
Retrograde approach with IOCVA	✓ Preserve contralateral venous access if the wire exit on the same side of preexisting leads	× Increased complexity and operative time
		× Concern for vascular injury, pneumothorax or hemothorax when blindly passing a wire
		× Require special skill and equipment
Other transvenous access		
Supraclavicular venous access (IJV, EJV and supraclavicular puncture for SCV) with lead tunneling to infraclavicular pocket	✓ Straightforward option to bypass the occlusion in distal SCV	× Lead traversing over the clavicle, prone to skin erosion, pain and lead fracture, overcome by subclavian tunneling but with more extensive surgical dissection
		× The route is often tortuous in EJV, making it hard to place the pacing leads to RV
		× Only feasible in distal occlusion of SCV
Infraclavicular venous access (femoral or iliac vein)	✓ No risk of pneumothorax	× High lead dislodgement rate for the atrial (11–21%) and ventricular leads (5–7%)
	✓ Easier to achieve hemostasis by manual compression	× Higher risk of device infection
		× Concern about femoral vein thrombosis
No transvenous lead implantation		
Leadless pacemaker	✓ Alternatives for patients without upper limb venous access	× Higher risk of cardiac perforation and vascular complications
	✓ No risk of pneumothorax	× Only single chamber pacemaker with VVI mode
		× Not all modalities can provide AV synchrony
Surgical epicardial lead	✓ For congenital heart disease in which transvenous lead is not feasible	× Increased peri-operative mortality and prolonged hospital stay for 4–5 days
	✓ Bail-out option	× Higher pacing thresholds
		× Greater incidence of lead fractures

EJV, external jugular vein; IJV, internal jugular vein; SCV, subclavian vein; SVC, superior vena cava; IOCVA, inside-out central venous access; RV, right ventricle; AV, atrioventricular.

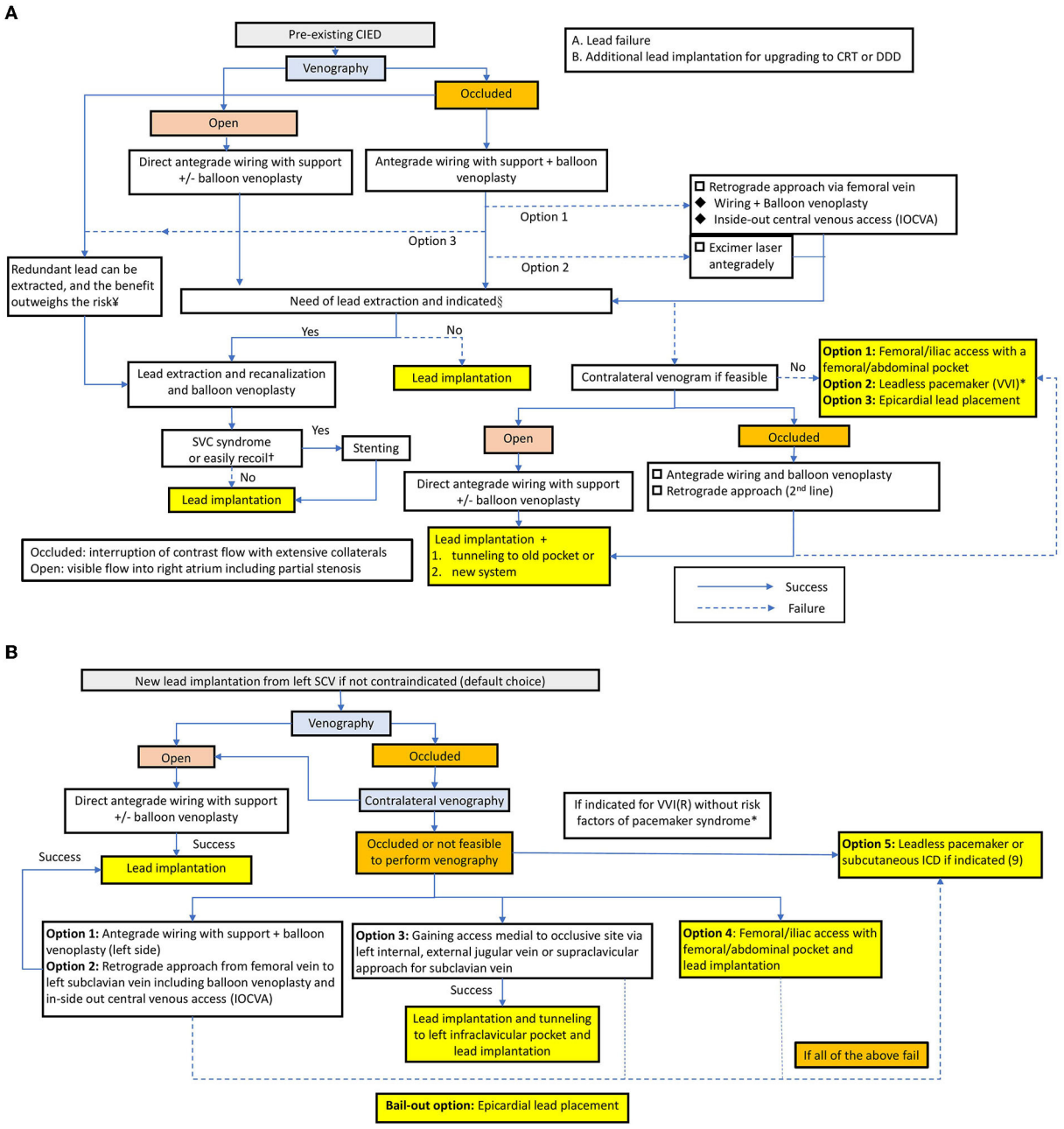

FIGURE 3
(A) Treatment algorithm in patients with a preexisting CIED. *In the setting of the pre-existing VVI mode with lead failure. §According to the Heart Rhythm Society expert consensus statement (9), the indications are as follows. Class I: Lead infection, thromboembolic events related to thrombus on the lead, SVC stenosis or occlusion preventing implantation of a necessary lead, planned stent deployment in a vein containing a lead, life-threatening arrhythmias secondary to retained leads. Class IIa: Severe chronic pain at the device or lead insertion site, CIED location interfering with the treatment of malignancy, if CIED implantation would require more than 4 leads on one side or more than 5 leads through the SVC, an abandoned lead interfering with the operation of a CIED system. In patients with lead infection, a new lead can be reimplanted after a complete antibiotic course. The duration depends on the type of infection and is described in the HRS expert consensus. ¥Extraction of lead as a first-line approach to lead revision or device upgrade for patients with venous occlusion can be useful in experienced centers, and the priority depends on the operator's discretion and expertise (9). †If the vascular recoil would hinder the lead implantation or patients present with SVC syndrome, venoplasty with subsequent stenting is needed (9). **(B)** Treatment algorithm in patients without preexisting CIED. *Indications for VVI: fixed atrial tachyarrhythmia with symptomatic bradycardia; Severe pacemaker syndrome occurred in nearly 20% of VVIR-paced patients, and the baseline predictors for pacemaker syndrome are lower sinus rate and higher programmed pacemaker rate (21).

pericardial effusion after the procedure in the study, and it was suspended permanently due to safety problems (17). In the following SELECT-LV study (18), successful implantations were achieved in 34 patients (97.1%) without significant periprocedural complications. Further clinical trials are needed to confirm the feasibility and safety of this pacing modality.

Wiring and balloon venoplasty, an effective and safe approach to overcome venous occlusion

Since 1990, it has been described that balloon angioplasty of occlusive venous access for implantation is feasible. One major complication of venoplasty is vessel perforation during balloon inflation or lead passage. Worley (19) and Worley et al. (20) detailed the subclavian venoplasty and performed lead implantation in 373 patients during a period of 11 years. The rate of total occlusion with collaterals was 65% *via* peripheral venogram but in only 20% of cases by contrast injection near the site of occlusion, indicating the importance of selective contrast injection for evaluation. Procedures were successful in 371 of 373 patients without complications, showing that venoplasty is highly effective and safe performed by experienced hands. Lead implantation can be promptly achieved after venoplasty for venous occlusion but is rarely performed because operating physicians often regard venoplasty as an area of expertise of a vascular interventionist, and consultation is less practical in the real world. It is noteworthy to attempt balloon venoplasty after consulting a vascular interventionist when confronted with the challenge of venous occlusion. Regarding the multiple strategies discussed previously, we tried to outline the characteristics and disadvantages of the strategies, as shown in Table 1.

Our proposed algorithm

Interventional strategies for lead implantation in patients with venous occlusion have not been optimized. On the basis of the approaches and outline reported by McCotter et al. (10), Burri (12) and Elayi et al. (14), herein, we emphasize the importance of balloon venoplasty and propose an algorithm as a step-by-step approach to deal with venous occlusion in lead implantation for patients with or without preexisting leads (Figures 3A,B). Further studies are needed to identify the optimal protocol to solve this situation.

Conclusion

We presented a case of venous access challenge in CRT lead implantation, which was overcome by retrograde wiring and balloon venoplasty. Venous occlusion is not an uncommon condition in patients without preexisting transvenous devices. Venography is imperative prior to CIED implantation. In patients with previous transvenous device implantation, the rate of any degree of venous occlusion increased to 31–61%. We performed a literature review of strategies to overcome the difficulty in venous access and proposed a treatment algorithm to be applied when we encounter this condition. We emphasize that balloon venoplasty is an effective and safe approach to recanalize the stenotic or occlusive vessel prior to CIED implantation. It is crucial for a device implanter to be familiar with the equipment and techniques to overcome the challenges associated with venous access. It is also important to be open-minded and consult a vascular interventionist for a venoplasty rather than promptly deciding to implant a leadless pacemaker.

Data availability statement

The raw data supporting the conclusions of this article will be made available by the authors, without undue reservation.

Ethics statement

The studies involving human participants were reviewed and approved by the National Cheng Kung University Hospital Institutional Review Board, (B-EC-111-026). Written informed consent for participation was not required for this study in accordance with the national legislation and the institutional requirements.

Author contributions

Y-PL and J-YC: conception and design. Y-PL, C-HL, and J-YC: data acquisition and critical revision of the article for important intellectual content. Y-PL: literature review and drafting and finalizing the article. J-YC: supervised the literature search and revision and approved the final version. All authors contributed to the article and approved the submitted version.

Funding

This study was supported by the Ministry of Science and Technology of Taiwan, China (MOST 110-2218-E-006-017 and MOST 110-2218-E-006-015) and Higher Education Sprout Project, Ministry of Education to the Headquarters of University Advancement at National Cheng Kung University (NCKU).

Conflict of interest

The authors declare that the research was conducted in the absence of any commercial or financial relationships that could be construed as a potential conflict of interest.

Publisher's note

References

1. McDonagh TA, Metra M, Adamo M, Gardner RS, Baumbach A, Böhm M, et al. 2021 ESC guidelines on cardiac pacing and cardiac resynchronization therapy. *Eur Heart J.* (2021) 42:3599–726. doi: 10.1093/eurheartj/ehab368

2. Oginosawa Y, Abe H, Nakashima Y. The incidence and risk factors for venous obstruction after implantation of transvenous pacing leads. *Pacing Clin Electrophysiol.* (2002) 25:1605–11. doi: 10.1046/j.1460-9592.2002.01605.x

3. Abu-El-Haija B, Bhave PD, Campbell DN, Mazur A, Hodgson-Zingman DM, Cotarlan V, et al. Venous stenosis after transvenous lead placement: a study of outcomes and risk factors in 212 consecutive patients. *J Am Heart Assoc.* (2015) 4:e001878. doi: 10.1161/JAHA.115.001878

4. Stanford W, Jolles H, Ell S, Chiu LC. Superior vena cava obstruction: a venographic classification. *Am J Roentgenol.* (1987) 148:259–62. doi: 10.2214/ajr.148.2.259

5. Sharma PS, Vijayaraman P. Conduction system pacing for cardiac resynchronisation. *Arrhythm Electrophysiol Rev.* (2021) 10:51–8. doi: 10.15420/aer.2020.45

6. Wang Y, Zhu H, Hou X, Wang Z, Zou F, Qian Z, et al. Randomized trial of left bundle branch vs. biventricular pacing for cardiac resynchronization therapy. *J Am Coll Cardiol.* (2022) 80:1205–16. doi: 10.1016/j.jacc.2022.07.019

7. Lickfett L, Bitzen A, Arepally A, Nasir K, Wolpert C, Jeong KM, et al. Incidence of venous obstruction following insertion of an implantable cardioverter defibrillator. A study of systematic contrast venography on patients presenting for their first elective ICD generator replacement. *Europace.* (2004) 6:25–31. doi: 10.1016/j.eupc.2003.09.001

8. Sudhakar BG. Left subclavian and innominate vein balloon venoplasty followed by permanent pacemaker implantation: a case report. *J Innov Card Rhythm Manag.* (2019) 10:3738–42. doi: 10.19102/icrm.2019.100704

9. Kusumoto FM, Schoenfeld MH, Wilkoff BL, Berul CI, Birgersdotter-Green UM, Carrillo R, et al. 2017 HRS expert consensus statement on cardiovascular implantable electronic device lead management and extraction. *Heart Rhythm.* (2017) 14:e503–51. doi: 10.1016/j.hrthm.2017.09.001

10. McCotter CJ, Angle JF, Prudente LA, Mounsey JP, Ferguson JD, DiMarco JP, et al. Placement of transvenous pacemaker and ICD leads across total chronic occlusions. *Pacing Clin Electrophysiol.* (2005) 28:921–5. doi: 10.1111/j.1540-8159.2005.00203.x

11. Van Putten JW, Schlosser NJ, Vujaskovic Z, Leest AH, Groen HJ. Superior vena cava obstruction caused by radiation induced venous fibrosis. *Thorax.* (2000) 55:245–6. doi: 10.1136/thorax.55.3.245

12. Burri H. Overcoming the challenge of venous occlusion of lead implantation. *Indian Pacing Electrophysiol J.* (2015) 15:110–2. doi: 10.1016/j.ipej.2015.07.006

13. Seow SC, Lim TW, Singh D, Yeo WT, Kojodjojo P. Permanent pacing in patients without upper limb venous access: a review of current techniques. *Heart Asia.* (2014) 6:163–6. doi: 10.1136/heartasia-2014-010546

14. Elayi CS, Allen CL, Leung S, Lusher S, Morales GX, Wiisanen M, et al. Inside-out access: a new method of lead placement for patients with central venous occlusions. *Heart Rhythm.* (2011) 8:851–7. doi: 10.1016/j.hrthm.2011.01.024

15. Beurskens NEG, Tjong FVY, de Bruin-Bon RHA, Dasselaar KJ, Kuijt WJ, Wilde AAM, et al. Impact of leadless pacemaker therapy on cardiac and atrioventricular valve function through 12 months of follow-up. *Circ Arrhythm Electrophysiol.* (2019) 12:e007124. doi: 10.1161/CIRCEP.118.007124

16. Sanchez R, Nadkarni A, Buck B, Daoud G, Koppert T, Okabe T, et al. Incidence of pacing-induced cardiomyopathy in pacemaker-dependent patients is lower with leadless pacemakers compared to transvenous pacemakers. *J Cardiovasc Electrophysiol.* (2021) 32:477–83. doi: 10.1111/jce.14814

17. Auricchio A, Delnoy PP, Butter C, Brachmann J, Erven LV, Spitzer S, et al. Feasibility, safety, and short-term outcome of leadless ultrasound-based endocardial left ventricular resynchronization in heart failure patients: results of the wireless stimulation endocardially for CRT (WiSE-CRT) study. *Europace.* (2014) 16:681–8. doi: 10.1093/europace/eut435

18. Reddy VY, Miller MA, Neuzil P, Søgaard P, Butter C, Seifert M, et al. Cardiac resynchronization therapy with wireless left ventricular endocardial pacing: the SELECT-LV study. *J Am Coll Cardiol.* (2017) 69:2119–29. doi: 10.1016/j.jacc.2017.02.059

19. Worley SJ. Implant venoplasty: dilation of subclavian and coronary veins to facilitate device implantation: indications, frequency, methods, and complications. *J Cardiovasc Electrophysiol.* (2008) 19:1004–7. doi: 10.1111/j.1540-8167.2008.01217.x

20. Worley SJ, Gohn DC, Pulliam RW, Raifsnider MA, Ebersole BI, Tuzi J. Subclavian venoplasty by the implanting physicians in 373 patients over 11 years. *Heart Rhythm.* (2011) 8:526–33. doi: 10.1016/j.hrthm.2010.12.014

21. Link MS, Hellkamp AS, Estes NA, Orav EJ, Ellenbogen KA, Ibrahim B, et al. High incidence of pacemaker syndrome in patients with sinus node dysfunction treated with ventricular-based pacing in the mode selection trial (MOST). *J Am Coll Cardiol.* (2004) 43:2066–71. doi: 10.1016/j.jacc.2003.10.072

frontiers | Frontiers in Cardiovascular Medicine

TYPE Case Report
PUBLISHED 24 October 2022
DOI 10.3389/fcvm.2022.1006435

OPEN ACCESS

EDITED BY
Ardan Muammer Saguner,
University Hospital Zürich, Switzerland

REVIEWED BY
Cristiano Pisani,
University of São Paulo, Brazil
Mark Gallagher,
St George's University Hospitals NHS Foundation Trust, United Kingdom

*CORRESPONDENCE
Jidong Zhang
zhangjidong78@163.com

SPECIALTY SECTION
This article was submitted to Cardiac Rhythmology, a section of the journal Frontiers in Cardiovascular Medicine

RECEIVED 29 July 2022
ACCEPTED 10 October 2022
PUBLISHED 24 October 2022

CITATION
Zhao L, Li R, Bai L, Wang D, Zhang J and Yang X (2022) Successful radiofrequency catheter ablation of Wolff-Parkinson-White syndrome in a patient with dextrocardia: A case report.
Front. Cardiovasc. Med. 9:1006435.
doi: 10.3389/fcvm.2022.1006435

Successful radiofrequency catheter ablation of Wolff-Parkinson-White syndrome in a patient with dextrocardia: A case report

Lei Zhao, Ruibin Li, Long Bai, Dong Wang, Jidong Zhang* and Xiaohong Yang

Department of Cardiology, The Second Hospital of Hebei Medical University, Shijiazhuang, China

Background: Dextrocardia is a congenital heart malformation with a low incidence that occurs in only 1 in 10,000–12,000 people. Wolff-Parkinson-White (WPW) syndrome is a congenital condition with additional accessory pathways between the atria and the ventricle, which affects up to three in 1,000 people worldwide. Experience of radiofrequency catheter ablation in patients with WPW syndrome and dextrocardia is scarce due to its rare incidence.

Case presentation: A 39-year-old female was hospitalized due to two episodes of palpitations in the latest 2 months. The morphology of the P-QRS-T complex of lead aVR and aVL, II, and III were presented invertedly as common conditions, and shortened P-R interval and a characteristic "delta" wave were shown on the electrocardiogram (EGM). The patient with dextrocardia and situs invertus malposition was confirmed by chest-X ray, cardiac color Doppler echocardiography. The patient was diagnosed with WPW syndrome with dextrocardia and underwent radiofrequency catheter ablation (RFCA) successfully. In this case, the key to the success of RFCA is to understand the anatomical structure of the heart and the great vessels before the operation and make a personalized operative plan.

Conclusion: Catheter ablation for tachycardia patients with dextrocardia is efficient and safe. For patients with dextrocardia, the key to successful ablation was adjusting for projection angulation and different catheter manipulation compared with a standard case because of the mirror image of a normal heart.

KEYWORDS

dextrocardia, Wolff-Parkinson-White (WPW) syndrome, radiofrequency catheter ablation, tachycardia, congenital heart malformation

Introduction

Dextrocardia with situs inversus is a rare congenital malformation characterized by the mirror-image location of the heart and viscera. Additionally, Wolff-Parkinson-White (WPW) is a congenital abnormality caused by an accessory pathway between the atria and ventricles that bypasses the atrioventricular (AV) node and the His-Purkinje system. WPW exists in 0.1–0.3% of the population (1, 2). Therefore, the morbidity rate of the two conditions is very low. Due to its rare incidence, the experience of radiofrequency catheter ablation (RFCA) of tachycardia in patients with dextrocardia is limited. Here, we report a WPW syndrome case in a patient with dextrocardia who successfully underwent RFCA.

Case presentation

An Asian 39-year-old female was admitted to the Second Hospital of Hebei Medical University in January 2022 due to

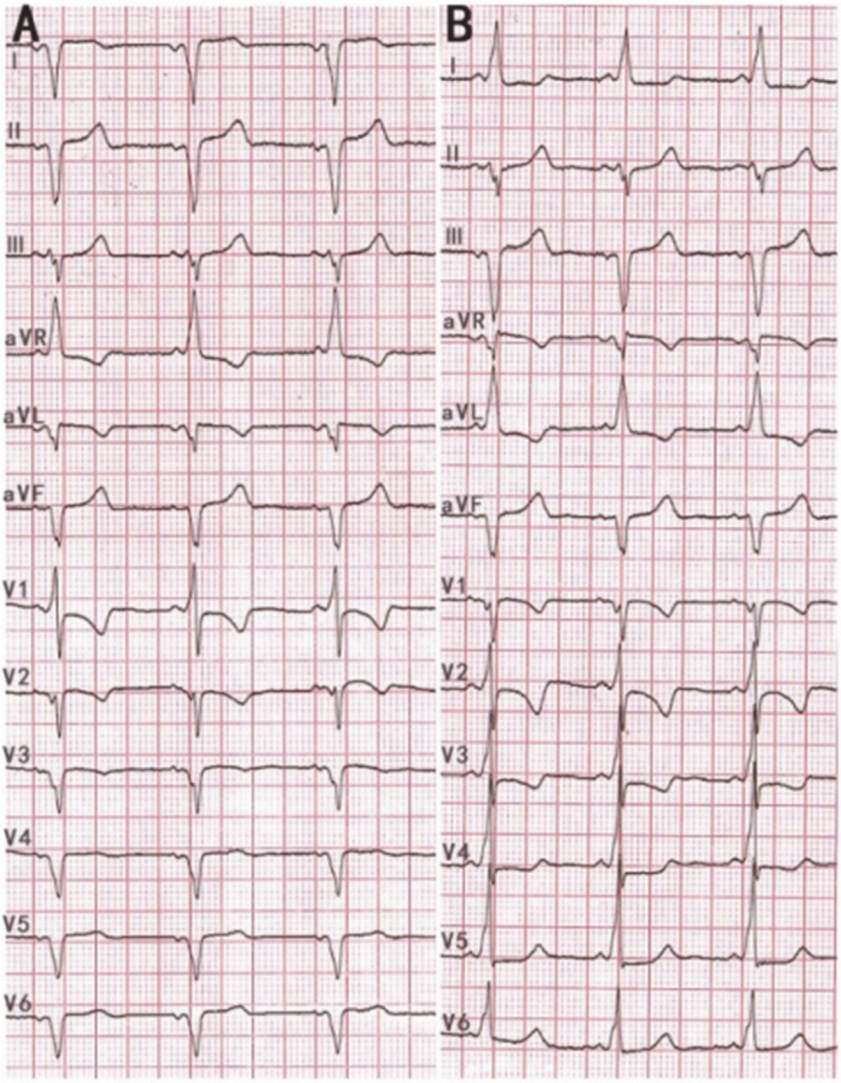

FIGURE 1
(A) 12 lead ECG with standard lead placement showing sinus rhythm with a heart rate of 68 beats per minute. ECG revealed inverted P-QRS-T complex waves in lead I and inverted P-QRS in lead aVL. Notably, the P-QRS-T complex in lead aVR and aVL appear reversed compared to their usual relationship. Likewise, the morphology of the P-QRS-T complex of lead II and III was also invertedly compared to their usual relationship. The ECG shows an RS morphology in V1, a reversed R wave from V2 to V6 leads, a shortened P-R interval, and a characteristic "delta" wave. **(B)** 12 lead ECG with reverse lead placement and right precordial leads V3R-V6R. The ECG showed a positive P-QRS complex in lead I. The morphology of the P-QRS-T complex of lead aVR and aVL, lead II, and III were reversed compared to their morphologies in panel **(A)**. R wave amplitude increases gradually, and the S wave decreases gradually in the precordial leads and the "delta" wave in 12 leads.

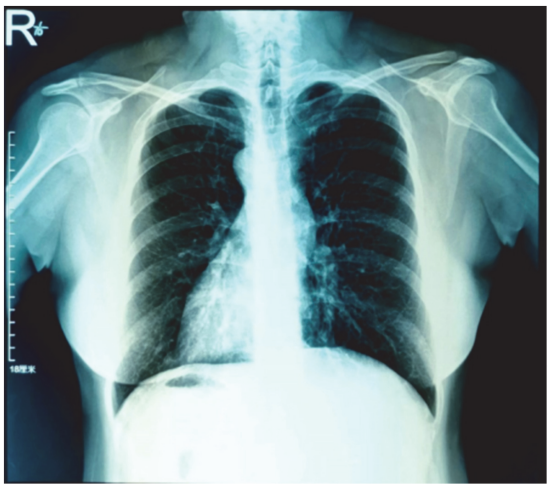

FIGURE 2
The PA view chest X-ray shows shadows of the heart and aortic arch in the right hemithorax along with gas in the fundus of the stomach on the right side.

two episodes of palpitations in the past 2 months. During the physical examination on admission, her resting heart rate was 71 beats per minute, her blood pressure was 117/64 mm Hg, and an apex beat was identified on the right side of the chest with no murmur. We completed the 12-lead electrocardiogram, chest-X ray, echocardiography, and blood examinations to evaluate the patient's condition. A twelve-lead EGM with standard lead placement showed inverted P-QRS-T complex waves in lead I and an inverted P-QRS in lead aVL. Notably, the P-QRS-T complex in lead aVR and aVL appear reversed compared to their usual relationship. Likewise, the morphology of the P-QRS-T complex of lead II and III were also reversed. The EGM shows an RS morphology in V1, a reversed R wave from V2 to V6, a shortened P-R interval, and a characteristic "delta" wave (a wide and initially slurred QRS complex) in precordial leads (**Figure 1A**). We completed a 12-lead EGM with reversed lead placement and right precordial leads V3R-V6R. From our results, the EGM showed a positive P-QRS complex in lead I. The morphology of the P-QRS-T complex of lead aVR and aVL, lead II, and III were reversed, as presented in **Figure 1A**. Furthermore, the R wave amplitude increased gradually, and the S wave decreased gradually in the precordial leads (**Figure 1B**).

The posteroanterior (PA) view chest X-ray shows shadows of the heart and aortic arch in the right hemithorax along with gas in the fundus of the stomach on the right side (**Figure 2**).

Echocardiography showed a normal size of each heart cavity and normal biventricular functions with an ejection fraction of 76.2%. No regional wall motion abnormalities and septal defects were detected. Furthermore, laboratory examinations showed no abnormalities.

Based on the above clinical manifestations and examinations, we diagnosed the patient with Wolff–Parkinson–White syndrome combined with dextrocardia. The following operation strategy of RFCA was performed successfully under local anesthesia.

Electrophysiological study and radiofrequency catheter ablation

This procedure was performed under standard local anesthesia and guided by CARTO electroanatomical

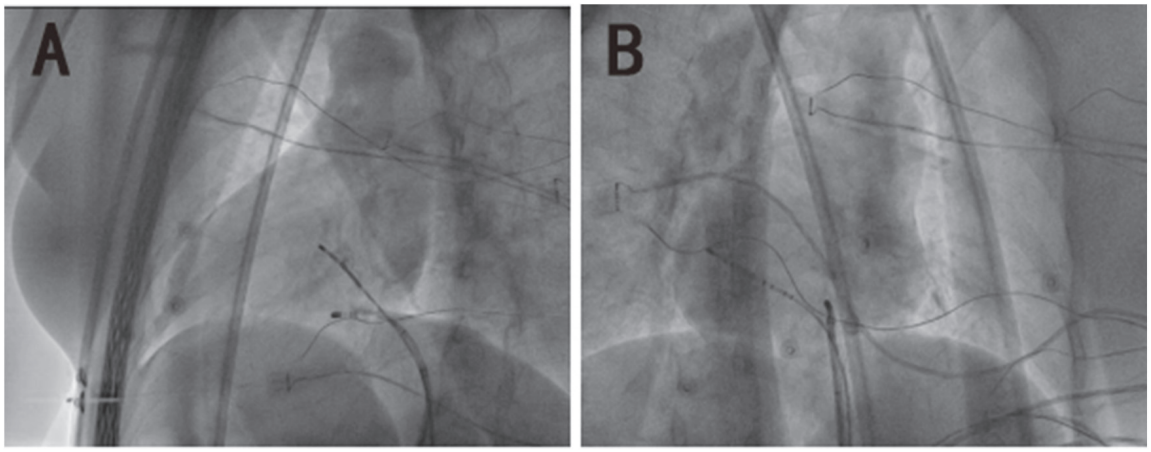

FIGURE 3
The X-ray image of mirror dextrocardia in the left anterior oblique view of 45° and right-anterior oblique view of 35°. **(A)** The image of dextrocardia in the left anterior oblique is presented as a common heart in the regular right anterior oblique. **(B)** The image of dextrocardia in the right anterior oblique is presented as a common heart in the regular left anterior oblique.

three-dimensional (3D) mapping system. A steerable Decapolar catheter (XTTM, Bard Electrophysiology, Lowell, MA, USA) and 4 polar catheters (AVAIL, Electrophysiology Cather, Biosense Webster, USA) were positioned in the coronary sinus (CS) through the right femoral vein. An 8.5-Fr long sheath (SL1, St. Jude Medical, MN, USA) was advanced into the right atrium through the right femoral vein, and a Thermocool Smart touch catheter was introduced to the region of His-bundle from SL1 (Figure 3). Supraventricular tachycardia was induced with the frequency of 180 beats per minute by ventricular S1S1, and A was reset by right ventricular apex entrainments and RS2 stimuli. The patient was diagnosed with dextrocardia with a posteroseptal tricuspid annulus accessory pathway by the intracardiac EGM (Figures 4A,B). After ablation at 43°C and 30W for 5 s, the accessory pathway was blocked and continued to ablate for 240 s. Retrograde Wenckebach conduction was stimulated by ventricular S1S1 for 400 ms, decreased conduction was stimulated by coronary sinus S1S1 stimulation, and Wenckebach conduction was found for 300 ms. No ventricular conduction with atria stimulated by S1S2 of 450/300 ms, indicating that the procedure was successful. Delta wave disappeared on intracardiac and surface EGM (Figure 4C).

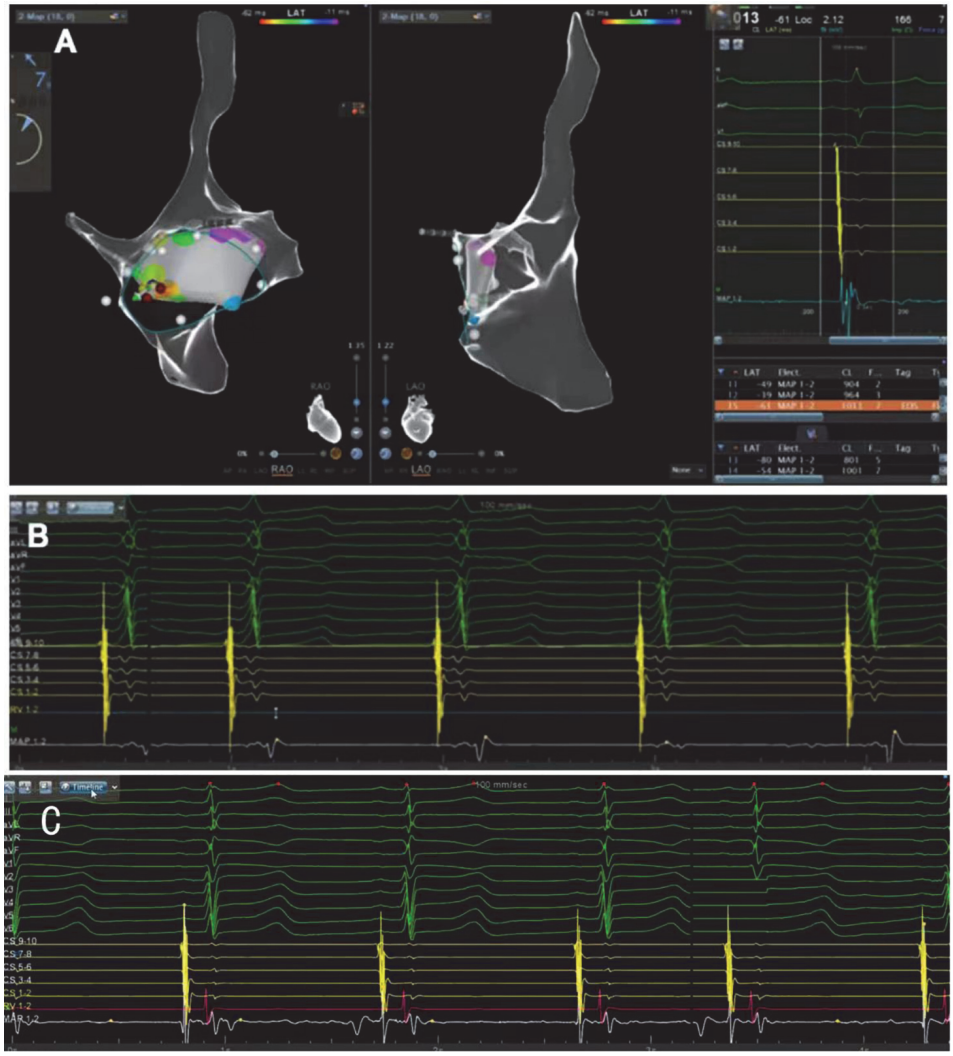

FIGURE 4
(A) CARTO electroanatomical 3-dimensional(3D) mapping system showing the right atrium is a mirror image of a normal heart in the right-anterior oblique view(RAO)and the left-anterior oblique view (LAO). **(B)** ECG (before RFCA) with reverse lead placement and right precordial leads V3R-V6R shows an inferoseptal tricuspid annulus accessory pathway. The prominent early V wave in 7/8 bipolar potentials of 10 polar coronary sinus electrodes also indicates the accessory pathway was in the inferoseptal nearby the coronary sinus ostium. Ventricular activation was marked by the red arrow. **(C)** The ECG after the radiofrequency catheter ablation shows "delta" wave disappeared, indicating that the procedure was successful.

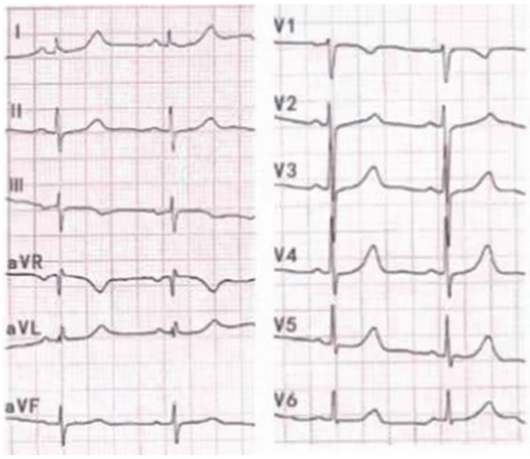

FIGURE 5
No characteristic "delta" wave was seen, and normal R/S transition was shown in precordial leads in 12 lead ECG with reverse lead placement.

After a 6-month of follow-up, the patient did not have complaints of onset palpitations, and no arrhythmia was observed on the EGM (**Figure 5**).

Discussion

Dextrocardia is a rare congenital abnormality that occurs in 1 in 10,000–12,000 people (3). There are three main types of dextrocardia. With situs solitus, dextrocardia is associated with the normal orientation of great arteries. With situs inversus, the great vessels are usually inversely placed in the thoracic cavity. Furthermore, with situs ambiguous, the presence and origin of great vessels from ventricles are variable and usually accompanied by asplenia or polysplenia (4). Notably, dextrocardia with situs inversus occurs in approximately 2 per 10,000 live births. Dextrocardia solitus or situs ambiguous is considerably less common, occurring in 1 in 20,000 live births (5). Wolff-Parkinson-White (WPW) syndrome is an inborn abnormality with an additional electrical conduction pathway between the atria and the ventricle, which affects up to three in 1,000 people worldwide (6). Therefore, the occurrence of the two conditions is uncommon. These two congenital anomalies can occur alone, or in concurrence. Dextrocardia can be associated with other additional cardiac anomalies (7). However, no clear evidence of a significant correlation relationship between dextrocardia and atrioventricular nodal reentrant tachycardia or atrioventricular reentrant tachycardia was found. Likewise,WPW syndrome occurs as often in patients with dextrocardia as in the general populations. Klug D (8) reported that a patient with mirror-image dextrocardia and WPW Syndrome underwent catheter ablation successfully in 1994 for the first time. Experience of RFCA in patients with tachyarrhythmia and dextrocardia is still limited due to its infrequent incidence. This paper presented the case of a patient with both conditions in whom radiofrequency catheter ablation was performed successfully.

Situs inversus is a rare congenital heart condition that can be divided into situs inversus totalis and situs inversus with levocardia (9, 10). According to chest X-ray and color Doppler echocardiography results, the patient reported in our case is cardiac dextrocardia, accompanied by visceral inversion. The aortic arch and great vessels are all mirror-inverted. Thus, the heart is located in the right of the chest, the apex of the heart points to the right, the aortic arch in the right of the chest, and the inferior vena cava are left-sided structures. Catheter ablation is an effective and safe strategy with a high success rate for managing patients suffering from WPW syndrome and dextrocardia (11). A previous study involving nine cases of patients with supraventricular tachycardia and dextrocardia showed that the successful rate of catheter ablation was 100% (12). Therefore, for situs inversus without additional anatomy malformations, adjusting for projection angulation and catheter manipulation are the key points to achieving a successful ablation (13).

In this particular case, the main challenge of the procedure is locating the ablation target accurately. The key point to a successful ablation in patients with dextrocardia is understanding the heart's anatomical structure nd the great vessels and identifying a strategy before conducting the operation. Relevant literature reported that the femoral vein is the most common ablation pathway in supraventricular tachycardia patients with dextrocardia when needed to RFCA (14, 15). In some cases, the superior vena cava is also the venous access to the heart (12). Fluoroscopy and 3D mapping during the procedure can help successfully ablate the accessory pathway in WPW syndrome. Besides, since mirror manipulation is required during the procedure in patients with supraventricular tachycardia and dextrocardia, catheter maneuvers are also crucial to a successful ablation.

Conclusion

Wolff-Parkinson-White syndrome with dextrocardia has been reported previously with left free wall, right free wall, and anteroseptal accessory pathways (16). We report a unique case of a posteroseptal accessory pathway in a patient with dextrocardia and situs invertus. An exact anatomical evaluation is critical in such a case with dextrocardia. Therefore, EGM, chest-X ray, cardiac CT, cardiac color Doppler echocardiography, and 3D mapping can help guide the catheter to the ablation

target, reduce the procedure duration, and decrease the risks of complications.

Data availability statement

The original contributions presented in this study are included in the article/supplementary material, further inquiries can be directed to the corresponding author.

Ethics statement

The studies involving human participants were reviewed and approved by the Research Ethics Committee of the Second Hospital of Hebei Medical University. The patients/participants provided their written informed consent to participate in this study. Written informed consent was obtained from the individual(s) for the publication of this case report and any potentially identifiable images or data included in this article.

Author contributions

LZ: conceptualization, data collection and curation, and writing-original draft. RL and LB: methodology. DW: visualization. JZ: validation. XY: writing-review and editing. All authors contributed to the article and approved the submitted version.

Acknowledgments

We thank AiMi Academic Services (www.aimieditor.com) for the English language editing and review services.

Conflict of interest

The authors declare that the research was conducted in the absence of any commercial or financial relationships that could be construed as a potential conflict of interest.

Publisher's note

All claims expressed in this article are solely those of the authors and do not necessarily represent those of their affiliated organizations, or those of the publisher, the editors and the reviewers. Any product that may be evaluated in this article, or claim that may be made by its manufacturer, is not guaranteed or endorsed by the publisher.

References

1. Janson CM, Millenson ME, Okunowo O, Dai D, Christmyer Z, Tan RB, et al. Incidence of life-threatening events in children with wolff-parkinson-white syndrome: analysis of a large claims database. *Heart Rhythm.* (2022) 19:642–7. doi: 10.1016/j.hrthm.2021.12.009

2. Kounis NG, Zavras GM, Papadaki PJ, Soufras GD, Kitrou MP, Poulos EA. Pregnancy-induced increase of supraventricular arrhythmias in wolff-parkinson-white syndrome. *Clin Cardiol.* (1995) 18:137–40. doi: 10.1002/clc.4960180306

3. Xu J, Jiang G, Zhang L, Chen Z, Wang H, Bai M, et al. Successful percutaneous left atrial appendage occlusion for atrial fibrillation in a patient with mirror-image dextrocardia: a case report. *BMC Cardiovasc Disord.* (2022) 22:20. doi: 10.1186/s12872-021-02369-9

4. Al-Khadra AS. Images in cardiovascular medicine. Mirror-image dextrocardia with situs inversus. *Circulation.* (1995) 91:1602–3.

5. Offen S, Jackson D, Canniffe C, Choudhary P, Celermajer DS. Dextrocardia in adults with congenital heart disease. *Heart Lung Circ.* (2016) 25:352–7.

6. Elitok A, Aksan G, Sonsöz MR, Tezcan M, Çevrim Ö. The coexistence of wolff-parkinson-white syndrome (WPW) and atrioventricular nodal reentrant tachycardia (AVNRT). *Turk J Emerg Med.* (2018) 18:131–3. doi: 10.1016/j.tjem.2017.12.002

7. Shi H, Sohn S, Wang S, Park S, Lee S, Kim SY, et al. A case of multiple cardiovascular and tracheal anomalies presented with wolff-parkinson-white syndrome in a middleaged adult. *J Korean Med Sci.* (2017) 32:2069–72. doi: 10.3346/jkms.2017.32.12.2069

8. Klug D, Dubuc M, Ferracci A, Nadeau R. Radiofrequency catheter ablation of an accessory pathway in a young man with dextroversion. *Pacing Clin Electrophysiol.* (1994) 17:981–5. doi: 10.1111/j.1540-8159.1994.tb01443.x

9. Karki S, Khadka N, Kashyap B, Sharma S, Rijal S, Basnet A. Incidental finding of dextrocardia with situs inversus and absent left kidney: a case report. *JNMA J Nepal Med Assoc.* (2022) 60:196–9. doi: 10.31729/jnma.6825

10. Goo HW, Park IS, Ko JK, Kim YH, Seo DM, Yun TJ, et al. CT of congenital heart disease: normal anatomy and typical pathologic conditions. *Radiographics.* (2003) 23:S147–65.

11. Zhang Y, Sun L, Luo F, Li J, Sun Y, Chen Y, et al. Result and technique consideration of radiofrequency catheter ablation of tachycardia in patients with dextrocardia. *Pacing Clin Electrophysiol.* (2022) 45:340–7. doi: 10.1111/pace.14452

12. Zhou GB, Ma J, Zhang JL, Guo XG, Yang JD, Liu SW, et al. Catheter ablation of supraventricular tachycardia in patients with dextrocardia and situs inversus. *J Cardiovasc Electrophysiol.* (2019) 30:557–64.

13. Ulus T, Dural M, Şener E, Al A, Mert KU, Görenek B. Atrial fibrillation and atrial flutter ablation using mirror image in a patient with dextrocardia with situs inversus. *Anatol J Cardiol.* (2020) 24:282–4. doi: 10.14744/AnatolJCardiol.2020.20766

14. Povoski SP, Khabiri H. Persistent left superior vena cava: review of the literature, clinical implications, and relevance of alterations in thoracic central venous anatomy as pertaining to the general principles of central venous access device placement and venography in cancer patients. *World J Surg Oncol.* (2011) 9:173. doi: 10.1186/1477-7819-9-173

15. Zheng Z, Zeng Z, Zhou Y, Li C, Zhang W. Radiofrequency catheter ablation in a patient with dextrocardia, persistent left superior vena cava, and atrioventricular nodal reentrant tachycardia: a case report. *Medicine.* (2020) 99:e22086. doi: 10.1097/MD.0000000000022086

16. Chin A, Phiri T. An anteroseptal accessory pathway in a patient with dextrocardia and situs inversus. *J Cardiovasc Electrophysiol.* (2015) 26:692–3. doi: 10.1111/jce.12616

frontiers | Frontiers in Cardiovascular Medicine

TYPE Case Report
PUBLISHED 28 October 2022
DOI 10.3389/fcvm.2022.1005952

OPEN ACCESS

EDITED BY
Matteo Anselmino,
University of Turin, Italy

REVIEWED BY
Pasquale Striano,
Giannina Gaslini Institute (IRCCS), Italy
Oscar Campuzano,
University of Girona, Spain
Przemyslaw Radwanski,
The Ohio State University,
United States

*CORRESPONDENCE
Hafiz Omer
omerh@ngha.med.sa

†These authors have contributed equally to this work and share first authorship

SPECIALTY SECTION
This article was submitted to Cardiac Rhythmology, a section of the journal Frontiers in Cardiovascular Medicine

RECEIVED 28 July 2022
ACCEPTED 10 October 2022
PUBLISHED 28 October 2022

CITATION
Omer H, Omer MH, Alyousef AR, Alzammam AM, Ahmad O and Alanazi HA (2022) Unmasking of Brugada syndrome by lamotrigine in a patient with pre-existing epilepsy: A case report with review of the literature.
Front. Cardiovasc. Med. 9:1005952.
doi: 10.3389/fcvm.2022.1005952

Unmasking of Brugada syndrome by lamotrigine in a patient with pre-existing epilepsy: A case report with review of the literature

Hafiz Omer[1,2*†], Mohamed H. Omer[3†], Abdulmohsen R. Alyousef[1], Ali M. Alzammam[4], Omar Ahmad[5] and Haitham A. Alanazi[1,2,6]

[1]Department of Adult Cardiology, King Abdulaziz Medical City, Riyadh, Saudi Arabia, [2]College of Medicine, King Saud Bin Abdulaziz University for Health Sciences, Riyadh, Saudi Arabia, [3]School of Medicine, Cardiff University, Cardiff, United Kingdom, [4]Department of Internal Medicine, King Abdulaziz Medical City, Riyadh, Saudi Arabia, [5]College of Medicine, Alfaisal University, Riyadh, Saudi Arabia, [6]King Abdullah International Medical Research Center, Riyadh, Saudi Arabia

Brugada syndrome is an inherited cardiac channelopathy arising from mutations in voltage-gated cardiac sodium channels. Idiopathic epilepsy portrays a coalescent underlying pathophysiological mechanism pertaining to the premature excitation of neuronal voltage-gated ion channels resulting in the disruption of presynaptic neurons and the unregulated release of excitatory neurotransmitters. The coexistence of epilepsy and Brugada syndrome may be explained by mutations in voltage-gated ion channels, which are coexpressed in cardiac and neural tissue. Moreover, the incidence of sudden unexpected death in epilepsy has been associated with malignant cardiac arrhythmias in the presence of mutations in voltage-gated ion channels. Lamotrigine is an antiepileptic drug that inhibits neuronal voltage-gated sodium channels, thus stabilizing neural impulse propagation and controlling seizure activity in the brain. However, lamotrigine has been shown to inhibit cardiac voltage-gated sodium channels resulting in a potential arrhythmogenic effect and the ability to unmask Brugada syndrome in genetically susceptible individuals. We are reporting a case of a 27-year-old male patient with a background of presumed idiopathic epilepsy who was initiated on lamotrigine therapy resulting in the unmasking of Brugada syndrome and the onset of syncopal episodes. This case provides further evidence for the arrhythmogenic capacity of lamotrigine and highlights the relationship between epilepsy and Brugada syndrome. In this report, we aim to review the current literature regarding the associations between epilepsy and Brugada syndrome and the impact of lamotrigine therapy on such patients.

KEYWORDS

Brugada syndrome, lamotrigine, epilepsy, syncope, sudden unexpected death in epilepsy (SUDEP), sudden cardiac death (SCD), ion channels

Introduction

Brugada syndrome (BrS) is an autosomal dominant channelopathy associated with mutations in voltage-gated ion channels within cardiac myocytes (1). Several genes have been implicated in the development of BrS; however, mutations in the *SCN5A* gene, which codes for the expression of voltage-gated sodium channels, have been correlated with most cases (2). The clinical features of BrS express wide heterogeneity and can range from complete lack of symptoms to malignant ventricular arrhythmias predisposing to sudden cardiac death (SCD) (1). BrS manifests with a characteristic electrocardiogram (EKG) pattern with coved-type ST-segment elevation in the right precordial leads (3). The malignant nature of BrS arises from the presence of arrhythmogenic epicardial substrate in the right ventricular outflow tract, leading to its association with approximately 20% of cases of SCD in individuals with structurally normal hearts (4, 5).

Idiopathic epilepsy portrays a similar pathophysiological mechanism to BrS, with mutations in the neuronal voltage-gated sodium channels implicated in the condition's development (6, 7). Moreover, some studies have reported the coexistence of idiopathic epilepsy amongst patients with BrS (7). Interestingly, with the conduction of genome-wide association studies amongst patients with idiopathic epilepsy and BrS, some gene mutations coexpressed in both conditions have been identified (8, 9). A recent emerging hypothesis explaining the coexistence of both conditions suggests that the coexpressed genes code for voltage-gated ion channels expressed within cardiac myocytes and neuronal cells (2, 7, 10).

Lamotrigine is an antiepileptic agent that inhibits neuronal voltage-gated sodium channels, stabilizing presynaptic membranes and hindering excitatory neurotransmitter release (11). However, *in vitro* studies have demonstrated that lamotrigine may exhibit class IB antiarrhythmic activity by inhibiting cardiac sodium channels (12, 13). There have been six reports in the literature of lamotrigine contributing to the unmasking of Brugada syndrome, which further supports the theory that lamotrigine may exert a sodium channel-blocking effect within cardiac myocytes (14–19).

In this paper, we aim to report a case of a patient with pre-existing epilepsy who was initiated on lamotrigine therapy resulting in the unmasking of a Brugada pattern on the electrocardiogram. As there have only been six reported cases of lamotrigine unmasking BrS, we aim to contribute to the pre-existing literature on the subject. Moreover, the case also highlights the rare coexistence of BrS with idiopathic epilepsy. Furthermore, we carried out an exhaustive literature review using the Medline database of all reports of lamotrigine-induced BrS as well as reports of the coexistence of epilepsy and BrS.

Abbreviations: BrS, Brugada syndrome; SCD, sudden cardiac death; SUDEP, sudden unexplained death in epilepsy; LQTS, long QT syndrome EKG, electrocardiogram; EEG, electroencephalogram; *SCN5A*, Sodium Voltage-Gated Channel Alpha Subunit 5; *SCN10A*, Sodium Voltage-Gated Channel Alpha Subunit 10; *SCN9A*, Sodium Voltage-Gated Channel Alpha Subunit 9; *SCN8A*, Sodium Voltage-Gated Channel Alpha Subunit 8; *AKAP9*, A-Kinase Anchoring Protein 9; *KCNQ1*, Potassium Voltage-Gated Channel Subfamily Q Member 1; FDA, Food and Drug Administration; UDP—glucuronosyltransferases, Uridine 5′′-diphospho-glucuronosyltransferase.

Case report

A 27-year-old Saudi-Arabian male with a 4-year history of idiopathic epilepsy was referred to the cardiology department at our hospital for an investigation of his recurrent syncopal episodes and an abnormal electrocardiogram. The patient's most recent admission was due to a generalized tonic-clonic seizure with lateral tongue biting lasting for 10 min. Seizure activity was rapidly terminated after four milligrams of intravenous lorazepam was administered. The patient recovered immediately with no evidence of confusion or weakness. However, an hour after seizure onset, the patient developed shortness of breath, which lasted for 10 min. A baseline electrocardiogram in the emergency department demonstrated a greater than 2 mm ST segment elevation in leads V1 and V2 with a prominent J wave followed by negative T waves (**Figure 1**). This was consistent with a type 1 Brugada pattern, facilitating the patient's referral to our department.

The patient described that he has been experiencing intermittent incidents of transient loss of consciousness preceded by light-headedness and palpitations. Moreover, he reported that this was unusual as he previously experienced one or two episodes annually of generalized tonic-clonic seizures with lateral tongue-biting and urinary incontinence. However, his recent syncopal episodes presented differently as described above and have occurred more frequently. A thorough evaluation of the patient's family history was undertaken, which did not reveal any history of cardiac disorders, epilepsy, or sudden death. Moreover, the patient described that the incidence of his syncopal episodes began after the initiation of lamotrigine therapy. The patient had previously been prescribed 1,000 milligrams of levetiracetam twice daily; however, 100 milligrams of lamotrigine twice daily was introduced to establish adequate control of seizure activity. Previous electrocardiograms before the initiation of lamotrigine therapy demonstrated normal sinus rhythm with no evidence of a type 1 Brugada pattern.

The patient underwent a transthoracic echocardiogram which revealed no evidence of structural heart disease. Further, electrocardiograms were repeated and were consistent with a type 1 Brugada pattern. Moreover, a CT scan of the head revealed no brain abnormalities. An electroencephalogram (EEG) reported during the awake stage revealed well-organized activity with no spike-and-wave discharges or lateralizing abnormalities. Subsequent phonic stimulation did not

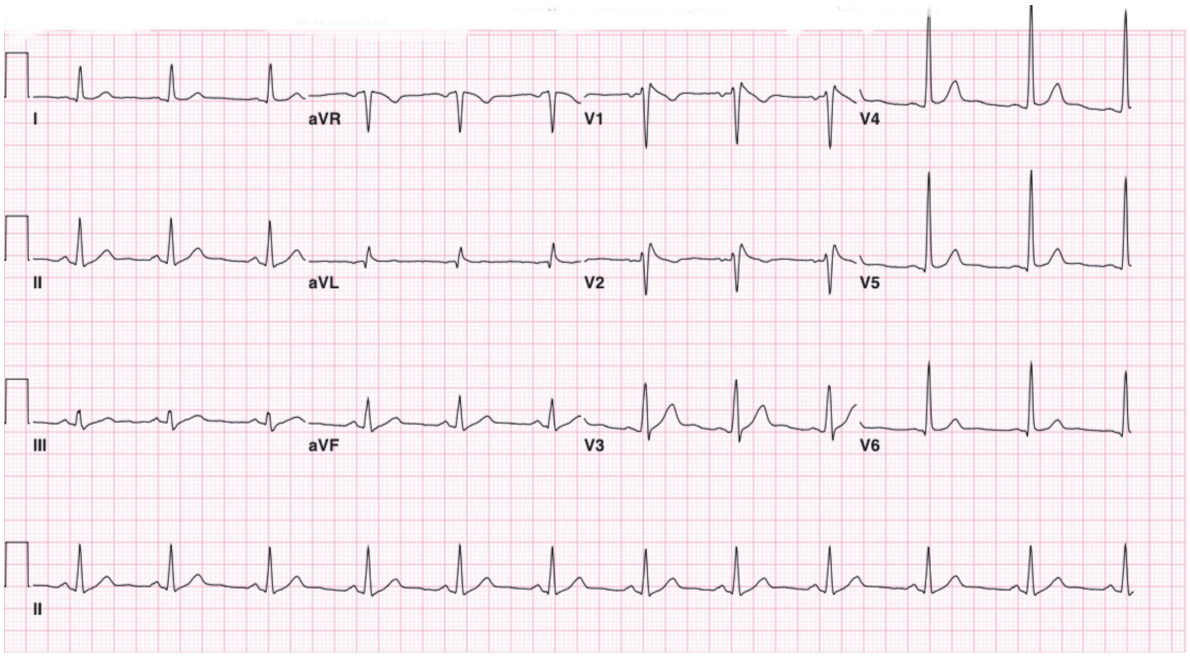

FIGURE 1
Twelve-lead electrocardiogram demonstrating 2 mm ST segment elevation in leads V1 and V2 with a prominent J wave followed by negative T waves. Suggestive of a type 1 Brugada pattern.

produce any abnormalities. An electrophysiological study was performed, which resulted in the induction of polymorphic ventricular tachycardia after programmed electrical stimulation of the right ventricular outflow tract (**Figure 2**). The ventricular tachycardia was terminated through cardioversion, and the patient remained comfortable throughout the study with no hemodynamic compromise.

Due to the presence of a type 1 Brugada pattern on electrocardiography along with a positive electrophysiological study and the presence of syncope, a recommendation for the placement of an implantable cardiac defibrillator (ICD) was made to the patient in accordance with current guidelines (1, 3). A thorough discussion regarding the risk of sudden cardiac death and the utility of ICD implantation was initiated; however, the patient refused further treatment. Moreover, the patient refused to undergo genetic testing to identify deleterious genetic variants in genes coding for voltage-gated sodium channels. A recommendation was made to the neurology team to discontinue lamotrigine therapy due to its potential arrhythmogenic effects.

The patient is currently receiving 1,000 milligrams of levetiracetam twice daily and has discontinued lamotrigine therapy after his initial admission. A follow-up assessment 3 months after the patient's initial admission revealed no further incidences of seizures or syncopal episodes. In addition, further electrocardiograms obtained after the discontinuation of lamotrigine therapy display normal sinus rhythm with near complete resolution of the J-point elevation and the type 1 Brugada pattern (**Figure 3**).

Discussion

We are reporting a case of lamotrigine-induced unmasking of BrS in a patient with idiopathic epilepsy. This case highlights two exceedingly rare associations, with one being lamotrigine's unmasking of BrS, while the other association encompasses the coexistence of epilepsy and BrS amongst specific individuals.

The pathophysiological mechanisms underlying BrS and idiopathic epilepsy share a coalescent theme pertaining to the dysregulation of cardiac and neuronal voltage-gated ion channels resulting in the premature excitability of cells, which manifests as cardiac arrhythmias and seizure-like activity, respectively (1, 6, 7). To identify reports highlighting the coexistence of epilepsy and BrS, we performed a Medline search using the keywords' Brugada syndrome', "Epilepsy," and "Seizure." Our initial search identified seventy-nine studies, and after abstract screening to identify relevant papers, we identified seventeen publications reporting cases of BrS in association with epilepsy (14–16, 19–32). The essential characteristic features of each paper, including electrocardiogram findings (EKG), electroencephalogram (EEG) findings, features of epilepsy, and the type of antiepileptic therapy, are highlighted in **Table 1**.

Mutations in voltage-gated sodium ion channels underlie the repolarization and depolarization abnormalities observed in

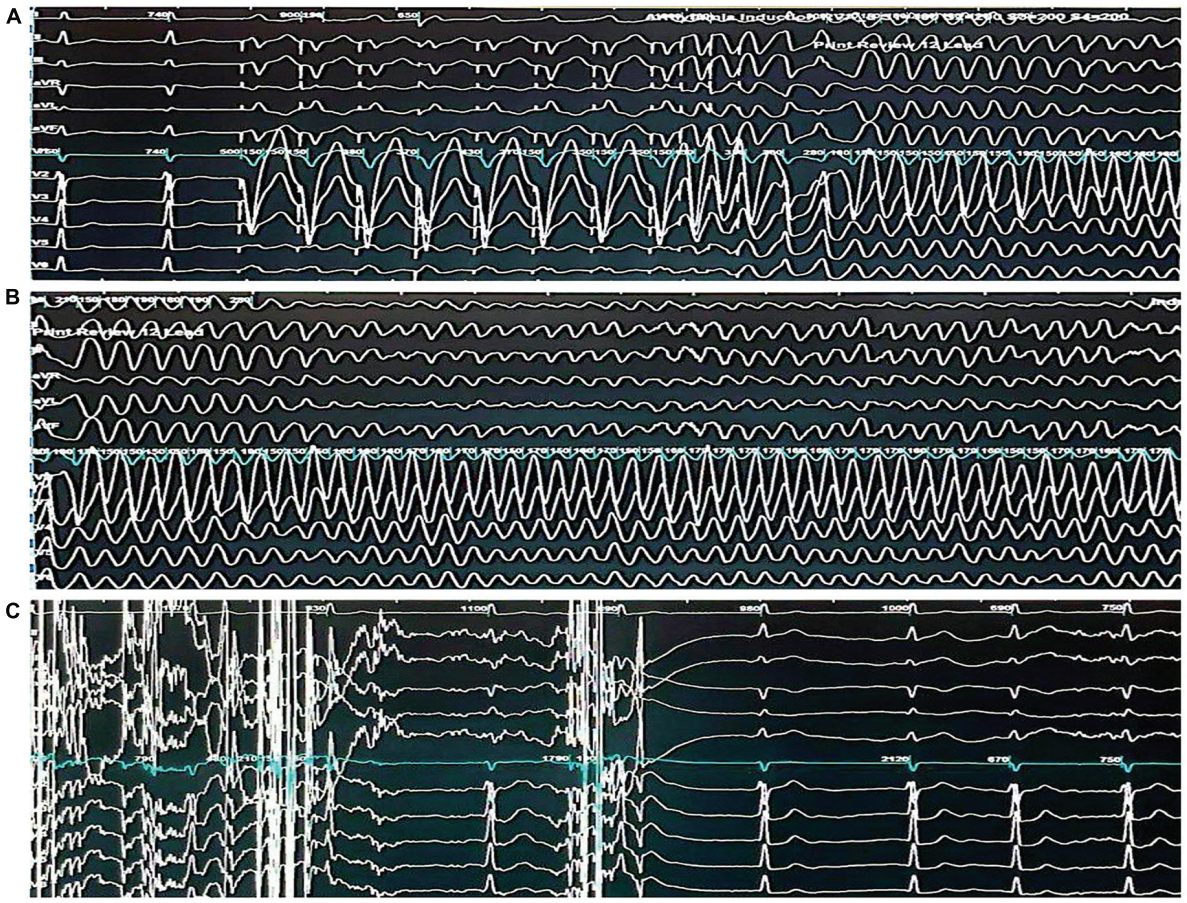

FIGURE 2
Electrophysiological study demonstrating the induction and termination of ventricular fibrillation. **(A)** Twelve -lead electrocardiogram demonstrating the induction of ventricular fibrillation through triple extrastimuli at the right ventricular outflow tract. **(B)** Twelve-lead electrocardiogram demonstrating sustained ventricular fibrillation. **(C)** Twelve-lead electrocardiogram demonstrating the termination of ventricular fibrillation through a 360-J transthoracic direct current shock and subsequent return to sinus rhythm.

BrS (1, 2). Over twenty individual genes have been associated with the development of BrS (2). Notably, loss of function mutations in the *SCN5A* gene, which codes for the alpha-subunit of the $Na_V1.5$ cardiac voltage-gated sodium channels, have been implicated in over 80% of identifiable mutations in BrS (2–33). Parisi et al. provide a report of a family with a mutation in *SCN5A* with co-expression of BrS and epilepsy along with characteristic EKG and EEG findings which can be found in **Table 1** (21). The authors of this paper suggest that individuals who possess the *SCN5A* mutation may have an age-dependent phenotypic expression of this mutation, with cerebral features presenting earlier in life and cardiac manifestations occurring in the later decades. This hypothesis is further supported by patients with gastrointestinal disease harboring the *SCN5A* mutation expressing variable symptoms within each age group (34). Furthermore, Leong et al. highlight a case of a patient harboring an *SCN5A* mutation with temporal lobe epilepsy and BrS (16). Animal studies in rats demonstrate the expression of *SCN5A* genes within the limbic system, suggesting that it can alter neuronal action potential propagation (35). More recently, the expression of *SCN5A* genes within the human brain has been described, with studies suggesting an increased expression within astrocytes and astrocytoma tumors (36–38). Hence, co-expression of *SCN5A* genes within the brain and cardiac tissue may underpin the concurrence of BrS and epilepsy amongst genetically susceptible individuals harboring the *SCN5A* mutation.

Recently, mutations in the *SCN10A* gene, which codes for the voltage-gated sodium channels subunit $Na_V1.8$, were implicated in a large percentage of BrS cases and were associated with an increased phenotypic expression of symptoms (39). Interestingly, despite the $Na_V1.8$ being mainly expressed in the peripheral nervous system, in certain pathologies the $Na_V1.8$ has been found within the central nervous system (40). Moreover, a recent genetic analysis has demonstrated that variants in the *SCN10A* gene were linked to certain

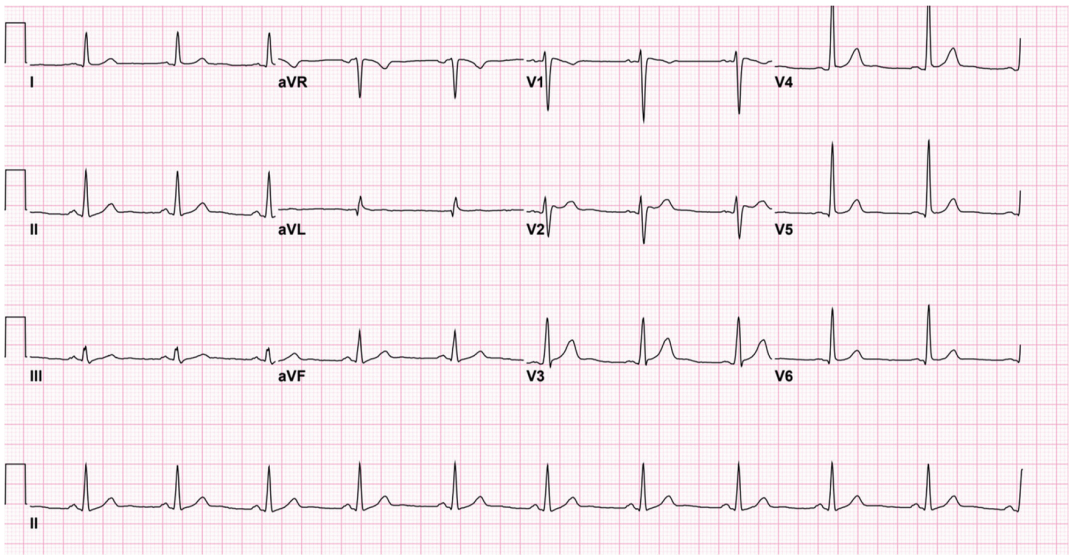

FIGURE 3
Twelve-lead electrocardiogram after the discontinuation of lamotrigine. The electrocardiogram demonstrates normal sinus rhythm with near resolution of the J-point elevation and type 1 Brugada pattern.

epilepsy-related phenotypes (41). Banfi et al. highlight a case of epilepsy associated with novel mutations identified in the voltage-gated sodium channel SCN9A gene, and the *AKAP9* gene, which have previously been implicated in cases of BrS (14, 42). The *SCN9A* gene is also expressed in the brain, with mutations in this gene being associated with the development of certain subtypes of epilepsy (43, 44). It is worth noting that BrS is not the only cardiac channelopathy that has been associated with epilepsy. Namely, the *KCNQ1* gene, which codes for voltage-gated potassium channels, has been correlated with epilepsy and long QT syndrome (LQTS) in a subgroup of patients (45).

Sudden unexplained death in epilepsy (SUDEP) is a phenomenon that carries tremendous morbidity among patients diagnosed with epilepsy. Approximately 18% of patients with epilepsy die due to SUDEP (8). One of the leading theories behind the pathophysiological mechanisms of SUDEP involves the onset of fatal cardiac arrhythmias (42). This theory is supported by retrospective cohort studies which suggest that patients with epileptic seizures have an increased incidence of abnormal electrocardiogram signs (46–48). It is also worth noting that SUDEP and sudden cardiac death have been shown to share similar risk factors, including sex and age (49). Furthermore, some gene mutations in genes that code for cardiac voltage-gated ion channels have been identified in patients with SUDEP. In particular, a few studies have reported mutations of the *SCN5A* and *SCN10A* genes amongst patients with SUDEP (50, 51).

Interestingly, mutations in the *SCN8A* gene, which codes for the alpha subunit type 8 of the voltage-gated sodium channel ($Na_V1.6$), have been implicated in cases of epilepsy and SUDEP (52). The $Na_V1.6$ voltage-gated sodium channel is predominantly expressed in the brain; hence mutations in the *SCN8A* gene are associated with a subtype of epilepsy termed early infantile-epileptic encephalopathy-13 (43). Individuals with *SCN8A* mutations possess up to a 10% higher risk of SUDEP (43). A possible explanation for this increased risk relates to the expression of $Na_V1.6$ in cardiac tissue, with mutations in this gene having been associated with cardiac arrhythmias in animal models (43, 53). Moreover, it is worth noting that the mere presence of the $Na_V1.6$ channel, under pathological conditions, may contribute to cardiac arrythmias. For instance, an *in vivo* study utilizing mouse models examined the effects of sodium-channel blockade on the induction of catecholaminergic polymorphic ventricular tachycardia (54). The authors of this study noted that blockade of the $Na_V1.6$ channel reduced the incidence of cardiac arrythmias (54). In addition, the authors hypothesize that $Na_V1.6$ blockade may interfere with sodium and calcium signaling within cardiac myocytes, thus, specific blockade of $Na_V1.6$ may provide a novel approach for the treatment of cardiac arrythmias (54). Munger et al. also examined the impact of $Na_V1.6$ on calcium and sodium channel dysregulation on the induction of atrial fibrillation (55). The authors of this paper suggest that blockade of sodium-channel isoforms such as the $Na_V1.6$ provides a novel approach for the treatment of atrial fibrillation through modulation of calcium release within myocytes (55). Moreover, the *SCN1A* gene which codes for the $Na_V1.1$ voltage-gated sodium channel, has also been associated with epilepsy, SUDEP, and cardiac conduction abnormalities across *in vivo* and *in vitro* studies. Mutations in the *SCN1A* lead to the

development of Dravet syndrome (a form of early onset severe myoclonic epilepsy) in over 80% of cases (56). The incidence of SUDEP amongst patients with Dravet syndrome is the highest SUDEP rate reported amongst epilepsy subtypes, hence, examining the mechanisms which may underpin SUDEP in Dravet syndrome is essential to further the understanding of the role of sodium channel isoforms in cardiac arrhythmogenesis and epilepsy (57). Auerbach et al. explored the mechanisms behind the altered cardiac electrophysiology and SUDEP in a mouse model with Dravet syndrome (58). The authors of this study noted that the mice with Dravet syndrome exhibited abnormalities in transient and persistent sodium current density within cardiac myocytes (58). The authors also noted the presence of increased cardiac excitability and arrhythmogenic electrocardiogram changes within the Dravet mice (58). Kalume et al. also examined the mechanisms behind SUDEP in a Dravet mouse model (59). The findings of this study suggest that SUDEP in association with *SCN1A* mutations is triggered by parasympathetic overdrive resulting in fatal bradycardia and cardiac dysregulation (59). Experimental models examining the effects of *SCN1A* mutations in epilepsy have described the overexpression of the $Na_V1.1$ channels within cardiac myocytes and subsequent cardiac hyper-excitability resulting in a predisposition to cardiac arrhythmogenesis (60).

The coexistence of epilepsy and BrS poses a tremendous diagnostic challenge due to the overlap in presentations amongst both diseases. Differentiating true epileptic seizures from arrhythmia-induced syncope amongst patients with BrS is challenging. Seizure-like activity amongst patients with BrS may be a byproduct of cardiac arrhythmias resulting in cerebral hypoperfusion and subsequent syncope (61, 62). There have been four reports of BrS masquerading as a seizure disorder resulting in the misdiagnosis of patients (20, 25, 26, 32). One of the reports by Wee and Latorre was that of a 25-year-old male who was presumed to have epilepsy and presented to the emergency department with an anoxic brain injury resulting in his subsequent death (25). A type 1 BrS pattern was missed on the patient's previous electrocardiograms; thereby, this report illustrates the significant magnitude associated with a misdiagnosis of epilepsy amongst BrS patients. Moreover, clinical features characteristically associated with epilepsy, such as tongue-biting and generalized tonic-clonic convulsions, may be observed in patients with arrhythmia-induced syncopal episodes, making establishing a final diagnosis a tremendous hurdle (63). The BrS EKG pattern may also not be visible on the initial EKG and may require further assessment through sodium-channel blocker provocative testing. In addition, a multicenter prospective observational study amongst patients with drug-resistant epilepsy found that syncope and epilepsy were coexistent amongst 20% of subjects (64). The discovery of mutations in voltage-gated cardiac ion channels amongst patients with SUDEP may be explained by the existence of potentially undiagnosed cardiac channelopathies and arrhythmias. Misdiagnosis of cardiac channelopathies as epilepsy, is also common with LQTS. A study by MacCormick et al. found that patients diagnosed with epilepsy experienced a delay of approximately 12 years before a correct diagnosis of LQTS was made (65).

Lamotrigine is an antiepileptic drug that inhibits neuronal voltage-gated sodium channels, stabilizing presynaptic neurons and suppressing unregulated glutamate release (11). Recently in 2021, the United States Food and Drug Administration (FDA) issued a warning recommending against using lamotrigine in individuals with structural heart disease and conduction disorders due to its potential arrhythmogenic effect (12). The FDA's warning was based on *in vitro* studies suggesting that lamotrigine might inhibit cardiac voltage-gated sodium channels with similar pharmacodynamics to class IB antiarrhythmic agents (12, 13). It is well-established that sodium-channel blockers may induce malignant ventricular arrhythmias in patients with BrS (66). Moreover, sodium-channel blocking antiarrhythmic drugs such as flecainide and ajmaline are used to artificially induce ventricular arrhythmias in patients with BrS as part of the diagnostic process (64). An animal study by Goto et al. investigated the effects of lamotrigine therapy on EKG parameters (67). A notable finding from this study included the elevation of the J wave in over half of the animals (67). The J wave is a distinctive feature of BrS, thereby suggesting that lamotrigine may possess the ability to unmask a BrS pattern in genetically susceptible individuals. Lamotrigine exhibits blockade of the brain's most abundantly expressed voltage-gated sodium channels, including the $Na_V1.1$, $Na_V1.2$, and $Na_V1.6$ (68). However, lamotrigine has also been shown to impact the cardiac voltage-gated sodium channel isoform $Na_V1.5$ in several *in vitro* studies. In a paper by Ingleby-Talecki et al., lamotrigine was shown to block $Na_V1.5$ current even at therapeutic dosages (69). Lamotrigine demonstrated a half maximal inhibitory concentration (IC_{50}) of 280.2 and 28.8 μM at holding voltages of –120 and –95, respectively (69). Moreover, other *in vitro* studies have reported similar potencies regarding lamotrigine's $Na_V1.5$ blockade (13, 70). *In vitro* studies have also shown that lamotrigine demonstrates voltage-dependent blockade of the $Na_V1.5$ channels with rapid kinetics, closely resembling the class IB anti-arrhythmic agent mexiletine (69). The findings of the aforementioned *in vitro* studies suggest that lamotrigine may be capable of blocking $Na_V1.5$ channels at plasma concentrations observed within its therapeutic dosage range. Moreover, a human study by Dixon et al. analyzed the effects of lamotrigine on the PR interval in healthy subjects (71). The study demonstrates that lamotrigine may exhibit a dose-dependent prolongation of the PR interval (71). The PR interval may be prolonged due to $Na_V1.5$ blockade, however, other factors such as heart rate and autonomic stimulation may contribute to PR prolongation (72). The findings of the *in vitro* studies coupled with lamotrigine's effects on electrocardiogram markers such as the J wave and PR interval

TABLE 1 Characteristic features of seventeen publications reporting the association between epilepsy and Brugada syndrome.

First author and year of publication	Patient age and gender	Brugada pattern on EKG	SCN5A mutation status	Epilepsy and EEG features	Antiepileptic medication	Additional information
Abdelghani et al. (20)	30-year-old male	Type 1 Brugada pattern	Not available	- Prior history of transient loss of consciousness with convulsions and epileptiform activity	- Sodium valproate and phenytoin	- Patient presented with cardiac arrest with ventricular fibrillation - Patient underwent epicardial radiofrequency catheter ablation and ICD implantation and was followed-up for 14 months with no further episodes - Antiepileptic medication was discontinued after ablation and ICD implantation
Parisi et al. (21)	- Patient 1: deceased female - patient 2: 40-year-old male - Patient 3: 42-year-old male - patient 4: 5-year-old male patient	All 4 patients had evidence of a type 1 Brugada pattern on EKG	Positive across all four patients	- Patient 1: not available - patient 2: tonic clonic seizures. focal posterior left abnormalities on EEG. - patient 3: tonic clonic seizures. focal posterior left abnormalities on EEG. - patient 4: history of recurrent falls and generalized slow spike-waves on EEG.	- Patient 1: not available - patient 2: phenobarbital - patient 3: phenobarbital - patient 4: levetiracetam, clobazam	- All four patients were members of the same family - All patients had undergone ICD implantation
Sotero et al. (14)	64-year-old male	Type 1 Brugada pattern	Negative	- Focal epilepsy.EEG showed bilateral focal slow temporal activity and right temporal epileptic activity	- 100 mg Lamotrigine per day - 500 mg of sodium valproate twice daily	- The patient experienced an increase in syncopal episodes after initiation of lamotrigine - EKG prior to initiation of lamotrigine was normal. - Repeat EKG after discontinuation of lamotrigine was normal and flecainide provocative drug test was normal
Fauchier et al. (22)	24-year-old male	Type 1 Brugada pattern	Not available	- History of idiopathic epilepsy with generalized tonic clonic seizures. - One-off EEG was reported as normal.	- Diazepam and phenobarbital	- Patient had witnessed generalized tonic-clonic seizures with evidence of lateral tongue biting and urinary incontinence.
Gülşen and Eker (23)	52-year-old female	Type 1 Brugada pattern	Not available	- Generalized tonic clonic seizures. - EEG revealed bilateral frontal intermittent rhythmic delta wave activity just before the convulsive episode.	- Levetiracetam 1,000 mg per day	- Patient had a paternal history of sudden cardiac death.
Camacho Velásquez et al. (24)	Patient 1: 37-year-old man Patient 2: 49-year-old man	Patient 1: Type 1 Brugada syndrome after Ajmaline provocative drug testing patient 2: type 3 Brugada pattern	Not available in both patients	- Patient 1: tonic clonic seizures with confusion after episodes. No EEG available. - patient 2: tonic clonic seizures. EEG revealed right fronto-temporal spikes	- Patient 1: Valproic acid 1,500 mg daily. - Patient 2: Levetiracetam 2,000 mg per day	- Patient 1 had a positive ajmaline provocative drug test whereas patient 2 had a positive flecainide provocative drug test revealing a Brugada pattern on EKG after infusion

(Continued)

10.3389/fcvm.2022.1005952

TABLE 1 (Continued)

First author and year of publication	Patient age and gender	Brugada pattern on EKG	SCN5A mutation status	Epilepsy and EEG features	Antiepileptic medication	Additional information
Banfi et al. (15)	30-year-old male	Type 1 Brugada pattern	Negative	Generalized tonic clonic seizures. EEG revealed diffuse slow waves and spikes	- Lamotrigine 3 mg/Kg/day	- The patient had a history of autism spectrum disorder and intellectual disability - The patient was on 15 mg/kg/day of sodium valproate daily prior to being switched over to lamotrigine - EKG findings returned to normal after initiation of lamotrigine - Rare variants identified in SCN9A and AKAP9 genes
Wee and Latorre (25)	25-year-old male	Type 1 Brugada pattern	Not available	EEG revealed diffuse slowing with no epileptiform activity	- Not specified	- Patient was given an anti-epileptic prescription which was never filled. - Patient had previous episodes of loss of consciousness with one episode lasting for approximately 40 min.
Anabtawi et al. (26)	56-year-old female	Type 1 Brugada pattern	Not available	- Not available	- Not specified	
Strimel et al. (19)	22-year-old female	Type 1 Brugada pattern	Not available	- History of temporal lobe epilepsy EEG not available	- 550 mg of lamotrigine daily	- The patient's lamotrigine blood level was approximately five times the upper limit of the normal range. - Procainamide provocative drug test after normalization of lamotrigine levels demonstrated no appearance of a Brugada pattern on EKG.
Sandorfi et al. (27)	41-year-old male	Type 1 Brugada pattern after procainamide provocative testing	Not available	- History of generalized seizures. - Several EEGs reported as normal, however, continuous EEG monitoring revealed rhythmic seizure activity in the left hemisphere	- Levetiracetam and oxcarbazepine	- The patient underwent ICD implantation
Huang et al. (28)	41-year-old male	Type 1 Brugada pattern	Not available	- Presented to the emergency department in status epilepticus after over half an hour of generalized tonic clonic seizures	- No antiepileptic therapy	- The patient presented with status epilepticus and ventricular fibrillation and direct current cardioversion was delivered which revealed the underlying type 1 Brugada pattern.

(Continued)

10.3389/fcvm.2022.1005952

TABLE 1 (Continued)

First author and year of publication	Patient age and gender	Brugada pattern on EKG	SCN5A mutation status	Epilepsy and EEG features	Antiepileptic medication	Additional information
Van Gorp et al. (29)	8-year-old male	Type 1 Brugada pattern	Not available	- History of tics, urinary incontinence, and learning disability. Night-time EEG monitoring revealed rapid, rhythmic, and low voltage EEG activity in the left temporal region	- Valproic acid 300 mg twice daily	- This study reported 3-day monitoring of the initiation of antiepileptic medication in a pediatric patient with pre-existing Brugada syndrome.
Ali (30)	59-year-old male	Type 1 Brugada pattern	Not available	- Generalized tonic clonic seizures lasting 30 s with rapid recovery and urinary incontinence	- Not available	- Patient initially presented with ventricular tachycardia - Procainamide provocative drug testing revealed Type 1 Brugada pattern.
Leong et al. (16)	60-year-old female	- Type 1 Brugada pattern after ajmaline provocative drug test	Positive	- Temporal lobe epilepsy - EEG revealed Epileptiform activity in both temporal lobes	- Lamotrigine 125 mg twice daily and 1.5 g of levetiracetam twice daily	
Gigli et al. (31)	40-year-old female	Type 1 Brugada pattern	Negative	- History of juvenile myoclonic epilepsy and recent generalized tonic clonic seizures - EEG revealed generalized spike-wave and spike-slow wave complexes.	- Valproic acid 750 mg per day	- Novel mutation identified in plakophilin 2 (PKP2)
Negro et al. (32)	36-year-old male	Type 1 Brugada pattern after ajmaline administration	Not available	- History of recurrent syncopal episodes with loss of consciousness and convulsions. - EEG not available	- Phenytoin 100 mg per day	- The patient had a family history of epilepsy and sudden unexplained death - Phenytoin levels were recorded to be above therapeutic range - Patient experienced several episodes of ventricular fibrillation and cardiac arrest resulting in the patient's death - The authors suggest that the epilepsy was misdiagnosed, and the patient had Brugada syndrome which was exacerbated by phenytoin.

10.3389/fcvm.2022.1005952

TABLE 2 Characteristic features of six publications reporting the association between lamotrigine therapy and Brugada syndrome.

Author and year of publication	Patient age and gender	Lamotrigine dose	Brugada pattern on EKG	SCN5A mutation status	Additional information
Sotero et al. (14)	64-year-old male	100 mg per day	Type 1 Brugada pattern	Negative	- Patient had a prior diagnosis of focal epilepsy - The patient was on 500 mg of sodium valproate twice daily and experienced an increase in syncopal episodes after initiation of lamotrigine - EKG prior to initiation of lamotrigine was normal. - Repeat EKG after discontinuation of lamotrigine was normal and flecainide provocative drug test was normal
Banfi et al. (15)	30-year-old male	3 mg/Kg/day	Type 1 Brugada pattern	Negative	- The patient suffered from generalized tonic clonic seizures and had a history of autism spectrum disorder and intellectual disability - The patient was on 15 mg/kg/day of sodium valproate daily prior to being switched over to lamotrigine - EKG findings returned to normal after initiation of lamotrigine - Lamotrigine level was reported to be within the normal range - Rare variants identified in SCN9A and AKAP9 genes
Leong et al. (16)	60-year-old female	125 mg twice daily	No evidence of Type 1 Brugada pattern on initial baseline EKG	Positive	- Patient had a diagnosis of temporal lobe epilepsy - Patient had a family history of sudden cardiac death - The patient was also taking 1.5 g of levetiracetam twice daily - Ajmaline provocative drug test revealed appearance of Type 1 Brugada pattern and QRS widening with bigeminy after 3 min of infusion - Repeat ajmaline provocative drug test after discontinuation of lamotrigine revealed Type 1 Brugada EKG pattern with no QRS widening or bigeminy
Tessitore et al. (17)	62-year-old male	Not available	Type 1 Brugada pattern	Not available	- Patient has a medical history of bipolar disorder and paroxysmal atrial fibrillation - Patient overdosed on 1 gram of Flecainide in addition to an unknown amount of lamotrigine and quetiapine.
Rodrigues et al. (18)	52-year-old woman	100 mg per day	Type 1 Brugada pattern	Not available	- Three EKGS were performed after a flecainide provocative drug test and only one of three revealed a Type 1 Brugada pattern.
Strimel et al. (19)	22-year-old female	550 mg per day	Type 1 Brugada pattern	Not available	- The patient has a history of temporal lobe epilepsy. - The patient's lamotrigine level was approximately five times the upper limit of the normal range. - Repeat procainamide provocative drug test after normalization of lamotrigine levels demonstrated no appearance of a Brugada pattern on EKG.

10.3389/fcvm.2022.1005952

in *in vivo* studies suggest that at therapeutic concentrations, lamotrigine may possess the ability to inhibit $Na_V1.5$ channels and thus contribute to the Brugada phenotype in genetically susceptible individuals.

To explore the association between lamotrigine therapy and the unmasking of BrS, we performed a Medline search using the terms "Lamotrigine" and "Brugada Syndrome." A total of 11 publications were identified, and abstract screening resulted in the selection of six reports (14–19). The features of each report, including patient characteristics, EKG findings, and lamotrigine dosage, are summarized in **Table 2**.

Four of the six patients have been treated with lamotrigine for pre-existing epilepsy (14–16, 19). In addition, all patients demonstrated a type 1 BrS pattern on EKG. Interestingly, five patients had a previously normal EKG prior to the initiation of lamotrigine therapy, suggesting that lamotrigine may contribute to unmasking the BrS pattern in susceptible individuals (14–19). Furthermore, the blood levels of lamotrigine were reported to be elevated in a paper by Strimel et al., whereas Banfi et al. reported a lamotrigine level within the normal range (15, 19). The lamotrigine blood level was unavailable within other reports. However, the discrepancy in the lamotrigine blood levels between the two papers highlights that lamotrigine may exhibit an inhibitory effect on cardiac sodium channels at both therapeutic and supra-therapeutic levels. It has previously been hypothesized that lamotrigine may unmask BrS at higher drug concentrations due to loss of specificity for neuronal voltage-gated sodium channels resulting in downstream effects on cardiac voltage-gated channels (19). However, the unmasking of BrS at normal physiological blood levels of lamotrigine contradicts this theory. We hypothesize that individual genetics may interfere with lamotrigine metabolism resulting in significant disparities relating to its pharmacokinetic metabolism amongst different individuals. Lamotrigine exhibits first-order pharmacokinetics and has an excellent oral bioavailability resulting in its rapid absorption with maximal plasma concentrations of the drug occurring within 1–3 h (11). Moreover, the metabolism of lamotrigine is facilitated by different UDP−glucuronosyltransferase enzymes in the liver (11). Individuals express a wide range of heterogeneity amongst genes coding for UDP−glucuronosyltransferases, and multiple polymorphisms can be detected amongst the population (73). The variable pharmacokinetic profile of lamotrigine was investigated in a study of 100 epilepsy patients by Milosheska et al. (74). The study found that multiple factors influenced the clearance of lamotrigine, including genetic polymorphisms in UDP−glucuronosyltransferases, body weight, and renal function (74). Therefore, the authors of this paper suggested that the variability in lamotrigine's pharmacokinetics governs the need for more precise and individualized drug monitoring and dosage adjustments (74).

As mentioned previously, many patients with cardiac channelopathies have a prior diagnosis of epilepsy requiring antiepileptic drug treatment. The role of antiepileptic drugs in the management of true epileptic seizures is well-established. For instance, the therapeutic interventions used in our patient's case to manage his epilepsy diagnosis included levetiracetam and lamotrigine, which are supported by clinical and pharmacogenomic studies (75). However, using antiepileptic drugs in patients with non-epileptic seizures and concurrent cardiac channelopathies may result in an arrhythmogenic effect. For instance, a paper by Bardai et al. found an increase in the risk of SCD in association with both epilepsy and the use of antiepileptic drugs (76). Moreover, Ishizue et al. found that polytherapy with multiple sodium channel blocking antiepileptic drugs was associated with arrhythmogenic EKG abnormalities (77). The unmasking of a BrS pattern on EKG has also been observed with other antiepileptic drugs, such as carbamazepine and phenytoin (78, 79).

Nonetheless, the evidence for lamotrigine's arrhythmogenic effects remains unclear as the FDA's current recommendation is based solely on the findings of *in vitro* studies. The findings of the aforementioned *in vitro* studies regarding lamotrigine's impact on cardiac activity have yet to translate clinically. For instance, a recent systematic review by Restrepo et al. explored cardiac risk in patients undergoing lamotrigine therapy and found no clear evidence to support an increase in cardiac risk (80). Therefore, as it currently stands, lamotrigine and other sodium-channel blocking antiepileptic drugs are not contraindicated in patients with BrS.

Conclusion

As described previously, the coexistence of epilepsy and BrS has been associated with mutations in genes coding for voltage-gated ion channels, which are coexpressed in cardiac and neural tissue (7). However, it is worth noting that the relationship between genotypes and clinical phenotypes is often not linear; hence mutations in genes co-expressed in cardiac and neuronal tissue may independently induce epilepsy and cardiac arrhythmias. Sudden unexplained death in epilepsy has been associated with malignant cardiac arrhythmias due to the presence of mutations in genes coding for voltage-gated cardiac ion channels (7). Consequently, the identification of potentially pathogenic genetic variants which may underlie the pathogenesis of epilepsy, cardiac conduction disorders, and SUDEP requires the use of targeted next-generation sequencing technology and the execution of genome-wide association studies to further our understanding of the genetic basis of the aforementioned conditions (81). Moreover, the coexistence of epilepsy and BrS poses a diagnostic challenge due to the similar nature of clinical presentations. Therefore, we recommend a thorough neurological and cardiovascular evaluation of patients presenting with seizures and syncope to identify any underlying disorders.

Using sodium-channel blocking antiepileptic drugs such as lamotrigine in patients with coinciding epilepsy and BrS may promote arrhythmogenic effects in cardiac myocytes (12). Furthermore, individual genetic polymorphisms may influence the pharmacokinetic profile of lamotrigine, resulting in impaired metabolism and subsequent supratherapeutic blood levels (72). Accordingly, we propose the need for more research to understand the arrhythmogenic capacity of lamotrigine and other antiepileptic drugs. In addition, we recommend the need for precise and individualized therapeutic monitoring and dosage adjustments amongst patients receiving lamotrigine therapy.

Data availability statement

The original contributions presented in this study are included in the article/supplementary material, further inquiries can be directed to the corresponding author.

Ethics statement

The studies involving human participants were reviewed and approved by the King Abdullah International Medical Research Center (KAIMRC) Institutional Review Board. Written informed consent was obtained from the participant/s for the publication of this case report.

Author contributions

MO and AMA wrote the initial manuscript and carried out the literature review process. HO and HA contributed to the acquisition of clinical data and the clinical design of the manuscript. OA contributed to the review of the present literature. AA contributed to the collation of clinical data. All authors reviewed the manuscript and authorized its submission for publication.

Conflict of interest

The authors declare that the research was conducted in the absence of any commercial or financial relationships that could be construed as a potential conflict of interest.

Publisher's note

References

1. Li K, Lee S, Yin C, Liu T, Ngarmukos T, Conte G, et al. Brugada syndrome: a comprehensive review of pathophysiological mechanisms and risk stratification strategies. *Int J Cardiol Heart Vasc.* (2020) 26:100468. doi: 10.1016/j.ijcha.2020.100468

2. Watanabe H, Minamino T. Genetics of Brugada syndrome. *J Hum Genet.* (2015) 61:57–60.

3. Antzelevitch C, Yan G. J-wave syndromes: Brugada and early repolarization syndromes. *Heart Rhythm.* (2015) 12:1852–66.

4. Pappone C, Brugada J, Vicedomini G, Ciconte G, Manguso F, Saviano M, et al. Electrical Substrate elimination in 135 consecutive patients with Brugada syndrome. *Circ Arrhythm Electrophysiol.* (2017) 10:e005053. doi: 10.1161/CIRCEP.117.005053

5. Brugada R, Campuzano O, Sarquella-Brugada G, Brugada J, Brugada P. Brugada Syndrome. *Methodist Debakey Cardiovasc J.* (2014) 10:25.

6. Devinsky O, Vezzani A, O'Brien T, Jette N, Scheffer I, de Curtis M, et al. Epilepsy. *Nat Rev Dis Primers.* (2018) 4:18024.

7. D'Imperio S, Monasky M, Micaglio E, Ciconte G, Anastasia L, Pappone C. Brugada syndrome: warning of a systemic condition? *Front Cardiovasc Med.* (2021) 8:771349. doi: 10.3389/fcvm.2021.771349

8. Chahal C, Salloum M, Alahdab F, Gottwald J, Tester D, Anwer L, et al. Systematic review of the genetics of sudden unexpected death in epilepsy: potential overlap with sudden cardiac death and arrhythmia—related genes. *J Am Heart Assoc.* (2020) 9:e012264. doi: 10.1161/JAHA.119.012264

9. Ricci M, Menegon S, Vatrano S, Mandrile G, Cerrato N, Carvalho P, et al. SCN1B gene variants in Brugada syndrome: a study of 145 SCN5A-negative patients. *Sci Rep.* (2014) 4:6470. doi: 10.1038/srep06470

10. Costagliola G, Orsini A, Coll M, Brugada R, Parisi P, Striano P. The brain–heart interaction in epilepsy: implications for diagnosis, therapy, and SUDEP prevention. *Ann Clin Transl Neurol.* (2021) 8:1557–68. doi: 10.1002/acn3.51382

11. Rambeck B, Wolf P. Lamotrigine clinical pharmacokinetics. *Clin Pharmacokinet.* (1993) 25:433–43.

12. French J, Perucca E, Sander J, Bergfeldt L, Baulac M, Auerbach D, et al. FDA safety warning on the cardiac effects of lamotrigine: an advisory from the Ad Hoc ILAE/AES Task Force. *Epilepsia Open.* (2021) 6:45–8.

13. Harmer A, Valentin J, Pollard C. On the relationship between block of the cardiac Na+channel and drug-induced prolongation of the QRS complex. *Br J Pharmacol.* (2011) 164:260–73. doi: 10.1111/j.1476-5381.2011.01415.x

14. Sotero F, Silva C, Cunha N, Franco A, Pimentel J. Lamotrigine-induced Brugada syndrome: a rare adverse event. *Seizure.* (2022) 94:7–9. doi: 10.1016/j.seizure.2021.11.001

15. Banfi P, Coll M, Oliva A, Alcalde M, Striano P, Mauri M, et al. Lamotrigine induced Brugada-pattern in a patient with genetic epilepsy associated with a novel variant in SCN9A. *Gene.* (2020) 754:144847. doi: 10.1016/j.gene.2020.144847

16. Leong K, Seligman H, Varnava A. Proarrhythmogenic effects of lamotrigine during ajmaline testing for Brugada syndrome. *HeartRhythm Case Rep.* (2017) 3:167–71. doi: 10.1016/j.hrcr.2016.11.006

17. Tessitore E, Ramlawi M, Tobler O, Sunthorn H. Brugada pattern caused by a flecainide overdose. *J Emerg Med.* (2017) 52:e95–7. doi: 10.1016/j.jemermed.2016.10.045

18. Rodrigues R, Amador P, Rassi L, Seixo F, Parreira L, Fonseca N, et al. Brugada pattern in a patient medicated with lamotrigine. *Rev Port Cardiol.* (2013) 32:807–10. doi: 10.1016/j.repc.2013.01.009

19. Strimel W, Woodruff A, Cheung P, Kirmani B, Stephen Huang S. Brugada-like electrocardiographic pattern induced by lamotrigine toxicity. *Clin Neuropharmacol.* (2010) 33:265–7.

20. Abdelghani M, Chapra A, Asaad N, Hayat S. Epilepsy and brugada syndrome: association or uncommon presentation? *Heart Views.* (2020) 21:114.

21. Parisi P, Oliva A, Coll Vidal M, Partemi S, Campuzano O, Iglesias A, et al. Coexistence of epilepsy and Brugada syndrome in a family with SCN5A mutation. *Epilepsy Res.* (2013) 105:415–8. doi: 10.1016/j.eplepsyres.2013.02.024

22. Fauchier L, Babuty D, Cosnay P. Epilepsy, Brugada syndrome and the risk of sudden unexpected death. *J Neurol.* (2000) 247:643–4.

23. Gülşen K, Eker A. PP-205 Brugada syndrome and epilepsy in same patient: Na channel defect in both myocytes and neurons. *Am J Cardiol.* (2014) 113:S84.

24. Camacho Velásquez J, Rivero Sanz E, Velazquez Benito A, Mauri Llerda J. Epilepsy and Brugada syndrome. *Neurología.* (2017) 32:58–60.

25. Wee C, Latorre J. A fatal case of mistaken identity: Brugada syndrome masquerading as seizure disorder (P2.264). *Am Acad Neurol.* (2018). Available online at: https://n.neurology.org/content/90/15_Supplement/P2.264 (accessed July 19, 2022).

26. Anabtawi A, Anabtawi A, Kim A. A case of brugada syndrome presenting as seizure disorder. *J Am Coll Cardiol.* (2018) 71:A2547.

27. Sandorfi G, Clemens B, Csanadi Z. Electrical storm in the brain and in the heart: epilepsy and Brugada syndrome. *Mayo Clin Proc.* (2013) 88:1167–73. doi: 10.1016/j.mayocp.2013.06.019

28. Huang C, Chen T, Lin F, Huang M. Status epilepticus as an initial presentation of brugada syndrome: a case report. *Kaohsiung J Med Sci.* (2005) 21:387–91. doi: 10.1016/S1607-551X(09)70139-1

29. Van Gorp V, Danschutter D, Huyghens L, Hachimi-Idrissi S, Sarkozy A, Chierchia G, et al. Monitoring the safety of antiepileptic medication in a child with Brugada syndrome. *Int J Cardiol.* (2010) 145:e64–7. doi: 10.1016/j.ijcard.2008.12.156

30. Ali A. *Brugada Syndrome in a Black Man with Seizures and Urinary Incontinence*. Houston, TX: Texas Heart institute (2006).

31. Gigli L, Bertero G, Vidal M, Iglesias A, Campuzano O, Striano P, et al. Juvenile myoclonic epilepsy and Brugada type 1 ECG pattern associated with (a novel) plakophillin 2 mutation. *J Neurol.* (2017) 264:792–5. doi: 10.1007/s00415-017-8414-2

32. Negro G, Ciconte G, Borrelli V, Rondine R, Maiolo V, Pappone C. Sudden death of a patient with epilepsy: when Brugada syndrome mimicry can be fatal. *HeartRhythm Case Rep.* (2022) 8:205–8. doi: 10.1016/j.hrcr.2021.12.008

33. Li W, Yin L, Shen C, Hu K, Ge J, Sun A. SCN5A variants: association with cardiac disorders. *Front Physiol.* (2018) 9:1372. doi: 10.3389/fphys.2018.01372

34. Locke G, Ackerman M, Zinsmeister A, Thapa P, Farrugia G. Gastrointestinal symptoms in families of patients with an SCN5A-encoded cardiac channelopathy: evidence of an intestinal channelopathy. *Am J Gastroenterol.* (2006) 101:1299–304. doi: 10.1111/j.1572-0241.2006.00507.x

35. Wang J, Ou S, Wang Y, Kameyama M, Kameyama A, Zong Z. Analysis of four novel variants of Nav1.5/SCN5A cloned from the brain. *Neurosci Res.* (2009) 64:339–47. doi: 10.1016/j.neures.2009.04.003

36. Wang J, Ou S, Bai Y, Wang Y, Xu Z, Luan G. Multiple Nav1.5 isoforms are functionally expressed in the brain and present distinct expression patterns compared with cardiac Nav1.5. *Mol Med Rep.* (2017) 16:719–29. doi: 10.3892/mmr.2017.6654

37. Xing D, Wang J, Ou S, Wang Y, Qiu B, Ding D, et al. Expression of neonatal Nav1.5 in human brain astrocytoma and its effect on proliferation, invasion and apoptosis of astrocytoma cells. *Oncol Rep.* (2014) 31:2692–700. doi: 10.3892/or.2014.3143

38. Johnson J, Hofman N, Haglund C, Cascino G, Wilde A, Ackerman M. Identification of a possible pathogenic link between congenital long QT syndrome and epilepsy. *Neurology.* (2008) 72:224–31. doi: 10.1212/01.wnl.0000335760.02995.ca

39. Hu D, Barajas-Martínez H, Pfeiffer R, Dezi F, Pfeiffer J, Buch T, et al. Mutations in SCN10A are responsible for a large fraction of cases of Brugada syndrome. *J Am Coll Cardiol.* (2014) 64:66–79. doi: 10.1016/j.jacc.2014.04.032

40. Han C, Huang J, Waxman S. Sodium channel Nav1.8. *Neurology.* (2016) 86:473–83.

41. Kambouris M, Thevenon J, Soldatos A, Cox A, Stephen J, Ben-Omran T, et al. BiallelicSCN10Amutations in neuromuscular disease and epileptic encephalopathy. *Ann Clin Transl Neurol.* (2016) 4:26–35.

42. Wang M, Tu X. The genetics and epigenetics of ventricular arrhythmias in patients without structural heart disease. *Front Cardiovasc Med.* (2022) 9:891399. doi: 10.3389/fcvm.2022.891399

43. Menezes L, Sabiá Júnior E, Tibery D, Carneiro L, Schwartz E. Epilepsy-related voltage-gated sodium channelopathies: a review. *Front Pharmacol.* (2020) 11:1276. doi: 10.3389/fphar.2020.01276

44. Zhang S, Zhang Z, Shen Y, Zhu Y, Du K, Guo J, et al. SCN9A epileptic encephalopathy mutations display a gain-of-function phenotype and distinct sensitivity to oxcarbazepine. *Neurosci Bull.* (2019) 36:11–24. doi: 10.1007/s12264-019-00413-5

45. Goldman A, Glasscock E, Yoo J, Chen T, Klassen T, Noebels J. Arrhythmia in heart and brain: KCNQ1 mutations link epilepsy and sudden unexplained death. *Sci Transl Med.* (2009) 1:2ra6. doi: 10.1126/scitranslmed.3000289

46. Opherk C, Coromilas J, Hirsch L. Heart rate and EKG changes in 102 seizures: analysis of influencing factors. *Epilepsy Res.* (2002) 52:117–27. doi: 10.1016/s0920-1211(02)00215-2

47. Zare M, Salari M, Tajmirriahi M. Electrocardiographic changes in patients with refractory epilepsy. *J Res Med Sci.* (2013) 18(Suppl. 1):S32–4.

48. Zijlmans M, Flanagan D, Gotman J. Heart rate changes and ECG Abnormalities during epileptic seizures: prevalence and definition of an objective clinical sign. *Epilepsia.* (2002) 43:847–54. doi: 10.1046/j.1528-1157.2002.37801.x

49. Velagapudi P, Turagam M, Laurence T, Kocheril A. Cardiac arrhythmias and sudden unexpected death in epilepsy (SUDEP). *Pacing Clin Electrophysiol.* (2011) 35:363–70.

50. Ravindran K, Powell K, Todaro M, O'Brien T. The pathophysiology of cardiac dysfunction in epilepsy. *Epilepsy Res.* (2016) 127:19–29.

51. Coll M, Allegue C, Partemi S, Mates J, Del Olmo B, Campuzano O, et al. Genetic investigation of sudden unexpected death in epilepsy cohort by panel target resequencing. *Int J Legal Med.* (2015) 130:331–9. doi: 10.1007/s00414-015-1269-0

52. Gardella E, Møller R. Phenotypic and genetic spectrum of SCN 8A —related disorders, treatment options, and outcomes. *Epilepsia.* (2019) 60Suppl. 3:S77–85. doi: 10.1111/epi.16319

53. Frasier C, Wagnon J, Bao Y, McVeigh L, Lopez-Santiago L, Meisler M, et al. Cardiac arrhythmia in a mouse model of sodium channel SCN8A epileptic encephalopathy. *Proc Natl Acad Sci U.S.A.* (2016) 113:12838–43. doi: 10.1073/pnas.1612746113

54. Radwański P, Ho H, Veeraraghavan R, Brunello L, Liu B, Belevych A, et al. Neuronal Na+ channels are integral components of pro-arrhythmic Na+/Ca2+ signaling nanodomain that promotes cardiac arrhythmias during β-adrenergic stimulation. *JACC Basic Transl Sci.* (2016) 1:251–66. doi: 10.1016/j.jacbts.2016.04.004

55. Munger M, Olðar Y, Koleske M, Struckman H, Mandrioli J, Lou Q, et al. Tetrodotoxin—sensitive neuronal—type Na + channels: a novel and druggable target for prevention of atrial fibrillation. *J Am Heart Assoc.* (2020) 9:e015119. doi: 10.1161/JAHA.119.015119

56. Rosander C, Hallböök T. Dravet syndrome in Sweden: a population-based study. *Dev Med Child Neurol.* (2015) 57:628–33.

57. Cooper M, Mcintosh A, Crompton D, McMahon J, Schneider A, Farrell K, et al. Mortality in Dravet syndrome. *Epilepsy Res.* (2016) 128:43–7.

58. Auerbach D, Jones J, Clawson B, Offord J, Lenk G, Ogiwara I, et al. Altered cardiac electrophysiology and SUDEP in a model of dravet syndrome. *PLoS One.* (2013) 8:e77843. doi: 10.1371/journal.pone.0077843

59. Kalume F, Westenbroek R, Cheah C, Yu F, Oakley J, Scheuer T, et al. Sudden unexpected death in a mouse model of Dravet syndrome. *J Clin Investig.* (2013) 123:1798–808. doi: 10.1172/JCI66220

60. Biet M, Morin N, Lessard-Beaudoin M, Graham R, Duss S, Gagné J, et al. Prolongation of action potential duration and qt interval during epilepsy linked to increased contribution of neuronal sodium channels to cardiac late Na + current. *Circ Arrhythm Electrophysiol.* (2015) 8:912–20. doi: 10.1161/CIRCEP.114.002693

61. Petkar S, Hamid T, Iddon P, Clifford A, Rice N, Claire R, et al. Prolonged implantable electrocardiographic monitoring indicates a high rate of misdiagnosis of epilepsy–REVISE study. *Europace.* (2012) 14:1653–60. doi: 10.1093/europace/eus185

62. McKeon A, Vaughan C, Delanty N. Seizure versus syncope. *Lancet Neurol.* (2006) 5:171–80.

63. Akor F, Liu N, Besag F, Ahmed M. Value of tongue biting in differentiating between epileptic seizures and syncope. *Seizure.* (2013) 22:328.

64. Ungar A, Ceccofiglio A, Pescini F, Mussi C, Tava G, Rafanelli M, et al. Syncope and epilepsy coexist in 'possible' and 'drug-resistant' epilepsy (overlap

between epilepsy and syncope study - OESYS). *BMC Neurol.* (2017) 17:45. doi: 10.1186/s12883-017-0822-5

65. MacCormick J, McAlister H, Crawford J, French J, Crozier I, Shelling A, et al. Misdiagnosis of long QT syndrome as epilepsy at first presentation. *Ann Emerg Med.* (2009) 54:26–32.

66. Postema P, Wolpert C, Amin A, Probst V, Borggrefe M, Roden D, et al. Drugs and Brugada syndrome patients: review of the literature, recommendations, and an up-to-date website (www.brugadadrugs.org). *Heart Rhythm.* (2009) 6:1335–41. doi: 10.1016/j.hrthm.2009.07.002

67. Goto A, Hagiwara-Nagasawa M, Kambayashi R, Nunoi Y, Izumi-Nakaseko H, Kawai S, et al. Reverse translational analysis of clinically reported, lamotrigine-induced cardiovascular adverse events using the halothane-anesthetized dogs. *Heart Vessels.* (2020) 36:424–9. doi: 10.1007/s00380-020-01716-8

68. Qiao X, Sun G, Clare J, Werkman T, Wadman W. Properties of human brain sodium channel α-subunits expressed in HEK293 cells and their modulation by carbamazepine, phenytoin and lamotrigine. *Br J Pharmacol.* (2014) 171:1054–67. doi: 10.1111/bph.12534

69. Ingleby−Talecki L, van Dijkman S, Oosterholt S, Della Pasqua O, Winter C, Cunnington M, et al. Cardiac sodium channel inhibition by lamotrigine: in vitro characterization and clinical implications. *Clin Transl Sci.* (2022) 15:1978–89. doi: 10.1111/cts.13311

70. Guo D, Jenkinson S. Simultaneous assessment of compound activity on cardiac Nav1.5 peak and late currents in an automated patch clamp platform. *J Pharmacol Toxicol Methods.* (2019) 99:106575. doi: 10.1016/j.vascn.2019.04.001

71. Dixon R, Alexander S, Brickel N. Effect of lamotrigine on the PR interval in healthy subjects. *Br J Clin Pharmacol.* (2011) 71:961–2.

72. Erdemli G, Kim A, Ju H, Springer C, Penland R, Hoffmann P. Cardiac safety implications of hNav1.5 blockade and a framework for pre-clinical evaluation. *Front Pharmacol.* (2012) 3:6. doi: 10.3389/fphar.2012.00006

73. Miners J, McKinnon R, Mackenzie P. Genetic polymorphisms of UDP-glucuronosyltransferases and their functional significance. *Toxicology.* (2002) 18:453–6.

74. Milosheska D, Lorber B, Vovk T, Kastelic M, Dolžan V, Grabnar I. Pharmacokinetics of lamotrigine and its metabolite N-2-glucuronide: influence of polymorphism of UDP-glucuronosyltransferases and drug transporters. *Br J Clin Pharmacol.* (2016) 82:399–411. doi: 10.1111/bcp.12984

75. Wolking S, Moreau C, Nies A, Schaeffeler E, McCormack M, Auce P, et al. Testing association of rare genetic variants with resistance to three common antiseizure medications. *Epilepsia.* (2020) 61:657–66. doi: 10.1111/epi.16467

76. Bardai A, Blom M, van Noord C, Verhamme K, Sturkenboom M, Tan H. Sudden cardiac death is associated both with epilepsy and with use of antiepileptic medications. *Heart.* (2014) 101:17–22.

77. Ishizue N, Niwano S, Saito M, Fukaya H, Nakamura H, Igarashi T, et al. Polytherapy with sodium channel-blocking antiepileptic drugs are associated with arrhythmogenic ST-T abnormality in patients with epilepsy. *Seizure.* (2016) 40:81–7. doi: 10.1016/j.seizure.2016.06.004

78. Ota H, Kawamura Y, Sato N, Hasebe NA. Carbamazepine-induced Brugada-type electrocardiographic pattern in a patient with schizophrenia. *Int Med.* (2017) 56:3047–50. doi: 10.2169/internalmedicine.8875-17

79. Swe T, Bhattarai B, Dufresne A. Type 1 Brugada pattern ECG due to supra-therapeutic phenytoin level. *BMJ Case Rep.* (2016) 2016:bcr2016214899.

80. Restrepo J, MacLean R, Celano C, Huffman J, Januzzi J, Beach S. The assessment of cardiac risk in patients taking lamotrigine; a systematic review. *Gen Hosp Psychiatry.* (2022) 78:14–27.

81. Coll M, Striano P, Ferrer-Costa C, Campuzano O, Matés J, del Olmo B, et al. Targeted next-generation sequencing provides novel clues for associated epilepsy and cardiac conduction disorder/SUDEP. *PLoS One.* (2017) 12:e0189618. doi: 10.1371/journal.pone.0189618

frontiers | Frontiers in Cardiovascular Medicine

TYPE Case Report
PUBLISHED 07 November 2022
DOI 10.3389/fcvm.2022.985421

OPEN ACCESS

EDITED BY
Elsayed Z. Soliman,
Wake Forest University, United States

REVIEWED BY
Alexander Carpenter,
University of Bristol, United Kingdom
Mario Matta,
AOU Città della Salute e della Scienza, Italy

*CORRESPONDENCE
Grzegorz Sławiński
gslawinski@gumed.edu.pl

SPECIALTY SECTION
This article was submitted to Cardiac Rhythmology, a section of the journal Frontiers in Cardiovascular Medicine

RECEIVED 03 July 2022
ACCEPTED 25 October 2022
PUBLISHED 07 November 2022

CITATION
Hawryszko M, Sławiński G, Kozłowski D and Lewicka E (2022) Apple Watch-guided diagnosis of AVNRT in a pregnant woman—A case report and literature review. *Front. Cardiovasc. Med.* 9:985421. doi: 10.3389/fcvm.2022.985421

Apple Watch-guided diagnosis of AVNRT in a pregnant woman—A case report and literature review

Maja Hawryszko, Grzegorz Sławiński*, Dariusz Kozłowski and Ewa Lewicka

Department of Cardiology and Electrotherapy, Medical University of Gdańsk, Gdańsk, Poland

Cardiac arrhythmias occurring during pregnancy pose a therapeutic problem as antiarrhythmic drugs can be potentially harmful to the fetus. A 35-years-old woman in the 20th week of pregnancy was admitted to the Department of Cardiology due to the first episode of arrhythmia in her life. During the event, the patient was wearing an Apple Watch Series 6, which records a 30-sec single-channel ECG. The recording showed narrow QRS complex tachycardia of 216 bpm, and short RP interval and atrioventricular nodal reentrant tachycardia (AVNRT) was recognized. Due to the mild nature of the arrhythmia, antiarrhythmic pharmacotherapy was not initiated. The use of mobile health (mHealth) devices such as wearables and health monitoring applications is now a valuable addition to routine cardiac diagnostics for patients of all ages and levels of cardiovascular risk.

KEYWORDS

AVNRT, pregnancy, Apple Watch, mobile health (mHealth), arrhythmia

Introduction

Cardiac arrhythmias occurring during pregnancy pose a therapeutic problem as antiarrhythmic drugs can be potentially harmful to the fetus. Therefore, in the presence of mild arrhythmias, antiarrhythmic drug therapy is not recommended. The use of mobile health (mHealth) devices such as wearables and health monitoring applications is now a valuable addition to routine cardiac diagnostics for patients of all ages and levels of cardiovascular risk (1).

Case description

A 35-years-old woman in the 20th week of pregnancy was admitted to the Department of Cardiology due to the first episode of arrhythmia in her life. During normal activities, she developed palpitations and pre-syncope symptoms. Until now, she had no concomitant diseases and had no risk factors for cardiovascular disease. She was not taking any medications. On admission, the patient did not report any symptoms, was in good general condition, and was without any abnormalities in the

physical examination. ECG showed sinus tachycardia 113 bpm, normal cardiac axis, and T-waves inversion in leads V1—V3 (Figure 1A).

During the event, the patient was wearing an Apple Watch Series 6, which records a 30-sec single-channel ECG. The recording showed narrow QRS complex tachycardia of 216 bpm and short RP interval (Figure 1B), and atrioventricular nodal reentrant tachycardia (AVNRT) was recognized. During hospitalization, no cardiac arrhythmia was found during telemetric ECG monitoring, and transthoracic echocardiography showed no abnormalities. Due to the mild nature of the arrhythmia, antiarrhythmic pharmacotherapy was not initiated. The patient was informed about the possibility of terminating the arrhythmia with the Valsalva maneuver.

Discussion

Cardiac arrhythmias may appear for the first time in pregnancy, but they may also aggravate or recur previously observed arrhythmias. Atrial fibrillation and paroxysmal supraventricular tachycardia (PSVT) are, in addition to premature beats, the most common forms of arrhythmia in pregnancy. Atrioventricular recurrent tachycardia (AVNRT) predominates among PSVT. It is estimated that approximately 20% of patients with pre-pregnancy supraventricular tachycardia will exacerbate their symptoms during pregnancy.

According to the 2019 guidelines for the management of patients with supraventricular tachycardia, vagal maneuvers are a first-line treatment for AVNRT during pregnancy. It is also recommended to avoid the use of antiarrhythmic drugs in pregnant women with mild symptoms or rare and short episodes of arrhythmia (2). If symptoms are present and the arrhythmia is not tolerated by the woman, and if periodic disturbances in uteroplacental flow are present, treatment with a cardioselective beta-blocker should be considered, preferably after the first trimester of pregnancy. If there is no improvement after the treatment, the substrate of the arrhythmia may be ablated, preferably after the end of pregnancy (3).

Recently, watches have turned into devices that not only show the time, but provide a lot of information about life activity, sleep, and its phases, and some of them also have the function of recording a real-time electrocardiogram (ECG). By enabling patients to take their ECG recordings in situations such as palpitations or presyncopes, clinicians can increasingly review hard-to-reach arrhythmias and those occurring less often thanks to registration using a smartwatch (4). Research has been carried out on the diagnostic accuracy of smartwatches in all cardiac arrhythmias. They show that the detection of cardiac arrhythmias with smartwatches available on the market is possible with very high diagnostic accuracy. The overall sensitivity, specificity, and accuracy of these digital systems were 100, 95, and 97%, respectively. PPV and NPV were 85 and 100%, respectively (5).

In the case described above, the patient used the smartwatch ECG function when she felt palpitations. However, not all patients experience episodes of arrhythmia to benefit from the ECG recording. A good example is an atrial fibrillation, which is often asymptomatic. Measuring the heart rate, but also detecting cardiac arrhythmias basically uses two different technologies: photoplethysmography (PPG) and electrocardiography. The resulting pulse wave sequences can be analyzed with the help of special algorithms (their regularity and irregularity), and arrhythmias can be detected using the variability of the pulse frequency. This information is analyzed by numerous available applications designed for this purpose (6). A number of studies have demonstrated the high accuracy of a wide variety of mobile AF detection devices. However, studies are still being conducted to confirm such large-scale use of patients (7). One of the largest studies is conducted by Perez et al. (8), where of the 450 participants who were monitored with ECG patches, 153 identified AF—resulting in a diagnostic AF efficiency of 34%. In subjects 65 years of age or older, AF was detected in 35% of patients, while among participants under 40 years of age, the diagnostic efficiency of AF was 18%. The goal of the Apple Heart Study was to evaluate the ability of the Irregular Heart Rate Alert algorithm to identify AF with the Apple Watch application by consumers. Among participants who received a report of an abnormal heart rate, 84% of reports were consistent with AF (8).

Nowadays, when health awareness and the need to control it increases, more and more mHealth devices appear on the market. Smartphones and smartwatches are the most popular, but that's not all. One of the most interesting proposals is Google Glass, a gadget worn on the head, which is equipped with an accelerometer, gyroscope, and a camera, thanks to which we can get to know our heart rate (HR) and respiratory rate (RR). Another noteworthy invention is Plaster Zio. It is a waterproof patch applied to the left chest that provides a single-lead ECG and is used for continuous heart rhythm monitoring. The patch can be worn for up to 14 days and provides relatively long-term heart rate monitoring without the need to replace the battery or recharge, and includes an event marker button that can be pressed when a patient experiences symptoms (9, 10). Another example is AliveCor's Kardia Mobile, an ECG event recorder for smartphones that provides 30 sec of ECG. It integrates ECG leads in a smartphone case and enables the recording of heart rhythms and then electronic sharing of the recordings (10). Currently, Kardia Mobile devices from AliveCor enable recording one or even six ECG leads. Recently, a device in the form of a card with the same functions has also been made available for general use. Another type of heart rate monitoring device is the chest belt. Examples of these devices include BioHarness and Polar devices, among others. In addition to monitoring the heart rhythm, they enable the monitoring

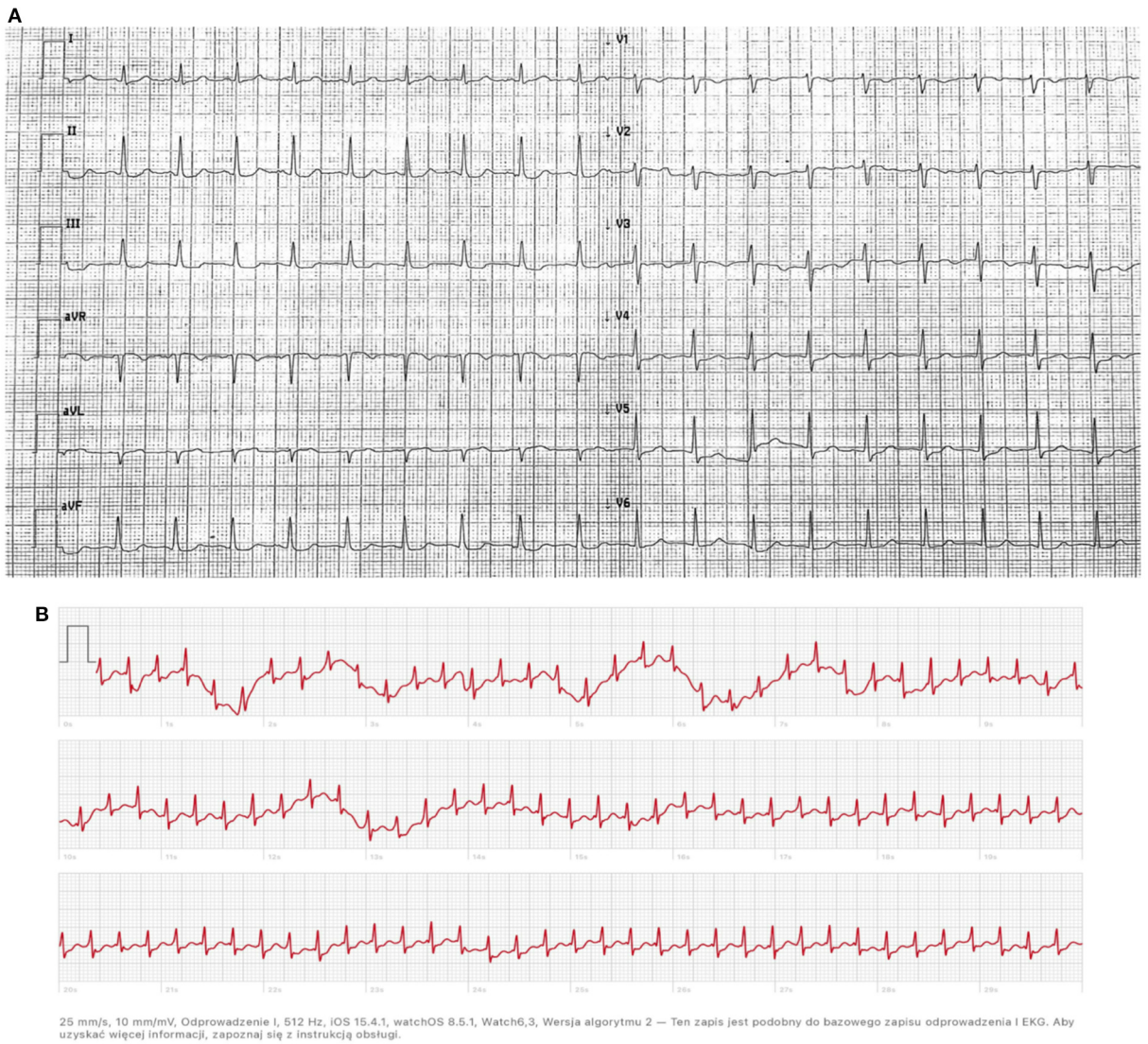

FIGURE 1
(A) ECG on admission to hospital: sinus tachycardia 113 bpm, normal cardiac axis, T-waves inversion in leads V1 - V3; **(B)** Recording from Apple Watch: narrow QRS complex tachycardia of 216 bpm with short RP interval.

of physical activity, respiratory rate and body temperature. These devices are dedicated primarily to people who practice sports intensively and want to monitor the circulatory and respiratory systems.

Current devices can monitor ECG, heart rate, arrhythmia, blood pressure, stress, respiratory rate, temperature, saturation, ischemia, and apnea. A comparison of the most popular devices used for mobile rhythm monitoring is presented in Table 1. Taking into account the capabilities of the existing mHealth devices, potential groups of patients for which the use of these devices would be an added value would be patients with palpitations, presyncope or syncope, heart failure, established AF, coronary artery disease, QTc prolongation in medical history, with a tendency to hyperkalemia, requiring cardiac rehabilitation and with peripheral vascular disease.

Measurement of HR during exercise and rest can be used to predict the risk of cardiovascular disease. In healthy populations, high resting HR is associated with an increased risk of coronary artery disease and is an unfavorable predictor of outcomes in patients with established heart failure (14). Disturbed return to resting heart rate after exercise correlates with increased rate of adverse cardiovascular events. HR variability (HRV) is also strongly associated with the risk of adverse cardiovascular events in healthy subjects and heart failure patients with reduced ejection fraction (14).

TABLE 1 Comparison of the most popular devices used for mobile rhythm monitoring.

Device	Type of product	The method used to detect heart rate or rhythm	AF detection accuracies	Continuous HRV measurement	Other medical functionalities	FDA approval
Apple Watch 4 or later (Apple, United States)	Watch	PPG—for long-term surveillance of HR Two-lead user-triggered ECG via one installed electrode in the digital crown and the other installed electrode in the back of the watch	90.5% (11)	No	PA, falls, sleep	Yes
KardiaMobile (AliveCor, United States)	Card, pocket mobile device	Up to six lead ECG	100% (11)	No	No	Yes
Fitbit Flex, One, Charge (Fitbit, United States)	Watch	PPG—an algorithm that can passively assess the heart rhythm in the background, and if there are any signs suggestive of AF, the user get notify	98.2% (12)	No	PA, sleep	Yes
Garmin (Garmin, United States)	Watch	PPG	nd	No	PA, sleep	No
Polar (Polar Electro, Finland)	Chest strap	Electrocardiac sensors which detects and monitor HR	nd	Yes	PA	No
Zio Patch (iRhythm Technologies, United States)	Patch	Single-use, adhesive, external ambulatory ECG device which continuously records up to 14 days of ECG data. The device has no external wires or electrodes; it records ECG data via a single lead contained in the device housing	100% (13)	No	No	Yes
Microsoft Band (Microsoft)	Band	PPG	nd	No	PA, sleep	No
BioHarness (Zephyr)	Chest belt	Continuous ECG sampled at 250 Hz by means of a couple of textrodes embedded on a chest strap	nd	Yes	PA, RR, skin temperature	Yes

AF, atrial fibrillation; ECG, electrocardiogram; HR, heart rate; HRV, heart rate variability; nd, no data; PA, physical activity; PPG, photoplethysmography; RR, respiratory rate.

10.3389/fcvm.2022.985421

A prolonged QT interval can predispose patients to life-threatening arrhythmias. The single-lead ECG patch BodyGuardian (Preventice Solutions Group, USA) and the algorithm-predicted QTc from the KardiaMobile 6-lead ECG compared to the 12-lead ECG confirmed the satisfactory quality of this type of measurements (15, 16). Hyperkalemia is another a reversible cause of life-threatening arrhythmias, which can manifest on the ECG in the form of: peaked T waves, QRS widening, PR interval shortening and bradycardia. It is observed especially in patients with chronic kidney disease. In these patients, efforts were made to evaluate the effectiveness of the detection of hyperkalemia with AliveCor devices. The sensitivity by the duration of hyperkalaemia was 94% and the specificity was 74%, however high false-positive, and false-negative rates and the need for continuous ECG monitoring decreased the enthusiasm supporting the use of wearables to find out hyperkalaemia (17). However, in the future, after improving the algorithms responsible for the detection of hyperkalaemia, it may be an interesting alternative to laboratory diagnostics in specific groups of patients. Cardiovascular telerehabilitation programs supported by real-time wearable data can revolutionize home-based rehabilitation and relieve the inconvenience and decrease the cost associated with center-based programs. A randomized trial comparing REMOTE-CR—a real-time, remote telerehabilitation platform that includes the use of a chest-worn wearable sensor (BioHarness 3, Zephyr Technology, United States) - with a classic center-based program showed that REMOTE-CR was associated with less sedentary time at 24 weeks and was even more cost-effective (18). In patients with peripheral vascular disease, the first-line treatment for intermittent claudication is a supervised exercise program of gradually increasing intensity. Two randomized trials with patients with peripheral vascular disease, each utilizing the ankle-based accelerometer StepWatch 3 (Modus, United States), proved that wearable-guided training was associated with a significant improvement in walking ability, speed, and peak oxygen consumption (19, 20).

Mobile applications for patients are very numerous and popular, which makes our phone a personal caregiver nowadays. Among the cardiological applications, the most popular are heart rate monitoring systems that simultaneously create history and graphs of the pulse wave. Some of them are related to algorithms for selecting/classifying ECG or other measurable symptoms of heart disease. In addition, you can also find programs for cardiac rehabilitation, blood pressure measurement, and systems for detecting heart failure. Other categories with a large number of cardiac applications include ECG education and interpretation, cardiology journals, calculators, and cardiopulmonary resuscitation (CPR) instructions (21).

Considering the potential of mHealth devices, the most important thing now would be to design a unified (at the beginning even within a given country) application that would enable direct data transfer to a doctor, for instance, when the patient's state of well-being has deteriorated.

Mobile devices have been conquering the world for several years. Recognizing their potential, the companies producing them try to meet customer requirements and the possibility of using them, for example in medicine. Despite the excellent results of research in this area, there are many problems that need to be solved in order to take advantage of their potential on a large scale. Barriers include heterogeneity in an application, lack of reimbursement structures, and socio-economic and demographic disproportions in access to technology. It is obvious that the devices mentioned above are most often used by young people who care about their health. Low-income people and older people will be less likely to access these tools, even though they are the group most likely to use them. When a patient uses mHealth devices, despite the diagnosis of arrhythmia by the application, there is no telemedicine network sufficiently built to send the results, such as ECG, to the doctor for evaluation. Some patients ignore the reports as irrelevant or are afraid of the diagnosis and initiation of chronic treatment (22). On the other hand, some patients may focus too much on interpreting the constantly accumulated information. The abundance of data can also, in extreme cases, become the basis for the overdiagnosis of diseases.

Conclusions

It usually takes months to register arrhythmias on the basis of multiple ECG recordings and frequent admissions to emergency departments (23). More importantly, this period is usually very stressful both for pregnant patients, as in the presented case, and for the other patient awaiting diagnosis. Due to the growing popularity of mHealth technology in the general population, cardiologists gain access to more data, which will enable faster diagnosis and treatment of arrhythmias (24). Arrhythmia recording with Apple Watch and other ECG recorders can be of great diagnostic value in preventing complications of arrhythmia, such as ischemic stroke in the case of patients with AF. It is also an important supplement to diagnostics and enables faster diagnosis in patients with paroxysmal palpitations. The widespread use of devices connected to the Internet makes it possible to collect a large amount of clinical information, without the need to visit the doctor directly, at relatively lower costs for hospitals and clinics.

Data availability statement

The original contributions presented in the study are included in the article/supplementary material, further inquiries can be directed to the corresponding author.

Ethics statement

Written informed consent was obtained from the participant/s for the publication of this case report.

Author contributions

MH, GS, and EL contributed to the conception and design of the study. MH wrote the first draft of the manuscript. MH, GS, EL, and DK wrote sections of the manuscript. All authors contributed to manuscript revision, read, and approved the submitted version.

Conflict of interest

The authors declare that the research was conducted in the absence of any commercial or financial relationships that could be construed as a potential conflict of interest.

Publisher's note

All claims expressed in this article are solely those of the authors and do not necessarily represent those of their affiliated organizations, or those of the publisher, the editors and the reviewers. Any product that may be evaluated in this article, or claim that may be made by its manufacturer, is not guaranteed or endorsed by the publisher.

References

1. Piotrowicz R, Krzesiński P, Balsam P, Piotrowicz E, Kempa M, Lewicka E, et al. Telemedicine solutions in cardiology: a joint expert opinion by the Information Technology and Telemedicine Committee of the Polish Cardiac Society, the Section Noninvasive Electrocardiology and Telemedicine of the Polish Cardiac Society, and the Clinical Research Committee of the Polish Academy of Sciences (short version, 2021). *Kardiol Pol.* (2021) 79:227–41. doi: 10.33963/KP.15824

2. Brugada J, Katritsis DG, Arbelo E, Arribas F, Bax JJ, Blomström-Lundqvist C, et al. 2019 ESC guidelines for the management of patients with supraventricular tachycardia. The task force for the management of patients with supraventricular tachycardia of the European Society of Cardiology (ESC). *Eur Heart J.* (2020) 41:655–720. doi: 10.1093/eurheartj/ehz467

3. Li JM, Nguyen C, Joglar JA, Hamdan MH, Page RL. Frequency and outcome of arrhythmias complicating admission during pregnancy: experience from a high- volume and ethnically-diverse obstetric service. *Clin Cardiol.* (2008) 31:538–41. doi: 10.1002/clc.20326

4. Strik M, Ploux S, Ramirez FD, Abu-Alrub S, Jaïs P, Haïssaguerre M, et al. Smartwatch-based detection of cardiac arrhythmias: beyond the differentiation between sinus rhythm and atrial fibrillation. *Heart Rhythm.* (2021) 18:1524–32. doi: 10.1016/j.hrthm.2021.06.1176

5. Nazarian S, Lam K, Darzi A, Ashrafian H. Diagnostic accuracy of smartwatches for the detection of cardiac arrhythmia: systematic review and meta-analysis. *J Med Internet Res.* (2021) 23:e28974. doi: 10.2196/28974

6. Veltmann C, Ehrlich JR, Gassner UM, Meder B, Möckel M, Radke P, et al. Wearable-basierte detektion von arrhythmien. *Kardiologe.* (2021) 15:341–53. doi: 10.1007/s12181-021-00488-3

7. Pearsons A, Hanson CL, Gallagher R, O'Carroll RE, Khonsari S, Hanley J, et al. Atrial fibrillation self-management: a mobile telephone app scoping review an content analysis. *Eur J Cardiovasc Nurs.* (2021) 20:305–14. doi: 10.1093/eurjcn/zvaa014

8. Perez MV, Mahaffey KW, Hedlin H, Rumsfeld JS, Garcia A, Ferris T, et al. Large-scale assessment of a smartwatch to identify atrial fibrillation. *N Engl J Med.* (2019) 381:1909–17. doi: 10.1056/NEJMoa1901183

9. Barrett PM, Komatireddy R, Haaser S, Topol S, Sheard S, Encinas J, et al. Comparison of 24-hour Holter monitoring with 14-day novel adhesive patch electrocardiographic monitoring. *Am J Med.* (2014) 127:95.e11-95.e9.5E17. doi: 10.1016/j.amjmed.2013.10.003

10. Sana F, Isselbacher EM, Singh JP, Heist EK, Pathik B, Armoundas AA. Wearable devices for ambulatory cardiac monitoring: JACC state-of-the-art review. *J Am Coll Cardiol.* (2020) 75:1582–92. doi: 10.1016/j.jacc.2020.01.046

11. Lee C, Lee C, Fernando C, Chow C-M. Comparison of Apple Watch series 4 vs. *kardiamobile: a tale of two devices CJC Open.* (in press). doi: 10.1016/j.cjco.2022.07.011

12. Lubitz SA, Faranesh AZ, Selvaggi C, Atlas SJ, McManus DD, Singer DE, et al. Detection of atrial fibrillation in a large population using wearable devices: the fitbit heart study. *Circulation.* (2022). doi: 10.1161/CIRCULATIONAHA.122.060291. [Epub ahead of print].

13. Rosenberg MA, Samuel M, Thosani A, Zimetbaum PJ. Use of a noninvasive continuous monitoring device in the management of atrial fibrillation: a pilot study. *Pacing Clin Electrophysiol.* (2013) 36:328–33. doi: 10.1111/pace.12053

14. Bayoumy K, Gaber M, Elshafeey A, Mhaimeed O, Dineen EH, Marvel FA, et al. Smart wearable devices in cardiovascular care: where we are and how to move forward. *Nat Rev Cardiol.* (2021) 18:581–99. doi: 10.1038/s41569-021-00522-7

15. Castelletti S, Dagradi F, Goulene K, Danza AI, Baldi E, Stramba-Badiale M, et al. A wearable remote monitoring system for the identification of subjects with a prolonged QT interval or at risk for drug-induced long QT syndrome. *Int J Cardiol.* (2018) 266:89–94. doi: 10.1016/j.ijcard.2018.03.097

16. Schram M, Shreibati J, Bos M, Galloway C, Valys A, Petterson F, et al. Prediction of the heart rate corrected qt interval (QTC) from a novel, multilead smartphone-enabled ecg using a deep neural network. *J Am Coll Cardiol.* (2019) 73:(9_Suppl. 1) 368. doi: 10.1016/S0735-1097(19)30976-3

17. Galloway CD, Valys AA, Petterson FL, Gundotra VP, Treiman DL, Albert DE, et al. Non-invasive detection of hyperkalemia with a smartphone electrocardiogram and artificial intelligence. *J Am Coll Cardiol.* (2018) 71:(Suppl. 11) A272. doi: 10.1016/S0735-1097(18)30813-1

18. Maddison R, Rawstorn JC, Stewart RAH, Benatar J, Whittaker R, Rolleston R, et al. Effects and costs of real-time cardiac telerehabilitation: randomised controlled non-inferiority trial. *Heart.* (2019) 105:122–9. doi: 10.1136/heartjnl-2018-313189

19. Gardner AW, Parker DE, Montgomery PS, Blevins SM. Step-monitored home exercise improves ambulation, vascular function, and inflammation in symptomatic patients with peripheral artery disease: a randomized controlled trial. *J Am Heart Assoc.* (2014) 3:e001107. doi: 10.1161/JAHA.114.001107

20. Gardner AW, Parker DE, Montgomery PS, Scott KJ, Blevins SM. Efficacy of quantified home-based exercise and supervised exercise in patients with intermittent claudication: a randomized controlled trial. *Circulation.* (2011) 123:491–8. doi: 10.1161/CIRCULATIONAHA.110.963066

21. Martínez-Pérez B. de la Torre-Díez I, López-Coronado M, Herreros-González J. Mobile apps in cardiology: review. *JMIR Mhealth Uhealth.* (2013) 1:e15. doi: 10.2196/mhealth.2737

22. Sepehri Shamloo A, Bollmann A, Dagres N, Arya A, Hindricks G. Smart watch devices for atrial fibrillation screening: it has to start somewhere. *J Am Coll Cardiol.* (2020) 75:1364–5. doi: 10.1016/j.jacc.2019.10.063

23. Siddeek H, Fisher K, McMakin S, Bass JL, Cortez D, AVNRT. captured by Apple Watch Series 4: can the Apple watch be used as an event monitor? *Ann Noninvasive Electrocardiol.* (2020) 25:e12742. doi: 10.1111/anec.12742

24. Carpenter A, Frontera A. Smart-watches: a potential challenger to the implantable loop recorder? *Europace.* (2016) 18:791–3. doi: 10.1093/europace/euv427

frontiers | Frontiers in Cardiovascular Medicine

TYPE Case Report
PUBLISHED 06 December 2022
DOI 10.3389/fcvm.2022.993903

OPEN ACCESS

EDITED BY
Matteo Anselmino,
University of Turin, Italy

REVIEWED BY
Kaveh Hosseini,
Tehran University of Medical Sciences, Iran
Zhuo Wang,
Renmin Hospital of Wuhan University, China
John Catanzaro,
University of Florida, United States

*CORRESPONDENCE
Mingxian Chen
xymignxianchen@csu.edu.cn

†These authors have contributed equally to this work

SPECIALTY SECTION
This article was submitted to Cardiac Rhythmology, a section of the journal Frontiers in Cardiovascular Medicine

RECEIVED 14 July 2022
ACCEPTED 14 November 2022
PUBLISHED 06 December 2022

CITATION
Wu Z, Tang J, Zhu Q, Hu L, Liu Z, Li X, Liu Q, Zhou S and Chen M (2022) Case report: Pacemaker lost capture after acute myocardial infarction in a patient with left circumflex coronary artery occlusion.
Front. Cardiovasc. Med. 9:993903.
doi: 10.3389/fcvm.2022.993903

Case report: Pacemaker lost capture after acute myocardial infarction in a patient with left circumflex coronary artery occlusion

Zhihong Wu†, Jianjun Tang†, Qingyi Zhu, Lin Hu, Zhenjiang Liu, Xuping Li, Qiming Liu, Shenghua Zhou and Mingxian Chen*

Department of Cardiology, The Second Xiangya Hospital of Central South University, Changsha, China

A 71-year-old female with a dual-chamber pacemaker presented to our hospital complaining of repeated chest pain. She was diagnosed with unstable angina. On day 7, the patient suddenly suffered cardiopulmonary arrest due to an inferior ST segment elevation myocardial infarction (STEMI). Pacemaker lost capture was suspected and was later confirmed by a pacemaker check with a high pacing threshold and a low sensing parameter. Emergency coronary angiography revealed that a large filling defect remained due to an extensive thrombus in the proximal left circumflex (LCX) with thrombolysis in myocardial infarction (TIMI) grade 2 flow, and then a repeat thrombus aspiration was performed. After reperfusion, the parameters of the right ventricular lead were gradually returned. We conclude that the loss of the right ventricular lead pacing occurred in this case of acute coronary syndrome (ACS) induced by an LCX thrombus due to an LCX supplying the right ventricular septal.

KEYWORDS

acute myocardial infarction, pacemaker, failure capture, sudden cardiac death, arrest

Introduction

There are several causes that contribute to the loss of a permanent pacemaker capture, such as battery depletion, lead dislodgement, and circuit problems. However, malfunction of a ventricular lead of a dual-chamber pacemaker following an acute myocardial infarction (AMI) is rare (1). There are few reports describing the pacemaker lost atrial capture as a consequence of an AMI (2–4). Herein, we report the rare case of failure pacing following an acute inferior wall myocardial infarction in a patient with an occlusion of the left circumflex (LCX) that supplied the right ventricular septal.

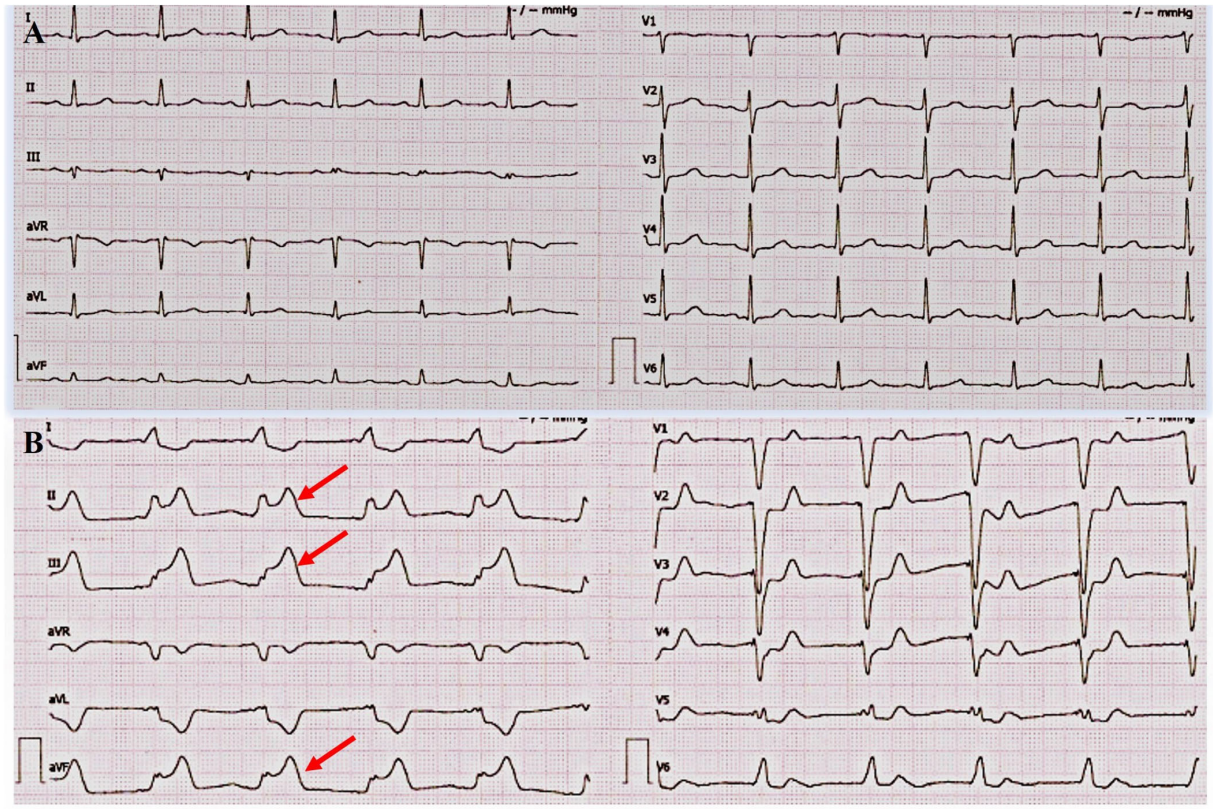

FIGURE 1
Admission electrocardiogram (ECG) and acute myocardial infarction (AMI) ECG. **(A)** ECG on admission. It showed a sinus rhythm at 76 bpm (beats per minute), normal conduction, and low amplitude of T wave in multiple leads. **(B)** ECG during AMI. It showed ST segment elevation in leads II, III, and aVF and ST segment depression in leads I, aVL, and v4-6.

Case report

A 71-year-old female presented to our hospital complaining of repeated chest pain. Her past history included coronary heart disease and sick sinus syndrome (SSS). Six years ago, she was first admitted to our hospital and diagnosed with unstable angina. Then, coronary angiography revealed a severe stenosis of the left anterior descending (LAD), and a stent was implanted into the LAD. One year ago, the patient was admitted to our hospital because of syncope. She was diagnosed as having SSS with 7.97 seconds of asystole and then received a dual-chamber pacemaker (Medtronic Inc., Minneapolis, MN, USA) implantation.

On admission, her heart rate was 76 bpm (beats per minute) and her blood pressure was 131/67 mmHg. Transthoracic echocardiography (TTE) showed a normal left ventricular size and function without regional wall motion abnormalities. Electrocardiogram (ECG) on admission shows a sinus rhythm at 76 bpm, normal conduction, and low amplitude of T wave in multiple leads. According to the ischemic symptom and previous history, the patient was diagnosed as having unstable angina. The concentration of hypersensitive cardiac troponin T (TnTsh, upper limit of normal = 14 pg/ml) was at a normal level (9.64 pg/ml). She received a secondary prevention of coronary heart disease. After admission, we confirmed that her pacemaker was functioning normally (a pacing threshold of 0.6 V @0.40 ms, a sensing threshold of 11.3–13.1 mV, and a lead resistance of 820 Ω). In addition, creatine kinase (CK) and TnTsh were normal.

On day 7, she suddenly presented with chest pain, then lost consciousness, and no carotid pulse was found. Subsequently, cardiopulmonary arrest ensued. Cardiopulmonary resuscitation (CPR) was performed immediately. ECG showed an ST segment elevation in leads II, III, and aVF and ST segment depression in leads I, aVL, and V4-6 (Figure 1). She was diagnosed as having AMI. A pacemaker malfunction was suspected and confirmed by a pacemaker check showing an increase in the pacing threshold to >10.0 V and a decrease in the sensing threshold to < 0.5 mV, despite a normal lead resistance (840 Ω). After CPR, her heart rate was 113 bpm (sinus rhythm) and her blood pressure was 128/68 mmHg (maintenance dose of norepinephrine: 1.2 mg/h). Pulse oximetry was 93% supported with mechanical ventilation. The results of arterial blood gases

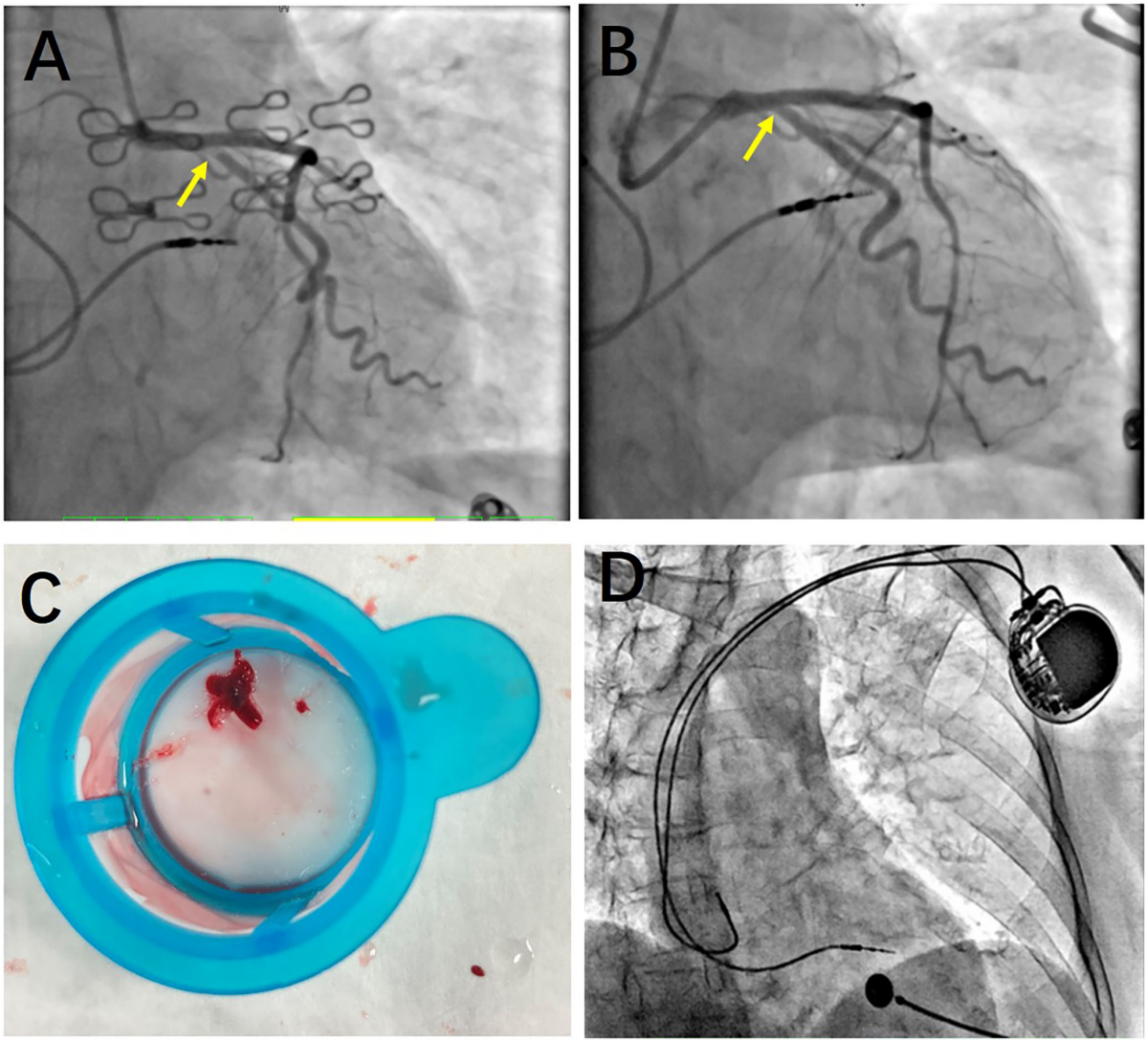

FIGURE 2
Coronary angiography. **(A)** Before thrombus aspiration, a large filling defect remained due to an extensive thrombus in the proximal left circumflex (LCX) with The Thrombolysis In Myocardial Infarction (TIMI) grade 2 flow. **(B)** After thrombus aspiration, the large filling defect appeared. And the TIMI grade of LCX improved. **(C)** A large thrombus was presented after thrombus aspiration. **(D)** Atrial and ventricular leads of dual-chamber pacemaker were normal. No leads' dislodgement or fracture was found.

TABLE 1 Summary of right ventricular lead testing before and after the acute myocardial infarction.

Date	Right atrium			Right ventricle		
	P-wave (mv)	Threshold (V/ms)	Impedance (Ω)	R-wave (mv)	Threshold (V/ms)	Impedance
Before AMI	>3.7	0.8@0.40	620	11.3–13.1	0.6@0.40	820
AMI	>2.8	1.0@0.40	660	<0.5	>10@1.5	840
After thrombus aspiration	>3.1	1.2@0.40	600	2.2	>5.0@1.5	760
Day 1 after AMI	>3.5	1.0@0.40	610	3.3	2.6@0.40	780
Day 2 after AMI	>3.5	1.0@0.40	580	5.7–5.8	2.2@0.40	800
Day 3 after AMI	>3.5	0.8@0.40	590	8.1–9.2	1.2@0.40	830

The infarction was associated with a complete right ventricular function. After an acute myocardial infarction (AMI), the ventricular lead sensing and pacing parameters were found to have gradually returned.

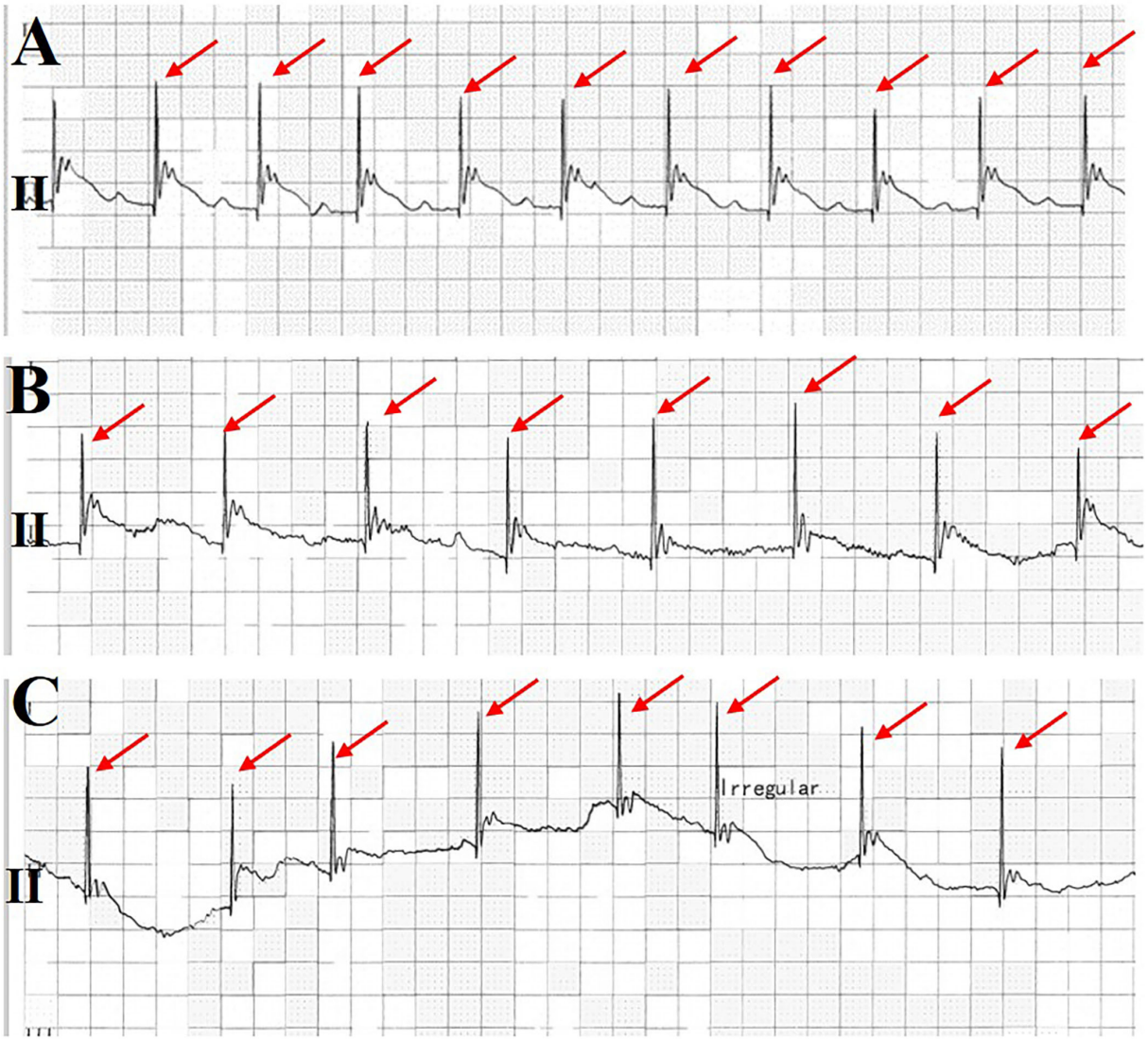

FIGURE 3
Monitoring electrocardiogram (ECG) at lead II. It was found that the pacemaker gradually lost capture before the patient lost consciousness **(A–C)**. Ventricular pacing spikes are shown in a red arrow.

and electrolytes showed a pH = 7.49, a potassium concentration (3.7 mmol/L, upper limit of normal = 5.3 mmol/L), and a magnesium concentration (0.8 mmol/L, lower limit of normal = 0.78 mmol/L). The concentration of TnTsh was elevated (437 pg/ml). The results of a routine blood panel showed a normal level of hemoglobin (131 g/L). Emergency coronary angiography showed that a large filling defect remained due to extensive thrombus in the proximal left circumflex (LCX) with TIMI grade 2 flow (Figure 2). The patient underwent repeated thrombus aspirations. The TIMI grade 2 flow had improved. The pacemaker reprogramming, it was found that an increase in the pacing threshold to >5.0 V and a decrease in the sensing threshold to 2.2 mV were noticed, despite a normal lead resistance (760 Ω) (Table 1). Looking back at the ECG monitor, ventricular pacing spikes were visible and failed to capture the myocardium (Figure 3). The atrial lead functioned normally. During the follow-up, from day 1 to day 3, the parameters of ventricular lead were gradually returned. In addition, CK showed the highest value [2,467 IU/L (international units/liter)] on day 1.

Discussion

There are several causes that result in the failure capture of a pacemaker, including battery depletion, lead dislodgement,

circuit problems, acidosis, and hyperkalemia (5). Although pacemaker malfunction induced by ischemia is rare, there are still some previous case reports that demonstrated an atrial lead malfunction after a myocardial infarction. In these cases, the pacing threshold was obviously increased due to myocardial necrosis. However, malfunction of a ventricular lead of a dual-chamber pacemaker following an acute myocardial infarction (AMI) is rarely reported (6). This case has illustrated the fact that loss capture (GA1) of a pacemaker took place after inferior STEMI in a patient. The anterior 2/3 of the interventricular septum is supplied by the left anterior descending or LAD, while the posterior 1/3 of the interventricular septum is supplied by the right coronary artery or LCX. The ventricular lead was implanted into the posterior 1/3 of the interventricular septum. Therefore, thrombotic LCX induced ventricular lead failure capture. A recent article reported by Saadatagah et al. (7) has also presented a similar scenario on the implantable cardioverter-defibrillator (ICD) malfunction during an AMI. It showed the case of a young woman with refractory vasospastic angina who happened to display a repeated dysfunction of her implantable cardioverter-defibrillator (ICD). Coronary angiography showed severe stenosis of three vessels (7).

A few hours after the AMI, an intercellular edema occurred. It is characterized by an obvious inflammatory response with neutrophil infiltration and progressive coagulative necrosis (8). It led to an increase in the pacing threshold in this patient, and it finally, resulted in a failure capture of the right ventricular lead. After thrombus aspiration and TIMI, blood flow recovered, and the parameters of the right ventricular lead were gradually returned. We concluded that the transient ischemia of the interventricular septum at the pacer–lead interface caused a transient loss of sensing and pacing functions (9).

Conclusion

Failure of ventricular capture of the pacemaker in an acute myocardial infarction is transient. Failure capture will reverse to normal after the timely intervention of reperfusion therapy.

Data availability statement

The original contributions presented in the study are included in the article/supplementary material, further inquiries can be directed to the corresponding author/s.

Ethics statement

The studies involving human participants were reviewed and approved by the Second Xiangya Hospital of Central South University. The patients/participants provided their written informed consent to participate in this study. Written informed consent was obtained from the individual(s) for the publication of this case report and of any potentially identifiable images or data included in this article.

Author contributions

MC, ZW, and JT participated in the study design and drafted the manuscript. QZ, LH, XL, and ZL contributed to data collection. MC and QL were responsible for writing the manuscript. SZ and MC contributed to the manuscript revision. All authors contributed to the article and approved the submitted version.

Funding

Financial support was obtained from the National Natural Science Foundation of China Grant No. 81800302 and the Provincial Natural Science Foundation of Hunan Grant Nos. 2019JJ50871 and 2022JJ30839.

Acknowledgments

We would like to thank Shuang Zhang for their modifications.

Conflict of interest

The authors declare that the research was conducted in the absence of any commercial or financial relationships that could be construed as a potential conflict of interest.

Publisher's note

References

1. Safavi-Naeini P, Saeed M. Pacemaker troubleshooting: common clinical scenarios. *Texas Heart Inst J.* (2016) 43:415–8. doi: 10.14503/THIJ-16-5918

2. Chen C, Fang CC, Wang SP. Reversible atrial lead dysfunction of DDD pacemaker after recent inferior myocardial infarction: a case report. *Angiology.* (2004) 55:451–4. doi: 10.1177/000331970405500413

3. Upadhyay S, Marshalko S, McPherson C. The stunned atrial lead: transient malfunction of a permanent atrial pacer lead following acute myocardial infarction. *Int J Crit Illn Injury Sci.* (2011) 1:161–3. doi: 10.4103/2229-5151.84806

4. Júnior FP, Chemello D, Mazzutti G, Pimentel M, Rabaioli P, Zimerman L. Early improvement of pacing threshold following primary right coronary angioplasty. *Heart Rhythm Case Rep.* (2017) 3:90–2. doi: 10.1016/j.hrcr.2016.09.007

5. Pothineni NVK, Liang JJ. Pacemaker malfunction? What is the mechanism? *J Electrocardiol.* (2021) 68:34–6. doi: 10.1016/j.jelectrocard.2021.07.002

6. Umei TC, Awaya T, Okazaki O, Hara H, Hiroi Y. Pacemaker malfunction after acute myocardial infarction in a patient with wrap-around left anterior descending artery supplying the right ventricular apex. *J Cardiol Cases.* (2018) 18:9–12. doi: 10.1016/j.jccase.2018.03.001

7. Saadatagah S, Hosseini K, Bozorgi A, A. Young woman with refractory vasospastic angina. *JAMA Cardiol.* (2019) 4:945–6. doi: 10.1001/jamacardio.2019.1667

8. Pasotti M, Prati F, Arbustini E. The pathology of myocardial infarction in the pre- and post-interventional era. *Heart.* (2006) 92:1552–6. doi: 10.1136/hrt.2005.086934

9. Cui W, Liu F, Xie R, Lu J, Li B, Wu J, et al. Abstract 3263: the effect of ischemia/reperfusion on the pacing threshold by trans-coronary pacing. *Circulation.* (2006) 114:691.

frontiers | Frontiers in Cardiovascular Medicine

TYPE Case Report
PUBLISHED 16 December 2022
DOI 10.3389/fcvm.2022.996644

OPEN ACCESS

EDITED BY
Patrick Badertscher,
University Hospital of
Basel, Switzerland

REVIEWED BY
Teodor Serban,
Cardiovascular Research Institute
Basel (CRIB), Switzerland
Hardik Dineshbhai Desai,
Gujarat Adani Institute of Medical
Sciences, India

*CORRESPONDENCE
Qiang Guan
✉ duanhy76@sxmu.edu.cn

SPECIALTY SECTION
This article was submitted to
Cardiac Rhythmology,
a section of the journal
Frontiers in Cardiovascular Medicine

RECEIVED 28 September 2022
ACCEPTED 30 November 2022
PUBLISHED 16 December 2022

CITATION
Duan HY, Guan Q, Guo YJ and Liang N (2022) Case report: Cardiac arrest during carotid body tumor resection indicating carotid sinus hypersensitivity.
Front. Cardiovasc. Med. 9:996644.
doi: 10.3389/fcvm.2022.996644

Case report: Cardiac arrest during carotid body tumor resection indicating carotid sinus hypersensitivity

Hong Yong Duan[1,2], Qiang Guan[1,2]*, Yu Jie Guo[1,2] and Ning Liang[1,2]

[1]Department of Vascular Surgery, Shanxi Provincial People's Hospital, Taiyuan, China, [2]Department of Vascular Surgery, The Fifth Clinical Medical College of Shanxi Medical University, Taiyuan, China

Background: Carotid body tumor surgery is associated with various complications. However, intraoperative cardiac arrest is very rare and no more than 10 cases have been reported.

Case description: A 58-year-old woman diagnosed with bilateral carotid body tumors underwent right carotid body tumor surgery. Sudden cardiac arrest occurred during the resection and was attributed to carotid sinus hypersensitivity. The patient recovered after prompt treatment and the tumor was removed completely with no complications.

Conclusion: Cardiac arrest attributed to carotid sinus hypersensitivity during carotid body tumor resection is very rare. Proper treatments can reverse intraoperative cardiac arrest. If carotid sinus hypersensitivity is detected preoperatively, prophylactic temporary pacemaker implantation may be appropriate.

KEYWORDS

carotid body tumors, carotid sinus hypersensitivity, intraoperative cardiac arrest, surgical complications, tumor resection

Introduction

Carotid body tumors (CBTs) are rare neurogenic tumors that arise from chemoreceptive tissue in the carotid body. It is the most common form of neck paragangliomas. Although there is no effective drug to treat CBT, several studies have shown that close monitoring and follow-up are an option in select CBT patients who were asymptomatic, showed no signs of accelerated enlargement, and presented with no evidence of malignancy or no somatic mutation (1–3). While complete surgical resection remains the mainstay of CBT treatment and the only definitive cure for CBT (4), tumor manipulation is associated with significant morbidity due to the nature of its anatomic structure and location. The rate of surgery-related complications has been reported to be in the range from 20 to 27% (5). Herein, we report on a female patient with bilateral CBTs who underwent surgical manipulation complicated by cardiac arrest during her first staged tumor resection. The clinical presentation of hemodynamic instability indicated carotid sinus hypersensitivity (CSH). Case details are provided and the related literature is comprehensively reviewed.

10.3389/fcvm.2022.996644

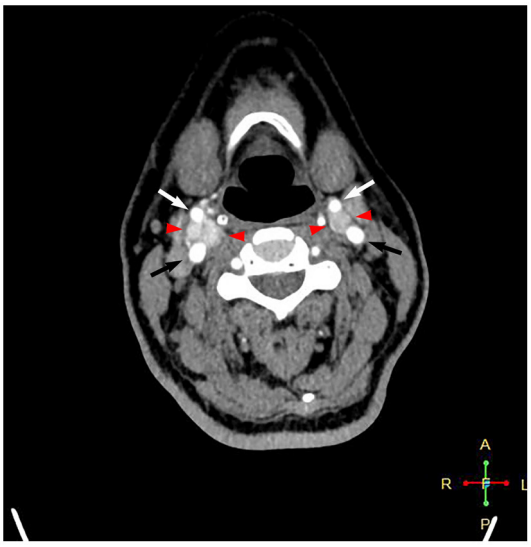

FIGURE 1
Computed tomography angiography showing intensely enhanced masses at the level of bilateral carotid bifurcations. Black arrows point to the internal carotid artery, white arrows point to the external carotid artery, and red arrowheads point to the carotid body tumor.

Case report

A 58-year-old female patient who was diagnosed with bilateral CBTs during a routine health check-up 3 years prior was admitted to the department of vascular surgery, Shanxi Provincial People's Hospital. She complained of a swelling sensation in her neck. The patient had no local pain, difficulty swallowing or breathing, voice changes, or palpitations. No systemic symptoms, such as fever, chills, and malaise, were present. There were no special records in her past medical history and family history. During a physical examination, a small, painless, firm, and pulseless mass was palpated on the right side of the neck at the carotid triangle located below the angle of the mandible. The Fontaine sign was positive. Physical examination did not reveal a left neck mass. The laboratory analyses did not suggest any other abnormalities, except slightly elevated low-density lipoprotein cholesterol and triglyceride levels. A routine electrocardiogram was normal. A computed tomographic angiography showed an intensely enhanced mass measuring 2.6 × 1.8 × 1.3 cm at the level of the right carotid bifurcation. A smaller mass measuring 1.1 × 0.9 × 0.9 cm was present on the left in a similar location (Figure 1). These findings were consistent with bilateral CBTs. According to the imaging results, the right tumor partially surrounded the carotid vessels, indicating Shambling II group tumor. The left-side tumor was of Shambling I group.

The therapy options were discussed with the patient after admission. She agreed to staged surgical dissection of the tumors. According to most experts' consensus, the smaller tumor should be removed first because of the low operative risk for permanent cranial nerve injury. This strategy facilitates the resection of large tumors in the second stage. However, the risk of manipulation in the right CBT was as low as that in the left after evaluation, and the patient requested removal of the large tumor first. Therefore, it was decided that the right CBT was to be resected in the first stage. The patient was informed of the possible surgical complications, and written consent was obtained before surgery.

Surgery was performed in a supine position under general orotracheal anesthesia, and the neck was slightly hyperextended and rotated to the left. A longitudinal incision along the anterior border of the right sternocleidomastoid muscle was made to expose the carotid bifurcation and the tumor (Figure 2). Proximal and distal arterial control was obtained by exposing the common carotid artery, internal carotid artery, and external carotid artery cephalad to the mass. Then, the tumor was gradually separated from the carotid arteries in cranial to caudal direction along the subadventitial plane using bipolar electrocautery. Cardiac arrest suddenly occurred when dissecting the tumor from the carotid bifurcation. The systolic blood pressure (sBP) dropped from 115 to 40 mmHg. This complication was managed immediately with external cardiac massage and administration of a single intravenous 0.5-mg atropine dose while simultaneously suspending CBT manipulation. The cardiac activity recovered ∼40 s after asystole. The heart rate and sBP returned to 72–80 bpm and 120 mmHg, respectively. The manipulation was then completed while gently assisted by topical anesthesia with 2% lidocaine. The patient was closely monitored after surgery and a decrease in the heart rate and blood pressure level was not noted. On the second day after surgery, the patient complained of left chest pain during exercise. Chest X-ray showed no rib fracture, and reexamination of the electrocardiogram indicated normal results. The level of myocardial enzymes was not elevated. The pain was relieved over time without analgesia treatment. The patient had no neurological sequelae or cranial nerve injuries after surgery and was discharged 1 week after surgery. Histopathological examination revealed a zellballen pattern characteristic of paraganglioma and did not show any evidence of malignancy (Figure 3A). Immunohistochemical results were positive for synaptophysin, chromogranin A, and CD56 in the tumor cells and S-100 protein was present in the sustentacular cells (Figures 3B–E). Both synaptophysin and chromogranin A are neuroendocrine markers located in neuroendocrine granules. CD56, known as a neuronal cell adhesion molecule, is a membrane glycoprotein present on the neural cell surface. These positive immunohistochemical stain profiles supported the diagnosis of CBT. The patient had no complaints at 1-month follow-up after surgery.

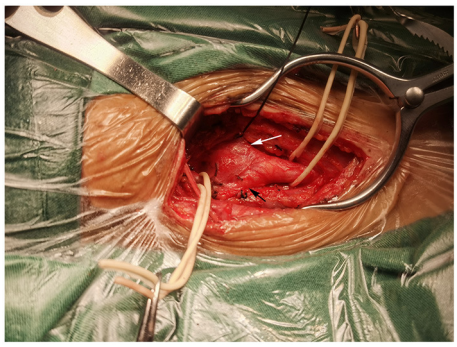

FIGURE 2
Intraoperation view of right carotid body tumor resection. A mass at the bifurcation splayed the internal carotid artery (black arrow) and external carotid artery (white arrow).

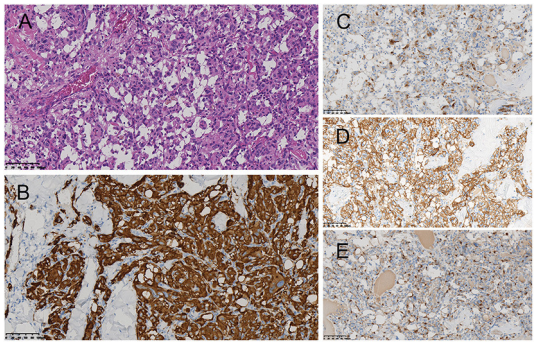

FIGURE 3
Histopathological examination revealed the zellballen pattern characteristic of paraganglioma **(A)**. Immunohistochemical results were positive for synaptophysin **(B)**, chromogranin A **(C)**, and CD56 **(D)** in the tumor cells and S-100 protein in the supporting cells **(E)**.

Discussion

CBTs can be divided into sporadic or familial types. Sporadic types account for the majority of cases, and bilateral tumors are detectable in only 5% of sporadic CBTs (6). A complete staged resection is suitable for most bilateral CBTs. Surgical CBT management can lead to various complications, including cranial nerve injury, vascular injury, stroke, and intraoperative blood loss. However, sudden cardiac arrest during CBT manipulations experienced by the patient described in the present report is very rare, with no more than 10 cases reported to date (7, 8). This complication can be attributed to CSH.

The carotid sinus is a baroreceptor with neurovascular structure located above the carotid bifurcation (9). CSH is an exaggerated response of the carotid sinus baroreceptor to local mechanical stimulation. According to the European Society of Cardiology (10), CSH is defined as asystole lasting for at least 3 s and/or a drop in sBP of at least 50 mmHg in response to carotid sinus massage. The prevalence of CSH is mainly concentrated in people over 60 years old and increases with age (11). It is rare in individuals younger than 50 years old. CSH is divided into three subtypes: (1) the cardioinhibitory type is characterized by a decrease in heart rate that leads to cardiac arrest; (2) the vasodepressor type results in a drop in sBP independent of heart rate; and (3) the mixed type has both features (12). The patient's CSH fell into the third category. CSH most commonly occurs in older males, probably owing to atherosclerotic vascular non-compliance and sternocleidomastoid denervation (11). Many systematic comorbidities and local morbidities are also associated with CSH. The former includes Alzheimer's disease, dementia with Lewy bodies, Takayasu arteritis, severe coronary artery disease, and internal carotid artery occlusion. The latter includes head and neck malignancy, scar in the neck, and radiotherapy to the neck (13, 14).

The study patient had no morbidities associated with CSH mentioned above. Special positioning necessary to obtain adequate tumor exposure might be a CSH trigger. Stretched carotid sinus and vagus nerve caused by hyperextension and rotation of the neck can led to a slowdown of the heart rate. Intraoperative dissection of the tumor from the carotid bifurcation and carotid arteries stimulated the carotid sinus, which was a response to the vessel wall deformation in any direction (15). These stimuli were carried out *via* the glossopharyngeal and vagus nerves to the nucleus tractus solitarius in the brainstem, with the efferent reflex arch carried through the vagus and sympathetic nerves to the heart and blood vessels, negatively influencing the heart rate and blood pressure (11). It is likely that the above two processes, especially the second one, were the main causes of CSH in the study patient.

The incidence of complications mentioned above increases with the expansion of the tumor (16). Intraoperative cardiac arrest seems to be not associated with tumor size. Prophylactic local anesthetic injection around the carotid sinus during the carotid bifurcation operation is routinely used by surgeons to inhibit the carotid sinus reflex (17, 18). However, the effect is questionable. Part of the causation may be due to the variations in carotid sinus location, which results in the inaccurate local anesthesia injection site (9).

The first staged surgery for the right CBT induced CSH in the present patient. The left CBT was smaller in size. The patient decided not to remove it for the time being, but to observe it instead. However, the patient provided consent for removing the tumor on the left side in the future, if necessary. How to prevent possible intraoperative CSH is a problem worthy of discussion. Bilateral CSH has been reported and atropine does not reverse bradycardia every time (19, 20). Temporary cardiac pacemaker implantation is a prophylactic option for CSH detected before

surgery (21, 22). The patient might need a temporary pacemaker before the surgery to remove the left CBT.

Conclusion

Intraoperative cardiac arrest caused by CSH is a very rare but life-threatening complication during the resection of CBT. Its incidence has little correlation with tumor size. Doctors should be alert to this potentially dangerous complication when performing surgery near the carotid sinus. Implantation of a temporary pacemaker is a possible preventive measure if CSH is detected on the surgical side prior to the operation.

Data availability statement

The original contributions presented in the study are included in the article/supplementary material, further inquiries can be directed to the corresponding author.

Ethics statement

The studies involving human participants were reviewed and approved by Ethics Committee of Shanxi Provincial People's Hospital. The patients/participants provided their written informed consent to participate in this study. Written informed consent was obtained from the individual(s) for the publication of any potentially identifiable images or data included in this article.

Author contributions

HYD made contributions to the conception, design of the work, acquisition, analysis, and interpretation of data and has drafted the manuscript. QG made contributions to the manuscript revision. YJG made contributions to the pictures collection. NL made contributions to the pictures editing. All authors approved the submitted manuscript for publication.

Conflict of interest

The authors declare that the research was conducted in the absence of any commercial or financial relationships that could be construed as a potential conflict of interest.

Publisher's note

References

1. Rodriguez-Cuevas S, Lopez-Garza J, Labastida-Almendaro S. Carotid body tumors in inhabitants of altitudes higher than 2000 meters above sea level. *Head Neck.* (1998) 20:374–8. doi: 10.1002/(sici)1097-0347(199808)20:5<374::aid-hed3>3.0.co;2-v

2. Langerman A, Athavale SM, Rangarajan SV, Sinard RJ, Netterville JL. Natural history of cervical paragangliomas: outcomes of observation of 43 patients. *Arch Otolaryngol Head Neck Surg.* (2012) 138:341–5. doi: 10.1001/archoto.2012.37

3. Reitz K, Ramos A, Speranza G, Chaer R, Singh M, Snyderman C, et al. Non-functional carotid body tumors in patients without somatic mutations may be considered for non-operative management. *Ann Vasc Surg.* (2022) 85:57–67. doi: 10.1016/j.avsg.2022.04.021

4. Davila VJ, Chang JM, Stone WM, Fowl RJ, Bower TC, Hinni ML, et al. Current surgical management of carotid body tumors. *J Vasc Surg.* (2016) 64:1703–10. doi: 10.1016/j.jvs.2016.05.076

5. Gonzalez-Urquijo M, Castro-Varela A, Barrios-Ruiz A, Hinojosa-Gonzalez DE, Salas AKG, Morales EA, et al. Current trends in carotid body tumors: comprehensive review. *Head Neck.* (2022) 44:2316–32. doi: 10.1002/hed.27147

6. Bobadilla-Rosado LO, Garcia-Alva R, Anaya-Ayala JE, Peralta-Vazquez C, Hernandez-Sotelo K, Luna L, et al. Surgical management of bilateral carotid body Tumors. *Ann Vasc Surg.* (2019) 57:187–93. doi: 10.1016/j.avsg.2018.10.019

7. Kakkos SK, Zampakis P, Lampropoulos GC, Paridis L, Kaplanis C, Bantouna D, et al. Successful resection of a large carotid body tumor masquerading complete encasement of the internal carotid artery on preoperative imaging. *Vasc Endovascular Surg.* (2018) 52:304–8. doi: 10.1177/1538574418761722

8. Li X, Zhang W, Shu C, Li Q, Zhang L, Zhu J. Diagnosis and outcomes of surgical treatment of carotid bifurcation tumors. *J Int Med Res.* (2020) 48:1–12. doi: 10.1177/0300060520976495

9. West CT, Brassett C, Gaunt ME. Variations in carotid sinus anatomy and their relevance to carotid interventions. *Folia Morphol.* (2018) 77:693–7. doi: 10.5603/FM.a2018.0017

10. Brignole M, Moya A, de Lange FJ, Deharo JC, Elliott PM, Fanciulli A, et al. 2018 ESC Guidelines for the diagnosis and management of syncope. *Eur Heart J.* (2018) 39:1883–948. doi: 10.1093/eurheartj/ehy037

11. Amin V, Pavri BB. Carotid sinus syndrome. *Cardiol Rev.* (2015) 23:130–4. doi: 10.1097/CRD.0000000000000041

12. McIntosh SJ, Lawson J, Kenny RA. Clinical characteristics of vasodepressor, cardioinhibitory, and mixed carotid sinus syndrome in the elderly. *Am J Med.* (1993) 95:203–8. doi: 10.1016/0002-9343(93)90261-m

13. Truong AT, Sturgis EM, Rozner MA, Truong DT. Recurrent episodes of asystole from carotid sinus hypersensitivity triggered by positioning for head and neck surgery. *Head Neck.* (2013) 35:E28–30. doi: 10.1002/hed.21812

14. Chung HS, Park CM, Kim ES, Ghil BG, Park CS. Temporary cardiac arrest in patient under robotically assisted total thyroidectomy causing carotid sinus hypersensitivity -a case report. *Korean J Anesthesiol.* (2010) 59(Suppl.):S137–140. doi: 10.4097/kjae.2010.59.S.S137

15. Kirchheim HR. Systemic arterial baroreceptor reflexes. *Physiol Rev.* (1976) 56:100–77. doi: 10.1152/physrev.1976.56.1.100

16. Hallett JW Jr, Nora JD, Hollier LH, Cherry KJ Jr, Pairolero PC. Trends in neurovascular complications of surgical management for carotid body and

cervical paragangliomas: a fifty-year experience with 153 tumors. *J Vasc Surg.* (1988) 7:284–91.

17. Casarim AL, Tincani AJ, Del Negro A, Aguiar CG, Fanni RV, Martins AS. Carotid body tumor: retrospective analysis on 22 patients. *São Pãulo Med J.* (2014) 132:133–9. doi: 10.1590/1516-3180.2014.13 23452

18. Gottlieb A, Satariano-Hayden P, Schoenwald P, Ryckman J, Piedmonte M. The effects of carotid sinus nerve blockade on hemodynamic stability after carotid endarterectomy. *J Cardiothorac Vasc Anesth.* (1997) 11:67–71. doi: 10.1016/s1053-0770(97)90256-1

19. Lilitsis E, Papaioannou A, Hatzimichali A, Spyridakis K, Xenaki S, Chalkiadakis G, et al. A case of asystole from carotid sinus hypersensitivity during patient positioning for thyroidectomy. *BMC Anesthesiol.* (2016) 16:85. doi: 10.1186/s12871-016-0255-5

20. Lacerda Gde C, Pedrosa RC, Lacerda RC, Santos MC, Perez Mde A, Teixeira AB, et al. Cardioinhibitory carotid sinus hypersensitivity: prevalence and predictors in 502 outpatients. *Arq Bras Cardiol.* (2008) 90:148–55. doi: 10.1590/s0066-782x2008000300002

21. Bauer AM, Smith RB, Thorell WE. Implications of carotid sinus hypersensitivity following preoperative embolization of a carotid body tumor. An indication for prophylactic intraoperative cardiac pacing. *JAMA Otolaryngol Head Neck Surg.* (2014) 140:459–63. doi: 10.1001/jamaoto.2014.144

22. da Gama AD, Cabral GM. Carotid body tumor presenting with carotid sinus syndrome. *J Vasc Surg.* (2010) 52:1668–70. doi: 10.1016/j.jvs.2010.07.016

frontiers | Frontiers in Cardiovascular Medicine

TYPE Case Report
PUBLISHED 12 January 2023
DOI 10.3389/fcvm.2022.1089694

OPEN ACCESS

EDITED BY
Masateru Takigawa,
Tokyo Medical and Dental University, Japan

REVIEWED BY
Stepan Havranek,
Charles University, Czechia
Seigo Yamashita,
Jikei University School of Medicine, Japan

*CORRESPONDENCE
Xiao-Lan Li
✉ wanders1396@hotmail.com

SPECIALTY SECTION
This article was submitted to Cardiac Rhythmology, a section of the journal Frontiers in Cardiovascular Medicine

RECEIVED 04 November 2022
ACCEPTED 19 December 2022
PUBLISHED 12 January 2023

CITATION
Huang X, Zhou H, Li X-M and Li X-L (2023) Case report: Left ventricular perforation caused by right ventricular pacemaker lead. *Front. Cardiovasc. Med.* 9:1089694. doi: 10.3389/fcvm.2022.1089694

Case report: Left ventricular perforation caused by right ventricular pacemaker lead

Xiang Huang, Heng Zhou, Xiao-Mei Li and Xiao-Lan Li*

Department of Cardiology, Xiangyang No.1 People's Hospital, Hubei University of Medicine, Xiangyang, Hubei, China

Background: Perforation of the interventricular septum and left ventricular (LV) free wall by a right ventricular (RV) lead is an extremely rare and potentially life-threatening complication. In this case report, we discussed the diagnosis and management of a very unusual complication of pacemaker (PM) implantation, i.e., LV perforation brought on by an RV pacing lead.

Case summary: A 92-year-old man was admitted to Xiangyang No.1 People's Hospital due to a complete atrioventricular block. We performed a dual-chamber PM implantation; however, on the second postoperative day (POD), pacemaker failure occurred. Thoracic computed tomography (CT) scan showed that RV lead had pierced the interventricular septum and LV free wall. A transvenous lead extraction of the penetrating lead was performed uneventfully, and RV lead was refixed at the lower RV septum on the 5th POD.

Discussion: Identification of high-risk patients is mandatory to prevent this serious complication, and transvenous lead extraction with cardiac surgery backup may be an option.

KEYWORDS

pacemaker, lead migration, left ventricular perforation, transvenous lead extraction, right ventricular pacemaker lead

1. Introduction

Iatrogenic ventricle perforation by pacing/defibrillation leads is a rare but potentially life-threatening complication which occurs in only 0.3–0.8% of pacemaker (PM) or implantable cardioverter defibrillator (ICD) implantation procedures (1). Although the right ventricular (RV) apex is the site of lead perforation that occurs most frequently, few cases have been reported of lead penetration through the interventricular septum and the left ventricular (LV) free wall to the left hemithorax (2). Appropriate management of lead migration in the left hemithorax is still uncertain. Among these reported cases, most patients underwent surgical extraction of the penetrating lead (3).

2. Case presentation

A 92-year-old man was referred to our center for syncope due to a complete atrioventricular block (Figure 1A). His medical history includes coronary atherosclerotic heart disease and chronic obstructive pulmonary disease. Coronary angiography was performed on account of effort angina 3 years ago (Figures 1E, F). Prior coronary angiography revealed a diffuse lesion (percent diameter stenosis 70–80%) in the middle segment of the left anterior descending (LAD) branch (Figure 1E). However, he refused to receive revascularization or medication treatment. During hospitalization, he had no finding of heart failure, and the transthoracic echocardiography (TTE) revealed minor mitral insufficiency and normal LV contraction (ejection fraction: 55%).

We performed dual-chamber PM (HeartTone LD300D, LifeTech Scientific Corporation, Shenzhen, China) implanted *via* the left subclavian vein on the next day after admission.

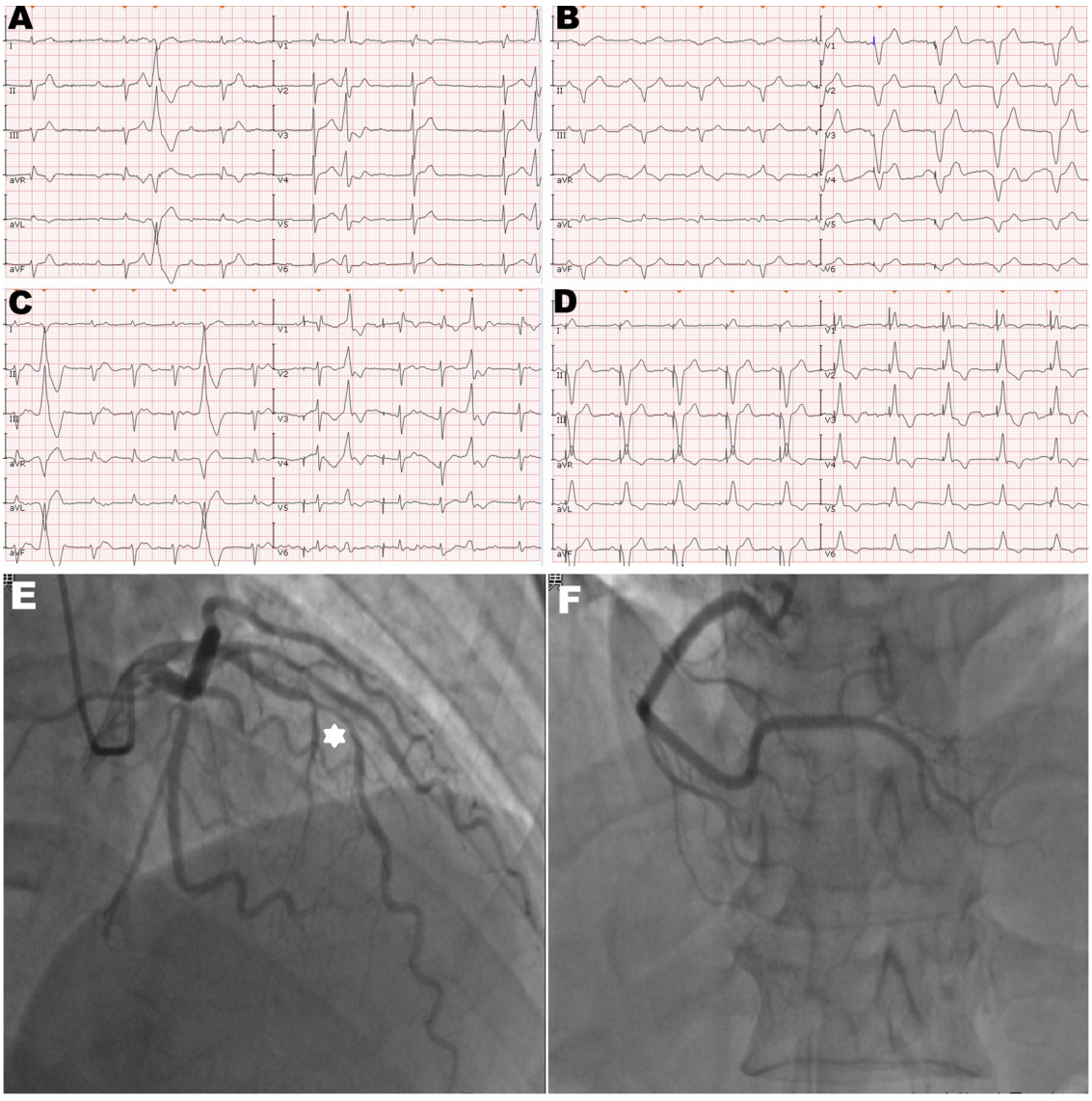

FIGURE 1
Twelve-lead electrocardiogram and coronary angiogram of the patient. **(A)** The initial electrocardiogram on the admission day showed complete atrioventricular block with frequent premature ventricular contractions. **(B)** The electrocardiogram immediately after pacemaker (PM) implantation showed the left bundle branch block pattern and the pacing model was VAT. **(C)** The electrocardiogram on the second post-operative day (POD) showed ventricular pacing failure. **(D)** The electrocardiogram after transvenous lead extraction and re-fixation showed the right bundle branch block and left axis deviation, and the right ventricular (RV) lead was refixed at the lower RV septum. **(E)** Hexagonal star symbol shows a diffuse atherosclerotic stenosis was observed in the middle segment of the left anterior descending branch, thus leading to insufficient coronary blood supply on the mid-portion of the interventricular septum. **(F)** Right coronary artery was relatively normal.

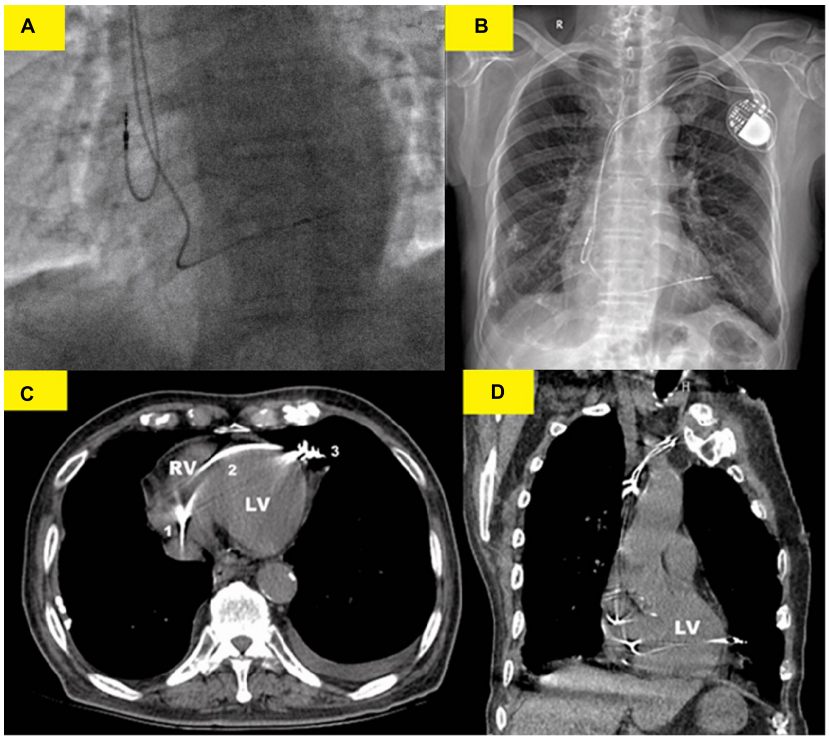

FIGURE 2
Various imaging modalities showed the lead perforation. **(A)** X-ray fluoroscopy image (right anterior oblique 30°) immediately after implantation showed that the RV lead was placed at the right ventricular (RV) apex. **(B)** Chest x-ray showed that the RV lead was beyond the left cardiac margin and clearly migrated in the left hemithorax. **(C)** Thoracic computed tomography (CT) scan showed the RV lead course from the right ventricle (1) to the left cardiac margin (3) in the patient and perforation of the interventricular septum (2) was well-evident. **(D)** Coronal CT images confirmed the RV lead migration in the left hemithorax. Thoracic CT scan should, therefore, be regarded as the gold standard for the strategical management of this complication.

The implantation procedure can be summarized as follows: under local anesthesia, after a successful puncture of the left subclavian vein, the patient was implanted with a common sheath. Although a superior vena cava stenosis might exist, we did not replace the common sheath with a long sheath. Thus, the manipulation of active fixation leads was very difficult; we attempted to fix RV lead at the RV septum, but it was not as successful. Finally, two active fixation leads were, respectively, placed at the RV apex (SureScan 5076; 58 cm, Medtronic, Minneapolis, MN, USA) and the right atrial appendage (SureScan 5076; 52 cm, Medtronic, Minneapolis, MN, USA) with excellent pacing parameters (intraoperative RV lead impedance and threshold were 1,300 Ω and 1.4 V, respectively). There were no abnormalities or complications during the implantation procedure. X-ray fluoroscopy image immediately after implantation showed that the RV lead was fixed properly (**Figure 2A**). Electrocardiogram immediately after implantation showed the left bundle branch block pattern (**Figure 1B**).

However, on the second postoperative day (POD), the patient complained of unrelenting chest pain and syncope. A subsequent immediate chest X-ray identified that the RV lead tip migrated to the region outside the left cardiac margin (**Figure 2B**). A thoracic computed tomography (CT) scan revealed that the RV lead passed through the interventricular septum and the left LV free wall, and finally reached the left of the pericardial cavity. Furthermore, as the thoracic CT scan also showed a small amount of left pleural effusion (**Figure 2B**) and there were no obvious symptoms of pericardial tamponade (**Figures 2C, D**), we deduced that the lead had already penetrated the pericardium. Electrocardiogram and interrogation showed loss of ventricular capture (**Figure 1C**).

The subsequent patient's management was thoroughly debated. Patients may not tolerate surgical lead extraction due to the variety of severe chronic diseases and advanced age. Therefore, on the 5th POD, we performed transvenous lead extraction under transesophageal echocardiography monitored and cardiac surgery backup. **Figures 3A–D** depict and describe the entire procedure in detail. Transvenous lead extraction was uncomplicated and did not have any hemodynamic instability, and intraoperative ultrasonography monitoring showed no increase in pleural effusion and pericardial effusion. The original RV lead was refixed at the lower RV septum to reduce the risk of perforation and consequent tamponade.

Subsequent electrocardiogram and PM interrogation revealed the PM functioning normally with excellent pacing parameters (intraoperative RV lead impedance and threshold were 1,020 Ω and 1.0 V, respectively) (**Figure 1D**). On the 10th POD, the patient was discharged, and the subsequent 6 months of follow-up were uneventful.

3. Discussion

Left ventricular perforation caused by an RV pacing lead is a rare and potentially life-threatening complication, and the lead can migrate to the outside of the pericardium with a potential risk of vascular or pulmonary damage. Although late-onset (> 1 month) ventricular perforations have also been observed, they often started within < 24 h after device placement (4). To the best of our knowledge, no specific recommendations are known to exist for this uncommon complication. In addition, it has not yet been extensively investigated what pathophysiological mechanisms are involved (5). All of the clinical cases with this complication documented in the literature are shown in **Table 1**, together with their lead type, model, location, migration course, clinical characteristics, treatment, and follow-up (2, 3, 5–12).

Although the mechanisms of interventricular septal perforation are still unknown, the reported cases suggest that inadequate blood supply and the twisting motion of the septal musculature from beat to beat may be associated with this complication (5). Besides, active fixation leads positioned on the thin-walled RV apex also seem to be related to an increased risk of left-sided lead migration, according to earlier observations on patients with lead perforation. Indeed, in this case, the perforation portion of the septal was the coronary angiogram that had previously shown insufficient coronary blood supply. Although active fixation leads positioned in the RV apex result in greater stability, the straight shape of the distal RV lead may bring about significant pressure perpendicularly transferred to the ventricular wall (13). Moreover, features of the lead (SureScan 5076; 58 cm, Medtronic) also seem to play a pivotal role in our case. This lead's non-retractable bare screw and substantial tipping load may have created excessive stress on the ventricular wall (12). Finally, excessive loop of the RV lead may generate more tension in the ventricular wall, which is also a potential cause of ventricular perforation. In this regard, to prevent the recurrence of this lead implantation complication, a leadless PM should be used in conjunction with a functioning AAI system as an alternate treatment.

A previous study found that pericardial effusion and tamponade only occurred in 38 and 19% of patients (14). However, detecting cardiac perforation brought on by ventricular leads with clinical symptoms was not difficult. Therefore, in instances with unclear results and/or a lack of symptoms, thoracic CT scans are essential to determine if the pleural or LV free wall is implicated and to establish an appropriate diagnosis.

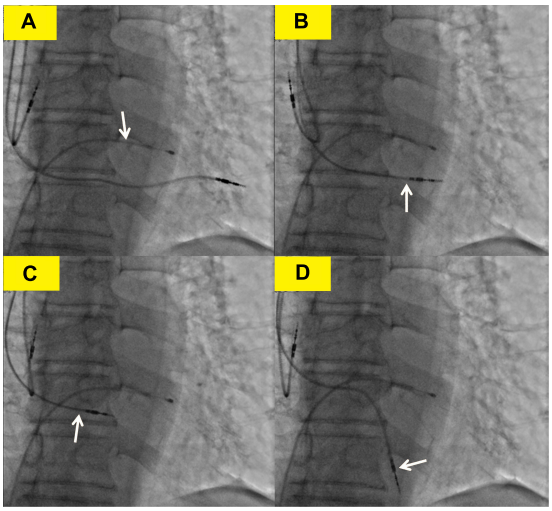

FIGURE 3
Transvenous lead extraction process. **(A)** The white arrow shows the lead of the temporary transvenous pacemaker. **(B)** The white arrow shows the right ventricular (RV) lead was screwed back to the left ventricle. **(C)** The white arrow shows the RV lead was screwed back to the right ventricle. **(D)** The white arrow shows the right ventricular lead was refixed at the lower right ventricular septum.

According to a consensus endorsed by the American Heart Association, transvenous lead extraction is not the preferred strategy for patients with cardiac perforation due to pacing/defibrillation lead (15). As indicated in **Table 1**, surgical lead extraction was carried out without incident in all instances of lead migration in the left hemithorax. Still, for patients who may not tolerate surgical extraction or refuse surgical extraction, transvenous lead extraction could be a potential alternative, especially in recent implantations. It is a less invasive method than open surgery that avoids the potential complications of sternotomy as well as long-term hospital stays (16).

In this report, to the best of our knowledge, we first demonstrated the transvenous lead extraction to treat the lead migration in the left hemithorax. From our experience, spontaneous closure of the perforated site with myocardial contraction is likely to occur immediately after lead withdrawal in LV or RV perforation. Therefore, transvenous lead extraction is feasible, but considering its high-risk characteristics, the whole procedure should be performed by an experienced intervention cardiologist specializing in transvenous lead extraction, preferably in a hybrid operating room, under careful hemodynamic and transesophageal echocardiographic monitoring with a cardiac surgical backup. In addition, transvenous lead extraction should be followed by a new lead implantation or re-fixing of the perforating lead in a different location.

TABLE 1 Summary of clinical cases of ventricular pacemaker/implantable cardioverter defibrillator (PM/ICD) leads migration in the left hemithorax including our case.

References	Sex	Age (y)	Lead type	Lead model	Lead position	Time from implantation to lead complication	Symptoms	Lead migration	Management	New lead position	Follow-up
Selcuk, et al. (6)	F	30	N/A	N/A	RV apex	2 weeks	headedness, chest pain	RV wall, pericardium, left pleura	surgical extraction	N/A	Uneventful
Migliore, et al. (7)	M	52	active fixation ICD lead	Linox SD 65/16, biotronik	RV apex	12 days	asymptomatic	septum, LV wall	surgical extraction	epicardial	Uneventful
Bohora, et al. (8)	M	44	active fixation PM lead	ICQ09B-58, vitatron	RV apex	5 days	chest pain, cough, fatigue, left hemithorax	RV wall, pericardium, left pleura	surgical extraction	epicardial	Uneventful
Kondoh, et al. (9)	M	82	active fixation PM lead	CapSureFix 5076-52, medtronic	RV sptum	3 months	chest pain	RV wall, pericardium, left pleura	surgical extraction	epicardial	Uneventful
Forleo, et al. (10)	F	81	active fixation PM lead	CapSureFix MRI, medtronic	RV apex	7 months	chest pain, left hemithorax, dyspnea, hypotension	RV wall, pericardium, left pleura	surgical extraction	RV septum	Uneventful
Pojar, et al. (11)	M	74	active fixation PM lead	N/A	RV apex	3 months	cardiogenic shock, left hemothorax, pericardial effusion	RV wall, pericardium, left pleura	surgical extraction	epicardial	Uneventful
Iribarne, et al. (2)	F	69	active fixation PM lead	CapSureFix 5076-52, medtronic	RV sptum	2 weeks	none	septum, LV wall	surgical extraction	epicardial	Uneventful
Satomi, et al. (3)	M	84	active fixation PM lead	Select secure 3830-69, medtronic	RV sptum	2 days	syncope	septum, LV wall	surgical extraction	RV septum	Uneventful
Marazzato, et al. (5)	F	78	active fixation PM lead	Solia S 60, biotronik	RV sptum	2 months	chest pain, syncope	septum, LV wall	surgical extraction	epicardial	Uneventful
Our report	M	92	active fixation PM lead	Surescan 5076-58, medtronic	RV apex	2 days	chest pain, syncope	septum, LV wall	transvenous extraction	RV septum	Uneventful

M, male; F, female; ICD, implantable cardioverter defibrillator; LV, left ventricular; N/A, not available; PM, pacemaker; RV, right ventricular.

10.3389/fcvm.2022.1089694

4. Conclusion

The presence of unrelenting chest pain should consider the possibility of a lead migration in the left hemithorax in cases of suspected cardiac perforation. To assess whether the pleural or LV free wall is involved, thoracic CT scans are essential. With respect to lead extraction, transvenous lead extraction with cardiac surgery backup can be feasible. In addition, less traumatic passive-fixation leads or leadless PM may be employed in these high-risk individuals with evidence of non-revascularizable coronary atherosclerotic heart disease and unequivocal need for PM/ICD implantation.

Data availability statement

The original contributions presented in this study are included in the article/**Supplementary material**, further inquiries can be directed to the corresponding author.

Ethics statement

Written informed consent was obtained from the individual(s) for the publication of any potentially identifiable images or data included in this article. The patient consent form was read and signed by the patient.

Author contributions

XH: methodology, investigation, formal analysis, and writing—original draft. HZ: conceptualization and visualization. X-ML: investigation and writing—review. X-LL: project administration and supervision. All authors contributed to the article and approved the submitted version.

Conflict of interest

The authors declare that the research was conducted in the absence of any commercial or financial relationships that could be construed as a potential conflict of interest.

Publisher's note

Supplementary material

The Supplementary Material for this article can be found online at: https://www.frontiersin.org/articles/10.3389/fcvm.2022.1089694/full#supplementary-material

SUPPLEMENTARY FIGURE 1
Transvenous lead extraction process.

References

1. Carlson M, Freedman R, Levine P. Lead perforation: incidence in registries. *Pacing Clin Electrophysiol.* (2008) 31:13–5. doi: 10.1111/j.1540-8159.2007.00943.x

2. Iribarne A, Sangha R, Bostock I, Rothstein E, McCullough J. Right ventricular lead perforation through the septum, left ventricle, and pleura, managed by an open surgical approach. *Heart Rhythm Case Rep.* (2018) 4:397–400. doi: 10.1016/j.hrcr.2018.05.004

3. Satomi N, Enta K, Otsuka M, Ishii Y, Asano R, Sawa S. Left ventricular free wall perforation by a right ventricular pacemaker lead: a case report. *Eur Heart J Case Rep.* (2021) 5:ytab125. doi: 10.1093/ehjcr/ytab125

4. Khan M, Joseph G, Khaykin Y, Ziada K, Wilkoff B. Delayed lead perforation: a disturbing trend. *Pacing Clin Electrophysiol.* (2005) 28:251–3. doi: 10.1111/j.1540-8159.2005.40003.x

5. Marazzato J, Caravati F, Blasi F, Refugjati T, Vilotta M, Torchio F, et al. Ventricular pacemaker lead in the left hemithorax: mechanisms and evidence-based management of a late-onset hazardous complication. *Clin Case Rep.* (2021) 9:e04617. doi: 10.1002/ccr3.4617

6. Selcuk H, Selcuk M, Maden O, Ozeke O, Celenk M, Turkvatan A, et al. Uncomplicated heart and lung perforation by a displaced ventricular pacemaker lead: a case report. *Pacing Clin Electrophysiol.* (2006) 29:429–30. doi: 10.1111/j.1540-8159.2006.00366.x

7. Migliore F, Leoni L, Torregrossa G, Guglielmi C, Tarantini G, Buja G, et al. Asymptomatic right ventricular perforation by an implantable cardioverter defibrillator lead detected by home monitoring system. *J Electrocardiol.* (2010) 43:673–5. doi: 10.1016/j.jelectrocard.2010.07.022

8. Bohora S, Unnikrishnan M, Ajit Kumar V, Nayyar S, Tharakan J. Left hemothorax: a presentation of a late ventricular perforation caused by an active fixation pacing lead. *Int J Cardiol.* (2010) 141:e43–6. doi: 10.1016/j.ijcard.2008.11.152

9. Kondoh H, Funatsu T, Taniguchi K. Late left ventricular perforation by active fixation pacemaker lead implanted in the right ventricular septum. *J Card Surg.* (2012) 27:530–1. doi: 10.1111/j.1540-8191.2012.01479.x

10. Forleo G, Zeitani J, Perretta T, Della Rocca D, Santini L, Simonetti G, et al. Acute left hemothorax as a late complication of an active-fixation pacemaker lead. *Ann Thorac Surg.* (2013) 95:1081–4. doi: 10.1016/j.athoracsur.2012.07.064

11. Pojar M, Vobornik M, Novy J. Left hemothorax: an unusual complication of delayed right ventricular perforation by a permanent pacemaker lead. *J Card Surg.* (2013) 28:325–7. doi: 10.1111/jocs.12080

12. Gammage M, Lieberman R, Yee R, Manolis A, Compton S, Khazen C, et al. Multi-center clinical experience with a lumenless, catheter-delivered, bipolar, permanent pacemaker lead: implant safety and electrical performance.

Pacing Clin Electrophysiol. (2006) 29:858–65. doi: 10.1111/j.1540-8159.2006.00452.x

13. Akbarzadeh M, Mollazadeh R, Sefidbakht S, Shahrzad S, Bahrololoumi Bafruee N. Identification and management of right ventricular perforation using pacemaker and cardioverter-defibrillator leads: a case series and mini review. *J Arrhythm.* (2017) 33:1–5. doi: 10.1016/j.joa.2016.05.005

14. Schwerg M, Stockburger M, Schulze C, Bondke H, Poller W, Lembcke A, et al. Clinical, anatomical, and technical risk factors for postoperative pacemaker or defibrillator lead perforation with particular focus on myocardial thickness. *Pacing Clin Electrophysiol.* (2014) 37:1291–6. doi: 10.1111/pace.12431

15. Wilkoff B, Love C, Byrd C, Bongiorni M, Carrillo R, Crossley G III, et al. Transvenous lead extraction: heart Rhythm Society expert consensus on facilities, training, indications, and patient management: this document was endorsed by the American heart association (AHA). *Heart Rhythm.* (2009) 6:1085–104. doi: 10.1016/j.hrthm.2009.05.020

16. Archontakis S, Sideris K, Aggeli K, Gatzoulis K, Demosthenous M, Tolios P, et al. Percutaneous lead extraction and repositioning: an effective and safe therapeutic strategy for early ventricular lead perforation with dislocation both inside and outside the pericardial sac following a cardiac device implantation. *J Cardiovasc Electrophysiol.* (2019) 30:299–307. doi: 10.1111/jce.13804

frontiers | Frontiers in Cardiovascular Medicine

TYPE Case Report
PUBLISHED 19 January 2023
DOI 10.3389/fcvm.2022.1035896

OPEN ACCESS

EDITED BY
Jedrzej Kosiuk,
Helios Clinic Koethen, Germany

REVIEWED BY
Riccardo Giossi,
ASST Grande Ospedale Metropolitano Niguarda, Italy
Abbas Alshami,
Jersey Shore University Medical Center (JSUMC), United States

*CORRESPONDENCE
Sy Duong-Quy
✉ sduongquy.jfvp@gmail.com
Vinh Nguyen-Nhu
✉ vinhnguyenmd@ump.edu.vn

SPECIALTY SECTION
This article was submitted to Cardiac Rhythmology, a section of the journal Frontiers in Cardiovascular Medicine

RECEIVED 03 September 2022
ACCEPTED 29 December 2022
PUBLISHED 19 January 2023

CITATION
Duong-Quy S, Huynh-Truong-Anh D, Tran-Xuan Q, Nguyen-Quang T, Nguyen-Thi-Kim T, Nguyen-Chi T, Tran-Ngoc-Anh T, Nguyen-Van-Hoai N, Do-Thi-Thu M, Tang-Thi-Thao T, Bui-Diem K, Hoang-Anh T, Nguyen-Ngoc-Phuong T and Nguyen-Nhu V (2023) Bradycardia unresponded to atropin testing was successfully treated with therapeutic plasma exchange in a patient with severe COVID-19 complicated by Guillain-Barré syndrome: A case report. *Front. Cardiovasc. Med.* 9:1035896. doi: 10.3389/fcvm.2022.1035896

Bradycardia unresponded to atropin testing was successfully treated with therapeutic plasma exchange in a patient with severe COVID-19 complicated by Guillain-Barré syndrome: A case report

Sy Duong-Quy[1,2,3,4]*, Duc Huynh-Truong-Anh[2], Quynh Tran-Xuan[5], Tien Nguyen-Quang[2], Thanh Nguyen-Thi-Kim[2], Thanh Nguyen-Chi[2], Thuy Tran-Ngoc-Anh[2], Nam Nguyen-Van-Hoai[2], Mai Do-Thi-Thu[2], Tram Tang-Thi-Thao[1], Khue Bui-Diem[6], Tien Hoang-Anh[7], Thu Nguyen-Ngoc-Phuong[4] and Vinh Nguyen-Nhu[8,9]*

[1]Biomedical Research Center, Lam Dong Medical College, Da Lat, Vietnam, [2]COVID-19 Unit of Phu Chanh, Binh Duong General Hospital, Thủ Dầu Một, Binh Duong, Vietnam, [3]Division of Pulmonary, Allergy, and Critical Care Medicine, Penn State College of Medicine, Hershey, PA, United States, [4]Faculty of Medicine, Pham Ngoc Thach University of Medicine, Ho Chi Minh City, Vietnam, [5]Department of Internal Medicine, Can Tho University of Medicine and Pharmacy, Can Tho, Vietnam, [6]Department of Physiology and Pathophysiology, University of Medicine and Pharmacy at Ho Chi Minh City, Ho Chi Minh City, Vietnam, [7]Department of Cardiology. Hue University of Medicine and Pharmacy, Hue University, Hue, Vietnam, [8]Department of Family Medicine, Faculty of Medicine, University of Medicine and Pharmacy at Ho Chi Minh City, Ho Chi Minh City, Vietnam, [9]Department of Respiratory Functional Exploration, University Medical Center, Ho Chi Minh City, Vietnam

The severe acute respiratory syndrome coronavirus 2 (SARS-CoV-2) pandemic has been an alarming situation worldwide for the past 2 years. The symptoms of coronavirus disease 2019 (COVID-19) are not only confined to the respiratory system but also affect a multitude of organ systems. Bradycardia associated with Guillain-Barré syndrome (GBS) is a rare autonomic and peripheral neurological complication of COVID-19. In this case report, we present the case of a 26-year-old man diagnosed with bradycardia associated with GBS after contracting COVID-19. Initially, this patient had the classical symptoms of COVID-19 and was hospitalized in the intensive care unit (ICU) for acute respiratory distress syndrome (ARDS). Then, he developed weakness in the lower extremities, diminished tendon reflexes, a loss of sensation without sphincter muscle disorders, and bradycardia. His bradycardia did not respond to atropine. The patient was treated concurrently with a high-flow nasal cannula, systemic corticosteroids, anticoagulation, and therapeutic plasma exchange (TPE) for COVID-19-induced ARDS, bradycardia, and GBS. His ARDS and bradycardia improved after the first cycle of TPE and medical treatment. After three cycles of TPE, the patient progressively recovered his muscle strength in the lower limbs and regained peripheral sensation. He was discharged from the hospital in stable condition after 4 weeks of hospitalization and was followed up after 6 months for cardiorespiratory and neurological complications. This case report elucidates the potential difficulties

and challenges that physicians may encounter in diagnosing and treating COVID-19-induced bradycardia and GBS during the pandemic outbreak. However, the patient outcomes with the treatment combining the conventional treatment with therapeutic plasma exchange seem to be optimistic.

KEYWORDS

SARS-CoV-2, COVID-19, bradycardia, Guillain-Barrée syndrome, therapeutic plasma exchange

Introduction

The coronavirus disease 2019 (COVID-19) is caused by a coronavirus called severe acute respiratory syndrome coronavirus 2 (SARS-CoV-2), which has affected more than 600 million people worldwide. Severe COVID-19 infections have been significantly reduced due to the global efficacy of vaccination campaigns. A few days after contracting the virus, patients with COVID-19 commonly present with a wide range of symptoms, ranging from mild to severe. These symptoms include fever, cough, shortness of breath, sore throat, nausea, vomiting, and/or diarrhea. However, patients with advanced age or serious comorbidities remain at higher risk for developing serious complications from COVID-19.

However, patients with COVID-19 could present at an emergency department with diverse neurological symptoms, including confusion, refractory headache, new onset of anosmia and/or ageusia, and acute peripheral impairment. Although COVID-19-induced inflammatory polyradiculoneuropathy or Guillain-Barré syndrome (GBS) has been described previously (1–5), patients with COVID-19 complicated by bradycardia-associated GBS remain a rare cardio-neurological complication of COVID-19.

In this case report, we present the case of a young man with bradycardia-associated GBS after contracting COVID-19-induced acute respiratory distress syndrome (ARDS). The clinical and laboratory features of this patient were appropriate for the diagnosis of ARDS and bradycardia-associated GBS due to COVID-19. Although the bradycardia did not respond to atropine testing and the symptoms of GBS did not improve after the conventional treatment for acute COVID-19, the patient was successfully stabilized with a normal heart rate and stable cardiorespiratory status after therapeutic plasma exchange (TPE) in combination with standard treatment. This case suggests that TPE might be considered a useful approach to treatment when used in combination with conventional treatments for patients with severe cardiorespiratory and neurological complications of COVID-19.

Case report

A 26-year-old man with a BMI of 34.6 kg/m^2 was admitted to the Medical Center of Binh Duong Province, Vietnam in the middle of October 2021 because of fever, cough, vomiting, diarrhea, and shortness of breath. His laboratory test for COVID-19 from a nasal swab reverse transcription polymerase chain reaction (RT-PCR) test was positive within the cycle threshold of 16. He was previously in good health without any past medical history. He had already received two doses of the inactivated COVID-19 vaccine, the last of which he received 2 months before he was tested positive without any side effects. After his admission to the medical center, he was treated with oxygen therapy (12 L/min *via* Venturi mask), intravenous corticosteroids (dexamethasone 8 mg, two times a day), and anticoagulation (heparin).

He was transferred to the intensive care unit (ICU) of the COVID-19 Hospital of Phu Chanh, Binh Duong General Hospital on day 5 of his admission due to severe dyspnea and pain in his lower limbs associated with muscular weakness. At the time of his ICU arrival, he was conscious; his blood pressure was 130/70 mmHg; his heart rate was 75 beats/min; and his oxygen saturation (SpO_2) was 90% with 15 L/min of oxygen through a mask. The neurological examination revealed the muscular weakness of the lower limbs with a Medical Research Council (MRC) scale of 3 out of 5 (vs. 5 out of 5 for the upper limbs), diminished sensation, and reflexes of the lower limbs without sphincter muscle disorders (Table 1). He had no neurogenic urinary or fecal incontinence.

The chest x-ray showed diffuse ground-glass opacity. Blood analysis and biochemical laboratory tests confirmed increased glucose, fibrinogen, ferritin, and lactate dehydrogenase (LDH) levels. He had normal white blood cells, electrolyte parameters, and liver and kidney functions. His cerebrospinal fluid (CSF) was clear and colorless and without an elevation in white blood cells; the analysis of the CSF demonstrated albuminocytologic dissociation. The result of magnetic resonance imaging (MRI) of the spine was normal. COVID-19-induced ARDS associated with Guillain-Barré syndrome was diagnosed by hospital-qualified neurologists. Other diagnoses, such as compressive myelopathy, transverse myelitis, or acute myelitis, were excluded at that time.

The patient was treated with a high-flow nasal cannula (HFNC) with a fraction of inspired oxygen (FiO_2) of 60%, an oxygen flow rate of 40 L/min, intravenous corticosteroids (dexamethasone: 8 mg, two times a day), anticoagulation (heparin), an intravenous antibiotic for nosocomial pneumonia prevention (ceftazidime and levofloxacin), and a subcutaneous insulin injection for hyperglycemia. The neurological symptoms worsened in the next 2 days, with an MRC scale of 1 out of 5 in the lower limbs and 2–3 out of 5 in the upper limbs, a decrease in the loss of superficial and deep sensation, and a decrease in reflexes. He did not have other autonomic symptoms such as blood pressure changes, bowel malfunctions, or urinary abnormalities. However, the patient then developed sinus bradycardia (40 beats/min), which did not respond to intravenous atropine.

The patient was then treated with therapeutic plasma exchange (TPE) after the decision was made by hospital experts. TPE was done every 2 days with 5% human albumin replacement (4,700 ml/cycle). His bradycardia improved to a normal resting heart rate (>55 beats/min) after the first TPE. He did not experience dyspnea after 5 days of HFNC treatment with flow decreased from 40 to 15

10.3389/fcvm.2022.1035896

TABLE 1 Laboratory data of the reported patient.

Parameters	Upon admission to ICU	After day 14th	Institutional normal range
RT-PCR SARS-CoV-2	+	Negative	Negative
White blood cell (10^9/L)	8.4	11.1	4.0–11.0
Neutrophil (%)	74.11	66.89	45–75
Lymphocyte (%)	17.77	21.83	20–45
Platelet (10^9/L)	351	246	140–500
CRP (mg/dL)	3.07	0.42	<1.0
Lactate (mmol/L)	0.72	–	0.5–2.2
LDH (U/L)	405	306	<247
Ferritin (ng/mL)	>1,500	347.4	23.9–336.2
Fibrinogen (g/L)	5.61	4.71	1.5–4.0
TP (%)	84	95	>70
APTT (s)	23.6	24.1	20–40
Arterial blood gas			
pH	7.32	7.32	7.35–7.45
$PaCO_2$ (mmHg)	25	43	35–45
HCO_3^- (mmol/L)	12.9	22.2	18–23
Base Excess$^-$ (mmol/L)	−11.2	−4	−2–+3
FiO2 (%)	95	21	21
PaO_2 (mmHg)	156	62	80–100
A-aDO_2	490	169	5–20
PaO_2/FiO_2 (ratio)	164	295	400–500
Sodium (mmol/L)	131	132	135–145
Potassium (mmol/L)	4.1	**3.4**	3.5–5.0
Calcium (mmol/L)	1.2	1.1	1.1–1.6
Magnesium (mmol/L)	1.05	0.74	0.73–1.06
Urea (mmol/L)	14.2	2.4	2.8–7.2
Creatinine (μmol/L)	77	52	72–127
eGFR-MDRD (mL/m/m^2)	113	126	≥ 60
HbA1c	12.5	6.2	< 5.7
AST (U/L)	34	22	0–50
ALT (U/L)	38	21	0–50
Glucose (mg/dL)	444	181	< 120
Total protein (g/L)	71	69	66–83
Albumin (g/L)	34	35	35–52
Cerebrospinal fluid			
Cells	0	–	0
Protein (g/L)	0.32	–	0.15–0.45
Glucose (mmol/L)	NA	–	NA
Lactate (mmol/L)	1.4	–	1.1–2.4
Pandy's test	negative	–	Negative

APTT, activated partial thromboplastin time; AST, aspartate aminotransferase; ALT, alanine aminotransferase; CRP, C-reactive protein; LDH, lactate dehydrogenase; eGFR, estimated glomerular filtration rate; FiO_2, fraction of inspired oxygen; MDRD, Modification of Diet in Renal Disease; PaO_2, partial pressure of oxygen in arterial blood; $PaCO_2$, partial pressure of carbon dioxide in arterial blood; RT-PCR, reverse transcription polymerase chain reaction; SARS-CoV-2, severe acute respiratory syndrome coronavirus 2; TP, prothrombin time.

L/min; he was then switched to a nasal cannula with 5 L/min, then 3 L/min, and finally stopped oxygen therapy on day 14 (Figure 1). The neurological symptoms of the patient also improved after day 10 with the progressive recovery of skin sensation and muscle tone in all four limbs evaluated by the MRC scale. The patient was discharged after 4 weeks of hospitalization and followed up regularly every 3 months until now. He recovered to his baseline health status after 3 months and returned to work without any health sequelae 6 months after discharge from the hospital. Currently, the patient is in good health with an MRC scale of 5 out of 5 in the lower and upper limbs and a normal resting heart rate. He has been seen regularly in the Outpatients Medical Center of Binh Duong General Hospital every 2–3 months.

Discussion

In this case report, we present the case of a patient with severe COVID-19 associated with ascending symmetrical limb weakness, external sensation disturbances, absent deep tendon reflexes, and bradycardia. Especially, the CSF showed albuminocytologic dissociation, which supported the diagnosis of GBS in this patient. Thus, clinical examination results and laboratory data were appropriate for the diagnosis of severe COVID-19 complicated by GBS associated with bradycardia.

Initially, the patient presented with acute polyneuropathy after being diagnosed with COVID-19-induced pneumonia. Thus, the diagnosis of GBS seemed to be more accurate. Other diagnoses were eliminated, such as spinal cord compression from degenerative disc disease, spinal cord infarction, and transverse myelitis. During his illness, the patient had no neurogenic urinary, fecal incontinence, or any history of spinal trauma; therefore, the possibility of spinal cord compression was less likely. In addition, he did not experience sudden and severe back pain accompanied by numbness and tingling along the circumference of the spinal cord for diagnosing spinal cord infarction. It was also less likely to be acute transverse myelitis as the major motor findings of this condition are paraparesis or quadriparesis. In addition, the result of the spinal MRI did not show any abnormalities.

Our patient had bradycardia and his heart did not respond to atropine testing. Therefore, severe COVID-19 complicated by GBS associated with bradycardia was diagnosed by the local expert committee of COVID-19 Phu Chanh Hospital. Indeed, following one of the first cases of GBS-associated SARS-CoV-2 infection reported by Zhao et al. in 2020, numerous cases have been published during the COVID-19 pandemic (6–25). Arrhythmias were also one of the significant complications of COVID-19 reported in the world literature. In a recent study from Wuhan, China, cardiac arrhythmias developed in 16.7% of hospitalized patients and 44.4% of ICU patients with COVID-19 (26). In some case reports, patients developed sinus bradycardia related to COVID-19 despite routine echocardiography and cardiac biomarkers (27, 28).

Guillain-Barré syndrome and arrhythmias can develop after immunization or the SARS-CoV-2 infection. According to the safety committee of the European Medicine Agency, 108 cases of GBS were reported worldwide among over 21 million people who had received the vaccine as of 30 June 2021 (29). A 2021 study of Adverse Events Reported From COVID-19 Vaccine Trials based on the WHO database reported 4,863 cardiovascular adverse events, in which

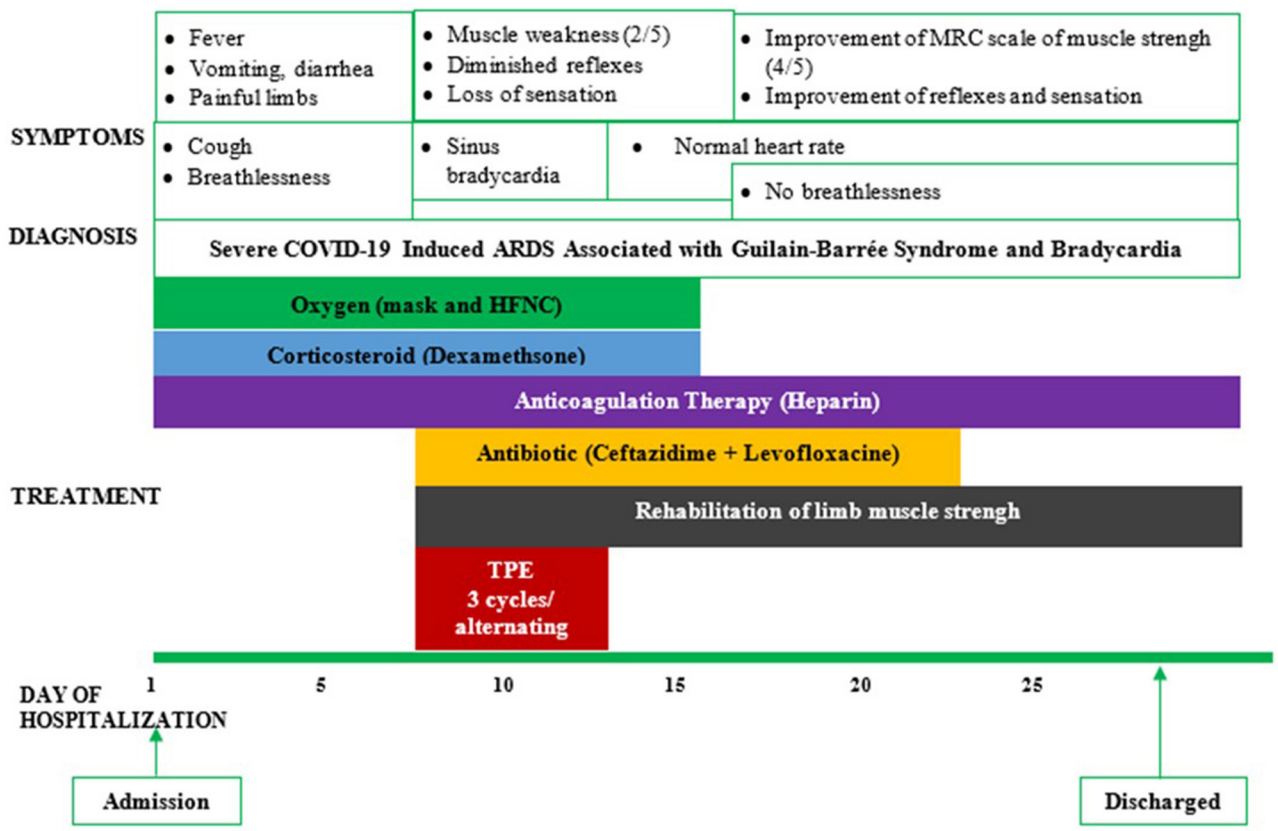

FIGURE 1
Symptoms, diagnosis, and treatment of a reported patient. ARDS, acute respiratory distress syndrome; HFNC, high-flow nasal cannula; TPE, therapeutic plasma exchange.

tachycardia was 16.41% and bradycardia was 5.2% (30). Our patient had his last vaccination dose 2 months before contracting COVID-19.

Autonomic neuropathy is a severe consequence of GBS. Overreactivity of vagal function, in particular, can cause major cardiac problems ranging from bradycardia to asystole (31). According to Mukerji et al., bradyarrhythmia can occur in up to 50% of patients with GBS (32). Cardiac arrhythmia was one of the adverse side effects observed during plasmapheresis procedures (33–35). Our patient recovered from sinus bradycardia after having the first TPE without recurrences during his hospital stay in the ICU. Therefore, this bradycardia could be considered a cardiac adverse event associated with GBS as a complication of COVID-19.

In this case report, TPE was used in combination with standard therapy, including oxygen therapy, anticoagulation, and corticosteroids, to treat severe COVID-19 (Figure 1). This combined treatment has demonstrated therapeutic effectiveness in our patient. Especially, the patient is currently in good health without any sequelae of GBS and post-COVID symptoms during his regular follow-up at our medical center. Although TPE, a therapeutic procedure used to eliminate antibodies and other potentially detrimental factors from the bloodstream (36), was the treatment option for patients with GBS before the COVID-19 pandemic, TPE may be used in COVID-19-induced GBS associated with bradycardia. In patients with severe COVID-19, TPE might be considered an efficient therapy for reducing the risk of cytokine storm-induced ARDS as it might reduce the inflammatory cytokines (including IL-6) and acute phase proteins (ferritin and CRP). This could help in improving tissue oxygenation and reducing the risk of hypercoagulation and improve tissue oxygenation and especially fatal cardiovascular events (37, 38).

Finally, the main limitation of this case report is the lack of other specific tests, such as electrophysiologic analysis, to confirm the diagnosis of GBS (39). It could not be performed on this patient due to the overcrowding of the local hospitals during the 4th wave of the COVID-19 pandemic in Vietnam (July–November 2021). Especially, at that moment, the mentioned ICU department held 125 patients with severe COVID-19 per day and more than half of them with mechanical ventilation, which induced the lack of medical staff for doing some specific tests in patients with COVID-19. Another possible limitation of this case report might be due to other potential causes of bradycardia that could not be eliminated in the reported patient (40–44).

Conclusion

COVID-19 remains a critical health problem worldwide. Encouragingly, severe cases of COVID-19 have been significantly reduced after implementing national and international COVID-19 vaccination campaigns. This case report suggests that, in a patient with severe COVID-19 complicated by GBS associated with bradycardia, early treatment with therapeutic plasma exchange

combined with standard therapy for COVID-19 may improve the outcome of the patient.

Data availability statement

The raw data supporting the conclusions of this article will be made available by the authors, without undue reservation.

Ethics statement

The studies involving human participants were reviewed and approved by Binh Duong General Hospital. The patients/participants provided their written informed consent to participate in this study.

Author contributions

The literature search was done by SD-Q, DH-T-A, QT-X, TN-Q, TN-T-K, TN-C, and TT-N-A, with significant contributions from NN-V-H, MD-T-T, TT-T-T, KB-D, TH-A, TN-N-P, and VN-N. Data collection was done by SD-Q, DH-T-A, QT-X, TN-Q, TN-T-K, TN-C, TT-N-A, NN-V-H, MD-T-T, and TT-T-T. SD-Q, QT-X, and DH-T-A drafted the manuscript, with significant contributions by TN-Q, TN-T-K, TN-C, TT-N-A, NN-V-H, MD-T-T, TT-T-T, KB-D, TH-A, and TN-N-P. All authors contributed equally to analyzing and interpreting the data in the case report.

Acknowledgments

The authors would like to thank Mrs. Hien-Pham-Thi-Minh, an English teacher at LMC, and Mr. Chandat Phan—Penn State University College of Medicine—for the English revision of the manuscript.

Conflict of interest

The authors declare that the research was conducted in the absence of any commercial or financial relationships that could be construed as a potential conflict of interest.

Publisher's note

References

1. Agosti E, Giorgianni A, Francesco D, Vinacci G, Balbi S, Locatelli D. Is Guillain-Barré syndrome triggered by SARS-CoV-2? Case report and literature review. *Neurol Sci.* (2021) 42:607–12. doi: 10.1007/s10072-020-04553-9

2. Elzouki AN, Osman MAM, Ahmed MAE, et al. COVID-19 infection presented as Guillain-Barré Syndrome: Report of two new cases and review of 116 reported cases and case series. *Travel Med Infect Dis.* (2021) 44:102169. doi: 10.1016/j.tmaid.2021.102169

3. Abrams RMC, Kim BD, Markantone DM, Reilly K, Paniz-Mondolfi AE, Gitman MR, et al. Severe rapidly progressive Guillain-Barré syndrome in the setting of acute COVID-19 disease. *J Neurovirol.* (2020) 26:797–9. doi: 10.1007/s13365-020-00884-7

4. Alberti P, Beretta S, Piatti M, Karantzoulis A, Piatti ML, Santoro P, et al. Guillain-Barré syndrome related to COVID-19 infection: case report. *Journal of Neurol Neuroimmunol Neuroinflamml.* (2020) 7:e741. doi: 10.1212/NXI.0000000000000741

5. Arnaud S, Budowski C, Tin SNW, Degos B. Post SARS-CoV-2 Guillain-Barré syndrome: case report. *Clin Neurophysiol.* (2020) 131:1652–4. doi: 10.1016/j.clinph.2020.05.003

6. Assini A, Benedetti L, Di Maio S, Schirinzi E, Del Sette M. New clinical manifestation of COVID-19 related Guillain-Barrè syndrome highly responsive to intravenous immunoglobulins: two Italian cases. *Neurol Sci.* (2020) 41:1657–8. doi: 10.1007/s10072-020-04484-5

7. Bigaut K, Mallaret M, Baloglu S, Nemoz B, Morand P, Baicry F, et al. Guillain-Barré syndrome related to SARS-CoV-2 infection. *Neurol Neuroimmunol Neuroinflamm.* (2020) 7:e785. doi: 10.1212/NXI.0000000000000785

8. Bracaglia M, Naldi I, Govoni A, Ventura DB, De Massis P. Acute inflammatory demyelinating polyneuritis in association with an asymptomatic infection by SARS-CoV-2. *J Neurol.* (2020) 267:3166–8. doi: 10.1007/s00415-020-10014-2

9. Börü ÜT, Toksoy CK, Bölük C, Demibras H, Yilmaz AC. A case of guillain-barré syndrome related to COVID-19 infection. *Int J Neurosci.* (2021) 12:1–3. doi: 10.1080/00207454.2021.1886097

10. Bueso T, Montalvan V, Lee J, et al. Guillain-Barre syndrome and COVID-19: a case report. *Clin Neurol Neurosurg.* (2021) 200:106413. doi: 10.1016/j.clineuro.2020.106413

11. Caress JB, Castoro RJ, Simmons Z, et al. COVID-19 – associated Guillain-Barré syndrome: The early pandemic experience. *Muscle Nerve.* (2020) 62:485–91. doi: 10.1002/mus.27024

12. Chakraborty N, Kumar H. Intravenous immunoglobulin may reverse multisystem inflammation in COVID-19 pneumonitis and Guillain-Barré syndrome. *Indian J Crit Care Med.* (2020) 24:1264–8. doi: 10.5005/jp-journals-10071-23688

13. Chan JL, Ebadi H, Sarna JR. Guillain-Barré syndrome with facial diplegia related to SARS-CoV-2 infection. *Can J Neurol Sci.* (2020) 47:852–4. doi: 10.1017/cjn.2020.106

14. Chan M, Han SC, Kelly S, Tamimi M, Giglo B, Lewis A, et al. case series of Guillain barré syndrome following covid-19 infection in New York. *Neurol Clin Pract.* (2021) 11:e576–8. doi: 10.1212/CPJ.0000000000000880

15. Coen M, Jeanson G, Culebras Almeida LA, Hübers A, Stierlin F, et al. Guillain-Barré syndrome as a complication of SARS-CoV-2 infection. *Brain Behav Immun.* (2020) 87:111–2. doi: 10.1016/j.bbi.2020.04.074

16. Colonna S, Sciumé L, Giarda F, Innocenti A, Beretta G, Costa DD. Case Report: Postacute rehabilitation of Guillain-Barré syndrome and cerebral vasculitis-like pattern accompanied by SARS-CoV-2 infection. *Front Neurol.* (2021). doi: 10.3389/fneur.2020.602554

17. Defabio AC, Scott TR, Stenberg RT, Simon EL. Guillain-Barré syndrome in a patient previously diagnosed with COVID-19. *Am J Emerg Med.* (2020) 45:154–5. doi: 10.1016/j.ajem.2020.07.074

18. Duong-Quy S, Huynh-Truong-Anh D, Nguyen-Thi-Kim T, et al. Guillain-Barré syndrome in patient with SARS-CoV-2 PCR positivity treated successfully with therapeutic exchange plasma: a first case report from Vietnam. *Front Neurol.* (2022) 13:868667. doi: 10.3389/fneur.2022.868667

19. Farzia MA, Ayromloua H, Jahanbakhshb N, Bavil PH, Janzadeh A, Shayan FK. Guillain-Barré syndrome in a patient infected with SARS-CoV-2, a case report. *J Neuroimmunol.* (2020) 346:577294. doi: 10.1016/j.jneuroim.2020.577294

20. Gale A, Sabaretnam S, Lewinsohn A. Guillain-Barré syndrome and COVID-19: association or coincidence. *BMJ Case Rep.* (2020) 13:e239241. doi: 10.1136/bcr-2020-239241

21. Galán AV, Del Saz Saucedo P, Postigo FP, Paniagua EB. Guillain-Barré syndrome associated with SARS-CoV-2 infection. *Neurologia (Engl End).* (2020) 35:268–9. doi: 10.1016/j.nrl.2020.04.007

22. Hirayama T, Hongo Y, Kaida K, Kano O. Guillain-Barré syndrome after COVID-19 in Japan. *BMJ Case Rep.* (2020) 13:e239218. doi: 10.1136/bcr-2020-239218

23. Khan F, Sharma P, Pandey S, Sharma D, V V, Kumar N, et al. COVID-19-associated Guillain-Barré syndrome: Postinfectious alone or neuroinvasive too? *J Med Virol.* (2021) 93:6045–9. doi: 10.1002/jmv.27159

24. Lampe A, Winschel A, Lang C, Steiner T. Guillain-Barré syndrome and SARS-CoV 2. *Neurol Res Pract.* (2020) 2:19. doi: 10.1186/s42466-020-00066-0

25. Zhao H, Shen D, Zhou H, Liu J, Chen S. Guillain-Barré syndrome associated with SARS-CoV-2 infection: causality or coincidence? *Lancet Neurol.* (2020) 19:383–4. doi: 10.1016/S1474-4422(20)30109-5

26. Wang D, Hu B, Hu C, Zhu F, Liu X, Zhang J, et al. Clinical characteristics of 138 hospitalized patients with 2019 novel coronavirus-infected pneumonia in Wuhan. *China JAMA*. (2020) 323:1061. doi: 10.1001/jama.2020.1585

27. Goyal P, Choi JJ, Pinheiro LC, Schenck EJ, Chen R, Jabri A, et al. Clinical characteristics of Covid-19 in New York City. *N Engl J Med.* (2020) 382:2372–4. doi: 10.1056/NEJMc2010419

28. Peigh G, Leya MV, Baman JR, Cantey EP, Knight BP, Flaherty JD. Novel coronavirus 19 (COVID-19) associated sinus node dysfunction: a case series. *Eur Heart J Case Rep.* (2020) 4:1–6. doi: 10.1093/ehjcr/ytaa132

29. European Medicine Agency 2021. *COVID-19 Vaccine Janssen: Guillain-Barré Syndrome Listed as a Very Rare Side Effect*. Available online at: https://www.ema.europa.eu/en/news/covid-19-vaccine-janssen-guillain-barre-syndrome-listed-very-rare-side-effect

30. Kaur RJ, Dutta S, Charan J, Bhardwaj P, Tandon A, Yadav D, et al. Cardiovascular adverse events reported from COVID-19 vaccines: a study based on WHO database. *Int J Gen Med.* (2021) 14:3909–27. doi: 10.2147/IJGM.S324349

31. Flachenecker P, Toyka KV, Reiners K. Cardiac arrhythmias in Guillain-Barre syndrome. An overview of the diagnosis of a rare but potentially life-threatening complication. *Nervenarzt.* (2001) 72:610–7. doi: 10.1007/s001150170060

32. Mukerji S, Aloka F, Farooq MU, Kassab MY, Abela GS. Cardiovascular complications of the Guillain-Barré syndrome. *Am J Cardiol.* (2009) 104:1452–5. doi: 10.1016/j.amjcard.2009.06.069

33. Rodnitzky RL, Goeken JA. Complications of Plasma Exchange in Neurological Patients. *Arch Neurol.* (1982) 39:350–4. doi: 10.1001/archneur.1982.00510180028007

34. Szczeklik W, Wawrzycka K, Włudarczyk A, Sega A, Nowak I, Seczyńska B, et al. Complications in patients treated with plasmapheresis in the intensive care unit. *Anaesthesiol Intensive Ther.* (2013) 45:7–13. doi: 10.5603/AIT.2013.0002

35. Tombak A, Uçar MA, Akdeniz A. Therapeutic plasma exchange in patients with neurologic disorders: review of 63 cases. *Indian J Hematol Blood Transfus.* (2017) 33:97–105. doi: 10.1007/s12288-016-0661-3

36. Raphael JC, Chevret S, Hughes RAC, Annane D. Plasma exchange for Guillain-Barré syndrome. *Cochrane Database Syst Rev.* (2012) 7:CD001798. doi: 10.1002/14651858.CD001798.pub2

37. Duong-Quy S, Huynh-Truong-Anh D, Nguyen-Thi-Kim T, Nguyen-Quang T, Nguyen-Chi T, Nguyen-Thi-Y Net al. The use of therapeutic plasma exchange in the treatment of a pregnant woman with COVID-19 induced acute respiratory distress syndrome. *Pulm Ther.* (2022) 8:233–40. doi: 10.1007/s41030-022-00188-7

38. Zaid I, Essaad O, El Aidouni G, Aabdi M, Berrichi S, Taouihar S, et al. Therapeutic plasma exchange in COVID-19 pnemonia in intensive care unit: Cases series. *Ann Med Surg.* (2021) 71:102920. doi: 10.1016/j.amsu.2021.102920

39. Rumeileh SA, Abdelhak A, Foschi M, Tumani H, Otto M. Guillain-Barré syndrome spectrum associated with COVID-19: an up-to-date systematic review of 73 cases. *J Neurol.* (2021) 268:1133–70. doi: 10.1007/s00415-020-10124-x

40. Plasma Exchange/ Sandoglobulin Guillain-Barré Syndrome Trial Group. Randomised trial of plasma exchange, intravenous immunoglobulin, and combined treatments in Guillain-Barré syndrome. *Lancet*. (1997) 349:225–60. doi: 10.1016/S0140-6736(96)09095-2

41. Verboon C, van Doorn PA, Jacobs BC. Treatment dilemmas in Guillain-Barré syndrome. *J Neurol Neurosurg Psychiatry.* (2017) 88:346–52. doi: 10.1136/jnnp-2016-314862

42. Wilison HJ, Jacobs BC, A van Doorn P. Guillain-Barré syndrome. *Lancet.* (2016) 388:717–27. doi: 10.1016/S0140-6736(16)00339-1

43. Kilinc D, van de Pasch S, Doets AY, Jacobs BC, van Vliet J, Garssen MPJ. Guillain Barré syndrome after SARS-CoV-2 infection. *Eur J Neurol.* (2020) 27:1757–8. doi: 10.1111/ene.14398

44. Korem S, Gandhi H, Dayag DB. Guillain-Barré syndrome associated with COVID-19 disease. *BMJ Case Rep*. (2020) 13:e237215. doi: 10.1136/bcr-2020-237215

frontiers | Frontiers in Cardiovascular Medicine

TYPE Case Report
PUBLISHED 23 February 2023
DOI 10.3389/fcvm.2023.1088697

OPEN ACCESS

EDITED BY
Masateru Takigawa,
Tokyo Medical and Dental University, Japan

REVIEWED BY
Jean-benoît Le Polain de Waroux,
AZ Sint-Jan Brugge-Oostende AV, Belgium
Alexander H. Maass,
University Medical Center Groningen,
Netherlands

*CORRESPONDENCE
Matteo Santamaria
✉ matteo.santamaria@gemellimolise.it

SPECIALTY SECTION
This article was submitted to
Cardiac Rhythmology,
a section of the journal
Frontiers in Cardiovascular Medicine

RECEIVED 03 November 2022
ACCEPTED 31 January 2023
PUBLISHED 23 February 2023

CITATION
De Innocentiis C, Astore P, Buonpane A, Santamaria AP, Patragnoni F and Santamaria M (2023) Case report: An unusual case of phrenic nerve stimulation in a patient with single chamber implantable cardioverter defibrillator.
Front. Cardiovasc. Med. 10:1088697.
doi: 10.3389/fcvm.2023.1088697

Case report: An unusual case of phrenic nerve stimulation in a patient with single chamber implantable cardioverter defibrillator

Carlo De Innocentiis[1], Pasquale Astore[1], Angela Buonpane[2], Antonia Pia Santamaria[3], Francesco Patragnoni[4] and Matteo Santamaria[1]*

[1]Arrhythmology and Electrophysiology Unit, Gemelli Molise Hospital, Campobasso, CB, Italy, [2]Agostino Gemelli IRCCS University Hospital Foundation, Rome, Italy, [3]Cardiac Rehabilitation Unit, Gemelli Molise Hospital, Campobasso, CB, Italy, [4]Medtronic Italia, Milan, Italy

Background: Phrenic nerve stimulation is a well-recognized complication related to cardiac implantable electronic devices, in particular with left ventricular coronary sinus pacing leads for cardiac resynchronization therapy.

Case presentation: We report an unusual case of symptomatic phrenic nerve stimulation due to inadvertent placement of a right ventricular defibrillation lead in coronary sinus posterior branch in a patient with heart failure with reduced ejection fraction with a recently implanted single-chamber cardioverter defibrillator.

Discussion: Phrenic nerve stimulation is a relatively common complication of left ventricular pacing. Inadvertent placement of a right ventricular lead in a coronary sinus branch is a rare but possible cause of phrenic nerve stimulation. Careful evaluation of intraprocedural fluoroscopic and electrocardiographic appearance of pacing and defibrillation leads during implantation may prevent inadvertent placement of a right ventricular lead in the coronary sinus.

KEYWORDS

phrenic nerve stimulation, cardiac implantable electronic devices, implantable cardioverter defibrillator, cardiac resynchronization therapy, case report

Introduction

Phrenic nerve stimulation (PNS) may complicate up to 30% of cardiac implantable electronic devices (CIEDs) implantation procedures, mainly cardiac resynchronization therapy (CRT) with left ventricular pacing, due to the anatomic contiguity of phrenic nerve to left ventricle lateral wall (1). Although its clinical relevance is limited to a minority of cases, PNS may be responsible for significant symptoms with reduced quality of life and CRT failure (2, 3). Here we report a case of highly symptomatic PNS after single-chamber implantable cardioverter defibrillator (ICD) implantation in a patient with heart failure with reduced ejection fraction (HFrEF).

10.3389/fcvm.2023.1088697

Case presentation

A 68-year-old Caucasian male was referred to our Arrhythmology and Electrophysiology Unit for lead revision of a single-chamber ICD implanted ten months earlier in another center. Two months before ICD implantation, the patient was hospitalized for symptomatic heart failure, NYHA class 3. A 12-lead ECG showed atrial fibrillation (AF) with rapid ventricular response. A transthoracic echocardiography (TTE) demonstrated reduced left ventricular ejection fraction (LVEF, 30%) and severe left atrial enlargement without significant valvular disease. An invasive coronary angiography (ICA) showed multivessel coronary artery disease (MVCAD) with a low Syntax score. Myocardial revascularization with percutaneous coronary intervention (PCI) and two drug-eluting stents (DES) implantation in the left anterior descendent (LAD) coronary artery and the obtuse marginal branch of the left circumflex was performed without complication. The patient was discharged on heart failure and rate-control therapy with a beta-blocker (bisoprolol 5 mg bid), an angiotensin receptor-neprilysin inhibitor (ARNI, sacubitril/valsartan 49/51 mg bid), a mineralocorticoid receptor antagonist (MRA), a loop diuretic, and digoxin (0.125 mg qd). After two months, because of persistent severe left ventricular systolic dysfunction, a single-chamber ICD with a single-coil passive fixation lead was implanted for primary prevention of sudden cardiac death (SCD). During subsequent follow-up, the patient was referred to our center for symptomatic PNS. At admission, the patient presented with mild dyspnea and mild ankle swelling. Blood tests were in the range of normality except for increased levels of N-terminal pro-B-type natriuretic peptide (NT-proBNP, 1,230 pg/ml, nr <125 pg/ml). Device control showed an excessive ventricular pacing percentage (about 15%) although ICD programming in VVI mode with a lower rate of 30 beats per minute, indicating phases of slow ventricular response with the necessity of ventricular pacing. PNS at very low energy output was also confirmed. Several symptomatic

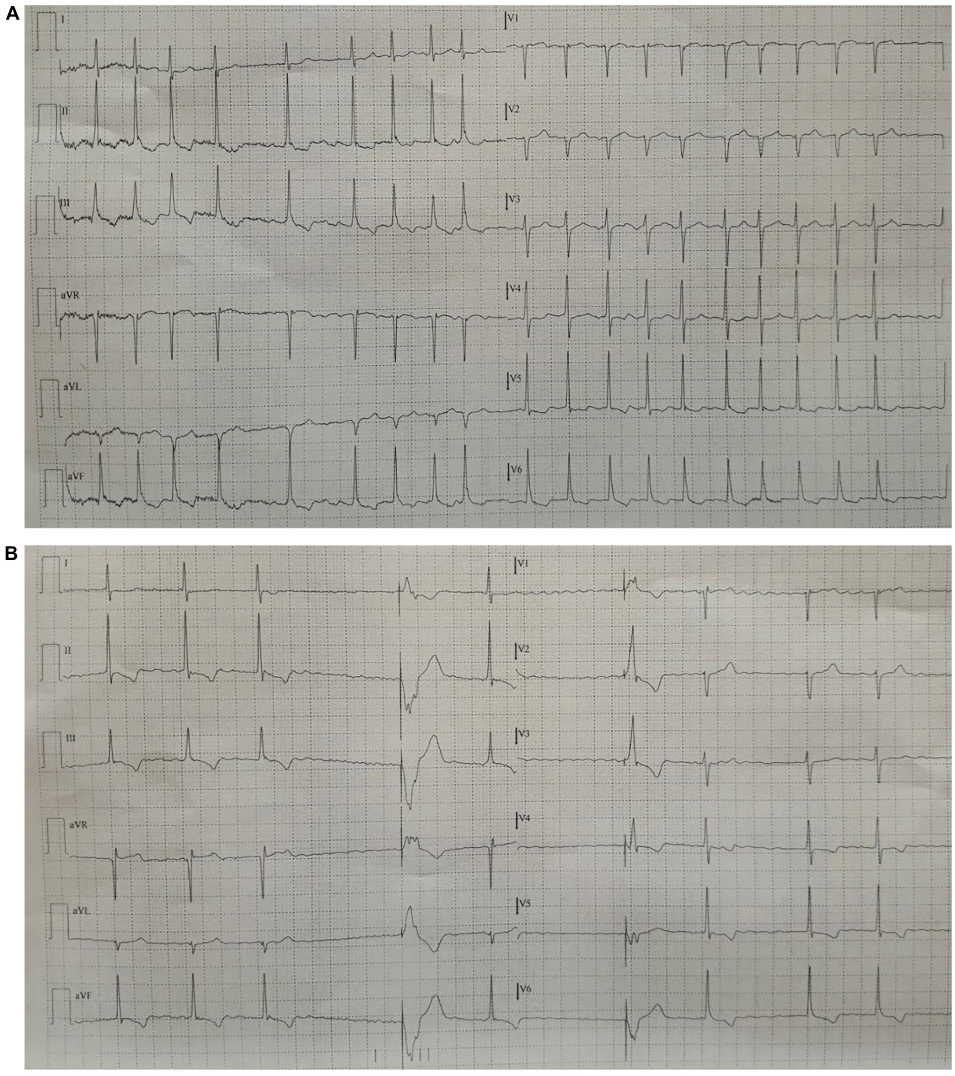

FIGURE 1
(A) 12-lead ECG at admission showing AF with rapid ventricular response despite rate-control therapy. **(B)** 12-lead ECG showing phases of AF with slow ventricular response with ventricular pacing at the lower rate (ICD in VVI 30). Note the morphology of the paced QRS with RBBB pattern, superior axis with R pattern in aVR. AF, atrial fibrillation; ICD, implantable cardioverter defibrillator; RBBB, right bundle branch block.

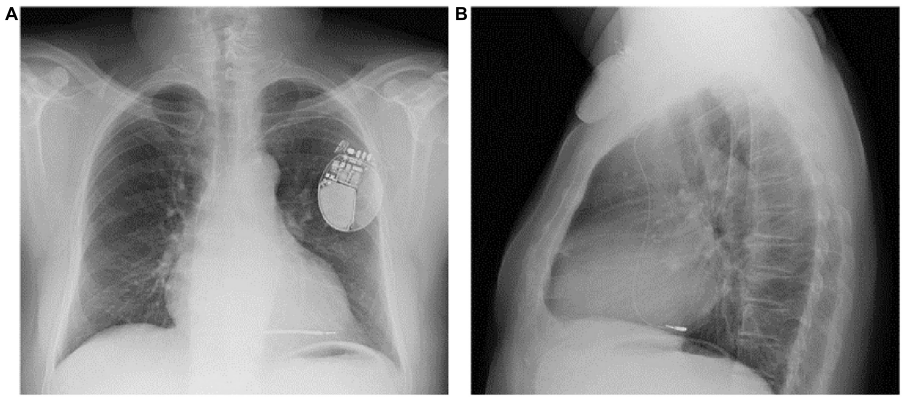

FIGURE 2
PA **(A)** and LL **(B)** chest x-ray of the patient showing inadvertent lead placement in the posterior branch of the coronary sinus. PA, posteroanterior; LL, laterolateral.

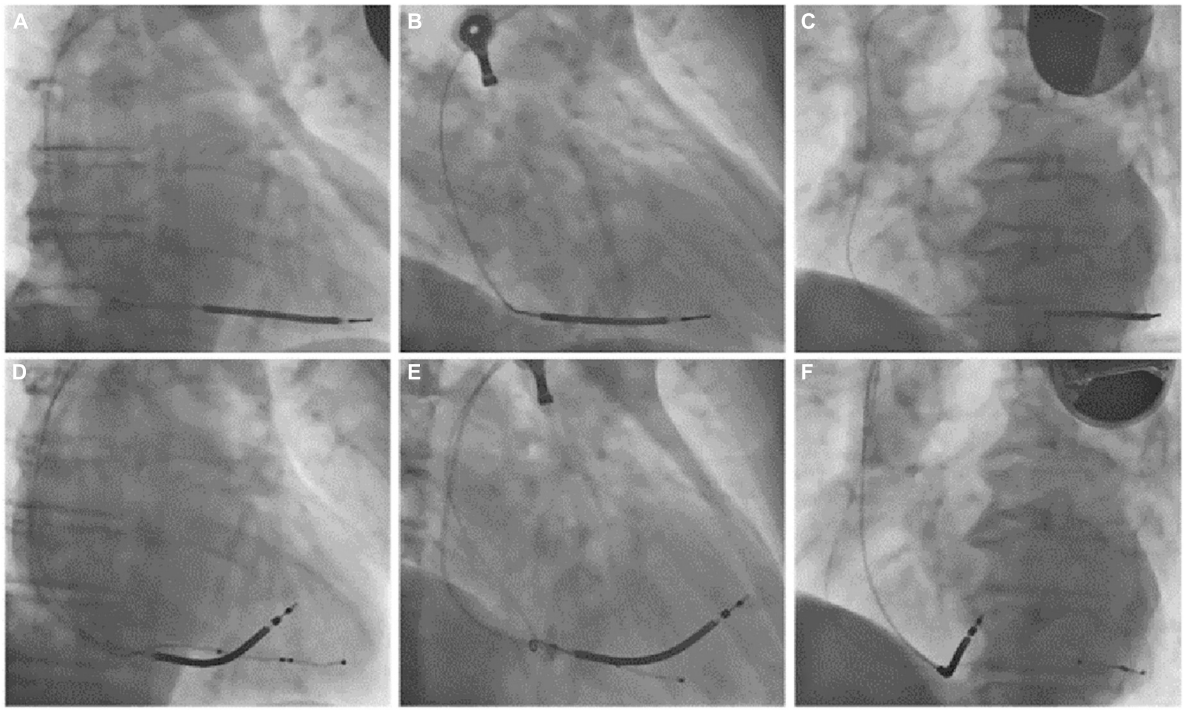

FIGURE 3
(Superior row) PA **(A)**, RAO 30° **(B)**, and LAO 45° **(C)** fluoroscopic views of the previously implanted single chamber cardioverter defibrillator with a single coil passive fixation defibrillation lead. (Inferior row) PA **(D)**, RAO 30° **(E)**, and LAO 45° **(F)** fluoroscopic views after lead extraction and the reimplantation of a new single-coil active fixation defibrillation lead on the mid portion of the interventricular septum and a coronary sinus quadripolar passive fixation lead for cardiac resynchronization therapy. PA, posteroanterior; RAO, right anterior oblique; LAO, left anterior oblique.

episodes of high ventricular rate (HVR) indicated an unsatisfactory pharmacological rate-control despite maximum tolerated drug dosage. Lead parameters were in the range of normality with a normal trend, thus excluding lead failure due to fracture or insulation defect. A 12-lead ECG showed AF with rapid ventricular response and normal QRS duration (90 ms) (**Figure 1A**). Unfortunately, a 12-lead ECG during ventricular pacing was not recorded before admission, however it was obtained during hospital stay from continuous ECG monitoring (**Figure 1B**). Paced QRS morphology showed a right bundle branch block (RBBB) pattern and superior axis. A chest X-ray (CXR) was obtained at admission (**Figure 2**). CXR showed a single-coil passive fixation defibrillation lead placed in coronary sinus posterior branch, thus explaining occasional PNS. Interestingly, the patient previously underwent two other CXR examinations but the incorrect lead placement was not recognized. A TTE was repeated and reduced LVEF without visualization of defibrillation lead in the right ventricle, in the absence of pericardial effusion, was confirmed. Lead explantation and CRT implantation for both high ventricular pacing percentage and predictable subsequent atrioventricular

10.3389/fcvm.2023.1088697

TABLE 1 Timeline.

Date	Event
12 months prior to admission	HFrEF.
	MVCAD treated with PCI.
	AF with rapid ventricular response.
10 months prior to admission	Single chamber ICD implantation for HFrEF and rate-control therapy.
	Symptomatic PNS during follow-up.
Day 1 admission	Hospital admission for lead revision for symptomatic PNS.
	Radiographic and electrocardiographic evidence of inadvertent lead placement in a coronary sinus branch.
	AF with both slow and rapid ventricular response.
Day 2 admission	Lead explantation and CRT-D implantation for both AF with slow ventricular response and subsequent "ablate-and-pace" therapy.
Day 3 admission	Hospital discharge with planned AVJ ablation for "ablate-and-pace" therapy.

AF, atrial fibrillation; AVJ, atrioventricular junction; CRT-D, cardiac resynchronization therapy-defibrillator; HFrEF, heart failure with reduced ejection fraction; ICD, implantable cardioverter defibrillator; MVCAD, multivessel coronary artery disease; PNS, phrenic nerve stimulation.

junction (AVJ) ablation for "ablate-and-pace" therapy were planned, because of reported suboptimal rate-control in patient history (alternance of slow and rapid ventricular response). A venogram was performed in order to confirm subclavian vein patency. A successful lead explantation with simple gentle traction using a non-locking stylet was performed. At the same time, we performed implantation of a CRT device with a single-coil active fixation defibrillation lead placed in the mid-ventricular septum, and a quadripolar passive fixation lead in coronary sinus posterior branch (the only available, **Figure 3**). The LV quadripolar lead was tested for PNS that was absent in pacing configurations excluding distal electrode, with optimal pacing threshold. Bedside echocardiographic examination ruled-out pericardial effusion. The patient was discharged the day after the procedure, and AVJ ablation was postponed after rate control evaluation at subsequent follow-up (**Table 1**).

Discussion

Phrenic nerve stimulation is a potential CIEDs complication, particularly in case of CRT with left ventricular pacing, due to the anatomic contiguity of the phrenic nerve to the lateral wall of the left ventricle. Direct diaphragmatic stimulation has also been hypothesized for LV pacing leads. PNS was more familiar with unipolar and bipolar coronary sinus leads due to the limited number of pacing configurations with such leads (3, 4). Contemporary quadripolar leads have markedly improved PNS management (5–8). However, in our patient, PNS was related to single-chamber ICD, a less common event. PNS after non-CRT devices implantation was previously reported following RVOT pacing (9) and as a consequence of lead fracture in subclavian crush syndrome (10). We excluded lead failure with fracture or insulation defect because lead parameters were in the range of normality. We excluded ventricular perforation for the same reason and for the absence of pericardial effusion. Therefore, we suspected inadvertent and erroneous lead malposition in a coronary sinus branch, confirmed by CXR. The 12-lead ECG obtained during hospital stay showed a RBBB with superior axis morphology of the paced QRS complexes further corroborating CXR findings (**Figure 1B**). The exact incidence of inadvertent lead malposition during CIEDs implantation remain unknown and is probably underestimated. A retrospective observational study reported an estimated incidence of inadvertent lead malposition of about 0.3% mainly due to endocardial left ventricular pacing

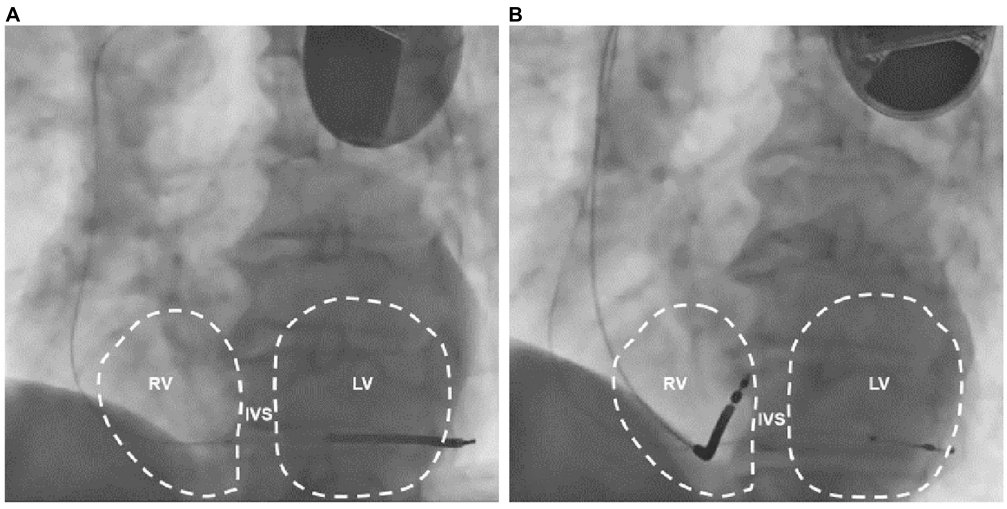

FIGURE 4
LAO 45° fluoroscopic views of the previously implanted single chamber cardioverter defibrillator **(A)** and the subsequently implanted biventricular cardioverter defibrillator **(B)**. Note that in A the defibrillation lead crosses the midline toward the left ventricle. LAO: left anterior oblique; RV, right ventricle; IVS, interventricular septum; LV, left ventricle.

through a patent foramen ovale (PFO), an atrial septal defect (ASD), or inadvertent arterial cannulation (11). A misplaced lead in a coronary sinus branch was the cause of inadvertent lead malposition in only one patient in the study cohort. Our case demonstrates the importance of accurate intraprocedural fluoroscopic and electrocardiographic evaluation of pacing and defibrillation leads during CIEDs implantation, and the necessity of specific training of radiologists in the evaluation of CIEDs related CXR. Anterior oblique fluoroscopic views during CIEDs implantation, particularly left anterior oblique (LAO) view, may prevent the inadvertent placement of a right ventricular lead in the coronary sinus (**Figure 4**).

Conclusion

The present case highlights the importance of early recognition of inadvertent placement of a right ventricular lead in a coronary sinus branch, mainly the middle cardiac vein or a posterior branch.

Such complication may be avoided with a careful fluoroscopic and electrocardiographic procedural examination. Both cardiologists and radiologists should be trained to interpret CIEDs' fluoroscopic appearance. Inadvertent placement of a right ventricular lead in a coronary sinus branch should always be considered in the case of PNS after single or dual chamber pacemaker or ICD implantation.

Data availability statement

The original contributions presented in this study are included in the article/supplementary material, further inquiries can be directed to the corresponding author.

Ethics statement

Written informed consent was obtained from all participants for their participation in this study. Written informed consent was obtained from the individual(s) for the publication of any potentially identifiable images or data included in this article.

Author contributions

CD drafted the manuscript. PA, AB, AS, FP, and MS revised it critically for important intellectual content and given final approval of the version to be published. All authors have been directly involved in patient care, have undertaken patient investigations, and agreed to be accountable for all aspects of the work in ensuring that questions related to the accuracy or integrity of any part of the work are appropriately investigated and resolved.

Conflict of interest

The authors declare that the research was conducted in the absence of any commercial or financial relationships that could be construed as a potential conflict of interest.

Publisher's note

All claims expressed in this article are solely those of the authors and do not necessarily represent those of their affiliated organizations, or those of the publisher, the editors and the reviewers. Any product that may be evaluated in this article, or claim that may be made by its manufacturer, is not guaranteed or endorsed by the publisher.

References

1. Goetze S, Defaye P, Bauer A, Merkel M, Bizeau O, Treusch S, et al. Phrenic nerve stimulation in CRT patients and benefits of electronic lead repositioning: the ERACE trial. *J Interv Card Electrophysiol.* (2013) 38:1–9. doi: 10.1007/s10840-013-9811-9

2. Biffi M, Exner D, Crossley G, Ramza B, Coutu B, Tomassoni G, et al. Occurrence of phrenic nerve stimulation in cardiac resynchronization therapy patients: the role of left ventricular lead type and placement site. *Europace.* (2013) 15:77–82. doi: 10.1093/europace/eus237

3. Biffi M, Moschini C, Bertini M, Saporito D, Ziacchi M, Diemberger I, et al. Phrenic stimulation: a challenge for cardiac resynchronization therapy. *Circ Arrhythm Electrophysiol.* (2009) 2:402–10. doi: 10.1161/CIRCEP.108.836254

4. Sardu C, Santamaria M, Funaro S, Sacra C, Barbieri M, Paolisso P, et al. Cardiac electrophysiological alterations and clinical response in cardiac resynchronization therapy with a defibrillator treated patients affected by metabolic syndrome. *Medicine (Baltimore).* (2017) 96:e6558. doi: 10.1097/MD.0000000000006558

5. Sardu C, Barbieri M, Santamaria M, Giordano V, Sacra C, Paolisso P, et al. Multipolar pacing by cardiac resynchronization therapy with a defibrillators treatment in type 2 diabetes mellitus failing heart patients: impact on responders rate, and clinical outcomes. *Cardiovasc Diabetol.* (2017) 16:75. doi: 10.1186/s12933-017-0554-2

6. Oswald H, Asbach S, Kobe J, Weglage H, Schulte-Pitzke B, Brachmann J. Effectiveness and reliability of selected site pacing for avoidance of phrenic nerve stimulation in CRT patients with quadripolar LV leads: the EffaceQ study. *Pacing Clin Electrophysiol.* (2015) 38:942–50. doi: 10.1111/pace.12664

7. Behar J, Bostock J, Zhu Li A, Chin H, Jubb S, Lent E, et al. Cardiac resynchronization therapy delivered via a multipolar left ventricular lead is associated with reduced mortality and elimination of phrenic nerve stimulation: long-term follow-up from a multicenter registry. *J Cardiovasc Electrophysiol.* (2015) 26:540–6. doi: 10.1111/jce.12625

8. Forleo G, Mantica M, Di Biase L, Panattoni G, Della Rocca D, Papavasileiou L, et al. Clinical and procedural outcome of patients implanted with a quadripolar left ventricular lead: early results of a prospective multicenter study. *Heart Rhythm.* (2012) 9:1822–8. doi: 10.1016/j.hrthm.2012.07.021

9. Sekihara T, Miyazaki S, Ishida T, Nagao M, Kakehashi S, Mukai M, et al. Phrenic nerve stimulation during right ventricular outflow tract pacing: a rare but possible complication. *J Cardiovasc Electrophysiol.* (2020) 31:3330–3. doi: 10.1111/jce.14760

10. Fujimori M, Sugimoto A, Shimizu T, Tamura T. Left phrenic nerve stimulation due to breakage of the endocardial right ventricular lead at the costoclavicular ligament. *J Arrhythm.* (2007) 23:250–4. doi: 10.1016/S1880-4276(07)80008-1

11. Ohlow M, Roos M, Lauer B, Von Korn H, Geller J. Incidence, predictors, and outcome of inadvertent malposition of transvenous pacing or defibrillation lead in the left heart. *Europace.* (2016) 18:1049–54. doi: 10.1093/europace/euv270

frontiers | Frontiers in Cardiovascular Medicine

TYPE Case Report
PUBLISHED 19 May 2023
DOI 10.3389/fcvm.2023.1143409

OPEN ACCESS

EDITED BY
Masateru Takigawa,
Tokyo Medical and Dental University, Japan

REVIEWED BY
Eduardo Sternick,
Biocor Institute, Brazil
Chin-Feng Tsai,
Chung Shan Medical University Hospital, Taiwan

*CORRESPONDENCE
Christopher V. DeSimone
✉ Desimone.Christopher@mayo.edu

RECEIVED 13 January 2023
ACCEPTED 28 April 2023
PUBLISHED 19 May 2023

CITATION
Raina A, Tan NY, Fatunde OA, Asirvatham SJ and DeSimone CV (2023) Case report: A case of perinodal atrial tachycardia and review of the relevant clinical anatomy surrounding the retroaortic node.
Front. Cardiovasc. Med. 10:1143409.
doi: 10.3389/fcvm.2023.1143409

Case report: A case of perinodal atrial tachycardia and review of the relevant clinical anatomy surrounding the retroaortic node

Anvi Raina[1], Nicholas Y. Tan[1], Olubadewa A. Fatunde[2], Samuel J. Asirvatham[1] and Christopher V. DeSimone[1]*

[1]Department of Cardiovascular Medicine, Mayo Clinic College of Medicine, Rochester, MN, United States, [2]Department of Cardiovascular Medicine, Mayo Clinic College of Medicine, Phoenix, AZ, United States

A 70-year-old female presented with incessant supraventricular tachycardia that was refractory to metoprolol and sotalol. ECG revealed a narrow complex tachycardia with a rate of 163 beats per minute with a short RP relationship. She had salvos of atrial tachycardia which led to a severe reduction in ejection fraction as noted on echocardiography and hemodynamic instability. An electrophysiological study was performed, and findings suggested this to be an atrial tachycardia with earliest activation in the perinodal area. Radiofrequency ablation was carried out along the septum and associated structures to surround this region including the right atrium, non-coronary sinus of Valsalva, and the left atrium (anterior wall outside of the right superior pulmonary vein) to isolate this area and surround the focus with ablation lesions. The patient has done well post-procedure and continues to do well without any recurrence on low-dose flecainide at 8 months.

KEYWORDS

perinodal atrial tachycardia, supraventricular tachycardia (SVT), retroaortic node, catheter ablation, electrophysiology study

Introduction

Perinodal atrial tachycardias (ATs) make up a minority of supraventricular tachycardia (SVT) cases and outcomes data on patients with this arrhythmia is limited to a few case reports and case series. Furthermore, ablation in this area can be challenging due to variations in atrial septal anatomy, difficulty with maintaining catheter contact, and proximity to the conduction system. It is critical for the electrophysiologist to appreciate the anatomy of the atrial septum and the potential arrhythmogenic role of the retroaortic node (RAN) in tachycardias originating from and around this region.

Case presentation

A 70-year-old female presented to the emergency department with recalcitrant palpitations and SVT. She noted a subacute onset of tachy-palpitations starting 2 months prior with accelerated frequency over the preceding week. She failed therapy with metoprolol and was admitted for sotalol loading given her symptoms. Her initial

Abbreviations
AT, Atrial tachycardia; AV, Atrioventricular; ms, milliseconds; SVT, Supraventricular tachycardia; bpm, beats per minute; RAN, retroaortic node.

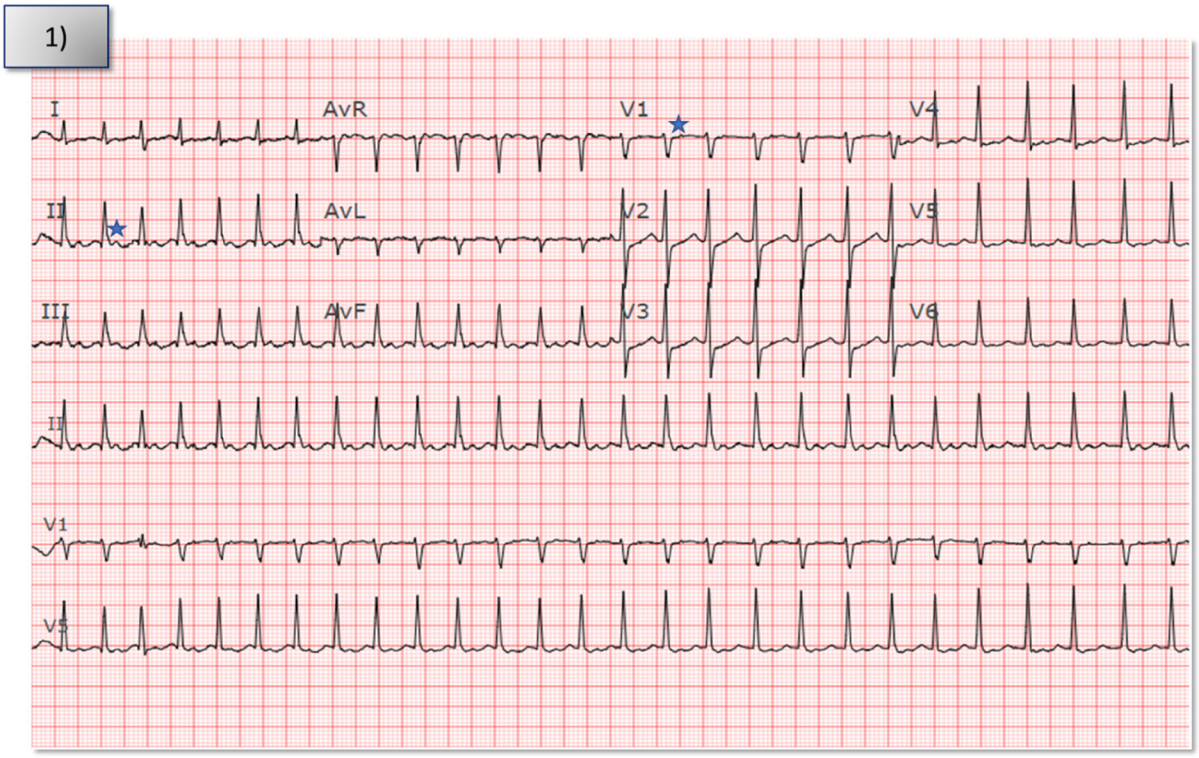

FIGURE 1
Index electrocardiogram from patient's presentation to the hospital showed narrow complex tachycardia with a short RP interval at a rate of 163 bpm. Star denotes *p* waves in V1 and lead II.

electrocardiogram showed a regular and narrow complex tachycardia with a rate of 163 bpm with a short RP relationship (**Figure 1**). The *p* wave morphology is biphasic in lead V1 (−/+), isoelectric in lead I, inferior directed axis, and narrower width when compared to sinus rhythm suggesting an origin in the atrial septum/perinodal region. The patient continued to have paroxysms of SVT during the hospitalization (other electrocardiograms and telemetry tracings shown in **Supplementary Figures S1A,B**). Echocardiography showed a preserved ejection fraction of 54% but a drastic decline in ejection fraction during with salvos of SVT. Given her symptoms, drop in ejection fraction during SVT, and failed drug therapy, she was offered an electrophysiologic study and ablation attempt.

Electrophysiologic study

Diagnostic catheters were placed in the high right atrium, coronary sinus, the bundle of His, and the right ventricle. At baseline, she had salvos of narrow complex tachycardia which were poorly tolerated hemodynamically. Initially, the earliest atrial signal appeared to be on the His catheter with an atrial cycle length of 300 milliseconds (ms) with 1:1 conduction to the ventricle. Changes in the atrial-atrial interval preceded and dictated changes in the ventricular-ventricular interval; this wobble in the atrial cycle length was suggestive of AT. Continued hemodynamic instability during tachycardia made further diagnostic maneuvers difficult to execute. Fine mapping was performed with a multi-polar catheter (OctaRay, Biosense Webster, Irvine, California) to map the earliest atrial electrograms. The earliest atrial signals were −27 ms ahead of the surface p wave and appeared to be along the septum, approximately 11:30 along the tricuspid annulus and around the superior limbus which appeared thick on imaging (**Figure 3A**).

Using an irrigated catheter (ThermoCool SmartTouch, Biosense Webster, Irvine, California), ablation was performed at the earliest site (**Figure 2A** shows electrograms during tachycarida, **Supplementary Figure S2A** shows same site during sinus rhythm) using radiofrequency energy of 30–40 Watts with 30 cc/minute flow for 30–90 s per lesion. We noted almost immediate suppression of the tachycardia with ablation (**Figure 3A** shows catheter position during ablation with intracardiac echocardiography; **Supplementary Figure S3A** shows corresponding fluoroscopic position). We then performed additional lesions around this region, in particular targeting the muscle bundle opposing the non-coronary aortic sinus of Valsalva and superior limbus. Despite extensive ablation around this area, the tachycardia continued with a similar cycle length.

We then performed mapping of the opposite side of the septum in the non-coronary sinus of Valsalva which was not particularly early. We did position our catheter slightly higher in order to be adjacent to the prior lesions from the right atrium and noted atrial electrograms −17 ms ahead of the surface *p* wave (**Figure 2B** shows

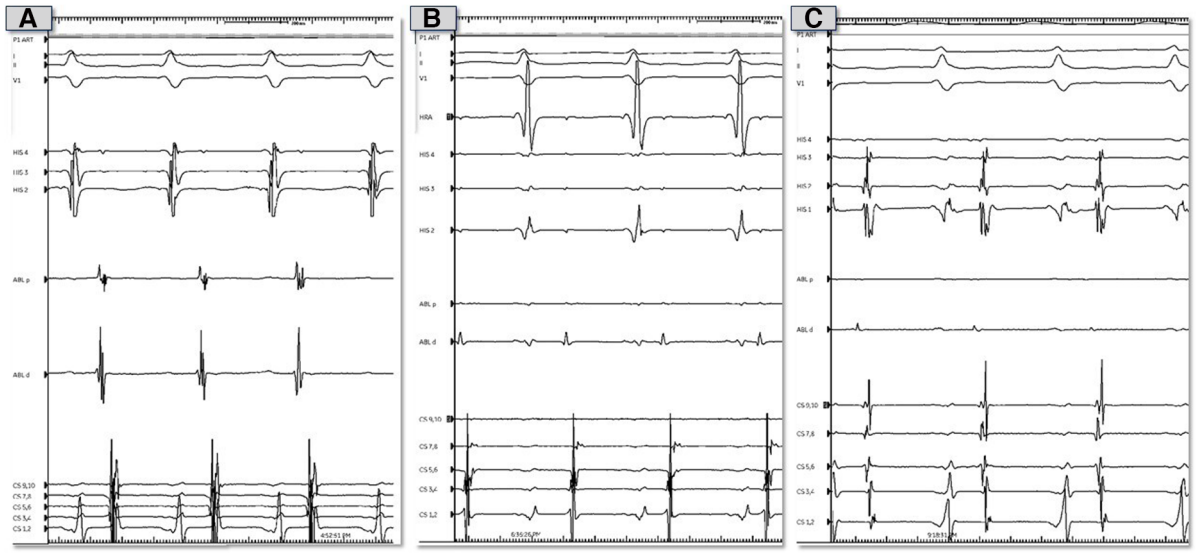

FIGURE 2
Representative electrocardiograms and intracardiac electrograms from electrophysiology study prior to ablation. (A) Tracings during tachycardia from theright atrial septum. (B) Tracings during tachycardia from the non-coronary sinus of Valsalva. (C) Tracings during tachycardia from the left atrial septum.

electrograms during tachycarida, **Supplementary Figure S2B** shows same site during sinus rhythm). Radiofrequency lesions were performed in this region at 30–40 Watts and 30 cc/min flow for 30–60 s per lesion (**Figure 3B** and **Supplementary Figure S3B** shows corresponding intracardiac echocardiography and fluoroscopic position of ablation catheter). Despite this, the tachycardia persisted, and we returned to the right atrium and performed additional radiofrequency ablation lesions in the same location along the septum as before. We noted transient suppression of tachycardia but afterwards we noted recurrence. Despite the use of a long sheath, some catheter movement was noted during ablation. To achieve better stability, we exchanged the radiofrequency ablation catheter for a cryoablation catheter (Medtronic CryoCath LP, Pointe-Claire, Canada), and created several lesions (freeze-thaw-freeze cycles to −80° Celsius for 3–4 min per lesion) along the superior limbus region. Despite initial suppression, AT recurred thereafter. This prompted transseptal access to map the left atrium. Mapping of the atrial septum was performed which revealed earlier (−29 ms relative to surface *p* wave) and fractionated signals near the left side of the superior limbus (**Figure 2C** shows electrograms during tachycarida, **Supplementary Figure S2C** shows same site during sinus rhythm) and close to the right superior pulmonary vein along the roof (directly adjacent to the area where right atrial ablation was performed). A series of ablation lesions were created using radiofrequency energy at 30–35 Watts and 30 cc/min flow for 30–60 s per lesion (**Figure 3C** shows corresponding ablation catheter position with intracardiac echocardiography; **Supplementary Figure S3C** shows corresponding fluoroscopic position). We noted temporary suppression and slowing of the tachycardia.

Given the extensive ablations already performed, we elected to end the procedure given the likelihood of automaticity from extensive ablation in the perinodal area. Immediately post-procedure she had salvos of SVT, prompting initiation of flecainide, metoprolol, and amiodarone bolus/drip overnight to allow the lesions and peri-ablation automaticity to settle. The patient recovered well from the procedure without any complications and was dismissed on flecainide and metoprolol.

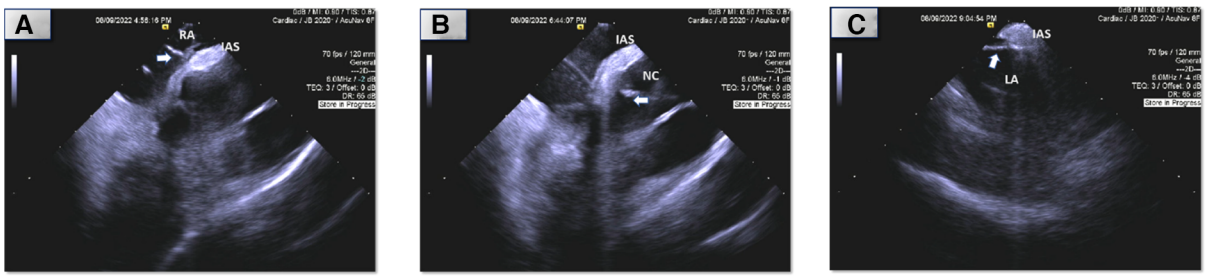

FIGURE 3
Intracardiac (ICE) echocardiography of ablation sites (arrow: ablation catheter, RA, right atrium; NC, non-coronary sinus of Valsalva; LA; atrial septum; IAS, interatrial septum). *Images are placeholders for videos which are attached. (A) Right atrial septum. (B) Non-coronary sinus of Valsalva. (C) Left atrial septum.

At her 3-month follow-up, she reported no further arrhythmia episodes and was tolerating flecainide without any ill effects and had reduced both flecainide and metoprolol dosing. At 8 months, she continues to do well without any recurrence and was offered to stop medications, but she preferred to stay on low doses given tolerance and improved symptoms as an added safeguard.

Discussion

We present a unique case of a 70-year-old female with recalcitrant SVT. The patient suffered from salvos of SVT which although short lived were poorly tolerated hemodynamically. Electrophysiologic study suggested perinodal AT to be the mechanism and ablation was carried out from the right atrium, non-coronary sinus of Valsalva, and the left atrium to consolidate lesions in the area of interest.

Relevant anatomy and arrhythmogenic role of the retroaortic node

The "true" atrial septum is limited to the floor of the fossa ovalis and its immediate muscular rims which are confluent with the apical portion of the triangle of Koch (1). This "true" or primum septum arises from the roof of the left side of the atrium and overhangs but does not reach the endocardial cushions. The roof of the right atrium then invaginates, resulting in an inner layer of adipose tissue between the myocardial layers, forming the septum secundum (2). After birth, left atrial pressure increases and pushes the septum primum against the septum secundum forming what we know clinically as the interatrial septum (3). The interatrial septum can serve as a potential arrhythmogenic focus for ATs and even facilitate tachycardias with intraseptal re-entry and atrial fibrillation (3). An increase in the thickness of the interatrial septum, often caused by fatty infiltration or fibrosis, is thought to be related to increased propensity for atrial arrhythmias (3, 4). Regardless, perinodal ATs remain a relatively less common focus accounting for 7%–13% of AT cases across different cases series (5–8).

Despite some clinical and animal studies on arrhythmias arising from the interatrial septum, little attention has been placed on the arrhythmogenic role of the RAN, a large remnant of the "atrioventricular (AV) ring" in the atrial septum. The AV rings and RAN are thought to be remnants of the AV canal. The RAN is composed of cardiomyocytes and is separated from the AV node by the antero-superior rim of the fossa ovalis and from the bundle of His by the membranous septum (9, 10). Its location within the antero-superior interatrial wall means that it does have potential continuity with the transitional cells of the AV node but is distinct from the compact node itself (9) (**Figure 4**).

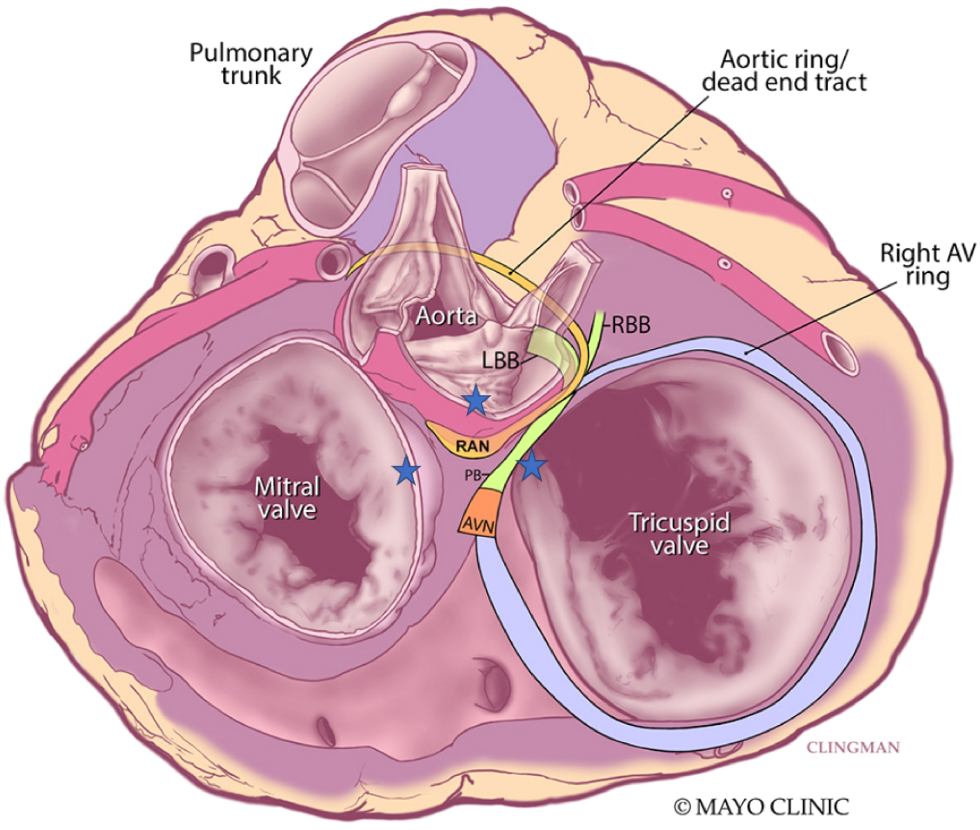

FIGURE 4
Superior view of the retroaortic node (RAN) and neighboring structures. Star represents vantage points of ablation to the area. AVN, atrioventricular node; PB, penetrating bundle; RBB, right bundle branch; LBB, left bundle branch. Adapted from Yanni et al. (14).

Electrophysiologic and molecular investigations of the RAN in animal studies suggest similar gene expression and ion channels as the compact AV node and point to its ability to serve as an ectopic source of ATs (11). Small clinical studies corroborate this notion with observations such as prompt termination of tachycardia with intravenous adenosine before production of AV block. In one such series of 43 patients, Bahora et al. (9) found all tachycardias (35/35) which were tested were found to be adenosine sensitive; the authors commented that this early termination was suggestive that the arrhythmic focus consists of node-like tissue but is distinct from the AV node itself. Clinical reports also suggest that the RAN may not respond to stress heating from radiofrequency ablation with automaticity (9, 12, 13). For ATs originating from this area, the right atrium offers a reasonable approach for ablation, although sometimes lesions need to be created from contiguous areas to "sandwich" the arrhythmic focus. The anterosuperior border of the fossa ovalis is marked by the non-coronary sinus of Valsalva and offers another vantage point for the proceduralist to approach perinodal ATs, including those tachycardias where the RAN may be implicated. While approaches from the right atrium and non-coronary sinus of Valsalva are well documented (12, 13), transeptal access and ablation of the left atrial septum must be considered in some patients where the septum is thicker, contact is not ideal, or atrial electrograms are not as early from the non-coronary sinus of Valsalva (**Figure 4**). In our case, ablation lesions were created from all three vantage points.

We must acknowledge some limitations in our case. Early termination of tachycardia in response to adenosine can be a clue for perinodal ATs. Unfortunately, due to the short-lived nature and hemodynamic instability of the tachycardia we were not able to test the effect of adenosine on the tachycardia in our patient. While cases of perinodal AT can be facile with ablation and termination from the right atrium or non-coronary sinus of Valsalva alone, we hope this report highlights a difficult case where different vantage points and energy sources had to be utilized. The use of unipolar recordings to corroborate the site of ablation could also be considered but was not done in our case. Lastly, the patient did have a short-lived episode of SVT post-procedure but has done well since suggesting durable lesion formation and the transient episode to be likely peri-ablation automaticity.

Conclusion

Perinodal ATs are an infrequent cause of SVT, especially with a robust decline in ejection fraction, and have unique electrocardiographic characteristics. Understanding the anatomy of the atrial septum and the potential arrhythmogenic role of the retroaortic node is imperative for the electrophysiologist who tackles these rhythms. A stepwise approach and ablation from various vantage points should be considered in difficult perinodal AT cases.

Patient perspective

Before treatment, the patient reported abrupt onset of symptoms with her tachycardia including palpitations, chest discomfort, and presyncope. She had to endure 6 ermegency room visits and two hospitalizations due to feeling extremely unwell due to SVT. Even when the episodes were short lived and self-terminated, she felt fatigued and out of energy for several hours afterwards. Particularly, during frequent salvos of tachycardia she felt unable to perform activities of daily living. After ablation, she is thankful for not having any more emergency room visits or even short runs of tachycardia at home. She was offered elimination of flecainide use, though she felt better keeping a low-dose as an added safeguard and tolerance.

Data availability statement

The original contributions presented in the study are included in the article/**Supplementary Material**, further inquiries can be directed to the corresponding author.

Ethics statement

Ethical review and approval was not required for the study on human participants in accordance with the local legislation and institutional requirements. The patients/participants provided their written informed consent to participate in this study.

Written informed consent was obtained from the individual(s) for the publication of any potentially identifiable images or data included in this article.

Author contributions

All authors contributed to this manuscript. All authors contributed to manuscript revision, read, and approved the submitted version. AR: writing and drafting of manuscript, editing and final completion NYT: conception and design of study, writing and drafting of manuscript, editing and final completion. OAF: writing and drafting of manuscript, editing and final completion. SJA: conception and design of study, editing and final completion. CVD: conception and design of study, editing and final completion. All authors contributed to the article and approved the submitted version.

Conflict of interest

The authors declare that the research was conducted in the absence of any commercial or financial relationships that could be construed as a potential conflict of interest.

Publisher's note

Supplementary material

The Supplementary Material for this article can be found online at: https://www.frontiersin.org/articles/10.3389/fcvm.2023.1143409/full#supplementary-material.

References

1. Ho SY, Sánchez-Quintana D. The importance of atrial structure and fibers. *Clin Anat*. (2009) 22(1):52–63. doi: 10.1002/ca.20634

2. Gard JJ, Swale MJ, Asirvatham SJ. Transseptal Access for the Electrophysiologist: Anatomic Considerations to Enhance Safety and Efficacy. (2011).

3. Kharbanda RK, Özdemir EH, Taverne Y, Kik C, Bogers A, de Groot NMS. Current concepts of anatomy, electrophysiology, and therapeutic implications of the interatrial septum. *JACC Clin Electrophysiol*. (2019) 5(6):647–56. doi: 10.1016/j.jacep.2019.04.013

4. Hutter AM Jr, Page DL. Atrial arrhythmias and lipomatous hypertrophy of the cardiac interatrial septum. *Am Heart J*. (1971) 82(1):16–21. doi: 10.1016/0002-8703(71)90156-6

5. Chen CC, Tai CT, Chiang CE, Yu WC, Lee SH, Chen YJ, et al. Atrial tachycardias originating from the atrial septum: electrophysiologic characteristics and radiofrequency ablation. *J Cardiovasc Electrophysiol*. (2000) 11(7):744–9. doi: 10.1111/j.1540-8167.2000.tb00045.x

6. Garg L, Pothineni NVK, Arroyo A, Rodriguez D, Garcia FC, Hyman MC, et al. Interatrial septal tachycardias following atrial fibrillation ablation or cardiac surgery: electrophysiological features and ablation outcomes. *Heart Rhythm*. (2021) 18(9):1491–9. doi: 10.1016/j.hrthm.2021.04.036

7. Iesaka Y, Takahashi A, Goya M, Soejima Y, Okamoto Y, Fujiwara H, et al. Adenosine-sensitive atrial reentrant tachycardia originating from the atrioventricular nodal transitional area. *J Cardiovasc Electrophysiol*. (1997) 8(8):854–64. doi: 10.1111/j.1540-8167.1997.tb00846.x

8. Lai LP, Lin JL, Chen TF, Ko WC, Lien WP. Clinical, electrophysiological characteristics, and radiofrequency catheter ablation of atrial tachycardia near the apex of Koch's triangle. *Pacing Clin Electrophysiol*. (1998) 21(2):367–74. doi: 10.1111/j.1540-8159.1998.tb00060.x

9. Bohora S, Lokhandwala Y, Sternick EB, Anderson RH, Wellens HJJ. Reappraisal and new observations on atrial tachycardia ablated from the non-coronary aortic sinus of Valsalva. *Europace*. (2018) 20(1):124–33. doi: 10.1093/europace/euw324

10. Anderson RH, Sanchez-Quintana D, Mori S, Spicer DE, Wellens HJJ, Lokhwandala Y, et al. Miniseries 2—septal and paraseptal accessory pathways—Part I: the anatomic basis for the understanding of para-Hisian accessory atrioventricular pathways. *EP Europace*. (2022) 24(4):639–49. doi: 10.1093/europace/euab292

11. Atkinson AJ, Logantha SJ, Hao G, Yanni J, Fedorenko O, Sinha A, et al. Functional, anatomical, and molecular investigation of the cardiac conduction system and arrhythmogenic atrioventricular ring tissue in the rat heart. *J Am Heart Assoc*. (2013) 2(6):e000246. doi: 10.1161/JAHA.113.000246

12. Liu X, Dong J, Ho SY, Shah A, Long D, Yu R, et al. Atrial tachycardia arising adjacent to noncoronary aortic sinus: distinctive atrial activation patterns and anatomic insights. *J Am Coll Cardiol*. (2010) 56(10):796–804. doi: 10.1016/j.jacc.2010.03.069

13. Wang Z, Liu T, Shehata M, Liang Y, Jin Z, Liang M, et al. Electrophysiological characteristics of focal atrial tachycardia surrounding the aortic coronary cusps. *Circ Arrhythm Electrophysiol*. (2011) 4(6):902–8. doi: 10.1161/CIRCEP.111.965640

14. Yanni J, Boyett MR, Anderson RH, Dobrzynski H. The extent of the specialized atrioventricular ring tissues. *Heart Rhythm*. (2009) 6(5):672–80. doi: 10.1016/j.hrthm.2009.01.021

Frontiers in
Cardiovascular Medicine

Innovations and improvements in cardiovascular treatment and practice

Focuses on research that challenges the status quo of cardiovascular care, or facilitates the translation of advances into new therapies and diagnostic tools.

Discover the latest Research Topics

See more →

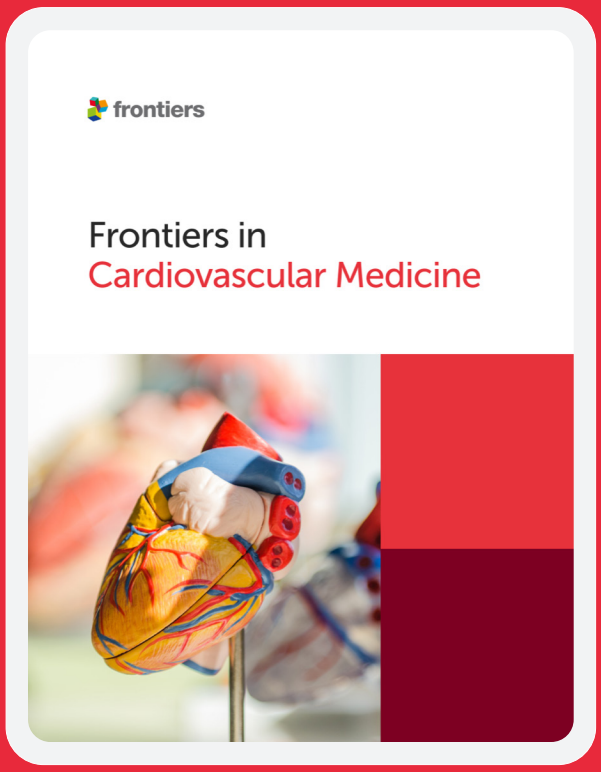

Frontiers

Avenue du Tribunal-Fédéral 34
1005 Lausanne, Switzerland
frontiersin.org

Contact us

+41 (0)21 510 17 00
frontiersin.org/about/contact